Aus dem Institut für Veterinär-Physiologie
des Fachbereichs Veterinärmedizin
der Freien Universität Berlin

Functional and molecular biological studies of the absorption of ammonia across porcine intestinal epithelia

Inaugural-Dissertation
zur Erlangung des Grades eines
Doktors der Veterinärmedizin
an der
Freien Universität Berlin

vorgelegt von
David Manneck
Tierarzt aus Potsdam

Berlin 2022
Journal-Nr.: 4352

Aus dem Institut für Veterinär-Physiologie

des Fachbereichs Veterinärmedizin

der Freien Universität Berlin

Functional and molecular biological studies of the absorption of ammonia across porcine intestinal epithelia

Inaugural-Dissertation

zur Erlangung des Grades eines

Doktors der Veterinärmedizin

an der

Freien Universität Berlin

vorgelegt von

David Manneck

Tierarzt aus Potsdam

Berlin 2022

Journal-Nr.: 4352

Gedruckt mit Genehmigung

des Fachbereichs Veterinärmedizin

der Freien Universität Berlin

Dekan:	Univ.-Prof. Dr. Uwe Rösler
Erster Gutachter:	Prof. Dr. Friederike Stumpff
Zweiter Gutachter:	Univ.-Prof. Dr. Jürgen Zentek
Dritter Gutachter:	Univ.-Prof. Dr. Heidrun Gehlen

Deskriptoren (nach CAB-Thesaurus): pigs, animal models, stomach, duodenum, jejunum, ileum, caecum, colon, digesta, mucosa, epithelium, muscle, ammonium, efflux, permeability, prostaglandins, cinnamaldehyde, essential oils, buffering capacity, polymerase chain reaction, western blotting, immunohistochemistry

Tag der Promotion: 21.10.2022

Table of Contents

List of Figures and Tables

List of Abbreviations

AITC	Allyl isothiocyanate
AQP	Aquaporin
Caco-2	Colorectal adenocarcinoma cell line
cAMP	Cyclin adenosine monophosphate
CFTR	Cystic fibrosis transmembrane conductance regulator
Cs^+	Caesium
GLP-1	Glucagon-like Peptide 1
G_t	Conductance
HCO_3^-	Bicarbonate (Hydrogencarbonate)
I_{sc}	Short circuit current
K^+	Potassium
Li^+	Lithium
Na^+	Sodium
NH_3	Ammonia
NH_4^+	Ammonium
NHE	Na^+-H^+ exchanger
NKCC	Na^+-K^+-2 Cl^- cotransporter
NSCC	Non-selective cation channel
OATP2A1	Solute carrier organic anion transporter family member 2A1
PGE2	Prostaglandin E2
pK_a	Acid dissociation constant
Rb^+	Rubidium
Rh	Rhesus
TRP	Transient Receptor Potential
UT-B	Urea transporter B

1. Introduction

The intestine, and in particular the colon, absorbs large amounts of ammonia that is formed during the digestive process from nitrogenous sources. The resulting ammonia is subsequently detoxified to urea and to smaller amounts of glutamine in the liver. Despite a certain reflux of urea into the intestine and utilization of glutamine as a precursor of non-essential amino acids, most of this nitrogen is ultimately excreted via the kidneys. Microbial decomposition leads to the formation of ammonia and nitrous oxides with adverse health and environmental effects. In Germany, 67 % of nitrogen emissions are attributable to agriculture (Geupel et al. 2021; Bach et al. 2020), while 95 % of ammonia emissions are of agricultural origin (Umweltbundesamt 2021). One way to reduce these emissions could be to make better use of the nitrogen sources supplied, but also to increase the microbial formation of nitrogen bound in protein. Although in monogastric species, this protein is subsequently excreted via the animals' feces, opportunities open up for reducing the rapid formation of volatile nitrogenous compounds while enhancing the amount of nitrogen that can be recycled into the food chain, e.g. as fertilizer (Béline 2002; Canh et al. 1998).

However, the transport mechanisms by which the large amounts of ammonia are intestinally absorbed have yet to be clarified. This is important for the reasons stated above, but also since in humans suffering from hepatic disease, absorption of ammonia from the gut contributes greatly to the lethal hyperammonemia in these patients (Romero-Gómez et al. 2009). The previously established hypothesis that ammonia is absorbed via simple diffusion through the lipid membrane surrounding epithelial cells must be considered obsolete (Al-Awqati 1999; Wrong 1978). Ammonia is in fact a highly polar compound, which severely limits its passage through cellular membranes. Instead, a rising number of studies indicate that ammonia can be taken up by different transport proteins (Weiner and Verlander 2017). This occurs either in the deprotonated form as NH_3 via Rh-Glycoproteins and aquaporins or in the protonated form as NH_4^+, as when uptake occurs via NKCC in the thick ascending loop of Henle (Weiner and Verlander 2016; Geyer et al. 2013b; Boron 2010; Knepper et al. 1989). Furthermore, at the pH found physiologically in the rumen of cattle and sheep, uptake of ammonia has been shown to occur primarily via a channel-mediated pathway as NH_4^+ (Abdoun et al. 2005; Bödeker and Kemkowski 1996). It should be noted that "ammonia" is used synonymously in this work for both forms, i.e. NH_3 and NH_4^+, with the structural formula used in specific places to indicate the relevance of the chemical compound.

Among transport systems for NH_4^+, diverse cation channels could play an important role (Burckhardt and Frömter 1992). These include the rather large family of Transient Receptor Potential (TRP) channels, which, as non-selective cation channels, perform a variety of tasks in the body. Given that recent studies have shown that TRPV3 and TRPV4 can conduct NH_4^+ (Liebe et al. 2022, 2021, 2020; Schrapers et al. 2018), one function may be to mediate absorption of ammonia. One special feature of many TRP channels including TRPV3 is that they can be specifically activated or inhibited by phytogenic components (Ramsey et al. 2006). Interestingly, studies of intact ruminal epithelia of sheep and cattle show that these tissues not only express TRPV3, but also conduct NH_4^+, and that the transport across the tissue can also be influenced by the use of phytogenic TRPV3 agonists such as thymol or menthol (Liebe et al. 2020; Rosendahl et al. 2016). Use of phytogenic compounds could thus be a promising solution to target the transport of ammonia across the gastrointestinal tract with the goal of improving the utilization of protein sources while reducing the environmentally hazardous renal excretion of nitrogen products.

To date, studies of the mechanisms behind the absorption of ammonia by porcine gastrointestinal epithelia are lacking. This is disturbing since pigs contribute considerably to ammonia emissions. Furthermore, pigs are a model species for humans. Therefore, one aim of this study was to investigate molecular biological evidence for the expression of relevant TRP channels by the porcine gut. Furthermore, this study attempted to investigate evidence for uptake of ammonia in the form of NH_4^+ and finally, to determine the effect of certain phytogenic agents in different intestinal segments on an electrophysiological level in more detail.

2. Literature Review

2.1 The Digestive System of the Pig

The digestive system of the pig can be divided into the upper and lower gastrointestinal tracts. The upper gastrointestinal tract consists of the oral cavity, salivary glands, esophagus, stomach, and duodenum, with the suspensory muscle (ligament of Treitz) being the demarcation to the lower gastrointestinal tract. The latter in turn contains the remaining parts of the small intestine (jejunum and ileum), as well as the entire large intestine (caecum, colon, rectum and anus). The greatly enlarged colon of the pig can be divided into a pars ascendens, transversum and descendens and has a spiral arrangement in the shape of a truncated cone. The length of the small intestine is about 20 m and that of the large intestine about 6 m, so that the intestine of the pig measures 15 times the length of the body (Salomon et al. 2008; Nickel et al. 2004).

2.1.1 Histology of the Intestinal Epithelium

The histological structure of the small and large intestine is generally similar. Thus, the intestinal mucosa consists of smooth muscles for self-motility of the mucosa (lamina muscularis mucosae), a cell-rich reticular connective tissue with lymphatic and blood vessels, nerve fibers and immune cells (lamina propria mucosae) and a single-layered highly prismatic epithelium (lamina epithelialis mucosae). The epithelial cells (enterocytes) of the lamina epithelialis mucosae have microvilli for surface enlargement. The small intestine also has circularly arranged folds (plicae circulares) to further increase its surface area, which are composed of mucosa and submucosa and are less common in the ileum. In addition, the small intestine contains protrusions of the lamina propriae mucosae and the mucosal epithelium, the villi intestinalis (Figure 1). Between the villi are the crypts (glandulae intestinales or Lieberkühn crypts), which are caved into the lamina propria mucosae. The crypts are particularly pronounced in the colon, where they play a decisive role in the aqueous secretion of chloride and bicarbonate. Regeneration of the intestinal epithelium from stem cells takes place in the lower third of the crypts. The newly formed cells differentiate and migrate to the tip of the villus, where they are finally extruded (Engelhardt and Breves 2010). In addition to the absorptive and secretory enterocytes, there are also secreting mucus-forming goblet cells, Paneth cells characterized by the formation of various enzymes, enteroendocrine cells, which act in a paracrine manner, and M cells that can transport antigens (Liebich 2010).

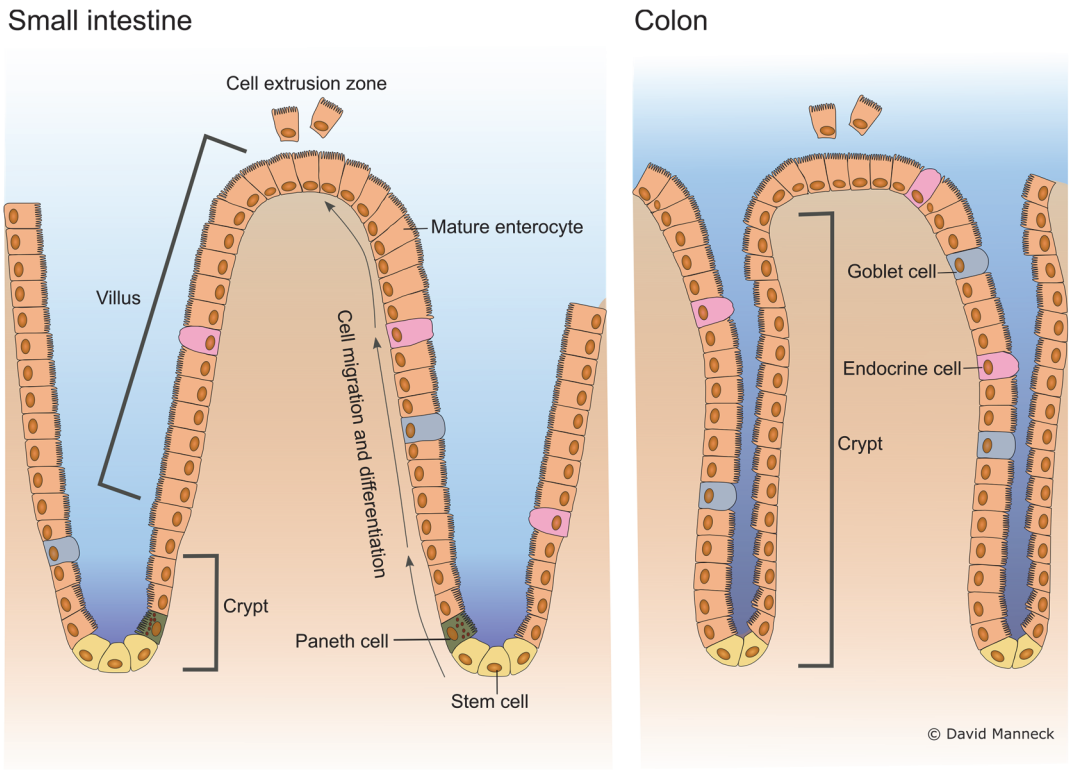

Figure 1. Schematic illustration of the intestinal mucosa of the small intestine and colon. A characteristic feature of the small intestine are the pronounced villi, which are responsible for the absorption of nutrients. Conversely, in the basal layer of the crypts, stem cells can be found which differentiate during migration to the tip. Furthermore, various types of crypt cells are responsible for secretions to the lumen. In the small intestine, the crypts are short and end between the villi, whereas in the large intestine, the crypts are more extensive and end in the intestinal lumen between the surface epithelium.

2.1.2 Digestion and Metabolism of Nitrogen

The main task of the gastrointestinal tract is to break down ingested nutrients into compounds that can be absorbed into the body's interior. The process of digestion begins in the cavity of the mouth by mechanical fragmentation of the feed and via enzymes of the saliva. The uptake of nitrogenous products is complex and begins with denaturation of the proteins via the acidic pH found in the stomach. After cleavage of the unfolded proteins via the peptidase pepsin, further digestion occurs in the small intestine with the help of pancreatic enzymes (e.g. trypsin, chymotrypsin, elastase) and other enzymes, such as the hydrolases of the brush border membrane (Kiela and Ghishan 2016). The absorptive epithelial cells of the brush border membrane then take up the amino acids with the help of different amino acid transporters, making them available to the body. In pigs, most of the nitrogen supplied is absorbed in the small intestine (Bergen and Wu 2009; Deglaire et al. 2009; Krawielitzki et al. 1990). Furthermore, a considerable amount of nitrogen enters the caecum and colon, where it is metabolized by microorganisms and used for microbial metabolism. This has been associated with a certain uptake of amino acids by the colon, but the relevance is not yet well understood and the effect is most likely of minor importance (van der Wielen et al. 2017;

Darragh et al. 1994). Accordingly and in contrast to ruminal fermentation, generation of microbial protein in the colon cannot cover the requirement of pigs for essential amino acids.

In parallel, however, large quantities of dietary protein and other nitrogenous compounds are degraded to ammonia via various mechanisms. Within the small intestine, glutamine deamination is thought to provide energy to enterocytes and to contribute considerably to the ammonia found in portal blood (Romero-Gómez et al. 2009). The highest concentrations of ammonia are found within the fermentative parts of the gut, where nitrogen containing compounds such as protein and urea are broken down via microbial enzymes. This ammonia can then be incorporated into microbial protein, thus promoting the fermentation process. However, large quantities are absorbed into the blood and must be detoxified in the liver – mostly to urea, which is then excreted via the kidneys. Eklou-Lawson et al. (2009) showed in starved pigs that within a 5-h period, a single dose of NH_4Cl did not result in an increase in blood ammonia until reaching the highest dose tested (5 g), from which the authors conclude that saturation of metabolic pathways occurs above 4.2 g of ammonia in the colon. The authors also observed that the addition of 2.5 g of NH_4Cl led to an increase in blood of L-glutamine, L-arginine, and urea, reflecting major products of ammonia metabolism.

The formation of glutamine, arginine and urea is a typical physiological process to counteract the toxic effect of ammonia. Ammonium is bound to α-ketoglutarate with the help of the enzyme glutamate dehydrogenase, which produces glutamate. Another molecule of ammonium can in turn be bound to glutamate with the help of the enzyme glutamine synthetase, resulting in glutamine. Both enzymes can be found in the colonic epithelium (Eklou-Lawson et al. 2009), but the liver is the main detoxification site for ammonia (Hakvoort et al. 2017; Spanaki and Plaitakis 2012). In the subsequent urea cycle, arginine is formed as an intermediary product (Walker 2009). The end product urea that is formed can finally be excreted via the kidneys into urine. However, relatively large quantities of urea are also secreted from blood back into the gastrointestinal tract, where the nitrogen can be utilized for the formation of microbial protein, or for the production of ammonia that is again absorbed into the portal circulation (Stumpff et al. 2013; Bindelle et al. 2008; Zervas and Zijlstra 2002). If the NH_3 that is produced from urea is absorbed in the protonated form as NH_4^+, this process might help to buffer the colonic lumen, as has been proposed for the rumen (Liebe et al. 2020).

2.2 Nitrogen Metabolism – Environmental and Health Impact

According to the German Environment Agency, 1547 kt per year of gaseous reactive nitrogen compounds or nitrates are emitted in Germany, with agriculture responsible for 67 % of these emissions (Geupel et al. 2021; Bach et al. 2020). A large part of these emissions, namely 589 kt per year or 38 %, are due to the emission of ammonia into the atmosphere

(Bach et al. 2020). Here, agriculture is responsible for 95 % (558 kt per year) of the ammonia emissions (Figure 2). With a total share of 70 %, most of these ammonia emissions are attributable to livestock farming, with pig farming alone responsible for 19 % of Germany-wide ammonia emissions (Umweltbundesamt 2021). The main source of the high emissions from pig farming is the rapid hydrolysis of urea from the pigs' urine to ammonia, which is converted bacterially via nitrate to nitrogen oxides (Philippe et al. 2011). Nitrates, which increasingly accumulate in groundwater (Zirkle et al. 2016), are carcinogenic and lead to eutrophication of water bodies, while nitrous oxides are highly potent climate gases (Gerber et al. 2013).

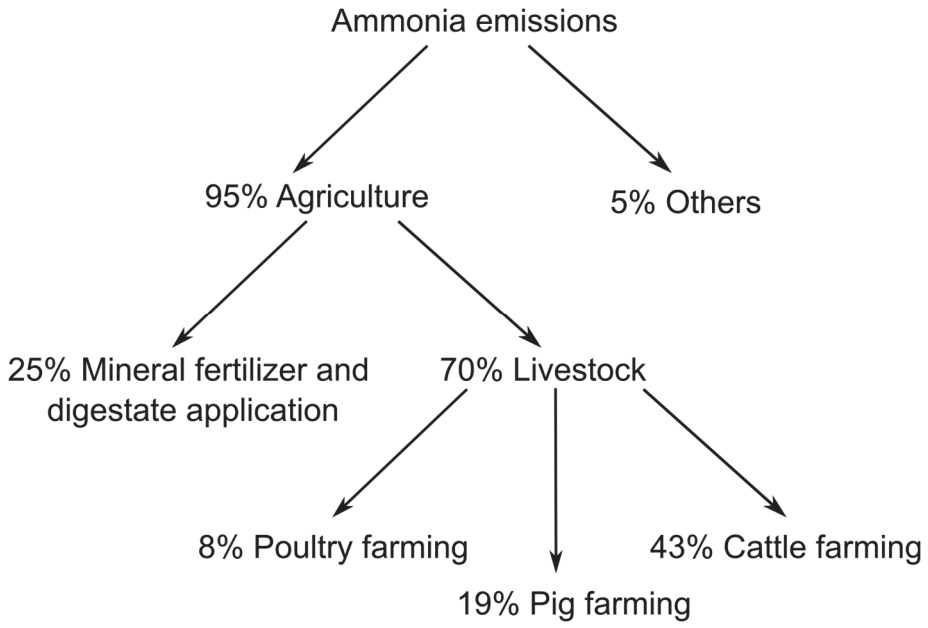

Figure 2. Diagram of emissions of ammonia in Germany. A total of 19 % of ammonia emissions are attributable to pig farming (Data from Umweltbundesamt 2021).

In contrast to urine, the degradation of protein in feces to ammonia occurs with a significant delay due to its high chemical stability and biological value (Béline 2002; Canh et al. 1998), allowing it to re-enter the food chain if disposed of in a favorable manner. In one study at 18 °C slurry temperature, 70 days were required to degrade 43 % of the protein (Spoelstra 1979). Accordingly, the housing system has a considerable influence on the ammonia emission rate. It has been shown that keeping pigs on a concrete floor system leads to a release of 2.8 kg of ammonia per animal per year, whereas keeping animals on slatted floors results in an annual emission rate of 2.5 kg that can be reduced to 2.2 kg per year when bedding with straw is provided that is changed weekly (Kavolelis 2006). Feeding studies on pigs have shown that increased fiber in the diet can reduce ammonia emissions by 17 % (O'Shea et al. 2009) and 33 % (Lynch et al. 2008), respectively, undoubtedly due to higher colonic fermentation with higher binding of nitrogen in microbial protein. The aim of any feeding strategy in pigs should therefore be, on the one hand, to improve overall protein efficiency and, on the other hand, to reduce the proportion of nitrogen excreted via urine.

In addition to the economic and ecological problems caused by nitrogen emissions, ammonia also creates direct health impacts. In pigs, even low concentrations of ammonia can trigger strong aversive reactions (Wathes et al. 2013). The toxicity of ammonia leads to impaired cleansing function of the cilia and altered flow properties of the mucus (Stombaugh et al. 1969), causing an increased predisposition to infectious diseases, such as infections with *Mycoplasma hyopneumoniae* (Michiels et al. 2015; Donham 1991). Thus, about 50 % of slaughter pigs show histological changes in terms of pneumonia despite costly vaccination strategies (Hillen et al. 2014; Maes et al. 2001; Grest et al. 1997). In addition, a significant proportion of farm employees are also susceptible to respiratory diseases. High ammonia concentrations are closely associated with respiratory symptomatology (Von Essen and Romberger 2003; de la Hoz et al. 1996). Workers on pig farms are considered as a high-risk group for lung diseases, with serious consequences for quality of life and life expectancy (Rushton 2007; Kirkhorn and Garry 2000).

In addition to the direct adverse effects of ammonia on the respiratory tract, absorption from the gut into the blood can also be a problem for patients with hepatic disease. In progressive liver diseases, the liver is no longer able to convert the cell-toxic amounts of ammonia into products such as glutamine or urea. This in turn leads to increased concentrations of ammonia in the blood, which causes inflammation in brain cells and fatal encephalopathy (Fiati Kenston et al. 2019; Mardini and Record 2013).

2.3 Transport of Ammonia and Ammonium

It is still unclear what mechanisms allow the intestine to absorb such high amounts of ammonia. According to classical theory, ammonia diffuses through the lipid bilayer surrounding intestinal cells in the uncharged form as NH_3 (Al-Awqati 1999; Wrong 1978). However, this theory has been challenged for several reasons. 1) The cell membrane does not consist of lipids only, but contains many other components such as cholesterol that reduce the permeation of lipid-soluable substrates. 2) NH_3 is a highly polar molecule with a high water solubility and low lipid permeability (Bell and Feild 1911), further reducing permeation. 3) Numerous biological preparations ranging from the lipid membrane surrounding Xenopus oocytes (Liebe et al. 2021, 2020; Burckhardt and Frömter 1992), the gastric epithelium (Boron et al. 1994; Waisbren et al. 1994) and the colonic epithelium of fish (Anderson et al. 2012) or chickens (Holtug et al. 2009) have been shown to be largely impermeable to a passive flux of ammonia in the form of NH_3. The low permeability of the ruminal epithelium to ammonia in the form of NH_3 has already been mentioned (Abdoun et al. 2005). 4) Ammonia has a pK_a value of 9.15 at 37 °C under physiologically relevant conditions (Weiner and Verlander 2017; Bromberg et al. 1960) and in the colon, where most ammonia is formed, a pH of about 6 is present (Pieper et al. 2012) (Figure 3a). As a result, over 99.9 % of ammonia is present in the

protonated form NH_4^+. Concentrations of NH_3 are thus minute, while for the charged ion NH_4^+, transport via simple lipid diffusion can be completely ruled out. 5) Influx of NH_3 into the cytosol will lead to a dramatic increase in the cytosolic pH. Note that the amount of NH_3 varies exponentially with changing pH, whereas the amount of NH_4^+ remains almost unchanged (Figure 3b). Therefore, transport of large quantities of NH_3 will lead to extreme challenges of pH regulatory mechanisms that can be avoided if transport occurs as NH_4^+. 6) Due to the fact that the radius and hydration energy of NH_4^+ is remarkably similar to that of K^+ in aqueous solutions, transport via corresponding transporters or ion channels seems likely (Weiner and Hamm 2007). This appears particularly relevant for organs with high rates of ammonia absorption.

More generally, proteins with a high selectivity for NH_3 over NH_4^+ favour the efflux of ammonia against the negative intracellular membrane potential, in particular if coupled to acid extrusion mechanisms with subsequent formation of NH_4^+, as in the collecting duct of the kidney (Ganz et al. 2020). Interestingly, such NH_3 transporters may also be involved in the transport of other uncharged but polar substrates, such as CO_2, which may explain their ubiquitous expression. Conversely, the selectivity of a protein for NH_4^+ over NH_3 facilitates the net uptake of ammonia into the cell. In situations with high extracellular concentrations of ammonia the permeation of both NH_4^+ and NH_3 through a transport protein will lead to a rather futile recirculation of both substrates across the cell membrane with a dissipation of ammonia and pH gradients (Ganz et al. 2020).

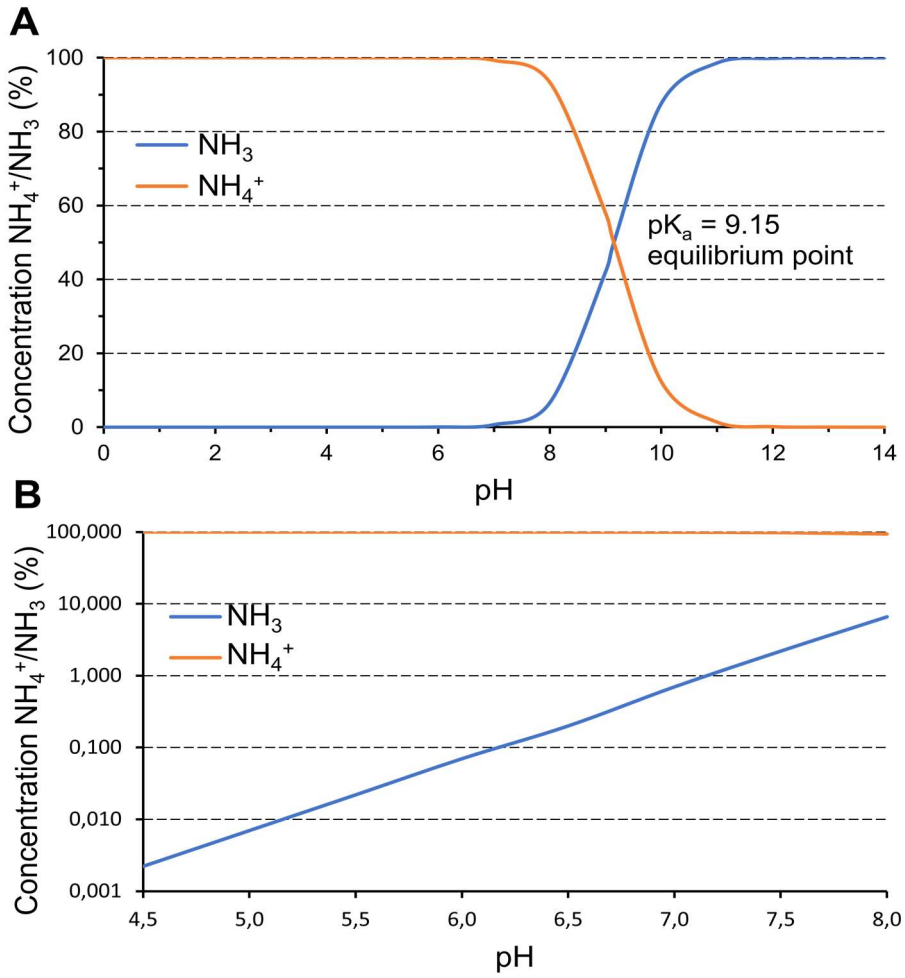

Figure 3. A Effect of pH on the distribution of NH_3 and NH_4^+. Both forms are in chemical equilibrium with each other with pK_a of 9.15 in biological systems. **B** Logarithmic plot of the concentrations of NH_4^+ and NH_3 at physiologically relevant pH values. Almost the total ammonia is present in the colon as NH_4^+ due to the low pH value of approx. 6. However, after absorption of the charged cation, the pH value within the cell increases to ~7.4, resulting in a substantial increase in NH_3 (Adapted from Weiner and Verlander 2017).

2.3.1 Transport of NH_3 via Aquaporins and Urea Transporters.

The intestine and the colon in particular, must absorb large amounts of water daily to maintain the body's water balance. To enable this, water can be transported either by paracellular mechanisms via tight junctions or by integral membrane water channels called aquaporins. In particular in the collecting duct of the kidney, the expression of these aquaporins is regulated to ensure water homoeostasis. The expression of the various aquaporins in the small and large intestine differs to a certain degree (Zhu et al. 2016). Since H_2O and NH_3 have similar electrostatic properties, transport via this channel family seems possible (Weiner and Verlander 2017). Some studies showed that many of the aquaporins can transport NH_3 (Assentoft et al. 2016; Kitchen et al. 2015; Litman et al. 2009), but the selectivity for NH_3 appears to vary among aquaporins (Musa-Aziz et al. 2009a). In addition, it is questionable so

far how relevant the transport of NH_3 via aquaporins really is. One study showed that knockout of the aquaporin AQP8 in mice did not impair NH_3 excretion, even at high ammonia concentrations (Yang et al. 2006).

Evidence from overexpressing systems suggests that NH_3 can also be transported through urea transporters, which is not surprising since NH_3 has physical properties that are similar to those of urea (Weiner and Verlander 2017). The UT-B transporter is amply expressed throughout the gastrointestinal tract (Inoue et al. 2005; Lucien et al. 2005) and transport of NH_3 via these channels appears possible (Geyer et al. 2013a).

2.3.2 Transport of NH_3/NH_4^+ via Rhesus Proteins

The rhesus (Rh) glycoprotein family includes RhAG, RhBG, and RhCG, with RhAG being expressed exclusively on erythrocytes and its precursors (Liu and Huang 1999). RhBG and RhCG are not expressed on erythrocytes, but in tissues such as liver, kidney, testis, and also in the gastrointestinal tract (Handlogten et al. 2005; Liu et al. 2001, 2000). This family of channels is related to the MEP proteins in yeasts and the AMT proteins in bacteria and plants, which transport ammonia (Thomas et al. 2000; Gazzarrini et al. 1999; Soupene et al. 1998; Marini et al. 1997). Whether transport through Rh proteins occurs as NH_4^+ or as NH_3 has not yet been fully clarified, as studies have yielded partly contradictory results. For example, some studies of RhBG have shown that transport is electrogenic, suggesting uptake of NH_4^+ (Nakhoul et al. 2010, 2005), whereas other studies suggest that this transport occurs as NH_3 (Geyer et al. 2013b; Zidi-Yahiaoui et al. 2005) or even that both forms are transported simultaneously (Caner et al. 2015). However, despite some controversy concerning the permeability to NH_4^+, the NH_3 transport function of Rh-like proteins is rarely disputed (Ganz et al. 2020). One reason for the different results could be due to the difficulties associated with experiments performed in heterologous expression systems (Neuhäuser et al. 2014; Javelle et al. 2007). Thus, high endogenous conductance values for NH_4^+ are found in *Xenopus laeves* oocytes, along with a sizable acidification after exposure to NH_4^+ (Liebe et al. 2020; Burckhardt and Frömter 1992).

In the case of RhCG, any transport of NH_4^+ appears to be minimal (Caner et al. 2015). A high selectivity of RhCG to NH_3 is considered to be crucial for extrusion of ammonia by the acid extruding cells within the collecting duct of the kidney, with a coupling of NH_3- transporting RhCG to apical H^+-ATPases (Bourgeois et al. 2013). Otherwise, a reflux of NH_4^+ would occur down the steep electrochemical gradient back into the cell (Weiner and Verlander 2017).

Most likely, highly selective Rh-like proteins initially bind NH_4^+, but catalyse a subsequent deprotonation into NH_3 which is then conducted along a pore that does not allow passage of

cations such as K^+ (Baday et al. 2015; Neuhäuser et al. 2014). However, mutations in the pore region can lead to a conductance for various cations, including NH_4^+ (Ganz et al. 2020).

2.3.3 Transport of NH_4^+ via Exchange Mechanisms

Due to the similar size and hydration energies, NH_4^+ can bind to the K^+-H^+ exchanger in the kidney so that H^+ is exchanged for NH_4^+ (Amlal and Soleimani 1997; Attmane-Elakeb et al. 1997). More surprisingly, the Na^+-H^+ Exchanger (NHE), which can be found in the intestine and kidney (Bookstein et al. 1994), has also been associated with the transport of NH_4^+. Some evidence suggests that the NHE3 in the kidney can accept NH_4^+ instead of H^+ at the cytosolic H^+-binding site, resulting in a Na^+-NH_4^+ exchange (Aronson et al. 1983; Kinsella and Aronson 1981). So far, however, it is not entirely clear why NH_4^+ can substitute for the much smaller H^+ ion, but it is suspected, among other factors, that these proteins do not transport H^+ but H_3O^+, which is biophysically closer to NH_4^+ (Weiner and Verlander 2017). In the jejunum and colon, NH_4^+ transport via NHE has also been discussed, but here NH_4^+ was thought to interact with the Na^+ binding site, thereby reducing sodium absorption (Gunther and Wright 1983). Cermak et al. (2002, 2000) were able to demonstrate this in a study on the rat colon and assumed the involvement of a Na^+-H^+ exchanger, although a role of either NHE2 or NHE3 was excluded. Conversely, studies of the ruminal epithelium, which expresses Na^+-H^+ exchangers such as NHE1 and NHE3 (Etschmann et al. 2006), showed stimulation of Na^+ transport by NH_4^+ administration (Abdoun et al. 2005) in conjunction with an intracellular acidification as measured by ion selective microelectrodes (Rosendahl et al. 2016; Lu et al. 2014). Interestingly, both experiments on the rumen and on the caecum of pigs have shown an increased short-circuit current (I_{sc}) after the addition of a solution containing NH_4^+, implying an increased transport of cations (Rosendahl et al. 2016; Lu et al. 2014; Stumpff et al. 2013; Abdoun et al. 2005; Bödeker and Kemkowski 1996). These observations cannot be explained with a model of either NH_3 transport or transport of NH_4^+ via NHE, since neither of these mechanisms involve intracellular acidification or the transepithelial transport of a net charge. Accordingly, there seems to be an additional, electrogenic route for NH_4^+ transport in the intestine.

2.3.4 Transport of NH_4^+ via NKCC

The Na^+-K^+-2 Cl^- cotransporter is classified into the isoforms NKCC1 and NKCC2, with NKCC1 expressed among others in the basolateral membrane of the colon (Haas and Forbush 1998). In contrast, NKCC2 is specific to the apical membrane of the thick ascending limb of the loop of Henle. A transport of NH_4^+ via the NKCC2 in the kidney was described many years ago, with NH_4^+ using the K^+ binding site (Karim et al. 2005; Kinne et al. 1986). A similar transport via NKCC1 has also been described in colonic crypt cells (Ramirez et al. 1999).

However, since NKCC1 is expressed basolaterally in the intestine, this would result in secretion of NH_4^+ and not cause absorption of NH_4^+. Interestingly, NKCC is expressed on the apical membrane of enterocytes in rainbow trout and may therefore serve as an absorption mechanism for NH_4^+ in this species (Rubino et al. 2019).

2.3.5 NH_4^+ Transport via K^+ Channels

As briefly mentioned at the beginning of this chapter, K^+ and NH_4^+ have similar physical properties, so a transport of NH_4^+ via potassium channels seems possible. Indeed, numerous studies show that NH_4^+ can be transported by a great number of potassium transporters (Choe et al. 2000; Heginbotham and MacKinnon 1993; Eisenman et al. 1986). Because of the expression of several of these channels in the gastrointestinal tract (Cosme et al. 2021; Heitzmann and Warth 2008), these transporters represent a possible transport pathway for NH_4^+. In rats and rainbow trout, transport of NH_4^+ via barium-sensitive K^+ channels in enterocytes appears to play a relevant role (Rubino et al. 2019; Hall et al. 1992).

Transport of NH_4^+ has also been described in various ATP-dependent transporters. Here, the K^+ binding site also acts as a shuttle for the NH_4^+, as is the case in the Na^+-K^+-ATPase (Wall 1996; Kurtz and Balaban 1986). However, this pump is expressed on the basolateral side of epithelia and would therefore lead to secretion of NH_4^+. A similar mechanism has also been described for the H^+-K^+-ATPase. Here, Cougnon et al. (1999) showed that *Xenopus laevis* oocytes overexpressed with rat H^+-K^+-ATPase react with an enhanced uptake of NH_4^+. Interestingly, as with the transport of NH_4^+ across the NHE, studies show that NH_4^+ appears to bind at both the K^+ and H^+ binding site (Nakamura et al. 1999; Garg and Narang 1988).

2.3.6 Transport of NH_4^+ via Non-Selective Cation Channels

Non-selective cation channels (NSCC) are formed by a variety of different proteins. Unlike classical, highly selective K^+, Na^+ or Ca^{2+} channels, these proteins discriminate poorly between these three and generally conduct other cations as well. Due to this fact, these channels can be considered prime candidates for the transport of NH_4^+. Unfortunately, there is very limited literature on the permeability of NSCCs to NH_4^+. The transport of NH_4^+ via NSCC channels has been described in some plant species (Pottosin and Dobrovinskaya 2014; Baluška et al. 2006; Roberts and Tyerman 2002), and has also repeatedly been reported in Xenopus Oocytes (Liebe et al. 2020; Burckhardt and Frömter 1992). However, the channels have not been identified so far and very few investigations have focussed on mammals.

2.3.7 Involvement of TRP Channels in NH_4^+ Transport across the Ruminal Epithelium

Recent research suggests an involvement of members of the transient receptor potential (TRP) family in NH_4^+ transport across the ruminal epithelium. TRP channels are

expressed in almost all tissues, including the intestine, although their function has not yet been fully elucidated (Jang et al. 2012; Holzer 2011; Kunert-Keil et al. 2006). The hypothesis that non-selective cation channels might be involved in NH_4^+ transport across the rumen arose more than 25 years ago (Bödeker and Kemkowski 1996). Later work showed that transport of NH_4^+ predominates at the pH found physiologically in the rumen (Rabbani et al. 2018; Abdoun et al. 2005) with acidification of the cytosol supported by the NH_4^+-induced stimulation of Na^+-fluxes and directly measured via ion-selective microelectrodes (Rosendahl et al. 2016; Lu et al. 2014). Patch clamp measurements on rumen epithelial cells confirmed the expression of non-selective cation channels permeable to NH_4^+ (Rosendahl et al. 2016; Abdoun et al. 2005; Leonhard-Marek et al. 2005). Later, functional evidence for the involvement of TRPV3 channels in ruminal Ca^{2+} and NH_4^+ absorption emerged using intact rumen tissue in the Ussing chamber (Geiger et al. 2021; Rabbani et al. 2018; Rosendahl et al. 2016), with a possible smaller additional participation of TRPV4 (Liebe et al. 2022). The expression of TRPV3 and TRPV4 by the apical membrane of the rumen has been verified using qPCR, immunoblots and immunohistochemistry (Liebe et al. 2022, 2020; Geiger et al. 2021; Rosendahl et al. 2016), while the permeability of TRPV3 and TRPV4 to NH_4^+ has been directly shown in overexpressing HEK-293 cells (Liebe et al. 2022, 2020; Schrapers et al. 2018) and, in the case of TRPV3, also in oocytes from *Xenopus laeves* (Liebe et al. 2020).

Physiological relevance of this finding has been reported in feeding studies with sheep and cattle fed supplements that activate TRPV3. Thus, increased blood calcium levels were found as a result of feeding (Kholif et al. 2020; Braun et al. 2019; Patra et al. 2019), and increased milk yield (Kholif et al. 2020; Braun et al. 2019) but increased amino acids such as glutamate/glutamine and aspartate/asparagine in the blood were also reported (Patra et al. 2019). This suggests that activation of TRP channels may improve nitrogen utilization in ruminants. Since electrogenic transport of NH_4^+ also occurs in the porcine caecum (Stumpff et al. 2013), this channel family is an interesting option for ammonia transport by the intestine.

2.4 Transient Receptor Potential (TRP) Channels

The term transient receptor potential arose in the late 1960s when studies found that a visually impaired *Drosophila melanogaster* mutant showed a transient response to steady light (Montell 2011; Cosens and Manning 1969). The animals were subsequently referred to as “transient receptor potential” (trp) mutants (Minke et al. 1975), but the discovery of the associated gene was not made until 1989 (Montell and Rubin 1989). Since this discovery, interest in the expression and function of this gene family increased over the next years and decades. An exciting feature is the sensitivity of many members of the family to a variety of pharmacological compounds, many of which are found in plants (Vennekens et al. 2008). The

nomenclature was initially quite confusing until a reorganization of the nomenclature was finally agreed upon (Catterall et al. 2003; Montell et al. 2002).

To date, 28 channels have been identified in mammals and are classified according to their homology to each other, as the exact function of these channels is often unknown. The channels are classified as canonical (TRPC), melastatin (TRPM), polycystin (TRPP), mucollipin (TRPML), vanilloid (TRPV) and ankyrin (TRPA) (Figure 4). A seventh subfamily, the no-mechanical-potential C channel (NOMP-C, TRPN), has also been described, but has not yet been detected in mammals (Nilius and Owsianik 2011). Common to all channels is that they consist of six-transmembrane domains with intracellular amino (N) and carboxy (C) termini. Thereby, they can form homo- or hetero-tetramers (Hoenderop 2003; Kedei et al. 2001). The cation conductivity of the pore region is expected to result from a hydrophobic stretch between TM5 and TM6 (Owsianik et al. 2006). Despite intensive studies in recent years of the various TRP channels, much has still to be discovered about their exact properties. These studies are complicated in part because some TRP channels can also form multiple splice variants (Vázquez and Valverde 2006; Walker et al. 2001). In addition, endogenous TRP channel expression is often low, which further complicates studies (Desai and Clapham 2005).

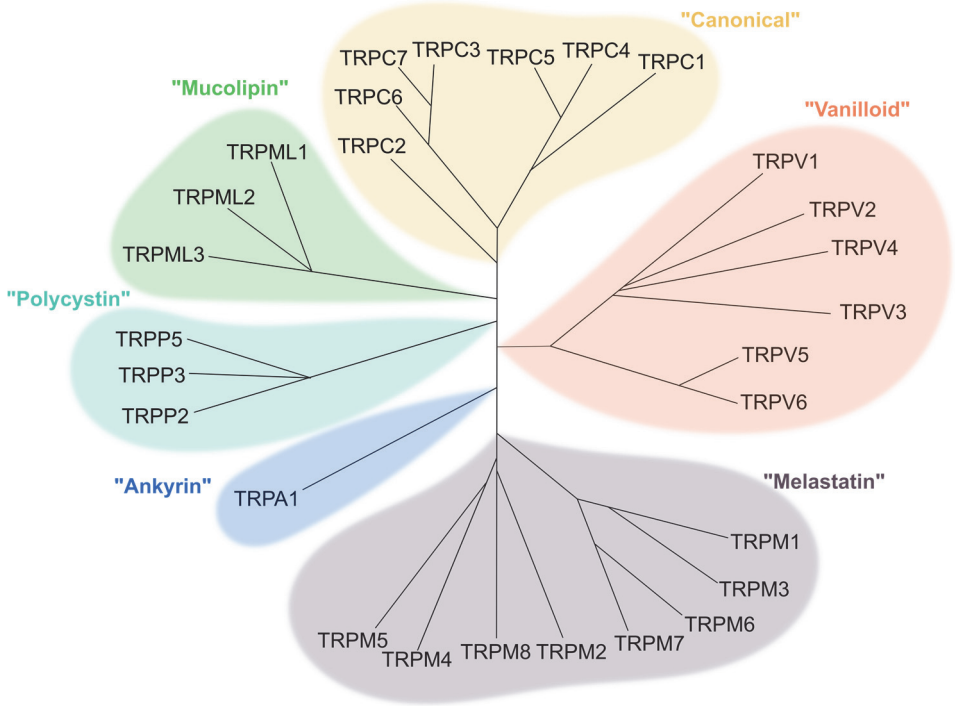

Figure 4. Phylogenetic tree of the TRP family detected in mammals to date (Adapted from Gees et al. 2010; Clapham 2003).

2.4.1 Expression and Function

TRP channels are expressed in almost all tissues, cells and cellular membranes, with some members showing very limited expression in a small number of tissues, whereas other members are found almost ubiquitously. In most cases, the channels are localized in the plasma membrane, where they transport cations with variable selectivity. For example, TRPV5 and TRPV6 have a very high selectivity for Ca^{2+} over other cations (Gees et al. 2010), whereas TRPM6 and TRPM7 predominantly conduct Mg^{2+} (Schlingmann et al. 2007). Other members of the family are more promiscuous and conduct both monovalent and divalent cations, with negative interactions typically observed.

The functions of the various TRP channels are as versatile as their expression. TRP channels are involved in sensory perception, such as taste transduction (Roper 2014), pain and temperature perception (Jardín et al. 2017), detection of pheromones (Lucas et al. 2003), but also have osmoregulatory functions (Janas et al. 2016) and are involved in muscle contractions (Dietrich et al. 2006). TRPV3 is also known for its participation in keratinization of the skin, with gain of function mutations leading to severe hyperkeratosis (Nilius and Bíró 2013). It is important to note that many functions of TRP channels are triggered by their activation with subsequent influx of cations, often Ca^{2+}, which serves as a second messenger. However, in the case of TRPV5, TRPV6, TRPM6 and TRPM7 the primary function is the epithelial transport of Ca^{2+} (TRPV5, TRPV6) and Mg^{2+} (TRPM6, TRPM7), in particular in the kidney and the intestine. The involvement of other members of the family in transepithelial transport has rarely been investigated, although many other TRP channels are expressed by epithelial cells.

2.4.2 Modulation by Phytogenic Compounds

The activation of TRP channels occurs via different mechanisms. In addition to G-protein coupled activation, certain TRP channels can also be activated more or less selectively by endogenous substances, osmotic pressure, pH, temperature, synthesized drugs or even phytogenic components (Ramsey et al. 2006). These phytogenic compounds predominantly include classes of monoterpenes (thymol, menthol, carvacrol, camphor, linalool), phenylpropanoids (cinnamaldehyde, eugenol), carboxamides (capsaicin, piperine), organosulfur compounds (allicin, allyl isothiocyanate), xanthines (caffeine) and cannabinoids (tetrahydrocannabinol (THC), cannabidiol (CBD)) (Vennekens et al. 2008). Interestingly, modulation by phytogenic substances appears to be somewhat specific for defined TRP channels and has so far only been demonstrated in some representatives, namely TRPV1-4, TRPA1, and TRPM8. Other TRP channels are apparently unaffected by phytogenic components.

The taste and perception of herbs and spices is due in part to the effects and hedonic sensations of these ingredients. Chili (capsaicin) and pepper (piperine), which are used to season and spice food worldwide, typically activate TRPV1, leading to sensations of stinging, heat and pain. This sensation is due to the fact that TRPV1 is substantially involved in the perception of heat (>40 °C) but also has a relevant role in the sensation of pain (Vennekens et al. 2008; Pingle et al. 2007). Activation of TRPV3 occurs at 22-40 °C and this channel can also be activated by phytogenic components such as carvacrol, thymol and menthol (Vennekens et al. 2008; Xu et al. 2006). Interestingly, menthol can also activate TRPM8, which mediates the sensation of cold (activation under <26 °C) (Bautista et al. 2007). The phytogenic substances cinnamaldehyde and allyl isothiocyanate are considered to be relatively specific for TRPA1 with high efficacy (Talavera et al. 2020). Conversely, TRPV4 is not activated by any of these compounds, although citral shows an inhibitory effect (Vincent and Duncton 2011; Stotz et al. 2008). However, TRPV4 can be activated by some cannabinoids, which also have an activating effect on other channels such as TRPV1, TRPV2, TRPV3 and TRPA1 (Muller et al. 2019). In addition, a specific synthetic agonist (GSK1016790A) exists for TRPV4 (Vincent and Duncton 2011).

The effect of phytogenic agents on TRP channels is being intensively studied, but there appear to be distinct species differences regarding concentration and action. Thus, at micromolar concentrations, menthol was found to activate mouse TRPA1, but at concentrations >50 $\mu mol \cdot l^{-1}$, it has a blocking effect (Xiao et al. 2008; Karashima et al. 2007). Conversely, human TRPA1 was found to be activated by concentrations as high as 250 $\mu mol \cdot l^{-1}$ (Xiao et al. 2008). Another example is caffeine, which can activate mouse TRPA1 but suppresses human TRPA1 (Nagatomo and Kubo 2008). It is also interesting to note that avian TRPV1 is insensitive to capsaicin (Chu et al. 2020; Uzura et al. 2020). These differences in effect are caused by changes in the amino acid residues, which alters the gating mechanism (Bianchi et al. 2012). Conclusions from rodents to humans or livestock are only possible to a limited extent due to these circumstances.

The exact mechanism of action on TRP channels has been studied in more detail for some phytogenic compounds and distinct differences emerge here as well. Activation of TRPA1 by cinnamaldehyde is due to covalent modification of cysteine and lysine residues within the N-terminus, resulting in dilatation of the permeation pore (Nilius et al. 2011; Macpherson et al. 2007; Hinman et al. 2006). The effect of cinnamaldehyde or allyl isothiocyanates is due to the bond with the α,β-unsaturated aldehyde group, so that it can be assumed that similar substances, such as citral, have a similar effect (Macpherson et al. 2007; Cavins and Friedman 1967). For the agonistic effect of menthol on TRPM8, it is not yet fully understood how channel activation occurs. In their studies, Xu et al. (2020) describe a "grab

and stand" mechanism, resulting in conformational changes that enable ion permeation. Whether the effect of the numerous other phytogenic agents is due to a similar mechanism can only be speculated on so far.

2.4.3 TRP Channels in the Gastrointestinal Tract

TRP channels are found throughout the gastrointestinal tract. They are expressed not only in nerve cells or muscles, but also on epithelial cells, where they fulfill different functions. In epithelial cells of the small intestine, the TRP channels TRP5/TRPV6 are critical for the absorption of Ca^{2+} in the small intestine (den Dekker et al. 2003), whereas TRPM6/TRPM7 are responsible for the absorption of Mg^{2+} (Schlingmann et al. 2007), with studies suggesting that most absorption occurs in the distal intestine (Hardwick et al. 1991). In ruminants, both Mg^{2+} secretion (mostly in the small intestine) and Mg^{2+} absorption (mostly in the hindgut and the rumen) are observed (Martens et al. 2018). In the balance, the rumen is required to ensure net uptake of Mg^{2+}, which again involves TRPM6/TRPM7. Some studies have reported that carvacrol has an antagonistic effect on TRPM7 (Cai et al. 2021; Chen et al. 2015), but no study has investigated an effect in the gastrointestinal tract yet, so any influence on magnesium absorption is speculatory.

TRPV1, one of the best-studied TRP channels, is mainly expressed in primary afferent sensory neurons and in neurons of the enteric nervous system, but has also been found in epithelial cells of the esophagus, stomach and colon (Rizopoulos et al. 2018; Holzer 2011; Cheng et al. 2009; Faussone-Pellegrini et al. 2005). On the one hand, TRPV1 is thought to be responsible for the perception of abdominal pain (Holzer 2011) and to have a protective effect of the mucosa (Massa et al. 2006), but on the other hand, it is also involved in inflammatory diseases, such as inflammatory bowel disease (Csekő et al. 2019). TRPA1 is also expressed in afferent nerve fibers, sometimes showing co-localization with TRPV1, and is thereby associated with pain and inflammation of the intestine (Talavera et al. 2020). However, TRPA1 is also expressed in epithelial cells of the intestine and in enterochromaffin cells (Cho et al. 2014). In this context, activation of TRPA1 in enterochromaffin cells is thought to lead to the release of serotonin (Lieder et al. 2020; Doihara et al. 2009).

In addition to TRPV1 and TRPA1, TRPV4 is also thought to play a significant role in abdominal pain. Since TRPV4 can be activated by mechanical influences in addition to chemical ones, TRPV4 is thought to play an important role in osmosensation and pain perception in the colon (Kollmann et al. 2020; Balemans et al. 2017; Shibasaki 2016; Cenac et al. 2008). This channel is also thought to be involved in inflammatory bowel diseases, such as ulcerative colitis (Toledo Mauriño et al. 2020). In the stomach, TRPV4 is reported to be involved in motility and emptying (Mihara et al. 2016). Recent evidence suggests that TRPV4

is also expressed by the ruminal epithelium (Liebe et al. 2022), where it may be involved in Ca^{2+} and NH_4^+ absorption. However, it should be noted that high concentrations of the TRPV4 agonist GSK1016790A were required for activation in the epithelium, suggesting a role that may lag behind that of TRPV3.

TRPV2 is also a mechanosensitive channel and is partly responsible for relaxation and emptying of the stomach (Mihara et al. 2013). Furthermore, some authors report that TRPV2-mediated motility in the gut is caused by nitric oxide production (Mihara et al. 2010). The role of TRPV2 in inflammatory bowel disease is currently poorly understood. In a dextran sulfate sodium induced colitis model, TRPV2 knockout mice showed weaker symptoms compared to controls (Issa et al. 2014). Another study reported that TRPV2 expression was unchanged in colitis patients compared with patients without inflammatory bowel disease (Rizopoulos et al. 2018). However, only a few phytogenic modulators of TRPV2 have been discovered so far, namely cannabinol, cannabidiol, and Δ^9-tetrahydrocannabinol as agonists and citral as an antagonist (Qin et al. 2008; Stotz et al. 2008). The far-reaching central nervous side effects of the TRPV2 agonists do not allow utilization in animal nutrition.

Various functions have been described for TRPM8, the only candidate of the TRP melastatin group that can be activated by phytogenic substances. In colonic smooth muscle, activation of TRPM8 is thought to cause relaxing effects by opening large-conductance Ca^{2+}-dependent K^+ channels (Amato et al. 2020). TRPM8 is co-localized with TRPV1 and TRPA1 in neurons of the colon. Activation of TRPM8 in these cells triggers mechanical desensitization with reduced agonist-triggered responses involving TRPV1 and TRPA1 (Takaishi et al. 2016; Harrington et al. 2011). In conjunction with studies describing an anti-inflammatory effect through activation of TRPM8, a positive influence in inflammatory bowel disease has been suggested (Peiris et al. 2021; Ramachandran et al. 2013), although contradicting findings have been reported (Hosoya et al. 2014).

The functions of TRPV3 in the gastrointestinal tract are almost unknown so far. A complicating factor is that although this channel can be modulated by numerous agonists and antagonists, they are all considered to be relatively non-specific. As a result, the search for specific modulators continues (Bischof et al. 2020). TRPV3 expression in the gastrointestinal tract has been detected in colonic epithelial cells, with localization primarily in the apical membrane, but the functional roles in these cells have not yet been elucidated (Bischof et al. 2020; Ueda et al. 2009). It has been suggested that TRPV3 is involved in inflammatory bowel disease, as studies have demonstrated increased expression (Toledo Mauriño et al. 2020). However, this finding could not be confirmed in other studies (Rizopoulos et al. 2018).

Some more information is available for the role of TRPV3 in the rumen of cattle and sheep. Here, TRPV3 emerged as a candidate gene when searching for the molecular identity of a divalent-sensitive cation conductance (Leonhard-Marek et al. 2005), which was found to conduct not only Na^+ and K^+, but also NH_4^+ and Ca^{2+}. Furthermore, and despite numerous attempts, it was not possible to detect mRNA for either TRPV5 or TRPV6 in this organ (Geiger et al. 2021; Rosendahl et al. 2016; Wilkens et al. 2012, 2009). Note that numerous functional studies of the ruminal epithelium support the channel-mediated absorption of Ca^{2+} by this organ (Schröder and Breves 2006; Schröder et al. 1999, 1997). Along with molecular biological evidence demonstrating the expression of TRPV3 by the apical membrane of the rumen, the effects of various TRPV3 agonists on the transport of Ca^{2+}, Na^+ and NH_4^+ suggest an involvement of TRPV3 in cation transport across the rumen (Liebe et al. 2022, 2020; Geiger et al. 2021; Rabbani et al. 2018; Rosendahl et al. 2016). Given that TRPV3 is also amply expressed by the apical membrane of the colon (Bischof et al. 2020; Ueda et al. 2009), the question naturally arises if these channels might also play a role in the uptake of NH_4^+ by this tissue.

3. Aims and objectives of this thesis

The main objective of the current thesis was to identify various TRP channels in the gastrointestinal tract of pigs by molecular techniques and to investigate functional evidence for the participation of these channels in ammonia transport in these tissues. Given that a number of these channels can be modulated by phytogenic agents, a further goal was to study the effects of typical agonists of some TRP channels on porcine gastrointestinal tissues *ex vivo*. The study was motivated by the desire to learn more about the pathways via which ammonia is absorbed from the porcine gut. Modulation of these pathways – e.g. by phytogenic agents – could potentially reduce the harmful impact of ammonia emissions from livestock on the environment.

In the first series of studies, the tissues of the stomach, duodenum, jejunum, ileum, caecum and colon were examined for expression of different TRP channels at the level of mRNA and protein. Furthermore, Ussing chamber experiments were conducted to functionally compare tissues from the different segments, to determine if these gastrointestinal tissues were conductive to ammonia and whether TRP channels might play a role.

The second series of studies investigated the effects of phytogenic agonists in the colon and jejunum of pigs in Ussing chambers. The agonists thymol and cinnamaldehyde, which have been described as relatively specific agonists for TRPV3 and TRPA1 respectively, were tested. The mechanism of action was further investigated using different solutions and blockers.

4. TRPV3 and TRPV4 as Candidate Proteins for Intestinal Ammonium Absorption

The manuscript

Manneck, D., Braun, H.-S., Schrapers, K.T., Stumpff, F., (2021): TRPV3 and TRPV4 as candidate proteins for intestinal ammonium absorption. Acta Physiol (Oxf), 233:e13694.

was published in Acta Physiologica and can be accessed here: https://doi.org/10.1111/apha.13694

An editorial article (Diener 2021) exists for this manuscript, which can be viewed here: https://doi.org/10.1111/apha.13711

Contribution	Contributor
Conceptualization	Stumpff, Manneck
Methodology	Stumpff, Braun, Schrapers, Manneck
Software	Stumpff
Validation	Braun, Manneck
Formal Analysis	Stumpff, Manneck
Investigation	Manneck
Resources	Stumpff, Schrapers
Data Curation	Stumpff, Manneck
Writing—Original Draft Preparation	Stumpff, Manneck
Writing—Review and Editing	Stumpff, Braun, Schrapers, Manneck
Visualization	Manneck
Supervision	Stumpff
Project Administration	Stumpff

License: https://creativecommons.org/licenses/by-nc/4.0/

Received: 22 January 2021 | Revised: 19 May 2021 | Accepted: 19 May 2021

DOI: 10.1111/apha.13694

ACTA PHYSIOLOGICA

REGULAR PAPER

TRPV3 and TRPV4 as candidate proteins for intestinal ammonium absorption

David Manneck[1] | **Hannah-Sophie Braun**[2] | **Katharina T. Schrapers**[2] | **Friederike Stumpff**[1]

[1]Institute of Veterinary Physiology, Freie Universität Berlin, Berlin, Germany

[2]PerformaNat GmbH, Berlin, Germany

Correspondence
Friederike Stumpff, Institute of Veterinary Physiology, Freie Universität Berlin, Oertzenweg 19b, Berlin 14163, Germany.
Email: stumpff@zedat.fu-berlin.de

Funding information
Akademie für Tiergesundheit; Deutsche Forschungsgemeinschaft, Grant/Award Number: DFG-STU 258/7-1

Abstract

Aim: Absorption of ammonia from the gut has consequences that range from encephalitis in hepatic disease to global climate change induced by nitrogenous excretions from livestock. Since patch clamp data show that certain members of the transient receptor potential (TRP) family are permeable to NH_4^+, participation in ammonium efflux was investigated.

Methods: Digesta, mucosa and muscular samples from stomach, duodenum, jejunum, ileum, caecum and colon of pigs were analysed via colourimetry, qPCR, Western blot, immunohistochemistry and Ussing chambers.

Results: qPCR data show high duodenal expression of TRPV6. TRPM6 was highest in jejunum and colon, with expression of TRPM7 ubiquitous. TRPM8 and TRPV1 were below detection. TRPV2 was highest in the jejunum but almost non-detectable in the colon. TRPV4 was ubiquitously expressed by mucosal and muscular layers. TRPV3 mRNA was only found in the mucosa of the caecum and colon, organs in which NH_4^+ was highest (>7 mmol·L^{-1}). Immunohistochemically, an apical expression of TRPV3 and TRPV4 could be detected in all tissues, with effects of 2-APB and GSK106790A supporting functional expression. In symmetrical NaCl Ringer, removal of mucosal Ca^{2+} and Mg^{2+} increased colonic short circuit current (I_{sc}) and conductance (G_t) by 0.18 ± 0.06 µeq·cm^{-2}·h^{-1} and 4.70 ± 0.85 mS·cm^{-2} ($P < .05$, N/n = 4/17). Application of mucosal NH_4Cl led to dose-dependent and divalent-sensitive increases in G_t and I_{sc}, with effects highest in the caecum and colon.

Conclusion: We propose that TRP channels contribute to the intestinal transport of ammonium, with TRPV3 and TRPV4 promising candidate proteins. Pharmacological regulation may be possible.

KEYWORDS
ammonium, colon, gastrointestinal transport, TRP channel, TRPV3, TRPV4

See editorial article: Diener M. 2021. How to manage N-waste in the intestine? *Acta Physiol* (Oxf). e13711.

This is an open access article under the terms of the Creative Commons Attribution-NonCommercial License, which permits use, distribution and reproduction in any medium, provided the original work is properly cited and is not used for commercial purposes.
© 2021 The Authors. *Acta Physiologica* published by John Wiley & Sons Ltd on behalf of Scandinavian Physiological Society.

1 | INTRODUCTION

Transient receptor potential (TRP) channels are expressed throughout the gastrointestinal tract where they play multiple roles that are incompletely understood.[1,2] Perhaps owing to the fact that the first member of the family to be discovered is central to phototransduction in drosophila flies,[3] the major focus of attention has so far mostly been on the role of these proteins as molecular sensors for various stimuli. Importantly, certain members of the family can be gated by heat (eg TRPV1 or TRPV3) or cold (TRPA1 or TRPM8).[4] Furthermore, the channels are modulated by a plethora of chemical stimuli including fragrant mono- and diterpenes found naturally in plants,[5] by hormones, by pH or osmolarity.[1,2,6,7] In the gastrointestinal tract, stimuli generally activate channels on submucosal neurons, leading to influx of Ca^{2+} with initiation of signalling cascades that lead both to central sensory perception or local responses. Thus, the stimulation of TRPA1 expressed by neuronal fibres of the enteric nervous system is thought to play a role in inflammatory responses with secretion of signalling molecules associated with hypersensitivity and pain as in inflammatory bowel disease.[8] On the other hand, the interaction of cinnamaldehyde with the same channel triggers motility and secretion enhancing the digestive response while simultaneously contributing to the enjoyment of food.[9]

However, TRP channels are not only expressed by enteric neurons or sensory cells, but also by cells of the transporting epithelium. Thus, a role for apical TRPA1 channels has been proposed in the mediation of prostaglandin signalling leading to anion secretion.[10-12] So far, a direct role in cation absorption has only emerged for TRPV5 and TRPV6 as major pathways mediating the uptake of Ca^{2+} by the intestine and the kidney, and for TRPM6 as the epithelial Mg^{2+} channel, with a more ubiquitous role in cellular Mg^{2+} homeostasis played by TRPM7.[13]

There are some indications that further channels from the TRP family may be directly involved in the transport of cations. Our own interest in TRP channels was triggered when searching for candidate genes that mediate the uptake of cations from the forestomach of cattle and sheep. Having evolved from the oesophagus, forestomach epithelia show marked differences to those found in monogastric species. For example, all attempts to demonstrate the expression of classical epithelial calcium channels TRPV5 or TRPV6 in sheep or cattle rumen were futile,[14,15] despite the fact that over 50% of the formidable total gastrointestinal calcium absorption of these milk-producing mammals occurs via the forestomachs.[16,17] Another striking difference is that Na^+ transport across the rumen cannot be stimulated by aldosterone in vivo,[18] while in vitro, the micromolar concentrations of amiloride used to block electrogenic uptake of Na^+ via epithelial sodium channels (ENaC) are ineffective.[19] A similar lack of amiloride-sensitive ENaC channels has been described in the caecum of rabbits and rats,[20,21] in the colon of Xenopus frogs[22] and the omasum.[23] Instead, all of these tissues express non-selective channels for the transcellular uptake of Na^+ and other monovalent cations.[20,22,24,25] A characteristic feature of these conductances is their block by divalent cations.[26-28] In the case of the ruminal epithelium, considerable evidence points towards the involvement of TRPV3 channels, with participation of other TRP channels likely. The low selectivity of the pore region of TRPV3 allows permeation not only of Ca^{2+}, but also of K^+, Na^+ and other cations such as NH_4^+.[14,29,30] Given the notorious promiscuity of many members of the TRP channel family,[27] these results are not surprising.

The question thus naturally arises whether TRP channels expressed by epithelia of monogastric species might also play a role in the uptake of cations in general, and of the much-neglected metabolite NH_4^+ in particular. Large quantities of NH_4^+ are produced from fermentational and enzymatic degradation of nitrogenous compounds in the intestinal tract of humans or farm animals.[31,32] In principle, this NH_4^+ can be utilized by microbiota for the formation of protein that can either be utilized by the host directly or re-enter the food chain after excretion. In practice, large quantities of toxic NH_4^+ are absorbed and have to be detoxified by the liver, requiring copious amounts of energy. The major product is urea, which cannot be broken up by mammalian enzymes so that large quantities must be renally excreted. Excreted urea is then rapidly degraded to nitrogenous compounds that drive both eutrophication of surface waters and global warming.[32] In livestock, the absorption of NH_4^+ from the gut thus leads to a dramatic waste of protein and energy with an environmental fall-out that can only be considered as catastrophic. In human patients with hepatic disease, absorption of ammonia into blood contributes to encephalopathy with ultimately lethal consequences.[33]

Classically, uptake of ammonia from the gut was thought to occur via simple diffusion of the uncharged form, NH_3, across the lipid membrane surrounding the cell.[34] However, NH_3 is in fact a highly polar molecule, and lipid diffusion does not play a major role in transport across biological preparations. Instead, a role for AMT/Rh proteins[35] and aquaporins[36] has clearly emerged. Current models suggest that these proteins catalyse the deprotonation of NH_4^+, allowing NH_3 to permeate a protein pore,[35,37,38] resulting in a rapid and pH-independent net uptake of NH_3 via an electroneutral process, leading to cytosolic alkalinization. Apart from this pathway, in some preparations, there is clear evidence supporting electrogenic uptake primarily in the protonated form as NH_4^+ with acidification of the cytosol. This may involve bona fide K^+-channels,[39] but also non-selective cation channels, as has repeatedly been shown for Xenopus oocytes,[30,40] but also for epithelia from the rumen.[14,31] There is also evidence for

an electrogenic uptake pathway for NH_4^+ by the caecum of pigs.[41] The low selectivity of many TRPV channels[27] makes them prime candidates for the permeation of NH_4^+, as has been directly shown for the bovine TRPV3 via patch clamp measurements.[29,30]

Despite the importance of the pig both as a farm animal and as an experimental model for humans, very little is currently known about the distribution and function of TRP channels in gastrointestinal epithelia of this species and almost nothing about the absorption of NH_4^+. Based on our previous studies of the rumen, the current study investigated the semi-quantitative distribution of mRNA encoding for a selection of TRP channels along the porcine gastrointestinal tract. In a further step, we investigated the expression of two non-selective members (TRPV3 and TRPV4) on the protein level via Western blot and immunohistochemistry. In a final step, evidence for a possible functional participation of these two candidate proteins in the transport of monovalent cations was investigated via Ussing chamber measurements.

2 | RESULTS

2.1 | PCR

To screen for the presence of selected members of the TRP channel family in the porcine gastrointestinal tract, tissues from different segments (stomach (fundus and cardia), duodenum, middle jejunum, ileum, caecum and middle colon) of 4 different pigs of ~10 weeks killed within an in-house study (subsequently referred to as "T") were examined semi-quantitatively via qPCR (Table 1). Expression was investigated both in the stripped epithelium (containing residual submucosa) and in the muscular layers of the respective sections and mRNA levels were compared to the reference genes YWHAZ, GAPDH and ACTB and scaled to the average value of the samples. Relative to these genes, significantly different expression levels were found for the various tissues (Figure 1).

Signals corresponding to mRNA for the Mg^{2+} conducting channels TRPM6 and TRPM7 were found throughout the

TABLE 1 Amplicon length and primer sequences of the target genes

Gene	Length (bp)	A_t	Primer	Accession no.
TRPV1 fwd	107	59°C	ACCTTGTTTTCTTGTTCGGCT	XM_013981216.2
TRPV1 rev			AGACAAGCCCTCGACACTTG	
TRPV2 fwd	164	59°C	CAAGTGGTACCTGCCCCTG	XM_021067918.1
TRPV2 rev			AGAGGAAGACGAGGTAGACC	
TRPV3 fwd	202	59°C	ATGCTCATTGCCCTGATGGGAGAGAC	XM_005669116.3
TRPV3 rev			ACTTCACCTCGTTGATCCGCAGACAC	
TRPV6 fwd	291	59°C	CTTCTTTGGACAGACCATCC	XM_021078898.1
TRPV6 rev			ATGATAAAGAAAGCTGAGGCA	
TRPV4 fwd	194	60°C	CGCTCTATGACCTCTCCTCC	XM_021071776.1
TRPV4 rev			GGCACACAGATAGGAGACCA	
TRPM6 fwd	214	59°C	TGTAGCTGTGAGGAACGTAT	XM_021064975.1
TRPM6 rev			GGAGAGCCTTATCCTCTTGT	
TRPM7 fwd	254	59°C	GTTTTGCCTCCACCACTTAT	XM_013993003.1
TRPM7 rev			ATCTGAATGCACATCTGCTC	
TRPM8 fwd	183	59°C	TCTCGAAAGTTCCCACCTGT	XM_021074741.1
TRPM8 rev			TCATCATTGGCTAGGTCCAGC	
ACTB fwd	127	60°C	GACATCAAGGAGAAGCTGTG	XM_003124280.5
ACTB rev			CGTTGCCGATGGTGATG	
ACTB probe			CTGGACTTCGAGCAGGAGATGGCC	
YWHAZ fwd	113	60°C	AAGAGTCATACAAAGACAGCAC	XM_021088756.1
YWHAZ rev			ATTTTCCCCTCCTTCTCCTG	
YWHAZ probe			ATCGGATACCCAAGGAGATGAAGCTGAA	
GAPDH fwd	117	60°C	CAAGAAGGTGGTGAAGCAG	NM_001206359.1
GAPDH rev			GCATCAAAAGTGGAAGAGTGAG	
GAPDH probe			TGAGGACCAGGTTGTGTCCTGTGACTTCAA	

Abbreviation: A_t, annealing temperature.

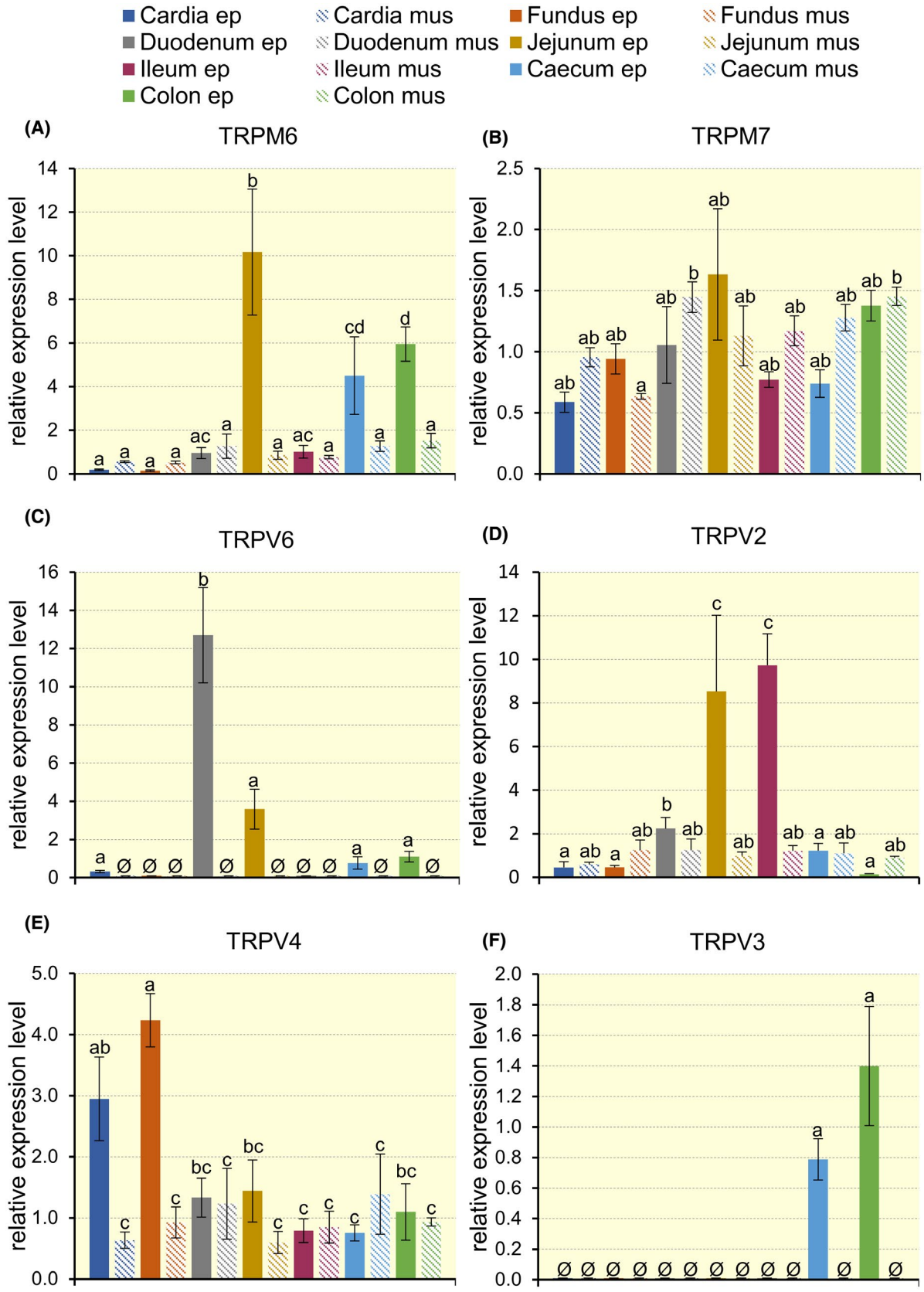

FIGURE 1 Semi-quantitative comparison of the mRNA expression of different gastrointestinal tissues (cardia and fundus of stomach, duodenum, jejunum, ileum, caecum, colon) from the stripped epithelium ("ep", containing residual submucosa) or muscle layer ("mus") of 4 pigs. The expression was normalized to the reference genes YWHAZ, GAPDH and ACTB and scaled to the average value of the samples. Bars that do not share a letter are significantly different ($P \leq .05$). Data are given as means ± SEM. Ø indicates when expression was below the detection level. TRPV1 and TRPM8 could not be detected in any segment

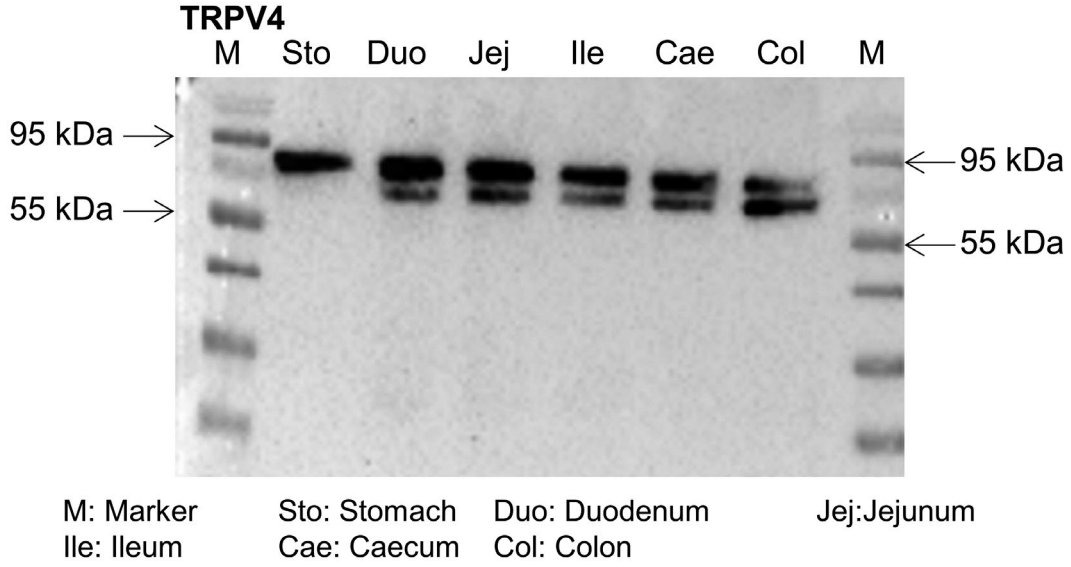

FIGURE 2 Western blot of protein from different porcine gastrointestinal tissues, stained by a TRPV4 antibody (PA5-41066). In all tissues a band at the expected level of ~90 kDa was visible. With the exception of the stomach, another band was visible at ~80 kDa

gastrointestinal tract, with expression of TRPM6 highest in the mucosal layers of the jejunum, followed by the caecum and colon (Figure 1A). Smaller amounts of TRPM6 mRNA were found in the remaining mucosa and in the muscular layers of all segments tested. Conversely, the expression of TRPM7 was high throughout and similar in muscular tissue and in the mucosa ($P = .2$; Figure 1B).

As expected, mRNA expression of TRPV6, which is a very well-established major uptake pathway for Ca^{2+} by the intestine, was highest in the duodenum. Lower levels were found in the jejunum, caecum, colon and cardia of the stomach. Interestingly, no signals for mRNA encoding for TRPV6 could be detected in ileum and fundus of the stomach or in tissue from the muscular layers (Figure 1C).

TRPV2 mRNA expression was highest in the mucosal layers of the small intestine, especially jejunum and ileum. Low mRNA expression was detected in the mucosal tissues of the stomach and caecum, as well as in the muscle layers. In the colon, signals were near the detection limit (Figure 1D).

An expression of mRNA for TRPV4 was found in both mucosal and muscular layers of all tissues studied, with the strongest expression occurring in the mucosa of the stomach (cardia and fundus; Figure 1E).

Messenger RNA encoding for TRPV3, the channel that has been proposed to serve as one pathway for the uptake of cations including NH_4^+ from the rumen,[14,29,30] could only be found in the mucosa of the caecum and colon, which are interestingly also the gastrointestinal organs with the highest levels of luminal NH_4^+ (Figure 1F and Table 2). No signals could be amplified in any of the other segments or in the muscular layers. However, it should be mentioned that the primer used in these experiments was only suitable for the amplification of the full-length 90 kDa TRPV3 protein. Apart from this long variant of TRPV3, a shorter variant of ~60 kDa has been described in mice[42] (XP_006533411.1) and in bovines[30] (AAI46079.1). We therefore designed several primers targeting segments common to both variants and which theoretically should capture them both (see Supporting Table A). Despite successful amplification by gel electrophoresis and subsequent sequencing, these 3 primers were not suitable for qPCR as they produced at least two melting curves. Only a 4th primer pair that binds to the long but not to the short variant was applicable for qPCR and produced the desired unitary melting curve. In retrospect, the failure of the other primers may indicate that mRNA of both variants might have been present in the tissue samples. The qPCR results thus suggest expression of the full-length TRPV3 mRNA sequence by caecum and colon, but neither confirm nor rule out the possibility that a further variant is expressed by these or other segments of the gastrointestinal tract.

Although control tissues tested positive (liver or medulla oblongata), no signals for TRPV1 or TRPM8 could be found in any of the porcine gastrointestinal sections in either the mucosa or the muscular layers. It should also be mentioned that despite numerous tries, we were unable to establish a porcine primer for TRPV5 that was clearly separate from TRPV6.

2.2 | Immunochemical detection of TRPV3 and TRPV4 via Western blot

In a further step, we attempted to investigate the expression of the non-selective cation channels TRPV3 and TRPV4 on the level of the protein. Since commercial antibodies for use in the porcine species are not available, we used epitope

screening to select suitable antibodies directed against a common sequence.

Staining for TRPV4 (directed against the epitope [AA 719-768]) was found in all sections at the predicted height of ~90 kDa. In all tissues but the stomach, a further band was observed at ~80 kDa that may reflect either a degradation product or a variant (Figure 2).

For staining of the porcine TRPV3, we used an antibody (ABIN863127) produced for the human, mouse and rat TRPV3 and which we previously established for use in the bovine species.[30] With the exception of a single E → V switch, the target epitope of this antibody (AA 458-474) is identical in pigs and bovines and interacts with both the large 797a (~90 kDa) and the smaller 526a (~60 kDa) variant of the bovine TRPV3 (see Supporting Table A and Ref. [30]). In porcine tissues, a weak band at 90 kDa could be detected in 2 of 9 blots of porcine colon (Figure 3A), while a stronger band at ~60 kDa was detected in all blots and all 6 intestinal sections from stomach to colon and in porcine skin (Figure 3A,B). Control samples of mouse skin showed a similar staining pattern (data not shown), in line with the reported long (NP_001357935.1) and short (XP_006533411.1) murine protein sequences. In samples with high expression, a doubling of the band could be observed, possibly reflecting degradation or phosphorylation.

2.3 | Confocal laser microscopy

To localize the expression pattern of these proteins, native tissues ("T") were stained with both TRPV3 and TRPV4 antibodies and investigated via fluorescent imaging, with

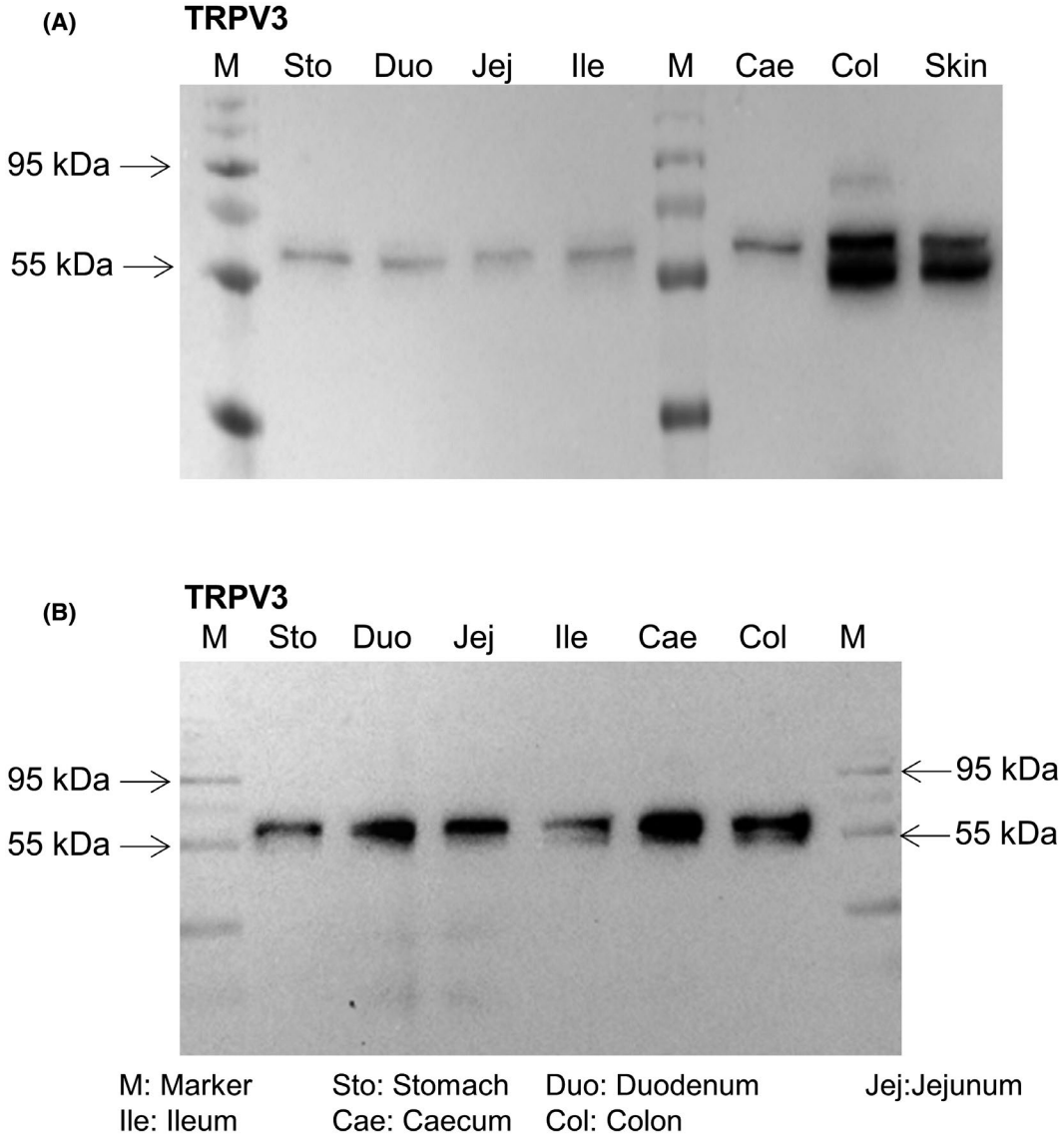

FIGURE 3 Western blot of protein from different porcine gastrointestinal tissues and from porcine skin, stained by a TRPV3 antibody (ABIN863127). A, In 2 of 9 blots a weak band at ~90 kDa was found in the colon. A and B, In all tissues a distinct band at ~60 kDa was found, sometimes doubled (see text for details)

DAPI used to mark the cell nuclei. Light settings were optimized for each preparation using standard software (ZEN, Zeiss, Jena, Germany). The same microscope settings were used to study the secondary antibody controls, which were routinely fixed onto the same slide. These controls only showed staining for DAPI. Otherwise, we made no attempt to work with fixed gain settings and the staining intensities seen in Figure 4 were optimized for each slide and do not allow a quantitative comparison of protein expression in the various segments.

In epithelia from the stomach, staining was observed along the gastric pits and in the surface epithelial cells. In the duodenum, staining of the epithelial cells was somewhat diffuse. In all more distal segments, staining was clearly strongest in the apical membrane of the cells facing the lumen (Figure 4). The staining of areas in the crypts or in the cytosol was often only subtle or not detectable.

2.4 | pH and NH_4^+ in ingesta

In order to get an overview of the physiological scenario, the ammonium concentrations and the pH of the ingesta of 4 pigs of ~10 weeks ("T") were examined in various intestinal sections, namely stomach, duodenum, middle jejunum, ileum, caecum and middle colon (Table 2). As expected, the pH value was found to rise steadily in the aboral sections of the small intestine, reflecting pancreatic secretion and chloride-bicarbonate exchange, and subsequently decreased in the fermenting sections of the caecum and colon, where resident microbiota produce short chain fatty acids from organic matter.[43,44] The ammonium concentrations remained at a relatively low level in the stomach and the small intestine, increasing substantially in the fermentative parts of the gut with microbial degradation of nitrogenous compounds.

TABLE 2 pH and ammonium content of gastrointestinal ingesta

		pH	NH_4^+ ($mmol \cdot L^{-1}$)
Tissue	**N**	**Mean ± SEM**	**Mean ± SEM**
Stomach	4	3.37 ± 0.34^a	2.78 ± 1.75^a
Duodenum	4	4.49 ± 0.51^a	1.83 ± 0.64^a
Jejunum	4	6.34 ± 0.12^b	3.13 ± 0.80^a
Ileum	4	6.39 ± 0.28^b	3.47 ± 0.66^a
Caecum	4	5.68 ± 0.13^b	7.98 ± 3.62^{ab}
Colon	4	5.92 ± 0.17^b	16.52 ± 5.47^b

Note: Values that do not share a letter in the superscript are significantly different ($P \leq .05$).

2.5 | Ussing chamber measurements

2.5.1 | Removal of mucosal Ca^{2+} and Mg^{2+}

A characteristic feature of non-selective cation channels of the TRP channel family is their negative interaction with divalent cations.[26-29] For screening purposes, we investigated the effect of a removal of divalent cations on the mucosal side of stripped intestinal mucosa ("T") in a custom-built, continuously perfused Ussing chamber, allowing artefact free solution changes.[14] Experiments were performed under symmetrical conditions with solutions containing identical amounts of NaCl on the mucosal and the serosal side (see Supporting Table B). A clear rise in I_{sc} was observed in 5 of 8 jejunal and 2 of 2 colonic epithelia tested when the divalent cations Ca^{2+} and Mg^{2+} in the mucosal standard NaCl Ringer buffer were replaced by 5 $mmol \cdot L^{-1}$ EDTA ($ØCa^{2+}$ $ØMg^{2+}$, Figure 5A), reflecting transport of Na^+ from the mucosal to the serosal side. To evaluate the isolated effect of a removal of Ca^{2+} more systematically, the effects were investigated in conventional Ussing chambers. In 17 colonic tissues from 4 different pigs ("T"), Ca^{2+} in the mucosal solution was replaced by EGTA, again resulting in a significant increase in I_{sc} by 0.18 ± 0.06 $\mu Eq \cdot cm^{-2} \cdot h^{-1}$. Simultaneously, G_t increased significantly. Control tissues that were incubated in parallel showed no response (N/n = 4/23; See Table 3).

2.5.2 | Removal of mucosal and serosal Ca^{2+}

Since a "calcium-switch" classically also opens tight junction proteins,[45] we conducted further experiments in which the buffer solution on both the serosal and the mucosal side of the epithelium was replaced by nominally Ca^{2+} free solution (Supporting Table B, "Ca^{2+} free"). As expected, a rise in G_t could again be seen, but no significant changes in I_{sc} emerged (Table 3).

2.5.3 | Effect of mucosal NH_4^+

In subsequent screening experiments ("T") in the perfused Ussing chamber, the effect of NH_4^+ on currents was tested (for solutions, see Supporting Table C). A clear and concentration-dependent increase in the I_{sc} could be observed after application of mucosal NH_4^+ in 7 of 8 tissues tested (from ileum (5), jejunum (1 of 2) and colon (1); Figure 5B). In subsequent experiments, both Ca^{2+} and Mg^{2+} were removed from the mucosal NH_4Cl solution, resulting in a rapid rise in I_{sc} with return to the original level after replacement in all tissues tested (2 from caecum, 4 from the colon and 3 from the jejunum; Figure 5C).

The effect of NH_4^+ on I_{sc} and G_t was subsequently systematically investigated in parallel in conventional Ussing chambers in different tissues from 4 pigs from a commercial slaughterhouse ("S"). After incubation in an NaCl Ringer buffer additionally containing 40 mmol·L^{-1} N-methyl-D-glucamine ($NMDG^+$), this large cation was replaced by an equimolar amount of NH_4^+ on the mucosal side of the tissue in the Ussing chamber. This intervention led to significant increases in I_{sc} and G_t in all 6 tissues of the gastrointestinal tract (Figure 6) as to be expected if ammonia is transported as NH_4^+. Note that the increase in I_{sc} could not have been caused by a swelling of cells with reduction of paracellular leak flow, since G_t also increased. Subsequently, the divalent cations in the mucosal NH_4Cl buffer were replaced by 5 mmol·L^{-1} EDTA. This resulted in a further increase in I_{sc} that was significant in all tissues. G_t rose significantly in all tissues but the jejunum and the caecum. These effects were largely reversible after washout. The changes in I_{sc} and G_t induced by the solution changes (ΔI_{sc} and ΔG_t) were numerically largest in the colon and lowest in the stomach (Table 4).

Since it appears possible that the ammonia-induced rise in I_{sc} and G_t was caused by induction of an anion conductance (eg via changes in cytosolic pH), we performed additional experiments using solutions essentially as above (Supporting Table C), but in which 110 mmol·L^{-1} chloride was replaced by gluconate. As before, the solutions were bicarbonate free. After equilibration in bilateral Na-gluconate solution, 20 mmol·L^{-1} $NMDG^+$ was replaced by an equimolar amount of NH_4^+.

In colonic preparations (N/n = 2/14, "S"), I_{sc} rose from 1.04 ± 0.18 to 2.20 ± 0.23 μeq·cm^{-2}·h^{-1} after addition of 20 mmol·L^{-1} NH_4^+ ($P < .001$), or by about half of what was observed in 40 mmol·L^{-1} NH_4Cl solution (see Figure 6). G_t rose from 14.5 ± 1.08 to 18.7 ± 2.05 mS·cm^{-2} ($P < .001$). In the jejunum (N/n = 2/14, "S"), I_{sc} rose from 0.29 ± 0.044 to 1.39 ± 0.15 μeq·cm^{-2}·h^{-1} and G_t from 16.7 ± 1.46 to 21.5 ± 2.14 mS·cm^{-2} (both $P < .001$).

Further experiments were performed using tissues from piglets ("T") in bicarbonate Ringer gassed with carbogen.[14] In both colon and jejunum, replacement of 20 mmol·L^{-1} $NMDG^+$ by NH_4^+ induced a significant rise in I_{sc} and G_t (both $P < .001$), the magnitude of which did not depend on

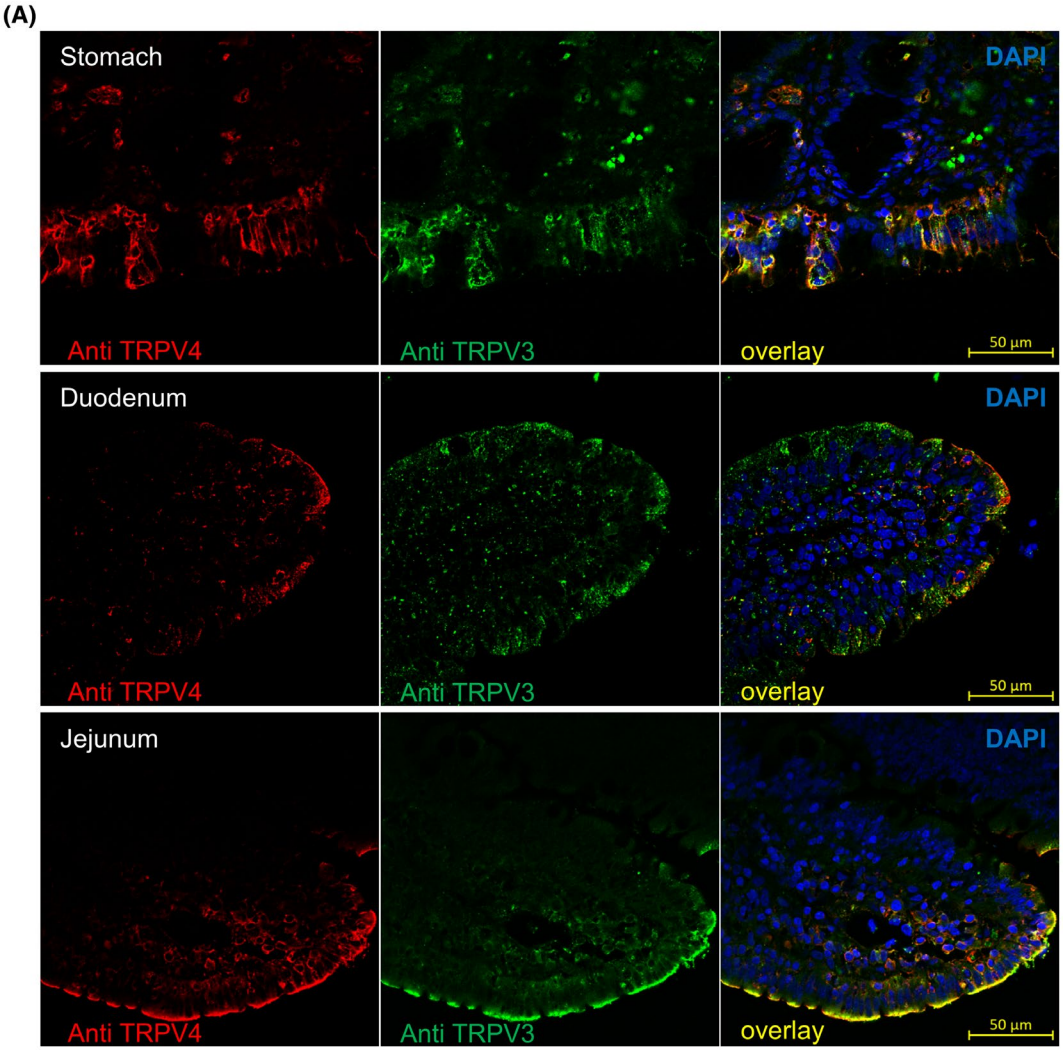

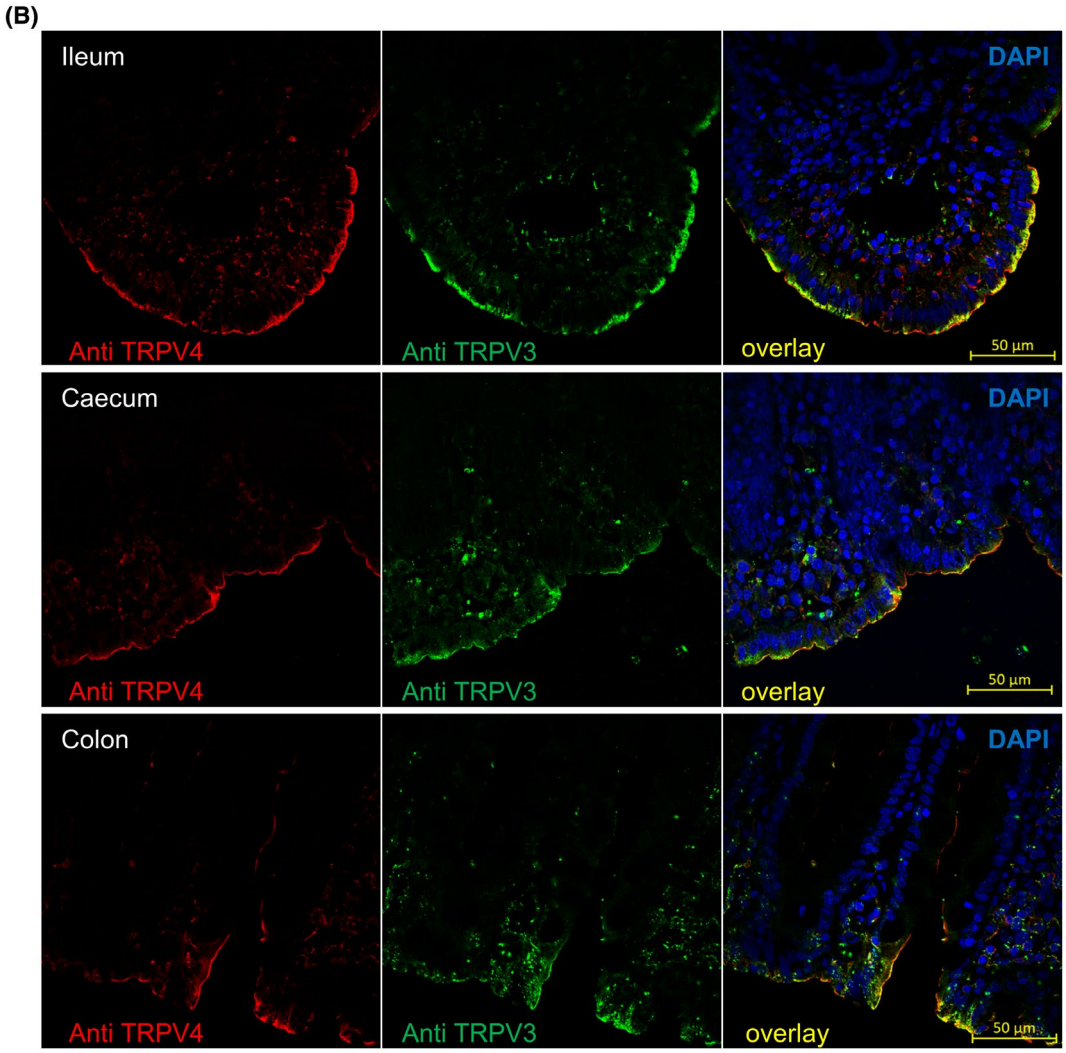

FIGURE 4 Immunohistological staining of gastrointestinal tissues of pigs using primary and secondary antibodies to mark TRPV3 (green, ABIN863127, Alexa Fluor 488) and TRPV4 (red, PA5-41066, Alexa Fluor 594). The merged pictures also show a staining for cell nuclei in blue (DAPI). A, Staining of stomach, duodenum and jejunum. The staining of TRPV3 and TRPV4 in the stomach occurred mainly in gastric pits and superficial epithelial cells. In the duodenum the staining was rather diffuse, whereas in the other tissues mainly the apical membrane was stained. Staining in the crypts was often only subtly present. B, Ileum, caecum and colon, stained as in a. Staining was most pronounced in the apical membrane

whether chloride was present (colon N/n = 3/17, jejunum N/n = 3/17) or replaced by gluconate (N/n = 3/16 and 3/18, respectively).

2.5.4 | TRP channel agonists

To test for functional involvement of TRP channels in electrogenic transport of ions across the colon, we investigated the effect of two TRP channel agonists, GSK106790A and 2-APB in Ussing chambers. A symmetrical arrangement with standard NaCl Ringer on both sides of the stripped mucosa ("T") was used (Supporting Table B). After mucosal addition, both agonists induced a steady increase in G_t over 15 minutes (P = .004 for GSK106790A; N/n = 3/6 versus control [Ethanol]; N/n = 3/6 and P = .002 for 2-APB, N/n = 3/6; Figure 7B,D). The short circuit current I_{sc} dropped rapidly in response to both agonists (P = .009 for GSK106790A, and P = .002 for 2-APB, both versus control; Figure 7A,C). The drops in I_{sc} (ΔI_{sc}) were -0.24 ± 0.06 µeq·cm^{-2}·h^{-1} (2-APB) and -0.089 ± 0.016 µeq·cm^{-2}·h^{-1} (GSK106790A), with corresponding increases in G_t (ΔG_t) of 8.56 ± 1.15 and 1.63 ± 0.44 mS·cm^{-2}.

Following the agonist-induced drop in I_{sc}, the current recovered and stabilized at a level clearly above zero after about five minutes (Figure 7). Conversely, G_t continued to rise in the 15-minute interval studied. This may mean that a paracellular pathway opened, or that a transcellular pathway opened, or, most likely, that both opened. In any case, the stabilization of I_{sc} could only occur because active, transcellular

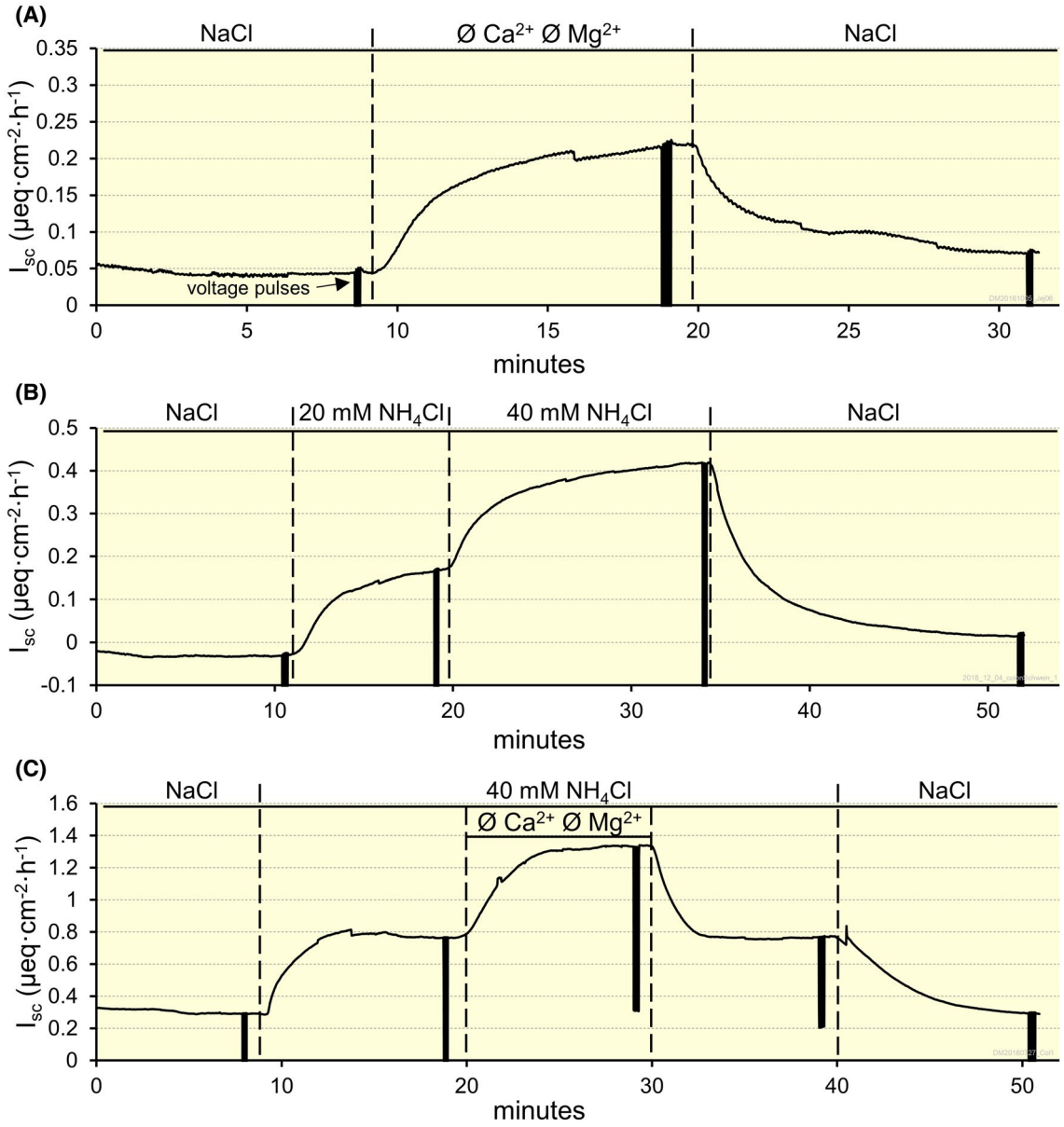

FIGURE 5 Effect of various solution changes on the mucosal side of intestinal epithelium in a modified continuously perfused Ussing chamber. The individual graphs represent original recordings from the jejunum (a) or the colon (b and c), with similar effects observed in the ileum and caecum. Before each solution change, voltage pulses were applied in order to determine epithelial conductance (vertical lines, marked with an arrow (→) in a). A, After replacing the divalent ions Ca^{2+} and Mg^{2+} with EDTA in a standard NaCl solution on the mucosal side, an immediate increase in I_{sc} could be observed. Serosally, standard NaCl Ringer solution was used. B, After the replacement of $NMDG^{+}$ by 20 or 40 mmmol·L^{-1} NH_4^{+} on the mucosal side, a distinct increase in I_{sc} could be observed. C, The change to mucosal 40 mmmol·L^{-1} NH_4^{+} increased the I_{sc}, which could be further increased by eliminating divalent ions. In all experiments the I_{sc} returned to normal values when the standard solution was used

transport increased, compensating for any loss in paracellular resistance. The simplest explanation for this is that 2-APB and GSK106790A directly opened TRP channels in the apical membrane.

3 | DISCUSSION

Despite the importance of the pig as a model for humans in biomedical research, surprisingly little is known about the expression of TRP channels by the porcine intestinal tract. This study attempted to begin to fill this gap by using qPCR to detect expression of a selection of TRP channels (TRPV6, TRPM6, TRPM7, TRPM8, TRPV2 and TRPV1) in addition to TRPV3 and TRPV4, with the expression of the latter additionally studied on the level of the protein using Western blots and immunohistochemistry. Finally, Ussing chamber measurements were utilized in order to assess the possible contributions of these channels to the transport of the monovalent cations Na^{+} and NH_4^{+}.

TABLE 3 Overview of the effect of calcium-free Ringer solutions on I_{sc} and G_t in the colon

	1. Mucosal side only Ca^{2+}-switch[a]		2. Mucosal and serosal Ca^{2+}-switch[b]		Comparison 1 vs 2
	N/n	Mean ± SEM	N/n	Mean ± SEM	*P*-value
ΔI_{sc} ($\mu eq \cdot cm^{-2} \cdot h^{-1}$)					
Ca^{2+}-switch	4/17	0.18 ± 0.06	5/14	0.008 ± 0.034	$P = .022$
Control	4/23	0.002 ± 0.012	5/29	−0.007 ± 0.009	n.s.
Switch vs control		$P = .029$		n.s.	
ΔG_t ($mS \cdot cm^{-2}$)					
Ca^{2+-}switch	4/17	4.70 ± 0.85	5/14	1.05 ± 0.35	$P < .001$
Control	4/23	−0.41 ± 0.13	5/29	−0.15 ± 0.19	n.s.
Switch vs control		$P < .001$		$P < .001$	

Note: The delta (Δ) was determined from the value immediately before the change to calcium-free Ringer to the value 15 min afterwards. Control tissues were exposed to the same standard Ringer solution throughout, although a sham solution change was performed.

[a]Mucosal solution was replaced by calcium-free Ringer with 1 $mmol \cdot L^{-1}$ EGTA.

[b]Mucosal and serosal solutions replaced by nominally calcium-free Ringer.

As mentioned, our interest in TRPV3 was sparked when searching for a candidate gene for the divalent-sensitive non-selective cation conductance of forestomach epithelia of ruminants.[23-25] Molecular biological approaches in conjunction with functional studies on native tissues, native cells and overexpressing systems confirm involvement of TRPV3 in the efflux of Na^+, NH_4^+ and Ca^{2+} from the rumen[14,29,30] with possible additional participation of other TRP channels. Similar divalent-sensitive, non-selective conductances for monovalent cations were first observed in frog and toad skin,[46,47] in the colon of Xenopus frogs[22] and in rabbit caecum.[20] Intriguingly, results of a very recent functional study of the rat caecum also point towards an involvement of non-selective TRP channels in ion transport across this segment of the gut.[21] Since the molecular identities of these divalent-sensitive conductances have remained obscure, a closer look appears merited.

Divalent cations permeate non-selective TRP channels by binding to negatively charged amino acid residues in the ion-conducting pore, which inhibits the permeation of monovalent cations with lower binding affinity (such as Na^+, Cs^+ or K^+).[27] Conversely, removal of divalent cations will result in an increase of current carried by the monovalent cation.[26-28] In line with this, a removal of divalent cations from the mucosal solution of porcine intestinal tissues incubated in Ussing chambers resulted in strong, reversible currents (Figure 5 and Table 3). Since experiments were carried out with no electrochemical gradient for NaCl present, two explanations for this rise in I_{sc} are possible: (a) an increase in current via activation of a transcellular pathway and (b) a reduction of leak backflow via tightening of the paracellular pathway. The possibility (b) can be ruled out since G_t increased significantly in all tissues studied, which is very much in line with the classical effects of a removal of Ca^{2+} on paracellular tight junction proteins.[45] Most likely, an apical cation channel opened, allowing more Na^+ to enter the cytosol and to be basolaterally driven out via the Na^+-pump. In the case of mucosal removal of divalent cations, I_{sc} increased strongly. In the case of bilateral Ca^{2+} removal, the I_{sc} did not drop despite the strong rise in G_t. In both cases, increased active transcellular transport compensated for the decrease in paracellular resistance.

In subsequent experiments, it could be shown that as in the rumen, application of mucosal NH_4^+ resulted in fully reversible, concentration-dependent and divalent-sensitive currents that tended to be highest in those compartments that physiologically have the highest concentrations of NH_4^+ (Figures 5 and 6; Tables 2 and 4).

Any involvement of chloride or bicarbonate in the NH_4^+-induced current was small since NH_4^+ induced currents of similar magnitude in gluconate solutions. However, it appears likely that pH effects contributed to the effects observed. Thus, many transport proteins, including TRPV3, are altered by changes in cytosolic pH.[48] On the other hand, the fact that the NH_4^+-induced I_{sc} could be increased by the removal of divalent cations is hardly explicable via a pH-sensitive mechanism.

It is also highly probable that the opening of tight junction proteins contributed to the rises in G_t. It appears possible that channel-like tight junctions with selectivity for NH_4^+ over Na^+ might explain the doubling of I_{sc} by replacement of as little as 20 $mmol \cdot L^{-1}$ $NMDG^+$ with NH_4^+ in a high NaCl background.[49] However, paracellular transport cannot explain the I_{sc} increase in bilateral NaCl Ringer solution after removal of divalents, which requires an active pumping mechanism. Since TRPV3 is clearly expressed by the apical membrane of the tissues studied (Figure 4), and since a divalent-sensitive permeability with $P(Na^+) < P(NH_4^+)$ has been shown directly in patch clamp experiments on cells

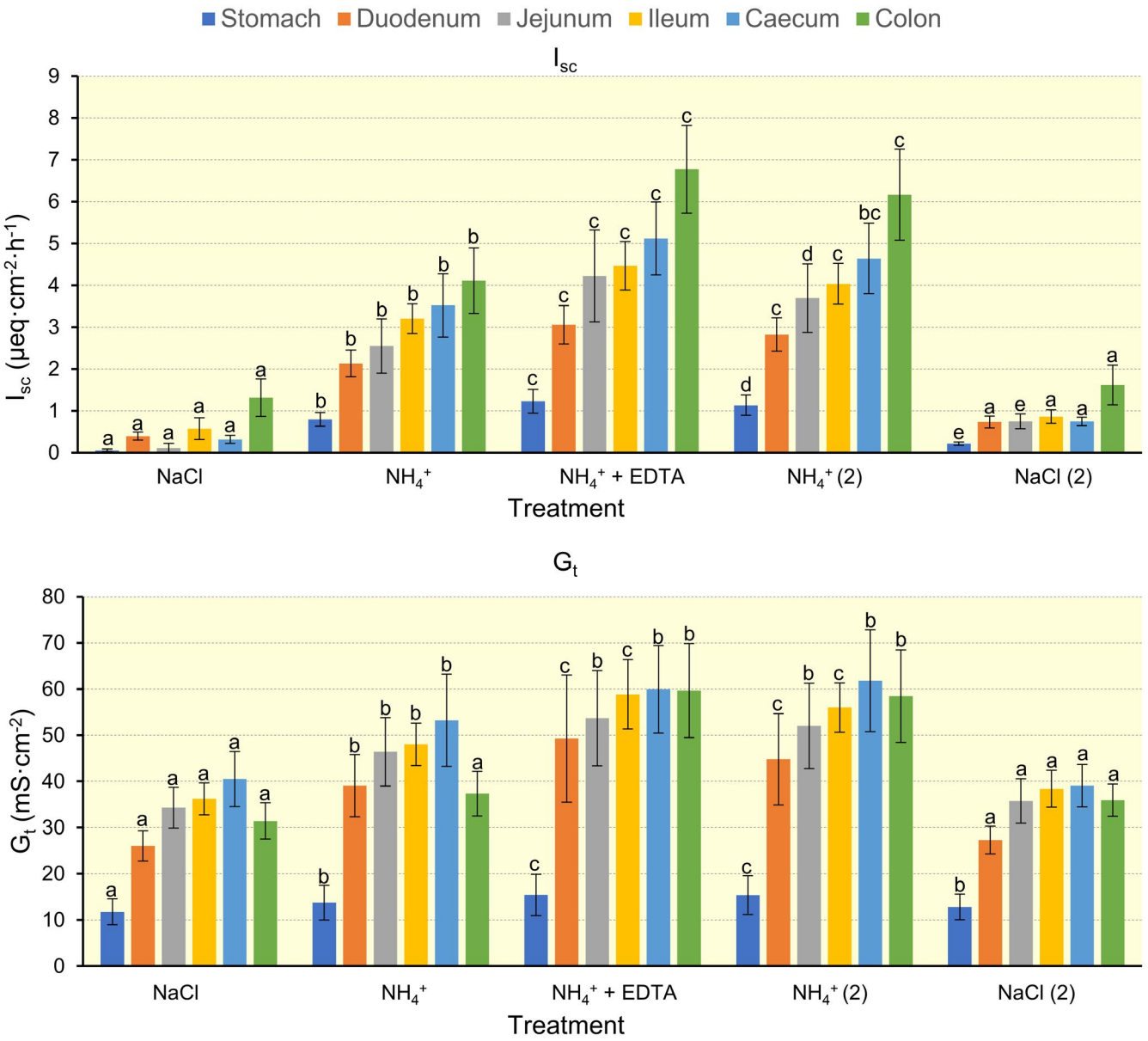

FIGURE 6 Effect of solution changes on the I_{sc} and G_t in different gastrointestinal tissues in the standard Ussing chamber. The solution change from NaCl to a 40 mmmol·L^{-1} NH_4^+ solution on the mucosal side caused an increase in I_{sc} and G_t in all tissues. After changing to a NH_4^+ solution, where Ca^{2+} and Mg^{2+} were replaced by EDTA, I_{sc} and G_t increased further. After return to the Ca^{2+} and Mg^{2+} containing NH_4^+ solution (NH_4^+ (2)) or to a NaCl (NaCl (2)) solution, a decrease to original values could be observed. Different letters indicate significant differences between solutions within a tissue type ($P \leq .05$). Data are given as means ± SEM. For differences between tissues, see Table 4

overexpressing TRPV3,[29,30] at least part of the effects should be attributable to TRPV3, with additional contributions by other pathways probable.

Functional expression of TRP channels is supported by electrophysiological effects of the TRP channel agonists GSK1016790A and 2-APB on colonic mucosa incubated in NaCl Ringer. Both agonists induced an immediate, steep drop in transepithelial resistance across the tissue that developed in the first minute after application and continued to rise (Figure 7). In contrast, the short circuit current I_{sc}, which reflects transcellular transport in this configuration, only dropped initially and then reached a new steady-state level which was clearly above zero. This means that a transcellular pathway must have been activated which eventually compensated for whatever rise in paracellular conductance continued to occur.[49]

GSK1016790A is currently thought to be selective for TRPV4. Unfortunately, there are currently no commercially available specific agonists or antagonists for TRPV3,[50] but if TRPV3 is functionally expressed, it should be activated by 2-APB. 2-APB is a classical TRP channel agonist that activates TRPV3, but also TRPV1, TRPV2 and TRPA1, but not TRPV4, TRPV5 or TRPV6,[51,52] with inhibitory effects on TRPC4, TRPC5, TRPC6, TRPM8 and TRPP1.[53] Note

TABLE 4 Overview of the changes (Δ) of I_{sc} (μeq·cm^{-2}·h^{-1}) and G_t (mS·cm^{-2}) 15 min after a solution change

ΔI_{sc} (μeq·cm^{-2}·h^{-1}) ± SEM				
	NaCl-NH_4Cl	**NH_4Cl-EDTA**	**EDTA-NH_4Cl**	**NH_4Cl-NaCl**
Tissue (N/n)	**ΔI_{sc}**	**ΔI_{sc}**	**ΔI_{sc}**	**ΔI_{sc}**
Stomach (4/8)	0.74 ± 0.18^{a}	0.43 ± 0.12^{a}	-0.09 ± 0.04^{a}	-0.92 ± 0.22^{a}
Duodenum (4/7)	1.73 ± 0.27^{ab}	0.93 ± 0.15^{ab}	-0.23 ± 0.07^{a}	-2.09 ± 0.30^{ab}
Jejunum (4/8)	2.44 ± 0.57^{ab}	1.67 ± 0.46^{ab}	-0.53 ± 0.31^{a}	-2.95 ± 0.68^{b}
Ileum (4/8)	2.63 ± 0.23^{b}	1.26 ± 0.35^{ab}	-0.43 ± 0.14^{a}	-3.17 ± 0.36^{b}
Caecum (4/8)	3.20 ± 0.68^{b}	1.60 ± 0.28^{b}	-0.48 ± 0.09^{a}	-3.9 ± 0.76^{b}
Colon (4/6)	2.80 ± 0.51^{b}	2.66 ± 0.71^{b}	-0.61 ± 0.19^{a}	-4.55 ± 0.91^{b}
ΔG_t (mS·cm^{-2}) ± SEM				
	NaCl-NH_4Cl	**NH_4Cl-EDTA**	**EDTA-NH_4Cl**	**NH_4Cl-NaCl**
Tissue (N/n)	**ΔG_t**	**ΔG_t**	**ΔG_t**	**ΔG_t**
Stomach (4/8)	2.00 ± 0.98^{a}	1.67 ± 0.73^{a}	-0.06 ± 0.33^{a}	-2.54 ± 1.55^{a}
Duodenum (4/7)	13.04 ± 5.73^{ab}	10.22 ± 7.93^{ab}	-4.51 ± 4.19^{a}	-17.50 ± 9.22^{ab}
Jejunum (4/8)	12.10 ± 3.12^{ab}	7.30 ± 3.99^{ab}	-1.71 ± 1.64^{a}	-16.25 ± 4.59^{ab}
Ileum (4/8)	11.83 ± 1.77^{b}	10.81 ± 3.96^{ab}	-2.99 ± 2.76^{a}	-17.57 ± 2.38^{b}
Caecum (4/8)	12.76 ± 4.14^{ab}	6.71 ± 2.51^{ab}	1.84 ± 2.13^{a}	-22.72 ± 7.49^{b}
Colon (4/6)	5.95 ± 2.45^{ab}	22.30 ± 9.36^{b}	-1.2 ± 1.76^{a}	-22.52 ± 6.72^{b}

Note: The first column gives ΔI_{sc} and ΔG_t after 40 mmol·L^{-1} $NMDG^+$ in an NaCl Ringer solution were replaced by an equimolar amount of NH_4^+ (NaCl-NH_4Cl). In the following column, Ca^{2+} and Mg^{2+} in the NH_4^+-solution were replaced by EDTA (NH_4Cl-EDTA). The next columns give values for a stepwise return to the original solutions (EDTA-NH_4Cl and NH_4Cl-NaCl). Different superscripts designate significant differences between tissues or within a solution (column; $P \leq .05$). The data are given as means ± SEM. For differences between solutions, see Figure 6.

that in the colon, we were unable to detect mRNA signals for TRPV1 or TRPM8, while levels for TRPV2 were almost below the detection level (Figure 1). Inhibition of TRPC4, TRPC5, TRPC6 or TRPP1 should have led to a drop in Gt, as observed in a recent study of rat caecum.[21] TRPA1, which is apically expressed by colonic epithelia,[11,12] may well have contributed to the response to 2-APB. However, TRPA1 has a high selectivity to Ca^{2+} and follows an Eisenman XI sequence with $P(Na^+) > P(K^+)$,[54] which does not predict a drop in I_{sc}. In line with this, in a recent study of the effects of the TRPA1 agonist cinnamaldehyde on porcine colon, we observed a rise in both I_{sc} and G_t.[12] These changes reflected an opening of TRPA1 with an increase in the conductance of the epithelium to cations, triggering subsequent prostaglandin-mediated secretion of anions. The latter confirms previous findings in rat colon[11] and highlights the established role of TRPA1 in cellular signalling.[8,11]

The effects in Figure 7 (decrease in I_{sc} with concomitant increase in G_t) can be understood if one assumes that 2-APB or GSK primarily activate channel(s) following an Eisenman sequence IV with $P(K^+) > P(Na^+)$, as is the case for TRPV3 and TRPV4.[26,27,30,55] Note that in our experiment, influx of Na^+ is further reduced by the high concentration of extracellular divalent cations, while efflux of K^+ can push obstructing Ca^{2+} or Mg^{2+} out of the external mouth of the pore region.[27] Accordingly, secretion of K^+ should exceed absorption of Na^+, predicting a drop in I_{sc} in conjunction with a drop in the potential across the apical membrane. The increasingly negative apical potential will enhance the driving force for Na^+, until influx of Na^+ and efflux of K^+ are equal. After a certain time, I_{sc} should reach a new steady-state equilibrium, precisely as observed (Figure 7). The rising G_t probably reflects both increases in permeation of Na^+ and K^+ through apical channels and an opening of paracellular tight junctions. On the other hand, the opening of channels may predominate since in studies of colonic or corneal cells, GSK1016790A led to a tightening of the tight junction in studies of colonic or corneal cells (with dropping G_t) and effects were visible only after 24 hours.[56,57]

In a further step, tissues from different segments of the porcine gastrointestinal tract were screened for relevant channels via qPCR. It should be mentioned in passing that establishing primers for the detection of TRP channels not just in the porcine species but also in ruminants has proved to be quite challenging.[14] In contrast to our experience with transporters such as NHE, an exceptionally high number of primers had to be tested before a primer delivered an acceptable melting curve. As emerged when attempting to establish a primer for the short variant of TRPV3, this may reflect the binding to more than one splice variant.

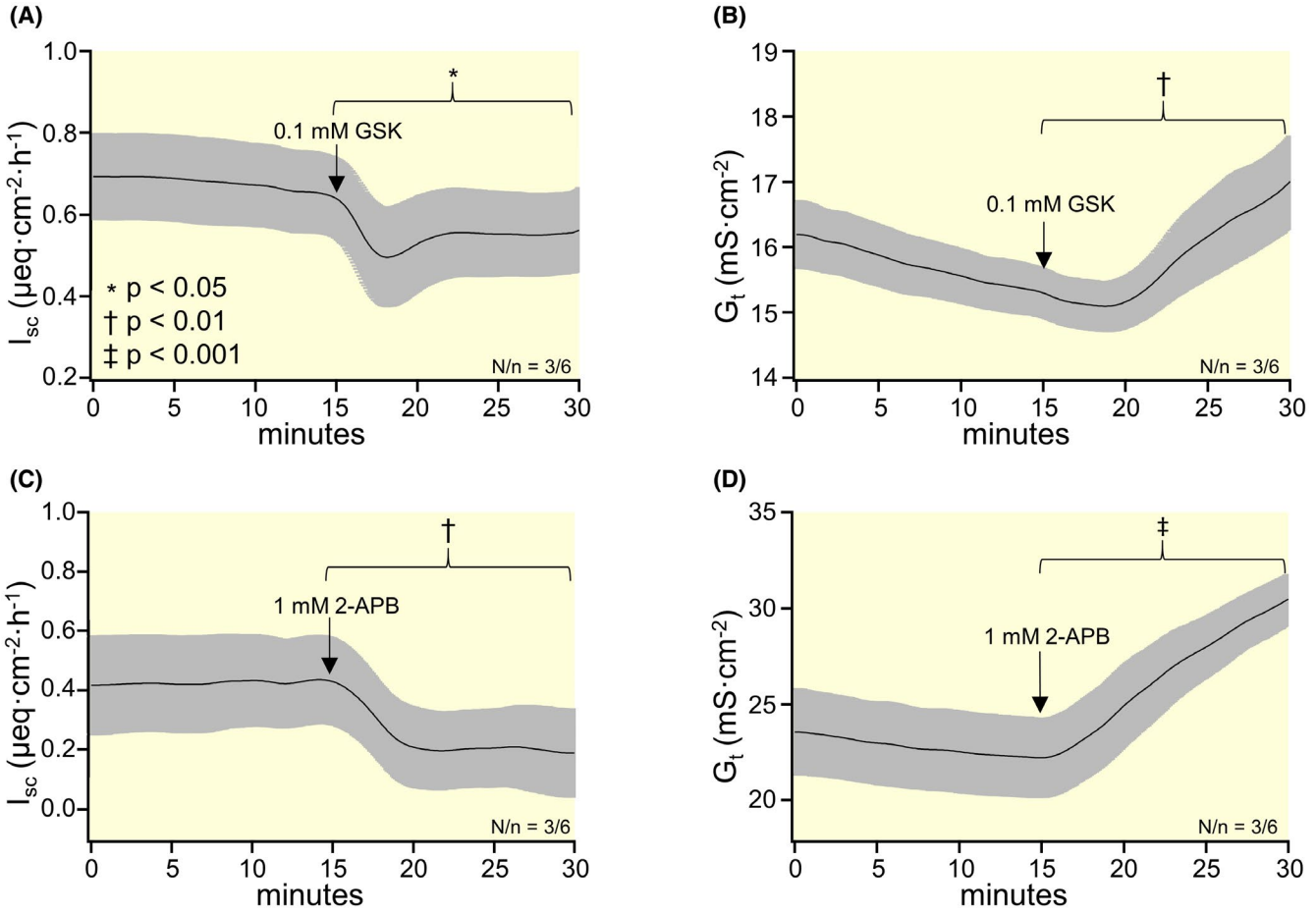

FIGURE 7 Effect of the TRP agonists 2-APB and GSK106790A (GSK) on I_{sc} and G_t in the Ussing chamber using colonic tissue of pigs. After addition of the respective agonist on the mucosal side, a decrease in I_{sc} (A and C) could be observed, while at the same time an increase in G_t occurred (B and D). Statistical comparisons were made between values taken immediately prior to addition of the agonist and after an incubation of 15 min. Data are given as means ± SEM

Our investigations started with TRP channels for which a direct role in (divalent) cation transport has been established. The expression pattern for TRPV6 confirms previously available data for the pig and other species and highlights the role of the duodenum as the major locus for Ca^{2+} absorption (Figure 1C).[16,58] Although data for the pig appear to be lacking, high mRNA expression levels of TRPM6 in the jejunum and the hindgut confirm what has been established in other species as the major locus of transcellular intestinal Mg^{2+} absorption (Figure 1A).[59-62] Interestingly, no signals for either TRPV6 or TRPM6 could be detected in samples from the muscular layers, highlighting their role in epithelial transport. Conversely, TRPM7 was found to be ubiquitously expressed by both the muscular and mucosal layers throughout the pig intestine (Figure 1B). This finding is in accordance with the proposed role of this channel in cellular Mg^{2+} homeostasis, although notably, TRPM7 may also be a primary player in epithelial Mg^{2+} uptake via formation of TRPM6/TRPM7 heteromers.[63] As mentioned, we were unable to establish a porcine primer for TRPV5 that was clearly separate from TRPV6.

In a second step, we turned to non-selective members of the TRP channel family. TRPM8 conducts both Na^{+} and Ca^{2+} and is known for its activation by cool temperatures and by plant terpenoids, notably menthol and thymol.[64] We found no evidence for an expression on the level of mRNA within the porcine gastrointestinal tract (Figure 1F). Notably, mRNA for TRPM8 was also not found in the rumen[14] or in the human intestine.[65] However, expression by human colonic muscle has been reported with weaker expression within the mucosa.[66]

TRPV1 is activated by heat (>40°C), by acidic pH, and by various exogenous and endogenous substrates (eg anandamide, capsaicin).[5,26] In the murine intestine, expression was found to be highest in the intestinal nerve fibres of the colon and distal rectum.[67] Both in mice and in humans, mucosal samples from colon and rectum express TRPV1 and a role in inflammatory bowel disease has been proposed.[8,68,69] In the current qPCR study of porcine mucosa and muscularis, mRNA encoding for TRPV1 was below the threshold of detection (set at 30 cycles). This may reflect species-dependent differences, our conservative cut-off value, or the fact that samples were taken from the mid colon and not from the

distal parts, where in mouse and human samples, TRPV1 is most highly expressed. Furthermore, great care was taken to strip the epithelium from the rest of the tissue where most neurons expressing TRPV1 for neuronal signalling can be found.

TRPV2 is activated by temperatures above 52°C and is typically expressed by neurons supplying the gastrointestinal tract.[62] In the current study, mRNA encoding for TRPV2 was found in equal small amounts in the muscular layers of all segments. In the mucosal layers, TRPV2 expression was comparable to those in the muscular layers, but reached increasingly higher levels in the small intestine (Figure 1F). In the mucosal layers of the caecum, TRPV2 was low while in the colon, TRPV2 was barely detectable. Given that our samples contained small amounts of submucosa, this finding is in line with the failure to detect mRNA for TRPV2 in isolated colonic crypts of the rat.[11]

A number of studies suggest an important role for TRPV4 in the regulation of gastric motility and emptying.[70] In the colon, the channel is thought to play diverse roles in osmosensation[6,71] and regulation of barrier function,[56] with possible implications for diseases such as ulcerative colitis.[72] In the current study, the largest amount of mRNA for TRPV4 was found in the mucosa of the stomach (cardia and fundus; Figure 1D). TRPV4-encoding mRNA expression by all other porcine mucosal tissues was lower and not significantly different from the muscular layers. In Western blots stained with a rabbit antibody against TPRV4 protein, a double band at the expected height of about 90 kDa could be observed, with the doubling possibly reflecting degradation or a variant (Figure 2). A doublet of similar height has been reported in Western blot analysis of TRPV4 expression in carotid artery, kidney or skeletal muscle of wild-type mice, and disappeared in TRPV4-/- mutants.[73,74] The same antibody was used in conjunction with a secondary antibody to localize the expression of TRPV4 protein within the intact tissue via confocal laser microscopy (Figure 4). In the gastric epithelium, strong staining for TRPV4 could be observed along the gastric crypts. In intestinal epithelia, staining for TRPV4 was clearly highest in the apical membrane of cells facing the lumen of the organ. Note that the staining intensity of the different sections reflects the gain chosen for each image and not the amount of protein expressed.

TRPV3 is known to be activated by numerous stimuli, such as heat (22-40°C) or various spices (eg thymol, menthol, carvacrol).[5,75,76] The physiological function of TRPV3 is generally poorly understood[77] and research is hampered by the lack of commercially available specific agonists or blockers although the race for the development of such agents is on.[50] TRPV3 is highly expressed by the keratinocytes of the skin, where gain of function mutations are linked to a hereditary hyperkeratosis that can be so severe that joints are immobilized.[78] Very little information is available for the role of TRPV3 in the gastrointestinal tract. A role in inflammation has been suggested, although attempts to correlate clinical findings in ulcerative colitis with the expression of TRPV3 have been frustrating.[68] In what was probably the pioneering study of TRPV3 expression by the colon,[10] the authors mention "the abundant expression by the superficial absorptive cells" and suggest that functions may include epithelial ion transport. This hypothesis is supported by the functional data of this study.

Interestingly, in the current study of the porcine gastrointestinal tract, mRNA encoding for TRPV3 could only be detected in mucosa of the colon and caecum, with no signal in the muscle layer or in any other segment (Figure 1E). Similar findings have been reported for the mouse intestine, where mRNA encoding for TRPV3 could also be detected in the colon, but not in the stomach or duodenum[10] while in the rat colon, mRNA for TRPV3 was significantly higher in the crypts than in residual tissues.[11] Notably, the colon and caecum are the parts of the gut where because of fermentational degradation of amino acids and urea, concentrations of NH_4^+ are highest (Table 2). Furthermore, these tissues showed the numerically highest divalent-sensitive conductance to NH_4^+ (Figure 6, Table 4).

A note of caution is necessary since our primer was only suitable for an amplification of the mRNA of the full-length 90 kDa protein (Supporting Table A). Apart from this long variant of TRPV3, a shorter variant of ~60 kDa has been described in mice (XP_006533411.1), in human epidermal keratinocytes[42] and in bovines (AAI46079.1 and Ref. [30]). Our finding that primer pairs matching both mRNA variants all produced more than one melting curve suggests that porcine gastrointestinal tissues may also express more than one splice variant. However, this is somewhat speculative and our qPCR results confirm mRNA expression only of the long variant. Western blots stained by a mouse TRPV3 antibody showed a clearly visible band at 60 kDa in all segments and all blots studied, with a further weak band at 90 kDa observed in two blots of colonic tissues (Figure 3) and in controls of mouse skin (not shown). A similar pattern emerged in Western blots of mouse distal colon using a rabbit antibody against TRPV3,[10] in human epidermal keratinocytes using an antibody from goats[42] and in our study of the ruminal epithelium, where the same murine antibody was used as in this study.[30] It should be mentioned that in our previous study, the TRPV3 antibody was validated both in overexpressing HEK 293 cells and in Xenopus oocytes.[30]

Immunohistochemical staining of porcine tissues against TRPV3 showed expression in the gastric crypts and a clear staining of the apical membrane of the intestinal segments, with colocalization of TRPV3 and TRPV4 frequent (Figure 4). Conversely, any staining of intracellular structures was very weak. This finding is in fascinating contrast to what is typically observed in keratinocytes from skin[42,79] or

the rumen,[30] where TRPV3 antibodies typically also strongly stain the cytosolic compartment. Whatever the reasons for these differences may be, apical expression as shown here supports the involvement of TRPV3 in epithelial transport.

Under physiological conditions, the intestinal absorption of Na^+ via TRP channels will be small relative to the much larger quantities transported via the highly Na^+ selective proteins NHE and ENaC that are abundantly expressed by the colon. Instead, we suggest that as in the rumen,[29,30] one function of these poorly selective channels[27] may be to serve as one of several routes for the uptake of NH_4^+. The bovine homologue of TRPV3 has been directly shown to be permeable to NH_4^+ on the single-channel level in two different expression systems, making it a prime candidate for the divalent cation conductance reported in this study.[29,30]

It should be stressed that our findings definitely do not exclude the participation of other cation channels, including other members of the TRP channel family, in the efflux of NH_4^+ from the intestine. Furthermore, it has been shown that protein-mediated pathways for the transport of NH_3 exist.[35-37] Notably, certain types of aquaporins conduct NH_3,[36] while the colon reportedly expresses the ammonia transporters RhCG (apical) and RhBG (basolateral).[35] Although in the past, there has been some controversy surrounding the exact transport mechanism and substrate specificity of RhBG,[37] there is a broad consensus that RhCG mediates net transport of NH_3 via an electroneutral mechanism.[80] Current models suggest that all Rhesus-like glycoproteins bind NH_4^+ and catalyse the conversion to NH_3, which is then conducted through a hydrophobic pore down the concentration gradient.[37,38] Accordingly, apical expression of RhCG by the colon cannot explain the divalent-sensitive NH_4^+-induced currents observed in this study.

Further work is required to determine the basolateral efflux route (which may involve transport of NH_4^+ through K^+ channels or a coupling of RhBG [35] and pH regulating transporters such as NHE or one of the various Na^+-HCO_3^- cotransporters) and to assess the relative contributions of different pathways to total intestinal ammonia transport. However, unlike absorption in the form of the base NH_3, absorption of NH_4^+ from the colon should be very useful for the maintenance of both luminal and intracellular pH homeostasis of an organ in which protons are continuously generated in the course of the breakdown of structural carbohydrates into short-chain fatty acids.[43,44,81] Colonic pH homeostasis is essential for the survival of both the epithelium, and the microbiota living within. On the downside, ammonia has to be detoxified by the liver and the urea that is formed has to be excreted, leading to a plethora of problems that have been discussed.

In summary, we present an overview of the mRNA expression of various TRP channels along the porcine gastrointestinal tract using qPCR. The expression of two non-selective members, TRPV4 and TRPV3, was also investigated on the protein level via Western blots and confocal laser microscopy. Expression was clearly highest in the apical membrane of the intestinal segments, suggesting a function in absorption. Although further work clearly needs to be done, the functional response to an exposure to NH_4^+ containing solutions, modulated by the removal of divalent cations and the response to TRP channel agonists, suggests that a role in the transport of monovalent cations in general and NH_4^+ in particular should be considered. A concert of protein-mediated pathways for the uptake of ammonia is thus replacing older models of an uptake via the lipid membrane.[14,29,30,35-37,39] Despite their redundancy, protein-mediated uptake pathways invite new approaches concerning pharmacological modulation of ammonia losses from the hindgut, with possible implications both for limiting nitrogen losses into the environment by livestock and for the treatment of hepatic encephalopathy in humans.

4 | MATERIALS AND METHODS

4.1 | Gastrointestinal epithelium

Gastrointestinal tissues from pigs were obtained according to German guidelines of the Animal Welfare Act with approval by the local authorities (LaGeSo Reg. Nr T0264/15 and T0297/17 or from local abattoir). The pigs from T0264/15 and T0297/17 (subsequently designated as "T") consisted of a hybrid of the breeds Danbred x Piétrain at around 10 weeks of age and weighed around 25 kg. The pigs were sedated by an intramuscular injection with ketamine hydrochloride (Ursotamin, Serumwerk Bernburg AG, Bernburg, Germany) and azaperone (Stresnil, Jansen-Cilag, Neuss, Germany) and subsequently killed by intracardiac injection of tetracaine hydrochloride, mebezonium iodide and embutramide (T61, Intervet Deutschland GmbH, Unterschleissheim, Germany). Other pigs were of different ages and breeds and came from a commercial slaughterhouse ("S"). The tissue was removed approximately 10 minutes after death and was then immediately washed with PBS or Ringer solution, after which the mucosa was immediately stripped from the submucosal layers.

4.2 | PCR

Stomach (fundus and cardia), duodenum, middle jejunum, ileum, caecum and middle colon were collected from 6 pigs ("T"). After manual separation, small pieces (1 cm^2) from the muscular layers or the stripped mucosa (containing small amounts of submucosal tissue) were then immediately transferred to RNAlater (1 mL tubes; Sigma-Aldrich,

Taufkirchen, Germany) and stored overnight at 4°C, followed by storage at −80°C. For primer establishment, control tissues (liver, kidney and medulla oblongata) were additionally collected. Total RNA was isolated from all samples using a commercially available kit including DNA digestion (Nucleospin RNA ll, Macherey-Nagel, Dueren, Germany). RNA quality was checked via determination of RNA integrity (RIN) values using a lab-on-chip technique (RNA 6000 Nano, Agilent, Waldbronn, Germany). Samples from 4 pigs with the best RIN values (RIN >6.8 (ileal mucosa) or RIN > 7.3, all other tissues) were selected for further processing. 1000 ng RNA were then transcribed into cDNA (iScript cDNA synthesis Kit, Bio-Rad Laboratories, Munich, Germany) according to the manufacturer's instructions, which was diluted 1:10.

Gene-specific intron-spanning primer pairs for the porcine TRP channels and reference genes were established based on the gene sequences of the NCBI database (Table 1). In order to ensure primer specificity, amplification products of all primer pairs (Eurofins Genomics Germany GmbH, Ebersberg, Germany) were sequenced at least once and matched with the target sequence.

For the three selected reference genes, corresponding primer-probe combinations were used with FAM as the reporter and BHQ1 (ACTB) or TAMRA (GAPDH, YWHAZ) as the quencher.[82] The qPCR was performed in triplicates for 40 cycles each on a thermal cycler (Applied Biosystems/Life Technologies, Waltham, MA, USA). Negative controls (no template controls) were included. The quantification cycle (C_q) was calculated automatically by the cycler software. Dilution-series-based gene-specific amplification efficiency of all genes and expression stability of the reference genes were determined using the software qbasePLUS (Biogazelle NV, Zwijnaarde, Belgium).

Expression of mRNA levels of the target genes TRPV1, TRPV2, TRPV3, TRPV4, TRPV6, TRPM6, TRPM7 and TRPM8 was evaluated in a three-step qPCR protocol (30 s 95°C, 30 s 59°C or 60°C, 30 s 72°C) with 4 µL cDNA, 5 µL SYBR green (IQ SYBR Green Supermix, Bio-Rad Laboratories GmbH, Feldkirchen, Germany), 0.6 µL water and 0.2 µL forward and reverse primer each.

For the primer-probe combinations of the reference genes, a two-step-protocol (1 s 95°C, 20 s 60°C) was applied using 3.7 µL cDNA and iTaq Universal Probes Supermix (Bio-Rad Laboratories GmbH, Feldkirchen, Germany) in a total volume of 10 µL.

According to the software qBASEplus, ACTB, GAPDH and YWHAZ showed sufficient expression stability and were therefore used for normalization of the target genes. Normalized C_q values of the target genes were then scaled to the average value of the samples and exported as calibrated normalized relative quantity (CNRQ) values. For statistical analysis, only CNRQ values were used.

4.3 | Western blot

The tissue was cut into 1 to 2 cm² pieces after stripping and washing with PBS. The samples were then frozen in liquid nitrogen and stored at −80°C. For protein extraction the thawed sample (approx. 300 mg) was mixed with RIPA buffer (1 mL; in mmol·L^{-1}:25 HEPES, 25 NaF, 1% sodium dodecyl sulphate (SDS), 2 EDTA, protease inhibitor [cOmplete, mini, Roche, Basel, Switzerland]) and two metal spheres. The sample was then homogenized in a mixer mill (4x 1.5 min, MM 200, Retsch GmbH, Haan, Germany) and centrifuged (15 min, 15 000 g, 4°C). The supernatant was filled into a new tube and stored at −80°C after the determination of the protein concentration by the Lowry method (DC Protein Assay, Bio-Rad Laboratories GmbH, Feldkirchen, Germany). Proteins were denatured at 95°C for 5 minutes in SDS sample loading buffer. Electrophoresis with polyacrylamide gels (10%, SDS-PAGE) was performed in tris-glycine buffer (0.1% SDS) and electroblotting was done onto polyvinylidene difluoride membranes (PVDF, Immunoblot, Bio-Rad Laboratories GmbH, Munich, Germany) in tris-glycine buffer (0.037% SDS, 20% methanol, 4°C).

For the primary antibodies, dilution factors 1:500 for mTRPV3 and 1:3000 for rTRPV4 were used. The detection of the primary antibodies was done via a horseradish peroxidase-conjugated secondary antibody (anti-mouse 1:1000 and anti-rabbit 1:1000, Cell Signalling Technology, Frankfurt, Germany). Visualization was performed via Clarity Western ECL substrate (Bio-Rad Laboratories GmbH, Munich, Germany).

4.4 | Immunohistological staining

For histological investigations, the tissue was carefully washed after removal and pinned on cork plates to avoid curling during fixation in 4% paraformaldehyde.

After fixation for 24-48 hours, the tissue was dehydrated with ascending concentrations of ethanol according to the following protocol: 3x 70% (1 h), 1x 70% (overnight), 3x 80% (1 h), 1x 80% (overnight), 1x 90% (1 h), 2x 96% (1 h), 3x 99.5% (1 h); followed by ethanol: xylene (1:1, 40 min), 2x xylene (0.5 h), and liquid paraffin (overnight and 2x 1 h). Samples were then stored at room temperature until cutting (Leica RM 2245 microtome, Leica Microsystems, Heidelberg, Germany) and mounting. For deparaffinization, the slides were preheated for 1 hour at 56°C and then transferred to xylene at room temperature for 10 minutes. Afterwards the rehydration was performed by using descending alcohol series (>99.5%, 96%, 90%, 80%, 80%, deionized water) for 5 minutes each.

To expose the epitopes, the sections were incubated with 0.05% pronase in PBS for 10 minutes each at 37°C and then at room temperature, rinsed with 0.05% Tween20 in PBS (2x 2 min), and permeabilized with 0.5% Triton-X100 (5 min).

After washing (PBS, 2x 5 min), the sections were incubated (1 h) in blocking solution (5% Goat Serum + 1% BSA in PBS). The sections were then stained with the primary antibodies (rTRPV4 1:250, PA5-41066, ThermoFisher Scientific, Waltham, MA, USA and mTRPV3 1:500, ABIN863127, antibodies-online GmbH, Aachen, Germany) and stored at 4°C overnight. Each slide also carried a negative control, which was incubated with blocking solution only. The following day the slides were washed 5x 5 minutes with blocking solution and then incubated with the secondary antibody and 4′,6-diamidino-2-phenylindole (DAPI) in blocking solution (1:1000, Alexa Fluor 594 and 488, Thermo Fisher Scientific, Waltham, MA, USA) for 1 hour at 37°C in the dark. The slices were washed 5x 5 minutes with PBS, briefly rinsed in deionized water and ethanol and then embedded (ProTaqs Mount Fluor, Biocyc, Luckenwalde, Germany). The images were taken at 405, 488 and 543 nm using a confocal laser-scanning microscope (LSM 510, Axiovert200M, Zeiss, Jena, Germany).

4.4.1 | Analysis of digesta

For the analysis of ammonia and measurement of pH, the different segments of the gastrointestinal tract were clamped to avoid mixing of the digesta. After taking the sample, the pH value was immediately determined using a calibrated pH electrode and the sample was then frozen at −20°C until further analysis. The analysis of ammonia was determined by the Institute for Animal Nutrition of the FU Berlin by colorimetric determination.[83]

4.4.2 | Ussing chamber experiments

Tissues were removed about 10 minutes after the death of the animal, washed, stripped from the muscular layer and then transported with gassed (95% O_2 / 5% CO_2) ice-cooled transport buffer, which contained the following (in mmol·L^{-1}): 115 NaCl, 0.4 NaH_2PO_4, 2.4 Na_2HPO_4, 5 KCl, 25 $NaHCO_3$, 5 Glucose, 10 HEPES, 1.2 $CaCl_2$ and 1.2 $MgCl_2$ (pH 7.4).

The mucosal-submucosal preparations (stomach fundus, duodenum, middle jejunum, ileum, caecum or middle colon) were then mounted in 0.95 cm² Ussing chambers, initially filled with 10 mL NaCl-containing buffer solution per side at 37°C and gassed with either O_2 or carbogen (95% O_2/5% CO_2). All solutions were adjusted to 300 mosmol·kg^{-1} using mannitol. The measurements were performed in short-circuit mode; the transepithelial conductance G_t was continuously monitored via the potential response to a 100 µA current pulse (Mussler Scientific Instruments, Aachen, Germany). The mucosal bath was grounded and the sign convention is such that a positive I_{sc} reflects transport of cations from the mucosal to the serosal side. Recording commenced after a constant I_{sc} and G_t could be monitored or after 45 minutes at the latest.

In experiments that required a change in solution, the chamber liquid was drained off on both sides simultaneously and rapidly refilled with the test buffer on the mucosal side while the serosal side was refilled with the same standard serosal buffer as before. Both buffers were prewarmed and pregassed. In addition, some screening experiments were carried out in a small vertical Ussing chamber designed to allow continuous perfusion, thus minimizing artefacts because of solution changes.[14] For the composition of the solutions, see Supporting Tables B and C. For low chloride Ringer, NaCl, NMDGCl and NH_4Cl in Supporting Table C were replaced by Na-gluconate, NMDG-gluconate and NH_4-gluconate (generated via titration).

Stock solutions of the TRP channel modulators GSK106790A[70] and 2-APB[51] were prepared by dilution in ethanol and stored at −20°C and added directly to the mucosal bath (Supporting Table B) at 1:1000 yielding final concentrations of 100 µmol·L^{-1} (GSK106790A) and 1 mmol·L^{-1} (2-APB). Equivalent amounts of ethanol were added to the mucosal side of control tissues.

4.5 | Chemicals and modulators

Chemicals were purchased from Carl Roth (Karlsruhe, Germany), Sigma-Aldrich (Taufkirchen, Germany) or Merck (Darmstadt, Germany).

4.6 | Data and statistical analysis

Ussing chamber data were recorded at 10 points/min and binomially smoothed via Igor Pro 6.37 (WaveMetrics Inc, Lake Oswego, USA). Unless indicated otherwise, data were obtained 15 minutes after each intervention and tested for normal distribution (Shapiro–Wilk) and homogeneity of variance (Brown-Forsythe) using SigmaPlot 11.0 (Systat Software, Erkrath, Germany). Differences were evaluated with ANOVA or ANOVA on ranks using the Student-Newman-Keuls method. In some cases, the Dunn method was used, as suggested by SigmaPlot software. When comparing two groups, either the Student's *t*-test or the Mann-Whitney-U-test was performed.

Statistical analysis of the PCR results was performed with the resulting CNRQ values. Depending on the number of values to be compared, either a *t*-test or an ANOVA-test (two way, considering animal and respective localization of the tissue as factors) with a correction for multiple testing was applied.

The data are given as means ±SEM and the statistical significance was assumed if $P \leq .05$. The number of experiments is declared as N for the number of animals and n for the number of tissues.

ACKNOWLEDGEMENTS

This study was partly funded by a grant from the Akademie für Tiergesundheit (to DM). The antibodies and some other reagents were purchased with funding from Deutsche Forschungsgemeinschaft (DFG-STU 258/7-1). We would like to thank Prof. Dr Dorothee Günzel for the opportunity to produce the histological images and PD Dr Robert Pieper for the analysis of the intestinal ingesta. We would also like to thank Susanne Trappe, Martin Grunau and Katharina Söllig for their technical support.

CONFLICT OF INTEREST

This study was performed within a conventional academic setting for purely scientific reasons. At the time of the study, KTS and HSB were employees of PerformaNat GmbH, Germany, which also supplied some of the reagents for the study. Friederike Stumpff is not financially involved in Performanat in any way, but is the co-holder of patents EP2879662 (EU) and 9 693 971 (US) that were transferred to this start-up. There was no influence on the evaluation and interpretation of the data and there is no conflict of interest.

DATA AVAILABILITY STATEMENT

The data that support the findings of this study are available from the corresponding author upon reasonable request.

ORCID

David Manneck https://orcid.org/0000-0003-4478-1980
Hannah-Sophie Braun https://orcid.org/0000-0001-9293-7623
Katharina T. Schrapers https://orcid.org/0000-0003-0928-6394
Friederike Stumpff https://orcid.org/0000-0001-9518-9237

REFERENCES

1. Alaimo A, Rubert J. The pivotal role of TRP channels in homeostasis and diseases throughout the gastrointestinal tract. *Int J Mol Sci*. 2019;20(21):5277.
2. Holzer P. Transient receptor potential (TRP) channels as drug targets for diseases of the digestive system. *Pharmacol Ther*. 2011;131(1):142-170.
3. Montell C. The history of TRP channels, a commentary and reflection. *Pflugers Arch*. 2011;461(5):499-506.
4. Voets T, Droogmans G, Wissenbach U, Janssens A, Flockerzi V, Nilius B. The principle of temperature-dependent gating in cold- and heat-sensitive TRP channels. *Nature*. 2004;430(7001):748-754.
5. Vriens J, Nilius B, Vennekens R. Herbal compounds and toxins modulating TRP channels. *Curr Neuropharmacol*. 2008;6(1):79-96.
6. Diener M. Sensing osmolarity: a new player on the field. *J Physiol*. 2020;598(23):5297-5298.
7. Mergler S, Valtink M, Taetz K, et al. Characterization of transient receptor potential vanilloid channel 4 (TRPV4) in human corneal endothelial cells. *Exp Eye Res*. 2011;93(5):710-719.
8. Cseko K, Beckers B, Keszthelyi D, Helyes Z. Role of TRPV1 and TRPA1 ion channels in inflammatory bowel diseases: potential therapeutic targets? *Pharmaceuticals*. 2019;12(2):48.
9. Nozawa K, Kawabata-Shoda E, Doihara H, et al. TRPA1 regulates gastrointestinal motility through serotonin release from enterochromaffin cells. *Proc Natl Acad Sci U S A*. 2009;106(9):3408-3413.
10. Ueda T, Yamada T, Ugawa S, Ishida Y, Shimada S. TRPV3, a thermosensitive channel is expressed in mouse distal colon epithelium. *Biochem Biophys Res Commun*. 2009;383(1):130-134.
11. Kaji I, Yasuoka Y, Karaki S, Kuwahara A. Activation of TRPA1 by luminal stimuli induces EP4-mediated anion secretion in human and rat colon. *Am J Physiol Gastrointest Liver Physiol*. 2012;302(7):G690-G701.
12. Manneck D, Manz G, Braun H-S, Rosendahl J, Stumpff F. The TRPA1 agonist cinnamaldehyde induces the secretion of HCO3− by the porcine colon. *Int J Mol Sci*. 2021;22(10):5198.
13. Dimke H, Hoenderop JG, Bindels RJ. Molecular basis of epithelial Ca^{2+} and Mg^{2+} transport: insights from the TRP channel family. *J Physiol*. 2011;589(Pt 7):1535-1542.
14. Rosendahl J, Braun HS, Schrapers KT, Martens H, Stumpff F. Evidence for the functional involvement of members of the TRP channel family in the uptake of Na(+) and NH4 (+) by the ruminal epithelium. *Pflugers Arch*. 2016;468(8):1333-1352.
15. Wilkens MR, Kunert-Keil C, Brinkmeier H, Schröder B. Expression of calcium channel TRPV6 in ovine epithelial tissue. *Vet J*. 2009;182(2):294-300.
16. Schröder B, Breves G. Mechanisms and regulation of calcium absorption from the gastrointestinal tract in pigs and ruminants: comparative aspects with special emphasis on hypocalcemia in dairy cows. *Anim Health Res Rev*. 2006;7(1–2):31-41.
17. Wilkens MR, Muscher-Banse AS. Review: regulation of gastrointestinal and renal transport of calcium and phosphorus in ruminants. *Animal*. 2020;14(S1):s29-s43.
18. Martens H, Hammer U. Magnesium and sodium absorption from the isolated sheep rumen during intravenous aldosterone infusion (author's transl). *Dtsch Tierarztl Wochenschr*. 1981;88(10):404-407.
19. Martens H, Gabel G, Strozyk B. Mechanism of electrically silent Na and Cl transport across the rumen epithelium of sheep. *Exp Physiol*. 1991;76(1):103-114.
20. Sellin JH, Dubinsky WP. Apical nonspecific cation conductances in rabbit cecum. *Am J Physiol*. 1994;266(3 Pt 1):G475-G484.
21. Pouokam E, Diener M. Segmental differences in ion transport in rat cecum. *Pflugers Arch*. 2019;471(7):1007-1023.
22. Krattenmacher R, Voigt R, Clauss W. Ca-sensitive sodium absorption in the colon of Xenopus laevis. *J Comp Physiol B*. 1990;160(2):161-165.
23. Schultheiss G, Martens H. Ca-sensitive Na transport in sheep omasum. *Am J Physiol*. 1999;276(6 Pt 1):G1331-G1344.
24. Leonhard-Marek S, Stumpff F, Brinkmann I, Breves G, Martens H. Basolateral Mg2+/Na+ exchange regulates apical nonselective cation channel in sheep rumen epithelium via cytosolic Mg2+. *Am J Physiol Gastrointest Liver Physiol*. 2005;288(4):G630-G645.
25. Leonhard-Marek S. Divalent cations reduce the electrogenic transport of monovalent cations across rumen epithelium. *J Comp Physiol B*. 2002;172(7):635-641.
26. Voets T, Prenen J, Vriens J, et al. Molecular determinants of permeation through the cation channel TRPV4. *J Biol Chem*. 2002;277(37):33704-33710.
27. Owsianik G, Talavera K, Voets T, Nilius B. Permeation and selectivity of TRP channels. *Annu Rev Physiol*. 2006;68:685-717.

28. Bouron A, Kiselyov K, Oberwinkler J. Permeation, regulation and control of expression of TRP channels by trace metal ions. *Pflugers Arch*. 2015;467(6):1143-1164.
29. Schrapers KT, Sponder G, Liebe F, Liebe H, Stumpff F. The bovine TRPV3 as a pathway for the uptake of Na^+, Ca^{2+}, and NH^{4+}. *PLoS One*. 2018;13(3):e0193519.
30. Liebe F, Liebe H, Kaessmeyer S, Sponder G, Stumpff F. The TRPV3 channel of the bovine rumen: localization and functional characterization of a protein relevant for ruminal ammonia transport. *Pflugers Arch*. 2020;472(6):693-710.
31. Abdoun K, Stumpff F, Martens H. Ammonia and urea transport across the rumen epithelium: a review. *Anim Health Res Rev*. 2006;7(1-2):43-59.
32. Gerber PJ, Hristov AN, Henderson B, et al. Technical options for the mitigation of direct methane and nitrous oxide emissions from livestock: a review. *Animal*. 2013;7(Suppl. 2):220-234.
33. Mardini H, Record C. Pathogenesis of hepatic encephalopathy: lessons from nitrogen challenges in man. *Metab Brain Dis*. 2013;28(2):201-207.
34. Al-Awqati Q. One hundred years of membrane permeability: does Overton still rule? *Nat Cell Biol*. 1999;1(8):E201-E202.
35. Handlogten ME, Hong S-P, Zhang LI, et al. Expression of the ammonia transporter proteins Rh B glycoprotein and Rh C glycoprotein in the intestinal tract. *Am J Physiol Gastrointest Liver Physiol*. 2005;288(5):G1036-G1047.
36. Boron WF. Sharpey-Schafer lecture: gas channels. *Exp Physiol*. 2010;95(12):1107-1130.
37. Neuhäuser B, Dynowski M, Ludewig U. Switching substrate specificity of AMT/MEP/ Rh proteins. *Channels*. 2014;8(6):496-502.
38. Baday S, Orabi EA, Wang S, Lamoureux G, Bernèche S. Mechanism of NH4(+) recruitment and NH3 transport in Rh proteins. *Structure*. 2015;23(8):1550-1557.
39. Chepilko S, Zhou H, Sackin H, Palmer LG. Permeation and gating properties of a cloned renal K+ channel. *Am J Physiol*. 1995;268(2 Pt 1):C389-C401.
40. Burckhardt BC, Frömter E. Pathways of NH3/NH4+ permeation across Xenopus laevis oocyte cell membrane. *Pflugers Arch*. 1992;420(1):83-86.
41. Stumpff F, Lodemann U, Van Kessel AG, et al. Effects of dietary fibre and protein on urea transport across the cecal mucosa of piglets. *J Comp Physiol B*. 2013;183:1053-1063.
42. Szöllősi AG, Vasas N, Angyal Á, et al. Activation of TRPV3 regulates inflammatory actions of human epidermal keratinocytes. *J Invest Dermatol*. 2018;138(2):365-374.
43. Bergman EN. Energy contributions of volatile fatty acids from the gastrointestinal tract in various species. *Physiol Rev*. 1990;70(2):567-590.
44. Tappeiner H. Untersuchung über die Gärung der Cellulose, insbesondere über deren Lösung im Darmkanale. *Zeitschr f Biol*. 1884;20:52-134.
45. Gonzalez-Mariscal L, Contreras RG, Bolivar JJ, Ponce A, Chavez De Ramirez B, Cereijido M. Role of calcium in tight junction formation between epithelial cells. *Am J Physiol*. 1990;259(6 Pt 1):C978-C986.
46. Van Driessche W, Zeiske W. Ca^{2+}-sensitive, spontaneously fluctuating, cation channels in the apical membrane of the adult frog skin epithelium. *Pflugers Arch*. 1985;405(3):250-259.
47. Van Driessche W, Desmedt L, Simaels J. Blockage of Na^+ currents through poorly selective cation channels in the apical membrane of frog skin and toad urinary bladder. *Pflugers Arch*. 1991;418(3):193-203.
48. Cao X, Yang F, Zheng J, Wang K. Intracellular proton-mediated activation of TRPV3 channels accounts for the exfoliation effect of alpha-hydroxyl acids on keratinocytes. *J Biol Chem*. 2012;287(31):25905-25916.
49. Meoli L, Günzel D. Channel functions of claudins in the organization of biological systems. *Biochim Biophys Acta Biomembr*. 2020;1862(9):183344.
50. Bischof M, Olthoff S, Glas C, Thorn-Seshold O, Schaefer M, Hill K. TRPV3 endogenously expressed in murine colonic epithelial cells is inhibited by the novel TRPV3 blocker 26E01. *Cell Calcium*. 2020;92:102310.
51. Hu H-Z, Gu Q, Wang C, et al. 2-aminoethoxydiphenyl borate is a common activator of TRPV1, TRPV2, and TRPV3. *J Biol Chem*. 2004;279(34):35741-35748.
52. Hinman A, Chuang HH, Bautista DM, Julius D. TRP channel activation by reversible covalent modification. *Proc Natl Acad Sci U S A*. 2006;103(51):19564-19568.
53. Clapham DE. SnapShot: mammalian TRP channels. *Cell*. 2007;129(1):220.
54. Talavera K, Startek JB, Alvarez-Collazo J, et al. Mammalian transient receptor potential TRPA1 channels: from structure to disease. *Physiol Rev*. 2020;100(2):725-803.
55. Ma X, Nilius B, Wong JW, Huang Y, Yao X. Electrophysiological properties of heteromeric TRPV4-C1 channels. *Biochim Biophys Acta*. 2011;1808(12):2789-2797.
56. Huang Y-Y, Li J, Zhang H-R, et al. The effect of transient receptor potential vanilloid 4 on the intestinal epithelial barrier and human colonic cells was affected by tyrosine-phosphorylated claudin-7. *Biomed Pharmacother*. 2020;122:109697.
57. Martínez-Rendón J, Sánchez-Guzmán E, Rueda A, et al. TRPV4 regulates tight junctions and affects differentiation in a cell culture model of the corneal epithelium. *J Cell Physiol*. 2017;232(7):1794-1807.
58. Nijenhuis T, Hoenderop JG, Bindels RJ. TRPV5 and TRPV6 in Ca(2+) (re)absorption: regulating Ca(2+) entry at the gate. *Pflugers Arch*. 2005;451(1):181-192.
59. Schuchardt JP, Hahn A. Intestinal absorption and factors influencing bioavailability of magnesium-an update. *Curr Nutr Food Sci*. 2017;13(4):260-278.
60. Schlingmann KP, Weber S, Peters M, et al. Hypomagnesemia with secondary hypocalcemia is caused by mutations in TRPM6, a new member of the TRPM gene family. *Nat Genet*. 2002;31(2):166-170.
61. Rondón LJ, Groenestege WMT, Rayssiguier Y, Mazur A. Relationship between low magnesium status and TRPM6 expression in the kidney and large intestine. *Am J Physiol Regul Integr Comp Physiol*. 2008;294(6):R2001-R2007.
62. Holzer P. TRP channels in the digestive system. *Curr Pharm Biotechnol*. 2011;12(1):24-34.
63. Zou ZG, Rios FJ, Montezano AC, Touyz RM. TRPM7, magnesium, and signaling. *Int J Mol Sci*. 2019;20(8):1877.
64. Janssens A, Gees M, Toth BI, et al. Definition of two agonist types at the mammalian cold-activated channel TRPM8. *eLife*. 2016;5:e17240.
65. Fonfria E, Murdock PR, Cusdin FS, Benham CD, Kelsell RE, McNulty S. Tissue distribution profiles of the human TRPM cation channel family. *J Recept Signal Transduct Res*. 2006;26(3):159-178.
66. Amato A, Terzo S, Lentini L, Marchesa P, Mulè F. TRPM8 channel activation reduces the spontaneous contractions in human distal colon. *Int J Mol Sci*. 2020;21(15):5403.
67. Matsumoto K, Kurosawa E, Terui H, et al. Localization of TRPV1 and contractile effect of capsaicin in mouse large intestine: high

abundance and sensitivity in rectum and distal colon. *Am J Physiol Gastrointest Liver Physiol*. 2009;297(2):G348-360.
68. Rizopoulos T, Papadaki-Petrou H, Assimakopoulou M. Expression profiling of the Transient Receptor Potential Vanilloid (TRPV) channels 1, 2, 3 and 4 in mucosal epithelium of human ulcerative colitis. *Cells*. 2018;7(6):61.
69. Kun J, Szitter I, Kemény Á, et al. Upregulation of the transient receptor potential ankyrin 1 ion channel in the inflamed human and mouse colon and its protective roles. *PLoS One*. 2014;9(9):e108164.
70. Mihara H, Suzuki N, Boudaka AA, et al. Transient receptor potential vanilloid 4-dependent calcium influx and ATP release in mouse and rat gastric epithelia. *World J Gastroenterol*. 2016;22(24):5512-5519.
71. Kollmann P, Elfers K, Maurer S, Klingenspor M, Schemann M, Mazzuoli-Weber G. Submucosal enteric neurons of the cavine distal colon are sensitive to hypoosmolar stimuli. *J Physiol*. 2020;598(23):5317-5332.
72. Toledo Mauriño JJ, Fonseca-Camarillo G, Furuzawa-Carballeda J, et al. TRPV Subfamily (TRPV2, TRPV3, TRPV4, TRPV5, and TRPV6) gene and protein expression in patients with ulcerative colitis. *J Immunol Res*. 2020;2020:2906845.
73. Pritschow BW, Lange T, Kasch J, Kunert-Keil C, Liedtke W, Brinkmeier H. Functional TRPV4 channels are expressed in mouse skeletal muscle and can modulate resting Ca2+ influx and muscle fatigue. *Pflugers Arch*. 2011;461(1):115-122.
74. Hartmannsgruber V, Heyken W-T, Kacik M, et al. Arterial response to shear stress critically depends on endothelial TRPV4 expression. *PLoS One*. 2007;2(9):e827.
75. Xu H, Delling M, Jun JC, Clapham DE. Oregano, thyme and clove-derived flavors and skin sensitizers activate specific TRP channels. *Nat Neurosci*. 2006;9(5):628-635.
76. Ortar G, Morera L, Schiano Moriello A, et al. Modulation of thermo-transient receptor potential (thermo-TRP) channels by thymol-based compounds. *Bioorg Med Chem Lett*. 2012;22(10):3535-3539.
77. Nilius B, Biro T, Owsianik G. TRPV3: time to decipher a poorly understood family member! *J Physiol*. 2014;592(Pt 2):295-304.
78. Greco C, Leclerc-Mercier S, Chaumon S, et al. Use of epidermal growth factor receptor inhibitor erlotinib to treat palmoplantar keratoderma in patients with olmsted syndrome caused by TRPV3 mutations. *JAMA Dermatol*. 2020;156(2):191-195.
79. Peier AM, Reeve AJ, Andersson DA, et al. A heat-sensitive TRP channel expressed in keratinocytes. *Science*. 2002;296(5575):2046-2049.
80. Weiner ID, Verlander JW. Recent advances in understanding renal ammonia metabolism and transport. *Curr Opin Nephrol Hypertens*. 2016;25(5):436-443.
81. Stumpff F. A look at the smelly side of physiology: transport of short chain fatty acids. *Pflugers Arch*. 2018;470(4):571-598.
82. Braun HS, Sponder G, Pieper R, Aschenbach JR, Deiner C. GABA selectively increases mucin-1 expression in isolated pig jejunum. *Genes Nutr*. 2015;10(6):47.
83. Pieper R, Vahjen W, Neumann K, Van Kessel AG, Zentek J. Dose-dependent effects of dietary zinc oxide on bacterial communities and metabolic profiles in the ileum of weaned pigs. *J Anim Physiol Anim Nutr (Berl)*. 2012;96(5):825-833.

SUPPORTING INFORMATION

Additional Supporting Information may be found online in the Supporting Information section.

How to cite this article: Manneck D, Braun H-S, Schrapers KT, Stumpff F. TRPV3 and TRPV4 as candidate proteins for intestinal ammonium absorption. *Acta Physiol*. 2021;233:e13694. https://doi.org/10.1111/apha.13694

Supplemental Table A: primers, antibody, and alignment of different TRPV3 variants

Table A1 TRPV3 primers used in the study

Although all 4 primers produced a clear band at the expected level in gel electrophoresis and the amplification product could be confirmed by sequencing, only TRPV3d, which binds only to the long variant, produced a uniform melting curve and thus proved suitable for qPCR. Details see text.

Primer	Base pairs	Sense/antisense	Aminoacid sequence
TRPV3a	186	GCACGAAGGCTTCTACTTCG	HEGFYF
		ACGAAGTCGTTCTGCGTCTT	KTQNDF
TRPV3b	223	GAGCCTGTCCAGGAAATTCA	SLSRKF
		GAGGGTCAGGGTGATGTTGT	NITLTL
TRPV3c	230	ATGAAATGCTGACCCTGGAG	EMLTLE
		CCAGATGAGCACAAACATCC	MFVLIW
TRPV3d	202	ATGCTCATTGCCCTGATGGGAGAGAC	MLIALMGE
		ACTTCACCTCGTTGATCCGCAGACAC	CLRINEVK
Epitope ABIN863127			VSYYRPREVEALPHPL

Table A2 Different splice variants of four species

Species	Variant	Base pairs	Aminoacids	Gen Accession No.	Protein Accession No.
Homo sapiens	long	5930	791	NM_001258205.2	NP_001245134.1
Homo sapiens	short	-	-	-	-
Bos taurus	long	6369	798	XM_015458625.2	XP_015314111.1
Bos taurus	short	3237	526	NM_001099024.1	NP_001092494.1
Mus musculus	long	5708	791	NM_145099.3	NP_659567.2
Mus musculus	short	1964	565	XM_006533348.3	XP_006533411.1
Sus scrofa	long	3212	790	XM_005669116.3	XP_005669173.2
Sus scrofa	short	-	-	-	-

Table A3 Alignment of TRPV3 variants from four different species

Regions of interest (primers or antibody) are marked in colour as indicated above in Table A1

```
SUS SCROFA LONG      1    MNAHPKEMVPLVGKRAVIPSGNPAILQEKRPAEITPTKKSAHFFLEIEGFEPNPTVAKTS  60
MUS MUSCULUS LONG    1    ....S...A..M...TTA.G...VV.T.....DL.....................T...  60
BOS TAURUS LONG      8    .K.........T.R..T..FV....M.....S.............................  67
HOMO SAPIENS LONG    1    .K.........M...VAA........P.....................................  60
MUS MUSCULUS SHORT   1    ....S...A..M...TTA.G...VV.T.....DL.....................T...  60
BOS TAURUS SHORT     1    .K.........T.R..T..FV....M.....S.............................  60

SUS SCROFA LONG      61   PPIFSKPMDSNIRQCISGNCDDMDSPQSPQDDVTETPSNPNSPSAHLAKEEQRRKKKRLK  120
MUS MUSCULUS LONG    61   ...............L.............................N.......Q......  120
BOS TAURUS LONG      68   ...............V.............................N..............  127
HOMO SAPIENS LONG    61   ..V.....................................................R...  120
MUS MUSCULUS SHORT   61   ...............L.............................N.......Q......  120
BOS TAURUS SHORT     61   ...............V.............................N..............  120

SUS SCROFA LONG      121  KRIFAAVSEGCVEELVELLMELQELGKRRRGLDVSDFLMHKLTASDTGKTCLMKALLNIN  180
MUS MUSCULUS LONG    121  ...............R...QD..D.CR.......P.........................  180
BOS TAURUS LONG      128  ....T..........L...G.....C...HS...P.........L..............  187
HOMO SAPIENS LONG    121  ...................V.....CR..HDE..P.........................  180
MUS MUSCULUS SHORT   121  ...............R...QD..D.CR.......P.........................  180
BOS TAURUS SHORT     121  ....T..........L...G.....C...HS...P.........L..............  180

SUS SCROFA LONG      181  PNTKEVVRILLAFAEENDILDRFINAEYTEEAYRGQTALNIAIERRQGDITALLIHAGAD  240
MUS MUSCULUS LONG    181  .....I.............................E...................V..A....  240
BOS TAURUS LONG      188  .....I.............................E.................A..A....  247
HOMO SAPIENS LONG    181  .....I..............G............E................A....A....  240
MUS MUSCULUS SHORT   181  .....I.............................E...................V..A....  240
BOS TAURUS SHORT     181  .....I.............................E.................A..A....  240

SUS SCROFA LONG      241  VNAHAKGVFFNPKYQHEGFYFGETPLALAACTNQPEIVQLLMEHEQTDITSQDSRGNNIL  300
MUS MUSCULUS LONG    241  ..............................................N..............  300
BOS TAURUS LONG      248  ........................................M...N..............  307
HOMO SAPIENS LONG    241  .......A.....................................................R........  300
MUS MUSCULUS SHORT   241  ..............................................N..............  300
BOS TAURUS SHORT     241  ........................................M...N..............  300

SUS SCROFA LONG      301  HALVTVAEDFKTQNDFVKRVYDMILLRSGTWGLETTRNKDGLTPLQLAAKMGKAEILKYI  360
MUS MUSCULUS LONG    301  ...................M.........N.E...M..N.....................  360
BOS TAURUS LONG      308  ...................M.........R..E......N.....................  367
HOMO SAPIENS LONG    301  ...................M.........N.E......N.....................  360
MUS MUSCULUS SHORT   301  ...................M.........N.E...M..N.....................  360
BOS TAURUS SHORT     301  ...................M.........R..E......N.....................  360

SUS SCROFA LONG      361  LSREIKDKRLRSLSRKFTDWAYGPVSSSLYDLTNVDTTTENSVLEIIVYNTNIDNRHEML  420
MUS MUSCULUS LONG    361  ......E.P..............................D.....................  420
BOS TAURUS LONG      368  ......................................D.....................  427
HOMO SAPIENS LONG    361  ......E..............................D......T..............  420
MUS MUSCULUS SHORT   361  ......E.P..............................D.....................  420
BOS TAURUS SHORT     361  ......................................D.....................  420

SUS SCROFA LONG      421  TLEPLHTLLHMKWKKFAKYMFFLSFCFYFFYNITLTLVSYYRPREVEALPHPLALTHKMG  480
MUS MUSCULUS LONG    421  ..........T.....................................D.D.........S  480
BOS TAURUS LONG      428  ..............................................E..............  487
HOMO SAPIENS LONG    421  ..................H.........................E..I...........  480
MUS MUSCULUS SHORT   421  ..........T.................................D.D...........S  480
BOS TAURUS SHORT     421  ..............................................E..............  480

SUS SCROFA LONG      481  WLQLLGRMFVLIWAMCISVKEGIAIFLLRPSDLQSILSDAWFHFVFFVQAVLVILSVFLY  540
MUS MUSCULUS LONG    481  ...............T..............................................  540
BOS TAURUS LONG      488  ...............F.............................A............  547
HOMO SAPIENS LONG    481  ..............................................I............  540
MUS MUSCULUS SHORT   481  ..............T.............................LI              527
BOS TAURUS SHORT     481  ..............F.............................L               526

SUS SCROFA LONG      541  LFAYKEYLACLVLAMALGWANMLYYTRGFQSMGMYSVMIQKVILHDVLKFLFVYIVFLLG  600
MUS MUSCULUS LONG    541  ...........................................................L....  600
BOS TAURUS LONG      548  ...............................................................  607
HOMO SAPIENS LONG    541  ...............................................................  600
MUS MUSCULUS SHORT
BOS TAURUS SHORT
```

```
SUS SCROFA LONG     601  FGVALASLIEKCSKDNKDCTSYGSFSDAVLELFKLTIGLGDLNIQQNSKYPILFLFLLIT  660
MUS MUSCULUS LONG   601  ..............K...S.............................T...........  660
BOS TAURUS LONG     608  ............P.SHEN.S.....................................  667
HOMO SAPIENS LONG   601  ............P......S.....................................  660
MUS MUSCULUS SHORT
BOS TAURUS SHORT

SUS SCROFA LONG     661  YVILTFVLLLNMLIALMGETVEDVSKESERIWRLQRARTILEFEKMLPEWLRSRFRMGEL  720
MUS MUSCULUS LONG   661  ......................N.....................................  720
BOS TAURUS LONG     668  ......................N......................I..............  727
HOMO SAPIENS LONG   661  ......................N.....................................  720
MUS MUSCULUS SHORT
BOS TAURUS SHORT

SUS SCROFA LONG     721  CKVAEEDFRLCLRINEVKWTEWKTHVSFLNEDPGPGRRT-DFNKIQDSSRSNSKTTLNAF  779
MUS MUSCULUS LONG   721  ....D.............................I...A.L...............Y..  780
BOS TAURUS LONG     728  .....D................................A.S..................  787
HOMO SAPIENS LONG   721  .....D............................V...A..........N.........  780
MUS MUSCULUS SHORT
BOS TAURUS SHORT

SUS SCROFA LONG     780  DEMEEFPETSV  790
MUS MUSCULUS LONG   781  ..LD.......  791
BOS TAURUS LONG     788  E.ID.......  798
HOMO SAPIENS LONG   781  E.V........  791
MUS MUSCULUS SHORT
BOS TAURUS SHORT
```

References

Altschul SF, Madden TL, Schäffer AA, et al. Gapped BLAST and PSI-BLAST: a new generation of protein database search programs. *Nucleic Acids Res*. 1997; 25:3389-3402.

Altschul SF, Wootton JC, Gertz EM, et al. Protein database searches using compositionally adjusted substitution matrices. *FEBS J*. 2005; 272:5101-5109.

Supplemental Table B

NaCl Solutions used in Ussing chamber experiments

All solutions were adjusted to 300 mosmol•l^{-1} with mannitol and gassed with 95% CO_2 / 5% O_2.

(used in Fig. 5a and Table 3 (Ca^{2+}- switch) and Fig. 7 and 8 (TRP channel agonists))

	Mucosal (mmol·l^{-1})	Serosal (mmol·l^{-1})	Mucosal (mmol·l^{-1})	Mucosal (mmol·l^{-1})	Mucosal (mmol·l^{-1})	Serosal (mmol·l^{-1})
Item	**Standard**	**Standard**	**EDTA[1]**	**EGTA[1]**	**Ca^{2+}-free[2]**	**Ca^{2+}-free[2]**
NaCl	120	120	120	120	120	120
$NaHCO_3$	25	25	25	25	25	25
NaH_2PO_4	0.32	0.32	0.32	0.32	0.32	0.32
$MgSO_4$	1	1		1.15[3]	1	1
KCl	6.3	6.3	6.3	6.3	6.3	6.3
$CaCl_2$	2	2				
NMDGCl			4	4	4	4
EGTA				1		
EDTA			5			
Glucose		16				16
Mannitol	16		16	16	16	
pH	7.4	7.4	7.4	7.4	7.4	7.4

[1] solution used for the Ca^{2+}-switch on the mucosal side only
[2] nominally calcium free solution used for the bilateral mucosal and serosal Ca^{2+}-switch
[3] Magnesium was adjusted for chelation via EGTA to yield the same final magnesium concentration as in the standard NaCl Ringer using the program “Maxchelator”.
https://somapp.ucdmc.ucdavis.edu/pharmacology/bers/maxchelator/

Supplemental Table C:

Solutions used for Ussing chamber experiments with NH_4^+

All solutions were adjusted to 300 mosmol·l^{-1} with mannitol and gassed with 100% O_2.

(used in Fig 5, 6 and Table 4).

	Serosal (mmol·l^{-1})	Mucosal (mmol·l^{-1})			
Item	**NaCl**	**NaCl**	**20 NH_4Cl**	**40 NH_4Cl**	**40 NH_4Cl + EDTA**
NaCl*)	70	70	70	70	70
NaH_2PO_4	0.4	0.4	0.4	0.4	0.4
KCl	5	5	5	5	5
Glucose	5	5	5	5	5
NaGlu	30	30	30	30	30
NMDGCl*)	40	40	20		
$MgCl_2$	1.2	1.2	1.2	1.2	
$CaCl_2$	1.2	1.2	1.2	1.2	
Na_2HPO_4	2.4	2.4	2.4	2.4	2.4
MOPS	8				
MES		8	8	8	8
NH_4Cl*)			20	40	40
EDTA					5
pH	7.4	6.4	6.4	6.4	6.4

*) Chloride substituted by gluconate in experiments with low chloride Ringer

5. The TRPA1 Agonist Cinnamaldehyde Induces the Secretion of HCO_3^- by the Porcine Colon

The manuscript

Manneck, D., Manz, G., Braun, H.-S., Rosendahl, J., Stumpff, F., (2021): The TRPA1 Agonist Cinnamaldehyde Induces the Secretion of HCO_3^- by the Porcine Colon. Int J Mol Sci, 22:5198.

was published in International Journal of Molecular Sciences and can be accessed here: https://doi.org/10.3390/ijms22105198

Contribution	Contributor
Conceptualization	Stumpff, Manneck
Methodology	Stumpff, Braun, Manz, Manneck
Software	Stumpff
Validation	Braun, Manneck
Formal Analysis	Stumpff, Manneck
Investigation	Manz, Manneck
Resources	Stumpff, Rosendahl
Data Curation	Stumpff, Manneck
Writing—Original Draft Preparation	Stumpff, Manneck
Writing—Review and Editing	Stumpff, Braun, Rosendahl, Manz, Manneck
Visualization	Manneck
Supervision	Stumpff
Project Administration	Stumpff

License: https://creativecommons.org/licenses/by/4.0/

International Journal of
Molecular Sciences

MDPI

Article

The TRPA1 Agonist Cinnamaldehyde Induces the Secretion of HCO_3^- by the Porcine Colon

David Manneck [1], Gisela Manz [1], Hannah-Sophie Braun [2], Julia Rosendahl [2] and Friederike Stumpff [1,*]

[1] Department of Veterinary Medicine, Institute of Veterinary Physiology, Freie Universität Berlin, Oertzenweg 19b, 14163 Berlin, Germany; david.manneck@fu-berlin.de (D.M.); gisela.manz@fu-berlin.de (G.M.)
[2] PerformaNat GmbH, Hohentwielsteig 6, 14163 Berlin, Germany; hannah-sophie.braun@fu-berlin.de (H.-S.B.); rosendahl@performanat.de (J.R.)
* Correspondence: stumpff@zedat.fu-berlin.de; Tel.: +49-30-838-62595

Abstract: A therapeutic potential of the TRPA1 channel agonist cinnamaldehyde for use in inflammatory bowel disease is emerging, but the mechanisms are unclear. Semi-quantitative qPCR of various parts of the porcine gastrointestinal tract showed that mRNA for TRPA1 was highest in the colonic mucosa. In Ussing chambers, 1 mmol·L^{-1} cinnamaldehyde induced increases in short circuit current (ΔI_{sc}) and conductance (ΔG_t) across the colon that were higher than those across the jejunum or after 1 mmol·L^{-1} thymol. Lidocaine, amiloride or bumetanide did not change the response. The application of 1 mmol·L^{-1} quinidine or the bilateral replacement of 120 Na^+, 120 Cl^- or 25 HCO_3^- reduced ΔG_t, while the removal of Ca^{2+} enhanced ΔG_t with ΔI_{sc} numerically higher. ΔI_{sc} decreased after 0.5 NPPB, 0.01 indometacin and the bilateral replacement of 120 Na^+ or 25 HCO_3^-. The removal of 120 Cl^- had no effect. Cinnamaldehyde also activates TRPV3, but comparative measurements involving patch clamp experiments on overexpressing cells demonstrated that much higher concentrations are required. We suggest that cinnamaldehyde stimulates the secretion of HCO_3^- via apical CFTR and basolateral Na^+-HCO_3^- cotransport, preventing acidosis and damage to the epithelium and the colonic microbiome. Signaling may involve the opening of TRPA1, depolarization of the epithelium and a rise in PGE2 following a lower uptake of prostaglandins via OATP2A1.

Keywords: cinnamaldehyde; colon; colonic buffering; epithelial transport; essential oils; intestine; patch clamp; pig; prostaglandin; TRPA1; TRPV3; Ussing chamber

check for updates

Citation: Manneck, D.; Manz, G.; Braun, H.-S.; Rosendahl, J.; Stumpff, F. The TRPA1 Agonist Cinnamaldehyde Induces the Secretion of HCO_3^- by the Porcine Colon. *Int. J. Mol. Sci.* **2021**, *22*, 5198. https://doi.org/10.3390/ijms22105198

Academic Editor: Viktorie Vlachova

Received: 8 April 2021
Accepted: 10 May 2021
Published: 14 May 2021

Publisher's Note: MDPI stays neutral with regard to jurisdictional claims in published maps and institutional affiliations.

Copyright: © 2021 by the authors. Licensee MDPI, Basel, Switzerland. This article is an open access article distributed under the terms and conditions of the Creative Commons Attribution (CC BY) license (https://creativecommons.org/licenses/by/4.0/).

1. Introduction

The transient receptor potential ankyrin channel (TRPA1) is a non-selective member of the large family of transient receptor potential (TRP) channels that is expressed by sensory neurons, epithelia and a wide variety of other cells, where it plays a key role as a sensor of multiple external and internal stimuli. In comparison to most other members of the TRP channel family, TRPA1 has a fairly high permeability to Ca^{2+}, with $P(Na^+)/P(Ca^{2+}) \sim 6$, a value that can rise to about nine when the channel is opened by an agonist [1]. The selectivity for monovalent cations follows an Eisenman XI sequence with $Na^+ > K^+$ [2,3], with permeation dropping when Ca^{2+} or other divalent cations are present [4].

The name of the channel reflects the presence of 14–18 ankyrin repeats at its very long cytosolic NH_2 terminus, a distinct feature that is thought to be relevant for its promiscuous interaction with a very large number of dramatically different stimuli [1,2]. TRPA1 opens not only in response to intensive cold, but also to pungent compounds contained in certain plants, such as allyl isothiocyanate (AITC, contained in mustard oil), cinnamaldehyde and thymol. Furthermore, TRPA1 is a sensor for hyper- and hypoxia, various reactive oxygen species (ROS), H_2S, certain prostaglandins and an immense number of other chemical species and endogenous signals, many of which are associated with cell damage, and are

released in acute and chronic pain and inflammation. Accordingly, TRPA1 is involved in the pathophysiology of multiple organs [1,2].

A dominant role in the sensation pain is confirmed by the major symptom in the only TRPA1 channelopathy known at this point [5]. In what is known as Familial Episodic Pain Syndrome (FEPS), a gain of function mutation of TRPA1 causes episodes of severe pain localized principally to the upper body that are triggered by cold, fasting or physical stress. Interestingly, the baseline pain thresholds are not impaired. Furthermore, it has emerged that hyperalgesia can involve the direct action of mediators of oxidative stress on TRPA1 channels in addition to the classical receptor-mediated cascades [6–8].

The debate is ongoing concerning the function of TRPA1 in the intestinal tract. TRPA1 is expressed by sensory extrinsic and intrinsic afferent neurons that innervate the viscera [9–11], by intestinal myenteric and motor neurons which control motility [1,12,13], and by endocrine and transporting cells of the epithelial mucosa [14–16]. Although visceral symptoms have not been reported in gain of function mutations of TRPA1 [5], there is a clear association with visceral hypersensitivity which can be purely functional or associated with diseases such as colitis ulcerosa or Crohn's disease [10,17]. Apart from direct activation by prostaglandin and its metabolites [6–8], TRPA1 can also be activated by immunostimulatory cues such as the lipopolysaccharides (LPS) or outer wall glycolipids that are released by gram-negative bacteria after lysis [18]. Accordingly, in mouse models, tail-flick hyperalgesia and a fall in blood pressure is observed within a minute of LPS injection, which is clearly the result of the activation of neuronal afferents long before the production of immunomodulators such as TNF-α sets in [9,18].

Somewhat curiously and in contrast to their aversive role in signalling cellular damage in pain and inflammation, TRPA1 agonists in the form of spices have played an important role in the culinary arts for millenia [1]. Furthermore, grazers are known to show a preference for certain herbal compounds which activate TRPA1 and other TRP channels, but the reasons for this are unclear [19]. Having evolved to protect plants from bacteria, fungi and viruses, TRP channel modulators clearly have a multi-target antimicrobial potential [20]. However, the amounts that are voluntarily consumed by humans and animals are far lower than those required to achieve significant antibacterial effects.

In humans, the activation of TRPA1 has been suggested to lead to feelings of satiety after the ingestion of fragrant compounds found in spices such as cinnamaldehyde [21,22], allicin [23], menthol [24], or thymol [25], all of which directly activate the channel in vitro. Furthermore, these TRPA1 agonists were found to facilitate the secretion of cholecystokinin (CCK) and 5-HT from enteroendocrine cells (EEC), and thus to enhance the digestive response [26,27]. In addition, a growing body of literature suggests that TRPA1 agonists have anti-inflammatory effects with therapeutic potential in bowel diseases [20,28]. Thus, cinnamaldehyde was found to attenuate experimental colitis induced by 2,4,6-trinitrobenzene sulfonic or acetic acid in rat models of the human disease, with the reduction both of the symptoms and various markers of inflammation, such as TNF-α, myeloperoxidase and IL-6 [29,30]. While various signalling cascades are being discussed, it is striking that cinnamaldehyde activates TRPA1 with a specificity that surpasses that of the classical TRPA1 agonist AITC [1].

In farm animals, modulators of TRP channels in general and of TRPA1 in particular are increasingly being added to the feed of livestock as an alternative to antibiotic growth enhancers [31,32]. This is particularly important during weaning, during which young animals that have previously obtained readily digestible milk from their mothers are switched to diets rich in plant fiber. Because the structural carbohydrates contained in plants cannot be broken down by the mammalian enzymes found in the small intestine, after weaning, large quantities of undigested material suddenly begin to enter the caecum and the colon. Here, a growing community of bacteria and fungi break up previously undigested material, producing energy-rich short chain fatty acids that can then be absorbed and utilized by the young animal to produce glucose and other energy-rich carbohydrates within the liver [33,34]. However, in the process, large quantities of protons are set free and have

to be buffered in the hindgut lumen or within the cytosol to prevent epithelial damage. While the bacterial colonization of the hindgut is thus central for the survival and growth of the young animal, the transition can be harsh and many piglets develop inflammatory responses with severe or even lethal diarrhea [35,36].

Given the importance of the pig both in food production and as a model species for research on humans, it was the purpose of this study to compare the expression of TRPA1 in the various segments of the gastrointestinal tract via qPCR, and to identify segments with high expression. In order to assess the functional importance of TRPA1 in the segment with the highest level of expression, Ussing chamber experiments were performed on colonic epithelia using cinnamaldehyde, a classical agonist of TRPA1 with possible therapeutic potential [1,2,29,30]. Using the whole cell configuration of the patch clamp technique on HEK-293 cells overexpressing TRPV3, we investigated a potential additional contribution of TRPV3 to the cinnamaldehyde response [37]. A more detailed understanding of the mechanisms of action of this phytogenic substance could be useful for a better understanding of colonic function, but also for finding new therapy options for the rising number of individuals suffering from inflammatory bowel disease worldwide [38].

2. Results

2.1. PCR

RT-qPCR was used to investigate the relative amounts of mRNA encoding for TRPA1 in the gastrointestinal tissues of stomach (fundus and cardia), duodenum, jejunum, ileum, caecum, and colon of four pigs. The expression was analyzed in the mucosa and tunica muscularis; normalized to the reference genes ACTB, GAPDH, and YWHAZ; and scaled to the mean value of all of the samples. Messenger RNA encoding for TRPA1 could be detected in all of the gastrointestinal epithelia investigated except for the ileum. The expression of TRPA1 by the colonic epithelium varied strongly depending on the animal, and was significantly higher than that of all other epithelia, except for the duodenum and caecum. In contrast, any expression of TRPA1 by the muscular layers was under the limit of detection (Figure 1).

2.2. Ussing Chamber Studies

2.2.1. Effect of Cinnamaldehyde

Cinnamaldehyde is known as a classical agonist of TRPA1 with high specificity [1,2]. The functional expression of TRPA1 was tested via the response to the bilateral application of 100 $\mu mol \cdot L^{-1}$ or 1 $mmol \cdot L^{-1}$ cinnamaldehyde in the colon of two pigs with a total of five tissues in a first set of experiments. After an incubation period of 15 min, washout was performed. The addition of 100 $\mu mol \cdot L^{-1}$ cinnamaldehyde showed no effect on the short circuit current I_{sc} and tissue conductance G_t ($p > 0.1$) (Figure 2). Before the addition of cinnamaldehyde, the I_{sc} remained relatively constant with 0.69 ± 0.15 $\mu eq \cdot cm^{-2} \cdot h^{-1}$ immediately before addition, reaching a peak value of 0.66 ± 0.13 $\mu eq \cdot cm^{-2} \cdot h^{-1}$ within the 15 min period after the addition ($p > 0.1$). The conductance also essentially remained constant, with a value of 21.2 ± 4.14 $mS \cdot cm^{-2}$ before and 20.2 ± 3.57 $mS \cdot cm^{-2}$ 15 min after the addition of cinnamaldehyde ($p > 0.1$). Visible and statistically significant effects on I_{sc} and G_t were observed after the addition of cinnamaldehyde in a higher concentration. Within the 15 min period after the application of cinnamaldehyde in a concentration of 1 $mmol \cdot L^{-1}$, the I_{sc} increased from 1.10 ± 0.29 $\mu eq \cdot cm^{-2} \cdot h^{-1}$ to a peak value of 2.66 ± 0.49 $\mu eq \cdot cm^{-2} \cdot h^{-1}$, after which, in some tissues, a decline could be observed. The conductance rose continuously in all of the tissues from 23.1 ± 4.20 $mS \cdot cm^{-2}$ to 28.4 ± 5.42 $mS \cdot cm^{-2}$ at the end of the 15 min period (both $p < 0.05$). After the washout, I_{sc} returned to 1.31 ± 0.33 $\mu eq \cdot cm^{-2} \cdot h^{-1}$ and the conductance returned to 26.9 ± 6.60 $mS \cdot cm^{-2}$, values that were not significantly different from the baseline at the start of the experiment ($p > 0.1$). We also performed similar experiments in the jejunum, in which 1 $mmol \cdot L^{-1}$ cinnamaldehyde again led to significant rises in I_{sc} (ΔI_{sc}, $p = 0.029$) and a trend for a rise in G_t (ΔG_t, $p = 0.079$). Interestingly, the

effects tended to be smaller than those observed in the colon ($p = 0.015$ for ΔI_{sc} and $p = 0.063$ for ΔG_t) (see Supplementary Materials Figure S1).

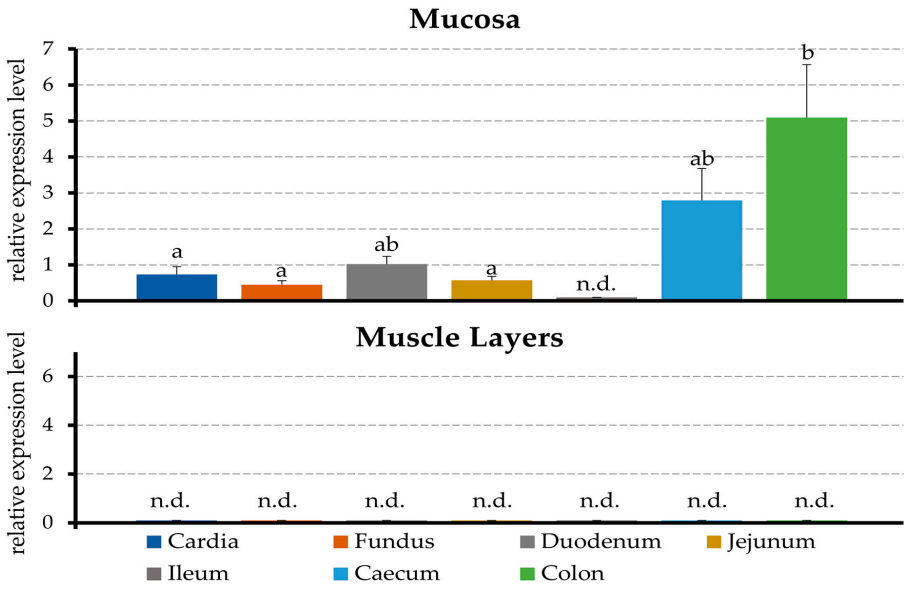

Figure 1. Relative mRNA expression of TRPA1 in the mucosa of the stomach (fundus and cardia), duodenum, jejunum, ileum, caecum and colon, and associated muscle layers of four young pigs from a controlled in-house study. Normalization was performed to the reference genes ACTB, GAPDH and YWHAZ, with scaling to the mean values of all of the samples. The letters above the bars indicate statistically significant differences between those bars that do not share a letter ($p < 0.05$) (n.d. = not detected).

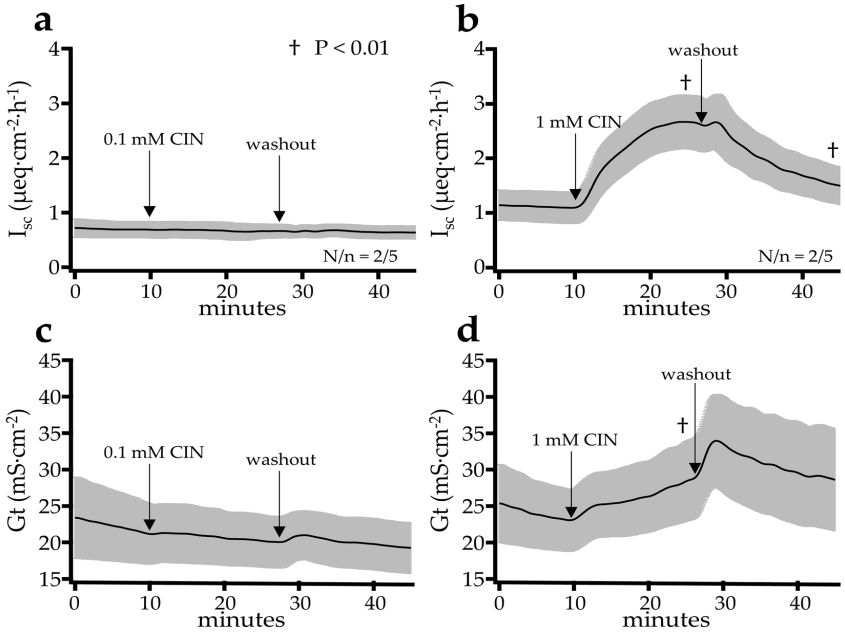

Figure 2. Effect of the TRPA1 agonist cinnamaldehyde at a concentration of 100 µmol·L^{-1} (**a**,**c**) and 1 mmol·L^{-1} (**b**,**d**) on I_{sc} and G_t in the Ussing chamber using the colonic tissue of young pigs (controlled in-house study). While the smaller concentration of 100 µmol·L^{-1} was insufficient, after the addition of 1 mmol·L^{-1}, a significant increase of the I_{sc} and G_t could be observed. After washout, the values dropped again. N/n = the number of animals/number of tissues, which was identical for G_t and I_{sc}.

In the next set of screening experiments, we examined the response to 1 mmol·L^{-1} cinnamaldehyde after the mucosal, serosal, or bilateral addition in the colon of five pigs with a total of nine or ten tissues per group (Figure 3). As in the previous series of experiments, we observed a rapid increase in I_{sc} from 0.59 ± 0.50 µeq·cm^{-2}·h^{-1} to peak values of 1.39 ± 0.71 µeq·cm^{-2}·h^{-1} (p = 0.016) within a 15 min period after the bilateral application of cinnamaldehyde, with a slightly slower increase in G_t from 24.8 ± 3.21 mS·cm^{-2} to 28.0 ± 2.83 mS·cm^{-2} (p = 0.006) at the end of the 15 min period. The same effect was also observed after the mucosal application, in which I_{sc} increased from 0.47 ± 0.23 µeq·cm^{-2}·h^{-1} to 1.09 ± 0.46 µeq·cm^{-2}·h^{-1} (p = 0.012) and G_t from 19.2 ± 1.81 mS·cm^{-2} to 21.8 ± 1.87 mS·cm^{-2} (p = 0.007). No effect on I_{sc} was observed after serosal application, which changed only slightly from 0.34 ± 0.24 µeq·cm^{-2}·h^{-1} to 0.34 ± 0.25 µeq·cm^{-2}·h^{-1} in the 15 min period (p = 0.85). G_t dropped from 23.2 ± 1.80 mS·cm^{-2} to 21.5 ± 1.46 mS·cm^{-2} during the same period (p = 0.013). However, the slope of the curve did not change after the application of cinnamaldehyde, so that this most likely reflects a baseline drift. Again, the response in the jejunum was different from that in the colon, where we observed increases in I_{sc} not only after mucosal and bilateral addition, but also after the serosal addition. Conversely, any effects of cinnamaldehyde on the G_t of the jejunum were subtle (see Supplementary Materials Figure S2).

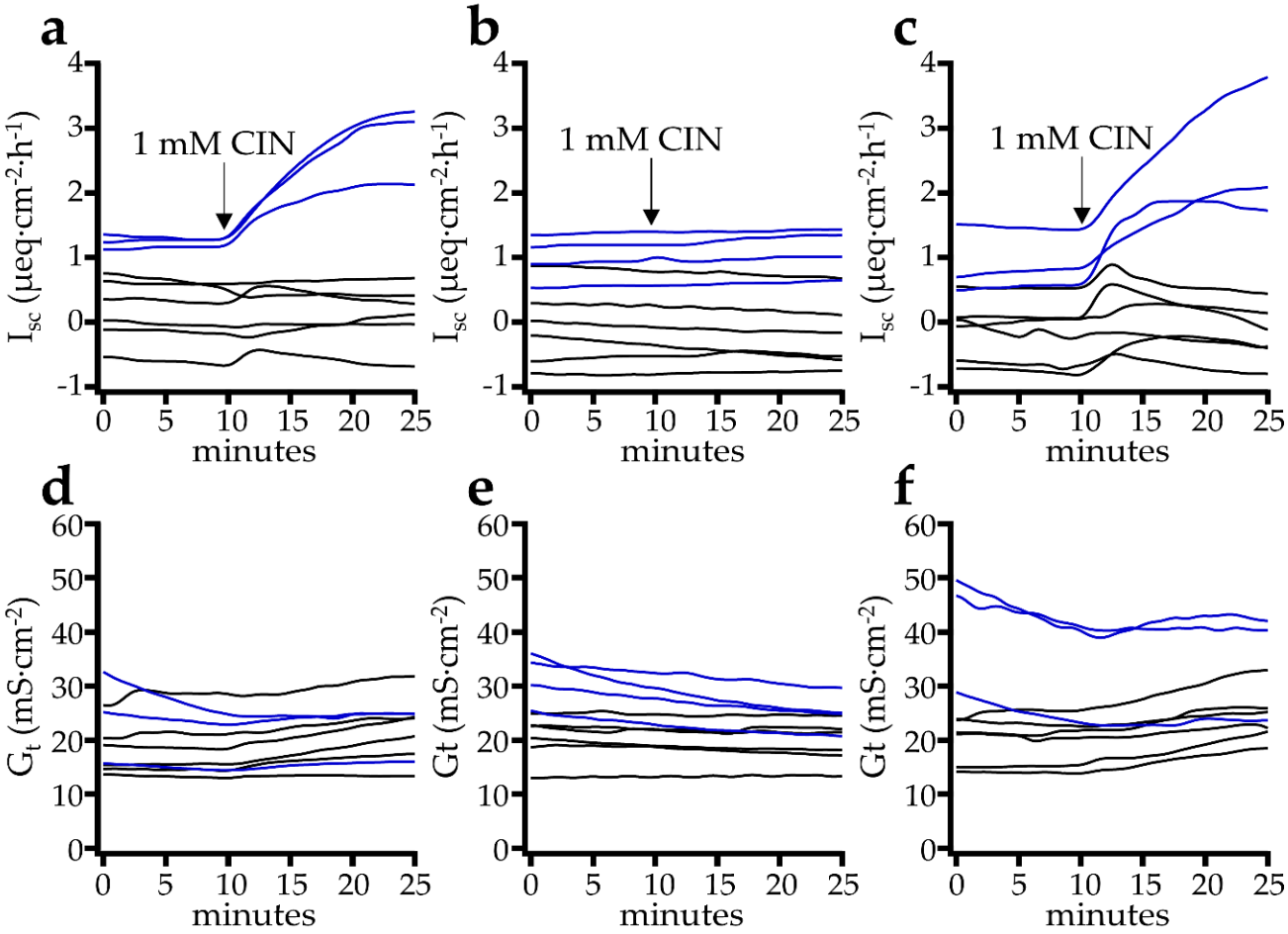

Figure 3. Effect of the TRPA1 agonist cinnamaldehyde (CIN) at a concentration of 1 mmol·L^{-1} after the mucosal (**a**,**d**), serosal (**b**,**e**) or bilateral addition (**c**,**f**) to I_{sc} and G_t in the Ussing chamber using the colonic tissue of pigs. After mucosal and bilateral addition, a significant increase in I_{sc} and G_t was observed, although the effects were absent after the serosal addition (details see text). In this figure, some tissues were obtained from older, larger pigs from a commercial slaughterhouse (blue lines), which showed a strong, sustained increase, while the black lines reflect the frequently biphasic responses that were seen in younger and smaller pigs slaughtered within a controlled study, as in the rest of the manuscript.

Finally, it should be mentioned that the tissues from three animals from a commercial slaughterhouse showed no response to cinnamaldehyde despite a positive reaction to theophylline (data not included). In these cases, there was a delay in the removal of the tissue from the carcass. It appears possible that cells from the absorptive surface epithelium (most exposed to gastrointestinal toxins and the major locus of TRPA1 expression [39]) were damaged more severely than the cells found within the crypts, where theophylline-induced secretion occurs. The subsequent experiments were therefore performed with tissues rapidly removed from piglets euthanized within a controlled study.

2.2.2. Effect of Blockers on the Cinnamaldehyde Response

In order to study the effect of cinnamaldehyde in a little more detail, we treated colonic tissues with different blockers 15 min before the addition of cinnamaldehyde to assess the response after the corresponding pretreatment. For each treatment, control tissues from the same animals were given the corresponding amount of solvent and served as a comparison. Delivery to the epithelium even in situations with the ample formation of mucus was ensured via bilateral application of cinnamaldehyde. The baseline parameters before and after the pretreatment are given in Table 1, while the data from before and after the cinnamaldehyde application are given in Table 2. The control values in the tables are the means of all of the control tissues used. The difference in the values before and after cinnamaldehyde application (ΔI_{sc} and ΔG_t) are given in the text, along with the respective control values. Because the animals in the different data sets showed individual variability, ΔI_{sc} and ΔG_t are also given as a percentage of the control value for each data set from the same group of animals in Figure 4.

Table 1. Baseline I_{sc} ($\mu eq \cdot cm^{-2} \cdot h^{-1}$) and G_t ($mS \cdot cm^{-2}$) in colonic tissue from young pigs (controlled in-house study) (baseline) and the peak value in the 15 min interval after the addition of blockers or ion replacement (treatment). For the concentrations and solutions, see Results and Supplementary Materials.

Treatment	N/n [1]	I_{sc} Baseline	I_{sc} Treatment	*p*-Value	G_t Baseline	G_t Treatment	*p*-Value
Control (all)	12/70	0.38 ± 0.056	0.37 ± 0.056	0.094	20.5 ± 0.62	20.3 ± 0.61	<0.001
Quinidine	4/21	0.39 ± 0.088	0.23 ± 0.085	<0.001	22.5 ± 1.02	19.9 ± 0.83	<0.001
Lidocaine	3/12	0.41 ± 0.070	0.27 ± 0.069	<0.001	23.6 ± 1.37	22.8 ± 1.10	0.151
Amiloride	3/15	0.55 ± 0.16	0.29 ± 0.15	<0.001	23.0 ± 1.65	21.3 ± 1.69	<0.001
Na^+ free bilat [2]	3/17	0.42 ± 0.066	−0.40 ± 0.052	<0.001	18.2 ± 1.58	8.9 ± 0.53	<0.001
Na^+ free muc [3]	5/28	0.34 ± 0.044	−0.69 ± 0.062	<0.001	17.6 ± 0.95	12.2 ± 0.39	<0.001
EGTA muc [2]	4/17	0.77 ± 0.16	0.95 ± 0.21	0.01	23.8 ± 1.38	28.5 ± 1.86	<0.001
Ca^{2+} free bilat [3]	5/14	0.98 ± 0.068	0.99 ± 0.065	0.819	19.3 ± 0.96	20.3 ± 0.86	0.011
Bumetanide	3/15	0.30 ± 0.11	0.19 ± 0.10	<0.001	20.1 ± 0.94	20.2 ± 0.90	0.528
NPPB	5/21	0.46 ± 0.10	0.26 ± 0.083	<0.001	21.9 ± 1.45	22.8 ± 1.53	0.008
Indometacin	3/9	0.24 ± 0.049	0.16 ± 0.036	0.04	22.6 ± 1.29	22.9 ± 1.39	0.212
Cl^- low [4]	5/30	0.29 ± 0.089	0.52 ± 0.071	0.050	21.5 ± 1.08	12.7 ± 0.99	<0.001
HCO_3^- free [4]	5/24	0.29 ± 0.089	0.59 ± 0.073	0.014	21.5 ± 1.08	14.1 ± 0.61	<0.001
HC-030031	3/7	0.33 ± 0.038	0.27 ± 0.028	0.028	17.7 ± 1.02	17.9 ± 1.15	0.813

[1] number of animals/number of tissues; [2] bilat = bilateral; [3] muc = mucosal; [4] test vs. control tissue.

Table 2. Cinnamaldehyde response in the colonic tissue from young pigs (controlled in-house study). The tissues were pretreated as indicated in the first column, yielding the values "I_{sc} treatment" ($\mu eq \cdot cm^{-2} \cdot h^{-1}$) and "$G_t$ treatment" ($mS \cdot cm^{-2}$) from Table 1. Subsequently, 1 $mmol \cdot L^{-1}$ cinnamaldehyde was added. The columns "I_{sc} cinn." ($\mu eq \cdot cm^{-2} \cdot h^{-1}$) and "$G_t$ cinn." ($mS \cdot cm^{-2}$) designate the peak value of the responses within a 15 min interval after the application of cinnamaldehyde.

Treatment	N/n [1]	I_{sc} Treatment	I_{sc} Cinn.	*p*-Value	G_t Treatment	G_t Cinn.	*p*-Value
Control (all)	12/70	0.38 ± 0.056	1.01 ± 0.10	<0.001	20.3 ± 0.61	24.4 ± 0.79	<0.001
Quinidine	4/21	0.23 ± 0.085	1.19 ± 0.21	<0.001	19.9 ± 0.83	21.7 ± 0.92	<0.001
Lidocaine	3/12	0.27 ± 0.069	1.05 ± 0.22	<0.001	22.8 ± 1.10	29.2 ± 1.44	<0.001
Amiloride	3/15	0.29 ± 0.15	1.29 ± 0.28	<0.001	21.3 ± 1.69	25.0 ± 1.96	<0.001

Table 2. *Cont.*

Treatment	N/n [1]	I_{sc} Treatment	I_{sc} Cinn.	*p*-Value	G_t Treatment	G_t Cinn.	*p*-Value
Na^+ free bilat [2]	3/17	−0.40 ± 0.052	−0.26 ± 0.060	0.002	8.90 ± 0.53	10.1 ± 0.58	<0.001
Na^+ free muc [3]	5/28	−0.69 ± 0.062	−0.19 ± 0.083	<0.001	12.2 ± 0.39	13.3 ± 0.43	<0.001
EGTA muc [2]	4/17	0.95 ± 0.21	2.13 ± 0.26	<0.001	28.5 ± 1.86	40.8 ± 3.36	<0.001
Ca^{2+} free bilat [3]	5/14	0.99 ± 0.065	1.78 ± 0.084	<0.001	20.3 ± 0.86	26.7 ± 1.56	<0.001
Bumetanide	3/15	0.19 ± 0.10	1.16 ± 0.27	<0.001	20.2 ± 0.90	25.2 ± 1.29	<0.001
NPPB	5/21	0.26 ± 0.083	0.71 ± 0.12	<0.001	22.8 ± 1.53	28.6 ± 2.19	<0.001
Indometacin	3/9	0.16 ± 0.036	0.54 ± 0.099	0.004	22.9 ± 1.39	30.6 ± 2.05	<0.001
Cl^- low [3]	5/30	0.52 ± 0.071	0.78 ± 0.10	<0.001	12.7 ± 0.99	16.1 ± 1.28	<0.001
HCO_3^- free [3]	5/24	0.59 ± 0.073	0.70 ± 0.11	0.054	14.1 ± 0.61	17.1 ± 0.61	<0.001
HC-030031	3/7	0.27 ± 0.028	0.91 ± 0.16	0.004	17.9 ± 1.15	22.3 ± 2.15	0.007

[1] number of animals/number of tissues; [2] bilat = bilateral; [3] muc = mucosal.

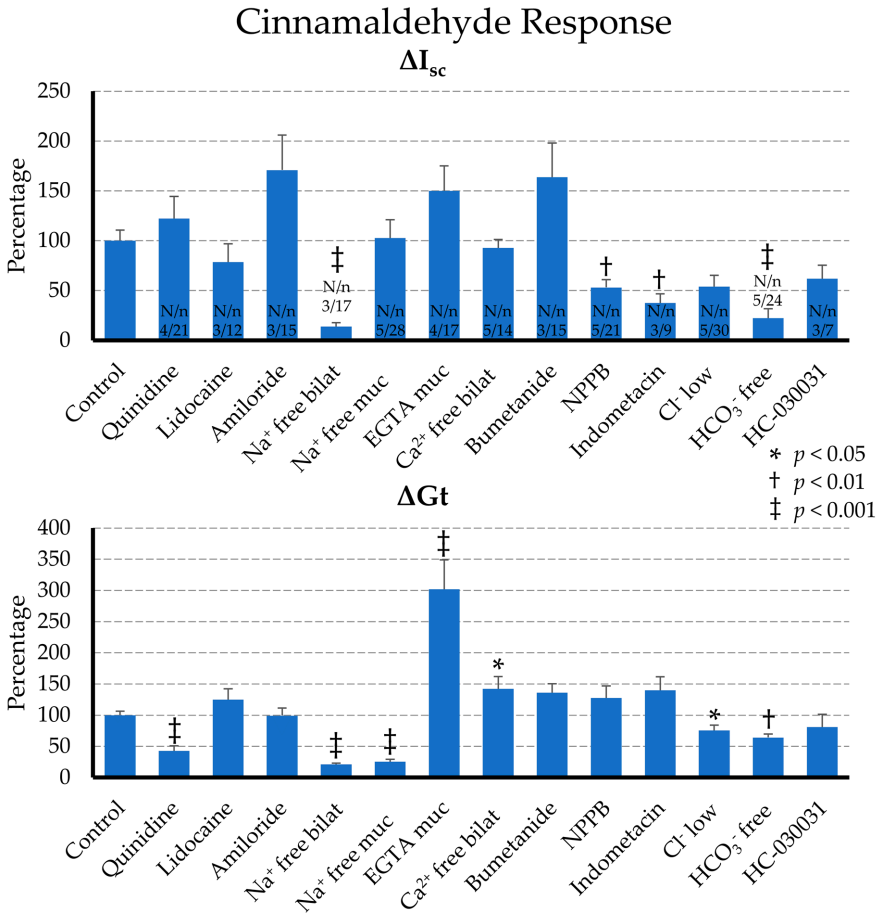

Figure 4. Comparison of the effect of cinnamaldehyde (1 mmol·L^{-1}) on the short circuit current (ΔI_{sc}) and the conductance (ΔG_t) of the colonic mucosa from young pigs (controlled in-house study) in Ussing chambers after preincubation with different blockers, or after the ion replacement. In order to allow a comparison of the data from different sets of experiments, the differences (deltas) were calculated by subtracting the peak value of the cinnamaldehyde response in the 15 min period after addition of cinnamaldehyde from the baseline value before addition. The delta values of the control tissues of each animal were set to 100%, and the deltas of the treated tissues were calculated as a percentage of the control tissues of the animal in question. Significant differences versus the control group are marked as *, †, or ‡ ($p < 0.05$, $p < 0.01$ or $p < 0.001$). For the concentrations of the blockers and the composition of the solutions used, see the results and the Supplementary Materials. N/n = number of animals/number of tissues, which were identical for G_t and I_{sc}; muc = mucosal; bilat = bilateral.

Neuronal involvement was tested in a first set of tissues (N/n = 3/12; number of animals/number of tissues), which were preincubated with serosal lidocaine (1 mmol·L^{-1}) before the bilateral addition of cinnamaldehyde (1 $mmol^{-1}$). The addition of lidocaine visibly decreased the baseline I_{sc} by $\Delta I_{sc} = -0.14 \pm 0.021$ μeq·cm^{-2}·h^{-1} ($p < 0.001$), with little change in G_t (which numerically shifted by $\Delta G_t = -0.87 \pm 0.50$ mS·cm^{-2}; $p = 0.15$) (Table 1). No response was seen in the control group (N/n = 3/12). After the addition of cinnamaldehyde, an identical increase in I_{sc} and G_t could be observed in both groups ($p > 0.1$). In the lidocaine group, I_{sc} increased by $\Delta I_{sc} = 0.78 \pm 0.18$ μeq·cm^{-2}·h^{-1} (or 78.6 ± 18.3% of the response of the control group, which was set to 100%), while the change in conductance (ΔG_t) was 6.41 ± 0.87 mS·cm^{-2} (or 125.0 ± 17.0% of the control; N/n = 3/12).

In a second set of tissues, preincubation with 1 mmol·L^{-1} mucosal quinidine was used (N/n = 4/21) as a blocker of non-selective cation channels. The addition of quinidine resulted in a significant decrease in the baseline I_{sc} by $\Delta I_{sc} = -0.17 \pm 0.022$ μeq·cm^{-2}·h^{-1}, and of G_t by $\Delta G_t = -2.52 \pm 0.35$ mS·cm^{-2} (both $p < 0.001$). After the subsequent addition of cinnamaldehyde, a ΔI_{sc} response of 0.96 ± 0.17 μeq·cm^{-2}·h^{-1} was observed, which remained at 122.4 ± 22.1% of the control (N/n = 4/23, $p > 0.1$). However, the ΔG_t response of 1.74 ± 0.34 mS·cm^{-2} (42.6 ± 8.3% of the control) was reduced strongly by more than half ($p < 0.001$).

Another set of epithelia was treated with 1 mmol·L^{-1} mucosal amiloride (N/n = 3/15), which decreased the baseline I_{sc} by $\Delta I_{sc} = -0.26 \pm 0.055$ μeq·cm^{-2}·h^{-1} and G_t by $\Delta G_t = -1.77 \pm 0.38$ mS·cm^{-2} (both $p < 0.05$), most likely reflecting a block of the epithelial sodium channel ENaC (SCNN1). After cinnamaldehyde addition, ΔI_{sc} was 1.00 ± 0.21 μeq·cm^{-2}·h^{-1} (170.8 ± 35.1% of the control, N/n = 3/8) and ΔG_t was 3.70 ± 0.45 mS·cm^{-2} (99.2 ± 12.2% of the control), both of which were not different from the control tissues ($p > 0.1$).

In order to selectively inhibit TRPA1, we used the antagonist HC-030031 with a concentration of 100 μmol·L^{-1} on both sides (N/n = 3/7). In rat colon, this concentration of HC-030031 blocked the cinnamaldehyde response [39]. Again, we observed a small but significant decrease in the baseline I_{sc} of $\Delta I_{sc} = -0.063 \pm 0.022$ μeq·cm^{-2}·h^{-1} after the preincubation period ($p = 0.028$), with the baseline G_t remaining unchanged ($p > 0.1$). The application of cinnamaldehyde (1 mmol·L^{-1}) resulted in a numerically smaller ΔI_{sc} of 0.63 ± 0.14 μeq·cm^{-2}·h^{-1} (or 61.8 ± 13.5% of the control, N/n = 3/18), but the effects did not show significance ($p = 0.138$). The ΔG_t remained at 4.41 ± 1.10 mS·cm^{-2} (81.0 ± 20.1% of the control).

An increase in I_{sc} may reflect either cation absorption or anion secretion, with the latter being classically driven by the Na^+-K^+-$2Cl^-$ cotransporter 1 (NKCC1) in the colon. Since NKCC1 is blocked by bumetanide, 1 mmol·L^{-1} were added to the serosal side (N/n = 3/15), which decreased the baseline I_{sc} by $\Delta I_{sc} = -0.10 \pm 0.023$ μeq·cm^{-2}·h^{-1} ($p < 0.001$). The baseline G_t was unchanged ($\Delta G_t = 0.035 \pm 0.23$ mS·cm^{-2}, $p > 0.1$). After the addition of cinnamaldehyde, I_{sc} increased by $\Delta I_{sc} = 0.96 \pm 0.20$ μeq·cm^{-2}·h^{-1} and G_t by $\Delta G_t = 5.07 \pm 0.53$ mS·cm^{-2}, values that were not different from the corresponding control (163.7 ± 34.4% and 135.9 ± 19.2%, respectively; $p > 0.1$, N/n = 3/8).

Further tissues were treated with the anion channel blocker NPPB at a concentration of 0.5 mmol·L^{-1} on the mucosal side (N/n = 5/21), which decreased the baseline I_{sc} by $\Delta I_{sc} = -0.20 \pm 0.047$ μeq·cm^{-2}·h^{-1} ($p < 0.001$) and the baseline G_t by $\Delta G_t = -0.95 \pm 0.32$ mS·cm^{-2} ($p < 0.008$). After the subsequent addition of cinnamaldehyde, a significantly smaller ΔI_{sc} was observed: 0.45 ± 0.07 μeq·cm^{-2}·h^{-1} (or 53.1 ± 7.87% of the control, $p = 0.06$). However, the ΔG_t response remained unchanged at 5.73 ± 0.86 mS·cm^{-2} (127.5 ± 19.2% of the control, N/n = 5/29).

In order to investigate whether the cinnamaldehyde response involves prostaglandin signalling, 10 μmol·L^{-1} indometacin was added to both sides to inhibit cyclooxygenases (N/n = 3/9). A slight decrease in the baseline I_{sc} level was observed by $\Delta I_{sc} = -0.079 \pm 0.032$ μeq·cm^{-2}·h^{-1} ($p = 0.04$), with no effect on G_t. In response to cin-

namaldehyde, a significantly smaller ΔI_{sc} of only 0.39 ± 0.10 μeq·cm^{-2}·h^{-1} or 37.5 ± 9.3% of the control was observed (p = 0.003, N/n = 3/18), while the ΔG_t of 7.63 ± 1.17 mS·cm^{-2} (140.1 ± 21.5% of the control) was not significantly changed by indometacin.

2.2.3. Effect of Ion Replacement on the Cinnamaldehyde Response

In a second experimental section, we replaced certain ions in the solutions in order to evaluate the effect of cations and anions on the cinnamaldehyde response (see Suplementary Materials Table S1). In the control tissues, a sham solution change was performed. Again, all of the results are summarized in Tables 1 and 2, and in Figure 4.

First, we switched to a Na^+-free solution 15 min before the addition of cinnamaldehyde on both sides (N/n = 3/17), replacing sodium with equivalent amounts of $NMDG^+$. This led to a sharp drop of I_{sc} by ΔI_{sc} = −0.81 ± 0.063 μeq·cm^{-2}·h^{-1} (or from 0.42 ± 0.066 to −0.40 ± 0.052 μeq·cm^{-2}·h^{-1}), while the G_t dropped by about half (ΔG_t = −9.30 ± 1.17 mS·cm^{-2}, from 18.2 ± 1.58 to 8.9 ± 0.53 mS·cm^{-2}, both $p < 0.001$). However, even in the bilateral absence of Na^+, an increase in I_{sc} and G_t could still be observed after the application of cinnamaldehyde of ΔI_{sc} = 0.14 ± 0.039 μeq·cm^{-2}·h^{-1} (p = 0.002) and ΔG_t = 1.16 ± 0.10 mS·cm^{-2} ($p < 0.001$), respectively. However, the magnitude of the response to cinnamaldehyde was strongly reduced, with ΔI_{sc} at 13.8 ± 3.8% of the control (N/n = 3/18) and ΔG_t at only 21.2 ± 1.84% of the control (both $p < 0.001$).

The replacement of Na^+ on the mucosal side only (N/n = 5/28) decreased the basal I_{sc} by ΔI_{sc} = −1.03 ± 0.076 μeq·cm^{-2}·h^{-1} (or from 0.34 ± 0.044 to −0.69 ± 0.062 μeq·cm^{-2}·h^{-1}) and the basal G_t by ΔG_t = −5.41 ± 0.77 mS·cm^{-2} (or from 17.6 ± 0.95 to 12.2 ± 0.39 mS·cm^{-2}) (both $p < 0.001$). After the addition of cinnamaldehyde, a G_t response occurred with a ΔG_t of 1.15 ± 0.17 mS·cm^{-2} ($p < 0.001$), which corresponded to 25.3 ± 3.67% of the control response (N/n = 5/29, $p < 0.001$). This response was identical to that observed after the bilateral removal of Na^+ (p = 0.96). In marked contrast, ΔI_{sc} was not affected, but remained at 0.51 ± 0.089 μeq·cm^{-2}·h^{-1}, or 102.8 ± 18.2% of the control ($p > 0.1$).

In the next step, we wanted to investigate the involvement of the divalent cation Ca^{2+}. For this purpose, a set of epithelia was changed mucosally to a calcium-free solution with EGTA (N/n = 4/17). Otherwise, the composition of the NaCl solution remained identical on both sides. The basal level I_{sc} increased by ΔI_{sc} = 0.18 ± 0.060 μeq·cm^{-2}·h^{-1} (p = 0.01), reflecting the stimulation of a transcellular transport mechanism. The conductance G_t increased by ΔG_t = 4.70 ± 0.85 mS·cm^{-2} ($p < 0.001$). The subsequent application of cinnamaldehyde induced a ΔI_{sc} of 1.18 ± 0.20 μeq·cm^{-2}·h^{-1} or 150.0 ± 25.1% of the control tissues from the pigs of the series (N/n = 4/17). When tested against all of the control tissues investigated (N/n = 12/70), this difference tested for significance (p = 0.022). The G_t response to cinnamaldehyde rose dramatically after the removal of calcium, with ΔG_t at 12.3 ± 1.92 mS·cm^{-2} or 301.8 ± 47.2% of the control ($p < 0.001$).

In a second similar set of experiments, we removed Ca^{2+} on both sides (N/n = 5/14). In order to prevent damage to the epithelium, the solution did not contain EGTA. No increase in the baseline I_{sc} was observed as a result of this pretreatment, although G_t increased by 1.05 ± 0.35 mS·cm^{-2} (p = 0.011). This suggests that here, too, the rate of transcellular transport must have increased to compensate for paracellular leak currents. The response to cinnamaldehyde did not change and ΔI_{sc} remained at 0.79 ± 0.072 μeq·cm^{-2}·h^{-1} (or 92.8 ± 8.37% of the control), although ΔG_t increased by 6.40 ± 0.87 mS·cm^{-2} (142.3 ± 19.4% of the control, p = 0.042).

The involvement of anions in the cinnamaldehyde response was tested by incubating the epithelia in a solution with a low Cl^- concentration (10.3 instead of 130.3 mmol·L^{-1}) or in a HCO_3^--free solution (buffered only with HEPES). Because these epithelia were incubated with the test solution from the beginning of the experiment, the baseline I_{sc} and G_t levels were compared to the control tissues.

Interestingly, the tissues in the low Cl^- solution (N/n = 5/30) had a higher mean baseline I_{sc} level of 0.52 ± 0.071 μeq·cm^{-2}·h^{-1} compared to the controls in a standard Ringer solution (0.29 ± 0.089 μeq·cm^{-2}·h^{-1}) (N/n = 5/29; p = 0.05), and an expectedly

lower G_t, which was 12.7 ± 0.99 mS·cm^{-2} rather than 21.5 ± 1.08 mS·cm^{-2} ($p < 0.01$). After cinnamaldehyde addition, a ΔI_{sc} response was observed that was numerically smaller than that of the control (0.26 ± 0.056 µeq·cm^{-2}·h^{-1} or 53.8 ± 11.5% of the control). The G_t increased by ΔG_t = 3.42 ± 0.38 mS·cm^{-2}, a value that was at 75.5 ± 8.3% of the control ($p = 0.037$).

The tissues that were incubated in parallel in the HCO_3^--free solution (N/n = 5/24) had a baseline I_{sc} of 0.59 ± 0.073 µeq·cm^{-2}·h^{-1}, which was again significantly higher than that of the controls mentioned above ($p = 0.014$). G_t was reduced to 14.1 ± 0.61 mS·cm^{-2} ($p < 0.01$). The response to cinnamaldehyde was strongly reduced, with ΔI_{sc} at 0.11 ± 0.046 µeq·cm^{-2}·h^{-1} in this group, or 22.3 ± 9.3% of the control ($p < 0.001$, N/n = 5/29). The ΔG_t of 2.90 ± 0.25 mS·cm^{-2} was at 64.2 ± 5.53% of the control ($p = 0.005$).

It is interesting to rank the effects of the removal of the ions on the cinnamaldehyde response in comparison to the effect in a standard Ringer solution using values from all of the controls studied (N/n = 12/70). The values of ΔI_{sc} increased in the order HCO_3^--free < Na^+-free < low Cl^- < standard Ringer < EGTA, with mean values of 0.11 ± 0.046^a, 0.14 ± 0.039^{ab}, 0.26 ± 0.056^b, 0.63 ± 0.067^c and 1.18 ± 0.20^d µeq·cm^{-2}·h^{-1}, respectively, in which the values that do not share a superscript are significantly different. The values of ΔG_t ranked in the order Na^+-free < HCO_3^--free < low Cl^- < standard Ringer < EGTA and were 1.16 ± 0.10^a, 2.90 ± 0.25^b, 3.42 ± 0.38^{bc}, 4.11 ± 0.31^c, 12.3 ± 1.92^d mS·cm^{-2}.

2.2.4. Effect of Thymol

In further experiments, the response to the herbal diterpene thymol was investigated. Thymol is known as an agonist of TRPM8, TRPV3 and TRPA1. A first set of screening experiments revealed that, as with cinnamaldehyde, thymol only showed effects after the mucosal or bilateral application in the colon, but not after the serosal application (all N/n = 2/4) (see Supplementary Materials Figure S3).

The response to the bilateral application of thymol was studied more rigorously in colonic tissues from 10 pigs. As before, a robust rise in G_t could be observed in all of the tissues studied (Figure 5, $p < 0.001$ colon). The effects of thymol on the short circuit current I_{sc} were quite variable. In colonic tissues from three pigs, I_{sc} went up; in six other pigs, I_{sc} went down; in one pig, the responses depended on the individual tissue (three down, one up). The means of the tissues that responded to thymol with a pronounced increase in I_{sc} ("up") are shown in Figure 5a ($p = 0.016$, N/n = 4/7), while the means of the tissues in which I_{sc} dropped ("down") are shown in Figure 5b ($p < 0.001$, N/n = 7/11).

Similar effects were observed in the jejunum (see Supplementary Materials, Figure S4, N/n = 10/18) and in the caecum (data not shown, N/n = 2/4).

2.3. Patch Clamp Studies

The effects of cinnamaldehyde on TRPA1 in overexpressing cells are extremely well documented [1,2]. However, one study has described the fact that cinnamaldehyde can activate TRPV3 in addition to TRPA1 [37], raising questions concerning its specificity. Accordingly, the effect of cinnamaldehyde on TRPV3 was studied using HEK-293 cells transfected with the human variant of TRPV3. As control cells, cells were transfected with the empty vector, essentially as described previously [40,41]. Cells were also treated with thymol, so that a subsequent comparison of the relative response of the TRPV3 expressing cells and the colonic tissues to cinnamaldehyde and thymol was possible.

The successful transfection of the cells was detected in a first step by the immunohistochemical staining of TRPV3 in the transfected HEK-293 cells. The transfected hTRPV3 cells showed green staining of the cytosol, reflecting co-expression of green fluorescent protein (GFP) as well as a red staining of the cell membrane, demonstrating the successful expression of the TRPV3 channel protein (Figure 6a). The control cells only showed green cytosolic staining (not shown). The transfected hTRPV3 and control cells were then examined with patch-clamp experiments under whole-cell conditions.

In a first series of experiments, cinnamaldehyde was applied to the cells in the concentration used in the Ussing chamber experiments (1 mmol·L^{-1}), which did not yield significant effects. In a second series, a higher concentration of 5 mmol·L^{-1} cinnamaldehyde was added to the cells, followed by a washout. At the end of the experiment, the addition of 1 mmol·L^{-1} thymol, which is a strong agonist of TRPV3, served as a control reaction. No response to 5 mmol·L^{-1} cinnamaldehyde was observed in hTRPV3 cells at 23 °C, although these cells reacted strongly to 1 mmol·L^{-1} thymol (Figure 6b). At 37 °C, a slowly increasing current was measured after the addition of cinnamaldehyde (5 mmol·L^{-1}), which decreased again after the washout. However, the response was discrete when compared to the response to 1 mmol·L^{-1} thymol (Figure 6c). In contrast, the control cells (also measured at 37 °C) showed no effect from either of the two agonists.

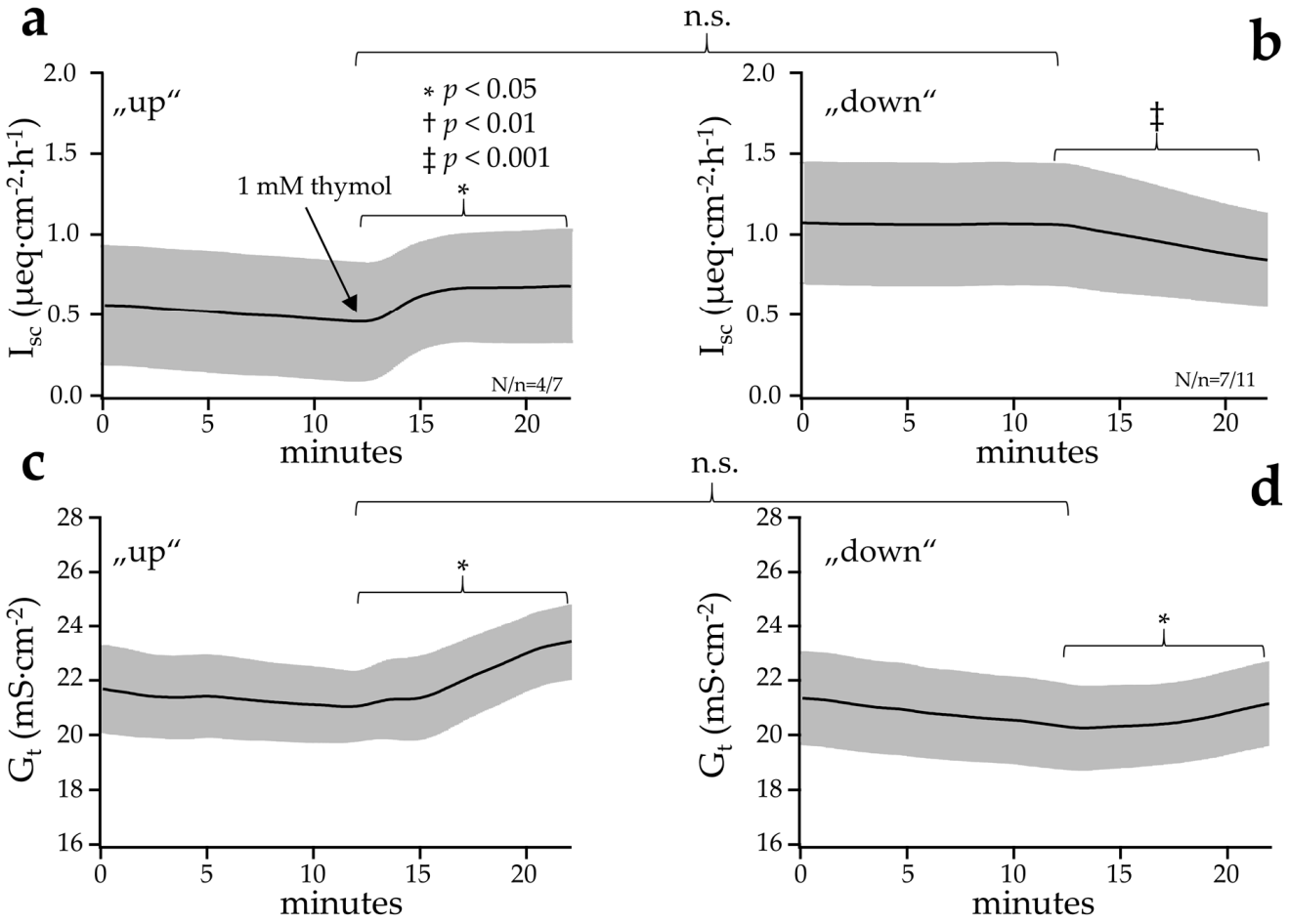

Figure 5. Effect of a bilateral application of thymol on the I_{sc} and G_t of the colon of ten young pigs (controlled in-house study). The data are given as means ± SEM. In some of the tissues, an increase ("up") in I_{sc} could be observed after the addition of thymol (**a**), whereas in other tissues a decrease or no effect ("down") was observed (**b**). An increase in G_t was observed in all of the tissues after the addition of thymol, ruling out barrier effects for increases in I_{sc} (**c**,**d**). The significance bars within graphs compare values taken immediately prior to addition of the agonist and after an incubation of 10 min. The significance bars between graphs indicate that in the colon, there was no difference between the "up" and the "down" groups before thymol was added. Significant differences are marked as *, †, or ‡ ($p < 0.05$, $p < 0.01$ or $p < 0.001$).

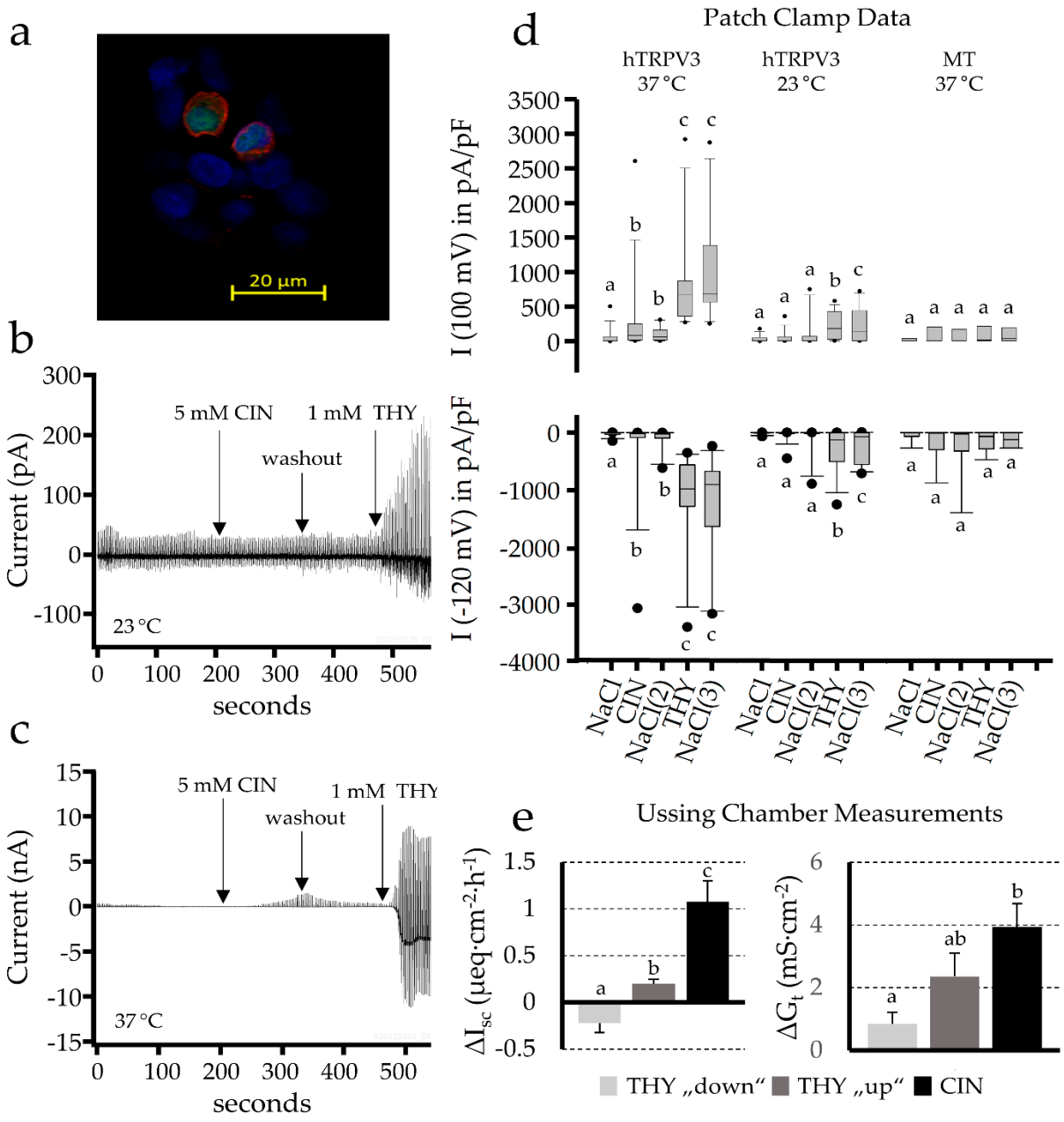

Figure 6. (**a**) Immunohistochemical staining of HEK-293 cells transfected with a vector for the simultaneous overexpression of human TRPV3 and green fluorescent protein (GFP, green), stained with a specific antibody against TRPV3 (red). The cell nuclei were stained with DAPI (blue). (**b**) An original recording of a patch clamp measurement of an hTRPV3 HEK-293 cell at 23 °C. No visible response was seen after the addition of 5 mmol·L^{-1} cinnamaldehyde (CIN), whereas 1 mmol·L^{-1} thymol (THY) elicited a clear response. (**c**) A patch clamp measurement of an hTRPV3 HEK-293 cell at 37 °C. The concentration of cinnamaldehyde had to be elevated to 5 mmol·L^{-1} before a small response could be observed. In contrast, at 1 mmol·L^{-1}, the effects of the thymol were very strong. (**d**) A boxplot of patch clamp data from hTRPV3 HEK-293 cells at 37 °C and 23 °C, and from control cells transfected with the empty vector (MT, 37 °C) at +100 mV and −120 mV. Within a group, significant differences after the addition of cinnamaldehyde or thymol and the subsequent washouts (NaCl(2) and NaCl(3)) are indicated via different letters above the bars. Comparisons between the groups are given in the main text (**e**) Data from Ussing chamber experiments from a subset of seven young pigs from Figure 5 (controlled in-house study), treated in parallel with either thymol (N/n = 7/13) or cinnamaldehyde (N/n = 7/14). In the native colonic tissues, 1 mmol·L^{-1} of cinnamaldehyde was sufficient to induce a clear change in the short circuit current and the conductance, which rose by ΔI_{sc} and ΔG_t, respectively. For comparison, the data for thymol (1 mmol·L^{-1}) are also shown. Here, the I_{sc} responses were clearly smaller, but diverse, with some tissues showing an increase in I_{sc} ("up", N/n = 4/7) and others a decrease ("down", N/n = 4/6). Bars that do not share a letter are significantly different.

Under the baseline conditions, the three groups of cells (hTRPV3 at 23 °C (N = 8), hTRPV3 at 37 °C (N = 14) and the control at 37 °C (N = 8)) did not show different currents at +100 mV and −120 mV pipette potential, respectively (Figure 6d). No effect was observed in the control group at 37 °C or in the hTRPV3 group at 23 °C. In hTRPV3 at 37 °C, the addition of cinnamaldehyde induced a significant increase in the Na^+ efflux from the pipette into the bath solution at +100 mV, which rose from 60 ± 35 pA·pF^{-1} to 284 ± 181 pA·pF^{-1} ($p < 0.001$ vs. the baseline and $p = 0.015$ vs. 23 °C), as well as an increase in the Na^+ influx from the bath solution into the pipette at −120 mV (from −27 ± 11 pA·pF^{-1} to −268 ± 217 pA·pF^{-1}, $p = 0.009$ vs. the baseline and $p = 0.052$ vs. 23 °C). After the washout, the currents in the hTRPV3 37 °C group decreased numerically at 100 mV (to 100 ± 31 pA·pF^{-1}) and at −120 mV (to −113 ± 54 pA·pF^{-1}), but they were still significantly higher than they were initially. In contrast to the 5 mmol·L^{-1} required to induce a response to cinnamaldehyde, a concentration of 1 mmol·L^{-1} thymol caused significant increases in the currents at 100 mV and −120 mV in both hTRPV3 groups, although the current increase was significantly greater in the 37 °C cells ($p < 0.001$ and $p = 0.002$). This difference makes sense because the TRPV3 is activated at warm temperatures (≥32 °C) [42–44].

For comparison, the Ussing chamber data of the colonic epithelia from a subset of seven pigs that were treated in parallel in separate chambers with either thymol or with cinnamaldehyde were used. The epithelia that responded to thymol (1 mmol·L^{-1}) with an increase in current (N/n = 4/7) were compared to the data from the same pigs treated with cinnamaldehyde (1 mmol·L^{-1}) (N/n = 7/14) (Figure 6e). The responsive tissues with a "down" response (N/n = 4/6) to thymol are included in the graph, but they were even smaller.

In summary, the maximal ΔI_{sc} after the addition of cinnamaldehyde (1.08 ± 0.22 µeq·cm^{-2}·h^{-1}) was significantly higher than after the thymol addition (0.20 ± 0.046 µeq·cm^{-2}·h^{-1}) ($p = 0.002$). The ΔG_t, which reflects both the secretion of K^+ and the absorption of Na^+ and Ca^{2+}, was similar (2.36 ± 0.74 mS·cm^{-2} for 1 mmol·L^{-1} thymol and 3.94 ± 0.75 mS·cm^{-2} for 1 mmol·L^{-1} cinnamaldehyde). In contrast, in the patch clamp experiments on TRPV3 expressing cells, a five-fold higher concentration of 5 mmol·L^{-1} cinnamaldehyde was required to observe a significant response. This response was small and much lower than the response to 1 mmol·L^{-1} thymol. It thus appears that TRPV3 only plays a marginal role, if any, in the response of the colonic epithelium to 1 mmol·L^{-1} cinnamaldehyde.

3. Discussion

As outlined in the introduction, TRPA1 agonists are emerging as promising pharmacological tools in the modulation of intestinal function in health and disease [20,32]. Despite this, only a handful of studies have systematically investigated the interaction of TPRA1 agonists with native gastrointestinal epithelia [14,16,39,45].

Because systematic quantitative studies of TRPA1 expression by the gastrointestinal tract seem to be lacking, we wished to find out more about the relative expression of TRPA1 along the porcine gastrointestinal tract via semiquantitative qPCR. In the second part, we studied the electrophysiological effects of the classical and therapeutically promising TRPA1 agonist cinnamaldehyde on epithelia in Ussing chambers. Although some of the experiments were performed on tissues from the porcine jejunum, the primary focus was on the colon as a major locus of fermentation and of inflammatory bowel disease, which also happened to be the tissue with the highest expression of mRNA for TRPA1. Finally, some patch clamp experiments were performed on overexpressing cells in order to assess a possible contribution of TRPV3 to the cinnamaldehyde response [37].

3.1. Expression of mRNA for TRPA1 by the Tissues of the Porcine Gastrointestinal Tract

In a first step, semiquantitative PCR was used to investigate the distribution of TRPA1 in various segments of the gastrointestinal tract, namely the fundus and cardia of the stomach, duodenum, jejunum, ileum, caecum, and (middle) colon (Figure 1). The signals

for TRPA1 in the muscular layers were below the detection level. With the curious exception of the ileum, the mucosa of all of the sections showed a clear expression of TRPA1, with the expression rising in the distal segments and highest in the colon. This finding is in agreement with immunohistochemical data showing that TRPA1 is expressed along the entire gastrointestinal tract of various species [11,27,39,46].

3.2. Effect of Blockers on I_{sc} and G_t in Ringer

Evidence for the functional expression of TRPA1 by the colon was obtained by applying various blockers to colonic epithelia in Ussing chambers. (Table 1). Quinidine is a highly potent, although unspecific, blocker of numerous cation channels, while HC-030031 is considered to be specific for TRPA1. Both blockers significantly reduced the baseline I_{sc} and G_t (Table 1 and Figure 7a). Conversely, the removal of Ca^{2+} can be expected to enhance the permeation of monovalent cations through TRP channels such as TRPA1 and TRPV3 [4]. In line with this, the mucosal replacement of Ca^{2+} with EGTA induced a highly significant increase of baseline G_t and I_{sc} (Table 1). Because the experiments were carried out in symmetrical solutions with no chemical gradient present, the rise in I_{sc} clearly reflects transcellular transport, most likely energized by the basolateral Na^+/K^+-ATPase. In addition, the removal of Ca^{2+} is known to enhance the permeability of the paracellular pathway by the decoupling of tight junction proteins [47,48], which may explain part of the rise in G_t.

The effects of the other treatments in Table 1 can be understood with textbook models of colonic transport [49]. The functional expression of ENaC (SCNN1) emerges from the amiloride response, while the effects of bumetanide point toward the basolateral expression of NKCC1, which drives the influx of Cl^- for secretion via NPPB-sensitive apical Cl^- channels (Figure 7c). These channels close when cAMP production is reduced after the application of the cyclooxygenase inhibitor indometacin, all of which is classically established [49].

3.3. Mucosal Cinnamaldehyde Induces an Increase in I_{sc} and G_t

In a second step, the effect of cinnamaldehyde on stripped epithelium from the jejunum and the colon was investigated in Ussing chambers (Figure 2 and Supplementary Material Figure S1).

Unlike in previous studies of rat colon [16,39] or porcine jejunum [45], the application of cinnamaldehyde in a concentration of 100 $\mu mol \cdot L^{-1}$ did not result in significant changes in the electrophysiological parameters. This may reflect the particularly thick mucus layer protecting the porcine colon, in conjunction with a partial degradation of cinnamaldehyde by the resident microbials. However, when applied at 1 $mmol \cdot L^{-1}$, significant increases in I_{sc} could be observed in both the colonic (Figure 2) and jejunal epithelia (Supplementary Materials Figure S1). Because, in our study, the colonic and jejunal responses from the same animals were monitored in parallel, they could be directly compared, and it emerged that the responses of the jejunum to cinnamaldehyde were significantly smaller in both ΔG_t and ΔI_{sc}. It is an attractive hypothesis that this reflects the lower expression of TRPA1 in this segment (Figure 1).

The jejunum responded not only to mucosal or bilateral application but also to the serosal application of cinnamaldehyde. In a previous study of porcine jejunum, the cinnamaldehyde response was inhibited by hexamethonium, but not by TTX. Conversely, the effects of thymol could be completely blocked by TTX [45]. It appears that an interplay of neuronal and epithelial TRP channels regulate the electrophysiological response of the jejunum in a complex manner that we did not attempt to unravel in the present study.

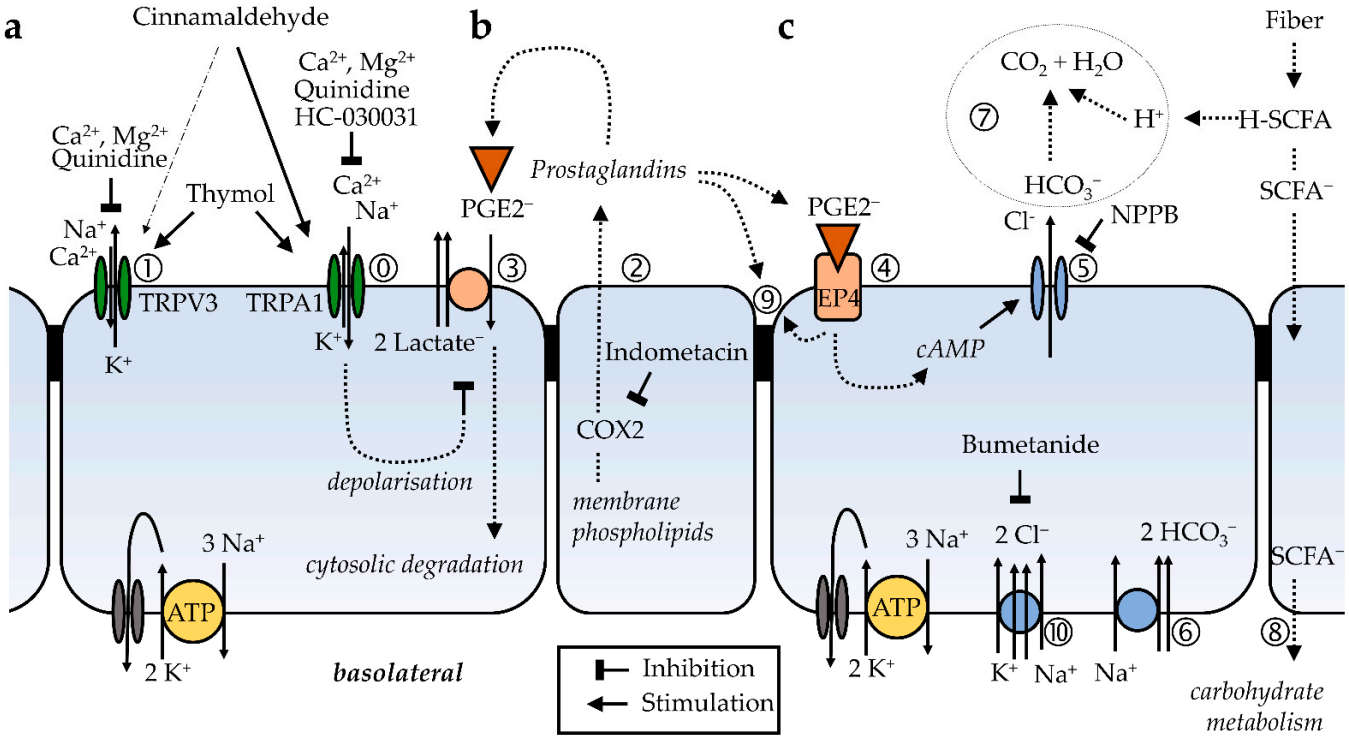

Figure 7. Model of the effects of cinnamaldehyde on the colon, based on the present study and the current literature. (**a**) Cinnamaldehyde opens apical, non-selective TRPA1 channels in the colonic mucosa near the lumen (⓪). The selectivity filter of the channel allows both the influx of Na^+ and Ca^{2+}, and a smaller efflux of K^+, so that the effects on I_{sc} are small. However, the cell is depolarised and a significant increase in conductance ΔG_t is observed, which is reduced by quinidine and enhanced by the removal of divalent cations. The effects of cinnamaldehyde on TRPV3 (①), which favors efflux of K^+ over influx of Na^+ and Ca^{2+}, are discrete. Thymol opens both channels. (**b**) Prostanoids such as PGE2 are anions that are synthesized from membrane phospholipids via cyclooxygenase-mediated pathways and secreted into the extracellular space via pathways that are being explored (②). For prostanoid signalling to end, the anionic prostaglandin has to be taken up into the cytosol via an electrogenic anion exchanger, OATP2A1 (SLCOA1) (③), after which the prostaglandin is degraded by cytosolic enzymes. Due to the electrogenic nature of the cotransporter, the depolarization of the cellular membrane, as occurs after the opening of TRPA1 channels via cinnamaldehyde (⓪), decreases the uptake of prostaglandins and thus increases the extracellular prostaglandin concentration. (**c**) After the binding of the PGE2 to EP4 receptors (④) expressed by the colonic mucosa, adenylyl cyclase is stimulated, resulting in rising levels of cAMP that open apical CFTR channels (⑤). Other anion channels may contribute to the secretion of HCO_3^-, which is driven by the uptake of Na^+ via basolateral NBCn1 (Slc4a7), NBCe1 (SLC4A4), or NBCe2 (Slc4a5) at a ratio of 1, 2 or 3 HCO_3^- for each Na^+ (⑥). Most of the NPPB-sensitive rise in I_{sc} that is observed after the activation of TRPA1 via cinnamaldehyde can be explained by this mechanism. The secretion of HCO_3^- is important for the buffering of protons formed in the fermentational process (⑦), and for the unfolding of mucines in the mucus layer, thus protecting the epithelium. Energy-rich short chain fatty acid anions ($SCFA^-$) are absorbed via various transport proteins (⑧) without challenging cytosolic pH homeostasis. In physiological concentrations, prostaglandins are also thought to have barrier-enhancing properties through interaction with tight junction proteins (⑨). Possibly, the secretion of HCO_3^- is highest in cells near the surface, while in the crypts, the expression of NKCC1 (SLC12A2) (⑩) predominates. The latter pathway leads to the secretion of Cl^- via CFTR, which can result in diarrhea when cAMP levels are pathologically high. Because the gradients favor a unilateral efflux of anions, the opening of CFTR will have higher effects on ΔI_{sc} than those after the opening of TRPA1.

In the colon, the effects were more straightforward because the serosal application of cinnamaldehyde showed no effect (Figure 3). While the serosal application of lidocaine as a blocker of neuronal Na^+ channels changed the baseline I_{sc} and G_t of the colonic epithelium (Table 1), underlining the importance of neuronal signalling for the regulation of transport function, the subsequent response of the tissue to cinnamaldehyde was not altered by pretreatment with lidocaine (Figure 4 and Table 2). Likewise, in previous investigations

of rat and human colon, agonists of TRPA1 were most effective when given mucosally, while preincubation with tetrodotoxin did not affect the response of the tissues to AITC, to cinnamaldehyde or to thymol [14,16,39]. In conjunction, these results suggest that the response of the colon to cinnamaldehyde involves mucosal receptors, with TRPA1 channels, as expressed by the apical membrane of human or rat colonocytes [39] being likely candidates.

3.4. Does Cinnamaldehyde Activate TRPV3?

Although it is generally considered to be specific for TRPA1, one study has suggested that cinnamaldehyde also opens TRPV3 channels [37]. TRPV3 is expressed by the apical membrane of colonocytes not only in rats and humans [50], but also in the pig (Manneck et al., submitted). Because commercially available specific agonists or inhibitors of TRPV3 are still in the process of being developed [51], we compared the responses of thymol (which strongly activates TRPV3 [25,41]) to those to cinnamaldehyde using Ussing chamber experiments on native epithelia and patch clamp experiments with overexpressing cells.

Previous studies of the thymol response in rat colon have shown a strong rise in I_{sc} and G_t, resembling the response to cinnamaldehyde, although the signalling differed [14,39]. In porcine colon, the responses to thymol were highly variable, with both increases in I_{sc} and decreases observed, in marked contrast to the uniform responses observed in parallel in tissues from the same pigs after the application of cinnamaldehyde. While changes in the barrier function may have contributed, the selectivity of TRPV3 to Ca^{2+} is poor, and it follows an Eisenman sequence IV with $P(K^+) > P(Na^+)$ [4,40], while TRPA1 follows an Eisenman XI sequence with $P(Na^+) > P(K^+)$ [1,2]. Accordingly, and depending on the gradients present, the opening of TRPV3 by thymol may lead to a secretion of K^+ with the hyperpolarization of the apical membrane and a drop in I_{sc}. Conversely, the opening of TRPA1 should lead to an increase in I_{sc}, as observed with cinnamaldehyde. The different relative expression of TRPA1 or TRPV3 may thus explain the variability of the response to thymol.

In patch clamp experiments overexpressing hTRPV3, as in a previous study of the bovine homologue [41], 1 mmol·L^{-1} thymol elicited the expected large response. However, despite numerous attempts, at 1 mmol·L^{-1}, no effect after the application of cinnamaldehyde could be observed. Small effects of cinnamaldehyde were only detectable at 5 mmol·L^{-1} and after the elevation of the bath temperature to 37 °C.

It thus appears that contributions of TRPV3 to the cinnamaldehyde response are possible, but most likely small.

3.5. G_t Is Sensitive to Quinidine

Further experiments were conducted in order to assess the contribution of cation absorption and/or anion secretion to the current. The lack of an effect of amiloride on the cinnamaldehyde response suggests that ENaC was not involved (Figure 4 and Table 2). Quinidine, a blocker of non-selective cation channels, had a strikingly negative impact on the increase in G_t observed after the application of cinnamaldehyde, with ΔG_t dropping by more than half (Figure 4), although ΔI_{sc} was not altered. Possibly, the quinidine effects were caused by a previously unknown negative interaction of quinidine with tight junction proteins. However, a more likely hypothesis is that quinidine blocked both the influx of Na^+ and the efflux of K^+ through TRP channels such as TRPV3 and TRPA1 by roughly equal amounts (Figure 7a), so that as a net effect, the I_{sc} level remained roughly the same, while the G_t dropped to about 40%.

In three different studies of rat colon, the response to AITC, cinnamaldehyde or thymol (100 µmol·L^{-1}) was significantly reduced by an equivalent concentration of HC-030031 [14,16,39]. On the other hand, the knockout of TRPA1 only partially reduced the AITC response, highlighting the possibility that TRPA1 may not be the only channel involved [16]. In our study, the TRPA1 blocker HC-030031 reduced the cinnamaldehyde response numerically, but the effects did not pass testing for significance (Figure 4 and

Table 2). The most likely explanation is that 100 µmol·L^{-1} of HC-030031 was insufficient to block the activity of the 1 mmol·l^{-1} cinnamaldehyde used in this study.

3.6. I_{sc} and ΔG_t Can Be Inhibited by Indometacin

The effects of the anion channel blocker NPPB suggest that the cinnamaldehyde-induced rise in I_{sc} is at least partially caused by the opening of an apical anion channel [49] (Figure 7c). Indometacin, which leads to reduced levels of cAMP, had identical effects, pointing towards an involvement of CFTR, although additional anion channels may participate. In our study, neither drug had a significant impact on ΔG_t. In contrast, in studies of the rat colon, the COX-inhibitor piroxicam reduced both ΔG_t and ΔI_{sc} in response to AITC [39].

In the study by Kaji et al. [39], the application of PGE2 induced increases in I_{sc} that could not be further enhanced by the subsequent application of AITC, suggesting that all of the CFTR channels were already at the maximal open probability. Furthermore, in both human and rat colon, the response to AITC could be strongly inhibited by ONO-AE3-208, a specific blocker which prevents the binding of PGE2 to the EP4 receptor.

3.7. Bicarbonate Is a Bigger Player Than Chloride in ΔI_{sc} and ΔG_t

As mentioned above, the basolateral uptake of Cl^- classically occurs via NKCC1 (SLC12A2). The responses of the rat and human colon to either thymol or AITC were partially blocked by bumetanide in two previous studies [14,39]. All of the responses could also be significantly reduced by the removal of Cl^-, with smaller effects after the removal of bicarbonate. Conversely, the cinnamaldehyde response of the pig jejunum was sensitive to the removal of HCO_3^-, but insensitive to either chloride removal or bumetanide [45].

In this study, the response of pig colon to cinnamaldehyde resembles the previous findings in pig jejunum [45]. The blocking of NKCC1 by bumetanide did not interfere with the cinnamaldehyde response, showing no significant effect on either ΔI_{sc} or ΔG_t. Furthermore, the bilateral reduction of Cl^- (from 130.3 to 10.3 mmol·L^{-1}) had no significant effect on ΔI_{sc}, although ΔG_t was significantly reduced by about half. Instead, dramatic effects were observed after the removal of only 25 mmol·L^{-1} bicarbonate from the solution via replacement with HEPES and gluconate (Supplementary Materials Table S1). Despite the continued presence of 130.3 mmol·L^{-1} Cl^-, the cinnamaldehyde-induced ΔI_{sc} dropped to less than a third of the control response, while ΔG_t dropped by about 40%. It thus appears that despite having a much lower concentration and only 60% of the mobility (see mobility listings in JPCalcWin 1.01, [52]) HCO_3^- contributes more to the cinnamaldehyde-induced ΔI_{sc} and ΔG_t than Cl^-.

These results are understandable if one assumes that NKCC1 does not contribute much to the cinnamaldehyde response. The basolateral uptake of HCO_3^- most likely occurs via basolateral cotransporters such as NBCe1 (SLC4A4), NBCe2 (Slc4a5) or NBCn1 (Slc4a7), which mediate the cotransport of Na^+ and HCO_3^-, and are amply expressed by the hindgut [53–55]. The apical efflux of HCO_3^- should be possible through apical Cl^- channels such as CFTR [49,56,57], which, like practically all of the anion channels known to date, are notoriously promiscuous. Either signalling complexes between the NBCs and CFTR or differential expression by distinct cell types may explain the preferential transport of HCO_3^- over Cl^-. In contrast to the secretion of chloride, the secretion of HCO_3^- should be useful to help with the buffering of short chain fatty acids fermentationally produced from fiber within the colonic lumen [33,34]. This may be of particular importance in pigs, which typically obtain about 30% of their energy from hindgut fermentation [34].

3.8. G_t Requires the Presence of Mucosal Na^+

At this point, some deliberations concerning the ΔG_t induced by cinnamaldehyde are possible. Given the low selectivity of anion channels, it is very hard to envision a paracellular tight junction protein with a high selectivity for HCO_3^- over Cl^-. It thus appears that the HCO_3^- dependent fraction, or about 40%, reflect changes in the transcellular passage

of HCO_3^-. Experiments in low chloride Ringer suggest that 25% of ΔG_t reflects the para- or transcellular flux of Cl^-. In conjunction with the quinidine data, it appears that, in total, roughly half of ΔG_t is caused by anions. Despite this, the removal of bilateral Na^+ had dramatic effects on the cinnamaldehyde response, with ΔI_{sc} and ΔG_t at a mere ~ 15 and 20% of the response in the control tissues, respectively. The collapse in ΔI_{sc} is clearly due to the lack of serosal Na^+ as a driving force for Na^+-HCO_3^- cotransport. However, if paracellular transport is assumed to be responsible for changes in conductance, the collapse in ΔG_t greatly exceeds reasonable expectations. Furthermore, ΔG_t collapsed by precisely the same amount when Na^+ was replaced on the mucosal side only. This observation is not compatible with the assumption of a paracellular flux of Na^+, because in this case, ΔG_t should have been much higher after the unilateral Na^+ removal than after the bilateral Na^+ removal. It appears that while a large part of the ΔG_t response reflects the passage of anions, the signalling to induce the response occurs via a quinidine-sensitive pathway and requires the presence of mucosal Na^+. The entry of Na^+ through TRPA1 is the most likely option.

While the mucosal removal of Na^+ dramatically reduced ΔG_t, it had absolutely no effect on the cinnamaldehyde-induced ΔI_{sc}. A possible reason for this is that the removal of mucosal Na^+ decreased the cytosolic Na^+, thus stimulating the basolateral influx of HCO_3^- via Na^+-HCO_3^- cotransport and the influx of Cl^- via NKCC1, with a subsequent increase in the apical secretion of anions. Another possibility is that the influx of Ca^{2+} was sufficient for the response.

3.9. Removal of Ca^{2+} Enhances ΔG_t

An attractive hypothesis is to assume that the cinnamaldehyde induced increase in I_{sc} is calcium dependent. Rising levels of cytosolic Ca^{2+} typically activate the apical Cl^- channels of the colonic epithelium both directly (in the case of calcium-dependent Cl^- channels) and indirectly (via calcium-dependent adenylyl cyclases with the production of cAMP) [49,58]. Thus, in rat colon, the thymol-induced ΔI_{sc} was reduced in bilateral Ca^{2+}-free Ringer, although notably, the ΔG_t remained the same [14]. In contrast, Ca^{2+} removal did not affect the AITC response of rat colon in a study by the same authors [39].

In the current study of porcine colon, bilateral nominally Ca^{2+}-free solution did not lead to a reduction in the cinnamaldehyde-induced ΔI_{sc}. Instead, the cinnamaldehyde-induced ΔG_t rose to almost twice the size observed in controls from the same animals. When Ca^{2+} was replaced by EGTA on the mucosal side only, ΔG_t rose even further to a striking 300% of the controls ($p < 0.001$). Simultaneously, ΔI_{sc} rose numerically to 150% of the controls from the same animals, a result that tested for significance when compared to the entire set of the controls. It thus appears that Ca^{2+} is very clearly not necessary for the response of the tissues to cinnamaldehyde.

3.10. Does the Opening of TRPA1 Inhibit the Uptake and Degradation of Prostaglandins?

While further work is clearly necessary, some speculation is possible. The synthesis of PGE2 by the colon is well-documented, and the effects of the inhibition of prostaglandin synthesis were significant and seen not only in this study, but also in two separate studies of rat colon using AITC as a TRPA1 agonist [16,39]. Prostanoids such as PGE2 are anions that are synthesized from membrane phospholipids via cyclooxygenase-mediated pathways. After secretion into the extracellular space, prostanoids are bound to specific prostanoid receptors [59,60]. For prostanoid signalling to end, the anionic prostaglandin has to be taken up into the cytosol where it is degraded. This uptake occurs via an electrogenic anion exchanger, OATP2A1 (SLCO2A1), with the efflux of two lactate anions driving the influx of one prostaglandin anion. Accordingly, the depolarization of the cellular membrane decreases the uptake of PGE2 [59–61]. The events are thus as follows: PGE2 is continuously produced by the colonic epithelium and taken back up into the cell via OATP2A1. If TRPA1 is opened via cinnamaldehyde or AITC, the entry of Na^+ and Ca^{2+} will exceed the efflux of K^+, depolarizing the cell. This reduces the reuptake of PGE2 via OATP2A1. There is thus

more PGE2 to bind to EP4, leading to the activation of adenyl cyclase, the production of cAMP, the opening of CFTR and, finally, the secretion of HCO_3^- and Cl^-. In conjunction, a rise in the current (ΔI_{sc}) and a rise in conductance (ΔG_t) are observed.

3.11. Barrier Effects

As outlined above, we do not think that an opening of the paracellular pathway can explain the major part of the cinnamaldehyde-induced ΔG_t response. From this study and others, there is considerable evidence to suggest that the activation of TRPA1 induces the secretion of PGE2 [16,39]. PGE2 has direct barrier-enhancing properties [62,63]. Thus, in cell culture models of colonic epithelia, prostaglandin-mediated signalling via the EP2 receptor prevented the proteosomal degradation of Claudin-4 [64]. The colon of EP4 deficient mice showed increased rates of apoptotic cells, as well as a defective mucosal barrier with signs of inflammation [65]. Furthermore, PGE2 was found to stimulate the recovery of the barrier function in porcine ischemia-injured ileal mucosa [66]. In addition, lower levels of PGE2 and other prostaglandins are thought to be involved in the classical gastrointestinal side-effects of cyclooxygenase inhibitors [67]. However, it is important to bear in mind that the pharmacology of PGE2 is notoriously complex, with numerous pro- and anti-inflammatory effects that are probably related to local concentrations of PGE2 and the expression patterns of its various receptors [62].

3.12. Cinnamaldehyde, Bicarbonate and the Buffering of Fermentational Acids in the Colon

More work is clearly necessary to understand the interaction of essential oils in general and of cinnamaldehyde in particular with colonic epithelia, but a picture is slowly emerging (Figure 7). In humans and in animals, the function of the colon is to serve as a fermentation chamber in which microbials can degrade the structural carbohydrates that are resistant to enzymatic digestion of the small intestine [33,34]. Anaerobic fermentation produces large quantities of short-chain fatty acids (Figure 7c). Large quantities of protons are released via dissociation and have to be removed, since low values of pH produce shifts in the colonic microbiome towards species that produce lactic acid. This is an occurrence associated with a further drop in colonic pH and subsequent damage to the epithelium [38,68,69]. The secretion of bicarbonate with the subsequent formation of CO_2 is a highly appropriate and well-established buffering mechanism [53,54,57]. While protons are removed via the formation of CO_2, the anions of short-chain fatty acids can then be transported across the epithelium without impairing the cellular pH homeostasis via various pathways that have been discussed elsewhere [33]. In a further twist, the secretion of HCO_3^- enhances the unfolding of the mucines that protect the epithelium from the bacterial invasion and inflammation seen in inflammatory bowel disease [38,70].

The current study suggests that the ingestion of plants rich in terpenes—such as those contained in the bark of the *Cinnamomum verum* tree—may help to stimulate HCO_3^- secretion. After the degradation of plant structures by microbials in the colon, cinnamaldehyde is released and binds to TRPA1, preventing the cellular uptake and degradation of PGE2 (Figure 7a,b). The rising levels of cAMP will then stimulate the secretion of HCO_3^- (Figure 7c). The removal of protons should certainly help to prevent damage to the epithelial cells, and may explain part of the anti-inflammatory action of essential oils such as cinnamaldehyde. Of course, the amounts consumed must not be too high, because otherwise the secretion of chloride might lead to diarrhea and other disagreeable or even toxic effects. It appears possible that humans and animals alike will use their outstanding ability to detect the smallest quantities of essential oils via their sense of smell to precisely assess just how much is needed to make the food tasty, but not too spicy [71].

4. Materials and Methods

4.1. Gastrointestinal Tissue

The porcine gastrointestinal tissues were obtained according to the guidelines of the German Animal Welfare Law under oversight by the local authority of the "Landesamt für

Gesundheit und Soziales Berlin" (LaGeSo Reg. Nr. T0264/15 and T0297/17). The pigs were a cross between the Danbred x Piétrain breeds, weighing ~25 kg and aged about 10 weeks, and were fed a normal diet. The animals were killed by prior sedation with ketamine (Ursotamin®, Serumwerk Bernburg AG, Bernburg, Germany) and azaperone (Stresnil®, Jansen-Cilag, Neuss, Germany) by intramuscular injection, followed by an intracardiac injection of tetracaine hydrochloride, mebezonium iodide and embutramide (T61®, Intervet Deutschland GmbH, Unterschleissheim, Germany). In a few experiments, older pigs from a commercial slaughterhouse were used, which is indicated where applicable. After death, the gastrointestinal tissue was immediately removed.

4.2. Molecular Detection of the TRPA1 Channel in the Gastrointestinal Tissue

For the molecular investigations, the removed gastrointestinal tissue (the fundus and cardia of the stomach, duodenum, mid-jejunum, ileum, caecum and mid-colon) was thoroughly rinsed with PBS, and small pieces of 1 cm^3 of the tunica muscularis or the mucosa were transferred into tubes containing 1 mL of RNAlater® (Sigma-Aldrich, Taufkirchen, Germany). These were cooled at 4 °C overnight and then stored at −80 °C. For the RNA isolation, a Nucleospin RNA II kit (Macherey-Nagel, Dueren, Germany) was used, and the RNA integrity numbers (RIN) were determined using an RNA 600 Nano kit (Agilent, Waldbronn, Germany). The samples from 4 pigs (out of 6) with the best RIN values (RIN > 6.8 for the ileal epithelium and RIN > 7.3 for all of the other tissues) were subsequently processed. For the reverse transcription into cDNA, an iScript® cDNA synthesis kit (Bio-Rad Laboratories, Munich, Germany) was used according to the manufacturer's instructions, whereby 1 µg RNA was transcribed per sample and then diluted 1:10.

Afterwards, an exon spanning FAM/BHQ1 labelled primer-probe combination was designed according to the predicted sequence of the porcine TRPA1 channel, and the corresponding reference genes were established (Table 3), which were synthesized by Eurofins (Eurofins Genomics Germany GmbH, Ebersberg, Germany). In order to ensure that the correct target was bound, the amplification product was sequenced and compared to the target sequence (Eurofins Genomics Germany GmbH, Ebersberg, Germany). Primer–probe combinations were also used for the three selected reference genes: ACTB (FAM/BHQ1), GAPDH [72] and YWHAZ (FAM/TAMRA). For the semi-quantitative analysis by qPCR, a 40-cycle 2-step protocol (1 s 95 °C, 20 s 60 °C) was performed on a thermocycler (ViiA 7, Applied Biosystems/Life Technologies, Waltham, MA, USA). The reactions were performed in triplicates with 3.7 µL cDNA and iTaq® Universal Probes Supermix (Bio-Rad Laboratories GmbH, Feldkirchen, Germany) with a total volume of 10 µL. Negative controls (no template controls) were routinely included. The quantification cycles (C_q) were calculated automatically by the cycler software. The dilution series-based gene-specific amplification efficiencies for the primer pairs were determined and the reference genes were tested for their expression stability (qbasePLUS, Biogazelle NV, Zwijnaarde, Belgium). The C_q values of the target gene TRPA1 were normalized using ACTB, GAPDH, and YWHAZ, and were scaled to the sample means. Subsequently, the values were exported as calibrated normalized relative quantity (CNRQ) values using qbasePLUS.

Attempts to find a suitable antibody against TRPA1 were unfortunately unsuccessful. Five commercial antibodies were tested, but yielded multiple or no bands in immunoblots of porcine tissues (sc-166469 and sc-376495, Santa Cruz Biotechnology Inc, Dallas, TX, USA; ACC-037, Alomone, Jerusalem, Israel; TA338564, OriGene, Herford, Germany and AG1346, Abgent, San Diego, CA, USA).

Table 3. Primer sequences and the amplicon length of the genes used.

Gene	Length (bp)	Primer	Gene Acession No.
TRPA1 fwd	192	ACAGGAAAGTCAGCCCTCTC	XM_001926115.4
TRPA1 rev		TATCCTGGCTGCCCGAATAG	
TRPA1 probe		TTTGCGGCCACCCAGGGAGC	
ACTB fwd	127	GACATCAAGGAGAAGCTGTG	XM_003124280.5
ACTB rev		CGTTGCCGATGGTGATG	
ACTB probe		CTGGACTTCGAGCAGGAGATGGCC	
YWHAZ fwd	113	AAGAGTCATACAAAGACAGCAC	XM_021088756.1
YWHAZ rev		ATTTTCCCCTCCTTCTCCTG	
YWHAZ probe		ATCGGATACCCAAGGAGATGAAGCTGAA	
GAPDH fwd	117	CAAGAAGGTGGTGAAGCAG	NM_001206359.1
GAPDH rev		GCATCAAAAGTGGAAGAGTGAG	
GAPDH probe		TGAGGACCAGGTTGTGTCCTGTGACTTCAA	

4.3. Ussing Chamber Studies

For the electrophysiological studies using a Ussing chamber, the tissue was washed with transport buffer after the removal. The tunica muscularis was stripped, and the tissue was transported with ice-cooled gassed (95% O_2/5% CO_2) transport buffer (in mmol·L^{-1}: 115 NaCl, 0.4 NaH_2PO_4, 2.4 Na_2HPO_4, 5 KCl, 25 $NaHCO_3$, 5 glucose, 10 HEPES, 1.2 $CaCl_2$, 1.2 $MgCl_2$). The tissue was then mounted in 0.95 cm^2 classical, custom-built Ussing chambers with perfusion maintained via a gas-lift system [73,74], which were filled with 10 mL Ringer's solution (in mmol·L^{-1}: 120 NaCl, 25 $NaHCO_3$, 0.32 NaH_2PO_4, 1 $MgSO_4$, 6.3 KCl, 2 $CaCl_2$) per side, unless otherwise declared. In order to exclude a glucose-induced sodium current, 16 mmol·L^{-1} glucose was added to the serosal side and 16 mmol·L^{-1} mannitol was added to the mucosal side. The final osmolality of the solutions was adjusted to 300 mosmol·kg^{-1} with mannitol. During the experiment, the tissue was kept permanently at 37 °C and gassed with 95% O_2 and 5% CO_2, whereas the solutions without HCO_3^- were gassed with oxygen. After the tissue mounting, the measurements were performed in short-circuit mode and the current (I_{sc}) was recorded, with positive values reflecting the transport of cations from the mucosal to the serosal side. Throughout, the I_{sc} represents the molar flux (in μeq·cm^{-2}·h^{-1}), which can be calculated from the current Φt (in μA·cm^{-2}) according to I_{sc} = Φt/F·3600s·h^{-1} = Φt/26.80 μeq·cm^{-2}·h^{-1}, where F is the Faraday constant. Using a 100 μA current pulse and the corresponding potential response, the conductance (G_t, in mS·cm^{-2}) was continuously recorded (Mussler Scientific Instruments, Aachen, Germany).

Measurements commenced after the I_{sc} and G_t values had stabilized, or after a maximum of 45 min. All of the agonists were added directly via a pipette to the bath solution in a ratio of 1:1000 to yield the target concentration, with the substances dissolved in either water (amiloride), ethanol (cinnamaldehyde, thymol, lidocaine, bumetanide, indometacin) or dimethyl sulfoxide (DMSO) (quinidine, 5-nitro-2-(3-phenylpropyl-amino) benzoic acid (NPPB), HC-030031). Cinnamaldehyde (1 mmol·L^{-1}) was added 15 min later. In the other experiments, the solution changes occurred 15 min before the addition of cinnamaldehyde. The composition of the solutions used can be found in the Supplementary Materials Table S1.

4.4. Patch Clamp Studies

A human construct of TRPV3 (hTRPV3) was used for the patch-clamp experiments, essentially as in [40,41]. The sequence (GeneArt, Thermo Fisher Scientific, Regensburg, Germany) was tagged with hemagglutinin (HA) and streptavidin (Strep). This construct was subsequently subcloned into pIRES2-AcGFP1 (Takara BioEurope, Saing-Germain-en-Laye, France). HEK-293 cells were used for transient transfection (DSMZ, Braunschweig, Germany). The cells were cultured using Dulbecco's modified Eagle's medium supplemented with 10% fetal bovine serum and 100 units·mL^{-1} of penicillin and streptomycin (Biochrom,

Berlin, Germany). Approximately 24 h before the start of the experiment, the cells were transfected with polyethyleneimine and the HA-Strep-hTRPV3-pIRES-AcGFP1 construct or the empty pIRES-AcGFP1 vector (control). Accordingly, the successfully transfected hTRPV3 cells should show green fluorescence. Furthermore, the cells were stained with a mouse TRPV3 antibody (ABIN863127, antibodies-online GmbH, Aachen, Germany) at a 1:1000 dilution, as in [40].

The whole-cell experiments were performed at room temperature (adjusted to 23 °C with an airconditioning system) and at 37 °C, using an inline solution heater to adjust the temperature (PH01 (S/N 1007), Multichannel Systems). Patchmaster software (HEKA Electronic) automatically performed the generation of pulses, data collection, filtering with a 2.9 kHz Bessel filter, and correction for capacity and series resistance. A low sampling rate (100 Hz) pulse protocol was used for the recording in order to assess the solution changes. This automatically switched to a classical step protocol with a high sampling rate (5 kHz) to assess the channel kinetics, as in previous studies [40,41]. After the measuring the osmolality, the solutions were adjusted to 300 mosmol·kg^{-1} with mannitol and buffered to a pH of 7.4. The pipette solution contained (in mmol·L[1]): 5 CsCl, 6.63 NaCl, 127.36 Na-gluconate, 10 EGTA, 10 HEPES, 1.91 $CaCl_2$, 2.27 $MgCl_2$, 1 Mg-ATP. The extracellular solution contained (in mmol·L^{-1}): 5 KCl, 1 NaH_2PO_4, 137 NaCl, 10 HEPES, 1.7 $CaCl_2$, 0.9 $MgCl_2$, 5 glucose. In the experiment, the effect of 1 and 5 mmol·L^{-1} cinnamaldehyde was studied at 37 °C and 23 °C, with 1 mmol·L^{-1} thymol serving as a control reaction at the end of the experiment.

4.5. Data and Statistics

The statistical analysis was performed with the program SigmaPlot 11.0 (Systat Software, Erkrath, Germany), with the data being tested for normal distribution (Shapiro-Wilk) and homogeneity of variances (Brown-Forsythe). Subsequently, data were tested using a parametric test (Student's t-test or ANOVA (Student-Newman-Keuls or Dunn's method)) or a non-parametric test (Mann-Whitney U test or ANOVA on ranks (Kruskal-Wallis method)), as appropriate. Statistical significance was assumed at $p < 0.05$. The data are presented as the mean values ± SEM. The number of experiments with pigs is expressed as N/n, where N is the number of animals and n is the number of tissues. The Ussing chamber data were binomially smoothed using Igor Pro 6.37 (WaveMetrics Inc., Lake Oswego, OR, USA). The statistical analysis of the qPCR data was performed using the calculated CNRQ data (qbasePLUS, Biogazelle NV, Zwijnaarde, Belgium). In the barplots, different letters were placed above the bars to designate significant differences. Bars that do not share a letter are significantly different ($p < 0.05$). Conversely, bars that share at least one letter are not different ($p > 0.05$).

Supplementary Materials: The following are available online at https://www.mdpi.com/article/10.3390/ijms22105198/s1, Figure S1: Concentration effects of cinnamaldehyde in the jejunum; Figure S2: Effect of cinnamaldehyde after the mucosal, serosal and bilateral addition in the jejunum; Figure S3: Effect of thymol after the mucosal, serosal and bilateral addition in the colon; Figure S4: Effect of the bilateral addition of thymol in the jejunum; Table S1: Ussing chamber solutions.

Author Contributions: Conceptualization, F.S., and D.M.; methodology, F.S., H.-S.B., G.M. and D.M.; software, F.S.; validation, D.M., and H.-S.B.; formal analysis, D.M. and F.S.; investigation, D.M. and G.M.; resources, F.S., J.R.; data curation, D.M. and F.S.; writing—original draft preparation, D.M. and F.S.; writing—review and editing, D.M., F.S., G.M., J.R. and H.-S.B.; visualization, D.M.; supervision, F.S.; project administration, F.S. All authors have read and agreed to the published version of the manuscript.

Funding: Funding for David Manneck was provided by "Akademie für Tiergesundheit (AfT)". The hTRPV3 vector and a few laboratory supplies were obtained in the course of a project funded by Deutsche Forschungsgemeinschaft (DFG STU 258/7-1). The porcine epithelia were obtained from an unrelated study. We acknowledge support by the Open Access Publication Fund of the Freie Universität Berlin.

Institutional Review Board Statement: The study was conducted according to German animal welfare and approved by the "Landesamt für Gesundheit und Soziales Berlin" (LaGeSo Reg Nr. T0264/15 and T0297/17).

Data Availability Statement: Data available on request.

Acknowledgments: We would like to thank Martin Grunau, Julius Dahl and Katharina Söllig for their great technical support.

Conflicts of Interest: D.M., G.M. and F.S. declare no conflict of interests. At the time of the study, H.-S.B. and J.R. were employees of PerformaNat GmbH. There was no influence on the results during the evaluation and interpretation.

References

1. Talavera, K.; Startek, J.B.; Alvarez-Collazo, J.; Boonen, B.; Alpizar, Y.A.; Sanchez, A.; Naert, R.; Nilius, B. Mammalian Transient Receptor Potential TRPA1 Channels: From Structure to Disease. *Physiol. Rev.* **2020**, *100*, 725–803. [CrossRef]
2. Nilius, B.; Appendino, G.; Owsianik, G. The Transient Receptor Potential Channel TRPA1: From Gene to Pathophysiology. *Pflugers. Arch.* **2012**, *464*, 425–458. [CrossRef] [PubMed]
3. Bobkov, Y.V.; Corey, E.A.; Ache, B.W. The pore properties of human nociceptor channel TRPA1 evaluated in single channel recordings. *Biochim. Biophys. Acta* **2011**, *1808*, 1120–1128. [CrossRef] [PubMed]
4. Owsianik, G.; Talavera, K.; Voets, T.; Nilius, B. Permeation and selectivity of TRP channels. *Annu. Rev. Physiol.* **2006**, *68*, 685–717. [CrossRef]
5. Kremeyer, B.; Lopera, F.; Cox, J.J.; Momin, A.; Rugiero, F.; Marsh, S.; Woods, C.G.; Jones, N.G.; Paterson, K.J.; Fricker, F.R.; et al. A gain-of-function mutation in TRPA1 causes familial episodic pain syndrome. *Neuron* **2010**, *66*, 671–680. [CrossRef] [PubMed]
6. Taylor-Clark, T.E.; Undem, B.J.; Macglashan, D.W., Jr.; Ghatta, S.; Carr, M.J.; McAlexander, M.A. Prostaglandin-induced activation of nociceptive neurons via direct interaction with transient receptor potential A1 (TRPA1). *Mol. Pharmacol.* **2008**, *73*, 274–281. [CrossRef]
7. Cruz-Orengo, L.; Dhaka, A.; Heuermann, R.J.; Young, T.J.; Montana, M.C.; Cavanaugh, E.J.; Kim, D.; Story, G.M. Cutaneous nociception evoked by 15-delta PGJ2 via activation of ion channel TRPA1. *Mol. Pain* **2008**, *4*, 30. [CrossRef] [PubMed]
8. Andersson, D.A.; Gentry, C.; Moss, S.; Bevan, S. Transient receptor potential A1 is a sensory receptor for multiple products of oxidative stress. *J. Neurosci.* **2008**, *28*, 2485–2494. [CrossRef]
9. Yilmaz, M.S.; Goktalay, G.; Millington, W.R.; Myer, B.S.; Cutrera, R.A.; Feleder, C. Lipopolysaccharide-induced hypotension is mediated by a neural pathway involving the vagus nerve, the nucleus tractus solitarius and alpha-adrenergic receptors in the preoptic anterior hypothalamic area. *J. Neuroimmunol.* **2008**, *203*, 39–49. [CrossRef]
10. Alaimo, A.; Rubert, J. The Pivotal Role of TRP Channels in Homeostasis and Diseases throughout the Gastrointestinal Tract. *Int. J. Mol. Sci.* **2019**, *20*, 5277. [CrossRef]
11. Holzer, P. Transient receptor potential (TRP) channels as drug targets for diseases of the digestive system. *Pharmacol. Ther.* **2011**, *131*, 142–170. [CrossRef] [PubMed]
12. Yang, Y.; Wang, S.; Kobayashi, K.; Hao, Y.; Kanda, H.; Kondo, T.; Kogure, Y.; Yamanaka, H.; Yamamoto, S.; Li, J.; et al. TRPA1-expressing lamina propria mesenchymal cells regulate colonic motility. *JCI Insight* **2019**, *4*. [CrossRef] [PubMed]
13. Brierley, S.M.; Hughes, P.A.; Page, A.J.; Kwan, K.Y.; Martin, C.M.; O'Donnell, T.A.; Cooper, N.J.; Harrington, A.M.; Adam, B.; Liebregts, T.; et al. The ion channel TRPA1 is required for normal mechanosensation and is modulated by algesic stimuli. *Gastroenterology* **2009**, *137*, 2084–2095 e2083. [CrossRef] [PubMed]
14. Kaji, I.; Karaki, S.; Kuwahara, A. Effects of luminal thymol on epithelial transport in human and rat colon. *Am. J. Physiol. Gastrointest. Liver Physiol.* **2011**, *300*, G1132–G1143. [CrossRef]
15. Kun, J.; Szitter, I.; Kemeny, A.; Perkecz, A.; Kereskai, L.; Pohoczky, K.; Vincze, A.; Godi, S.; Szabo, I.; Szolcsanyi, J.; et al. Upregulation of the transient receptor potential ankyrin 1 ion channel in the inflamed human and mouse colon and its protective roles. *PLoS ONE* **2014**, *9*, e108164. [CrossRef]
16. Fothergill, L.J.; Callaghan, B.; Rivera, L.R.; Lieu, T.; Poole, D.P.; Cho, H.J.; Bravo, D.M.; Furness, J.B. Effects of Food Components That Activate TRPA1 Receptors on Mucosal Ion Transport in the Mouse Intestine. *Nutrients* **2016**, *8*, 623. [CrossRef]
17. Balemans, D.; Boeckxstaens, G.E.; Talavera, K.; Wouters, M.M. Transient receptor potential ion channel function in sensory transduction and cellular signaling cascades underlying visceral hypersensitivity. *Am. J. Physiol. Gastrointest. Liver Physiol.* **2017**, *312*, G635–G648. [CrossRef]
18. Meseguer, V.; Alpizar, Y.A.; Luis, E.; Tajada, S.; Denlinger, B.; Fajardo, O.; Manenschijn, J.A.; Fernandez-Pena, C.; Talavera, A.; Kichko, T.; et al. TRPA1 channels mediate acute neurogenic inflammation and pain produced by bacterial endotoxins. *Nat. Commun.* **2014**, *5*, 3125. [CrossRef] [PubMed]
19. Startek, J.B.; Voets, T.; Talavera, K. To flourish or perish: Evolutionary TRiPs into the sensory biology of plant-herbivore interactions. *Pflugers Arch.* **2019**, *471*, 213–236. [CrossRef]

20. Spisni, E.; Petrocelli, G.; Imbesi, V.; Spigarelli, R.; Azzinnari, D.; Donati Sarti, M.; Campieri, M.; Valerii, M.C. Antioxidant, Anti-Inflammatory, and Microbial-Modulating Activities of Essential Oils: Implications in Colonic Pathophysiology. *Int. J. Mol. Sci.* **2020**, *21*, 4152. [CrossRef]
21. Bandell, M.; Story, G.M.; Hwang, S.W.; Viswanath, V.; Eid, S.R.; Petrus, M.J.; Earley, T.J.; Patapoutian, A. Noxious cold ion channel TRPA1 is activated by pungent compounds and bradykinin. *Neuron* **2004**, *41*, 849–857. [CrossRef]
22. Macpherson, L.J.; Dubin, A.E.; Evans, M.J.; Marr, F.; Schultz, P.G.; Cravatt, B.F.; Patapoutian, A. Noxious compounds activate TRPA1 ion channels through covalent modification of cysteines. *Nature* **2007**, *445*, 541–545. [CrossRef]
23. Macpherson, L.J.; Geierstanger, B.H.; Viswanath, V.; Bandell, M.; Eid, S.R.; Hwang, S.; Patapoutian, A. The Pungency of Garlic: Activation of TRPA1 and TRPV1 in Response to Allicin. *Curr. Biol.* **2005**, *15*, 929–934. [CrossRef] [PubMed]
24. Karashima, Y.; Damann, N.; Prenen, J.; Talavera, K.; Segal, A.; Voets, T.; Nilius, B. Bimodal action of menthol on the transient receptor potential channel TRPA1. *J. Neurosci.* **2007**, *27*, 9874–9884. [CrossRef] [PubMed]
25. Ortar, G.; Morera, L.; Moriello, A.S.; Morera, E.; Nalli, M.; Di Marzo, V.; De Petrocellis, L. Modulation of thermo-transient receptor potential (thermo-TRP) channels by thymol-based compounds. *Bioorg. Med. Chem. Lett.* **2012**, *22*, 3535–3539. [CrossRef]
26. Cho, H.J.; Callaghan, B.; Bron, R.; Bravo, D.M.; Furness, J.B. Identification of enteroendocrine cells that express TRPA1 channels in the mouse intestine. *Cell Tissue Res.* **2014**, *356*, 77–82. [CrossRef]
27. Purhonen, A.K.; Louhivuori, L.M.; Kiehne, K.; Kerman, K.E.; Herzig, K.H. TRPA1 channel activation induces cholecystokinin release via extracellular calcium. *FEBS Lett.* **2008**, *582*, 229–232. [CrossRef] [PubMed]
28. Qu, S.; Shen, Y.; Wang, M.; Wang, X.; Yang, Y. Suppression of miR-21 and miR-155 of macrophage by cinnamaldehyde ameliorates ulcerative colitis. *Int. Immunopharmacol.* **2019**, *67*, 22–34. [CrossRef]
29. Momtaz, S.; Navabakhsh, M.; Bakouee, N.; Dehnamaki, M.; Rahimifard, M.; Baeeri, M.; Abdollahi, A.; Abdollahi, M.; Farzaei, M.H.; Abdolghaffari, A.H. Cinnamaldehyde targets TLR-4 and inflammatory mediators in acetic-acid induced ulcerative colitis model. *Biologia* **2021**. [CrossRef]
30. Elhennawy, M.G.; Abdelaleem, E.A.; Zaki, A.A.; Mohamed, W.R. Cinnamaldehyde and hesperetin attenuate TNBS-induced ulcerative colitis in rats through modulation of the JAk2/STAT3/SOCS3 pathway. *J. Biochem. Mol. Toxicol.* **2021**, e22730. [CrossRef]
31. Jimenez, M.J.; Berrios, R.; Stelzhammer, S.; Bracarense, A. Ingestion of organic acids and cinnamaldehyde improves tissue homeostasis of piglets exposed to enterotoxic Escherichia coli (ETEC). *J. Anim. Sci.* **2020**, *98*. [CrossRef] [PubMed]
32. Bosetti, G.E.; Griebler, L.; Aniecevski, E.; Facchi, C.S.; Baggio, C.; Rossatto, G.; Leite, F.; Valentini, F.D.A.; Santo, A.D.; Pagnussatt, H.; et al. Microencapsulated carvacrol and cinnamaldehyde replace growth-promoting antibiotics: Effect on performance and meat quality in broiler chickens. *An. Acad. Bras. Cienc.* **2020**, *92*, e20200343. [CrossRef] [PubMed]
33. Stumpff, F. A look at the smelly side of physiology: Transport of short chain fatty acids. *Pflugers. Arch.* **2018**, *470*, 571–598. [CrossRef]
34. Bergman, E.N. Energy contributions of volatile fatty acids from the gastrointestinal tract in various species. *Physiol. Rev.* **1990**, *70*, 567–590. [CrossRef]
35. Heo, J.M.; Opapeju, F.O.; Pluske, J.R.; Kim, J.C.; Hampson, D.J.; Nyachoti, C.M. Gastrointestinal health and function in weaned pigs: A review of feeding strategies to control post-weaning diarrhoea without using in-feed antimicrobial compounds. *J. Anim. Physiol. Anim. Nutr. (Berl.)* **2013**, *97*, 207–237. [CrossRef] [PubMed]
36. Gresse, R.; Chaucheyras-Durand, F.; Fleury, M.A.; Van de Wiele, T.; Forano, E.; Blanquet-Diot, S. Gut Microbiota Dysbiosis in Postweaning Piglets: Understanding the Keys to Health. *Trends Microbiol.* **2017**, *25*, 851–873. [CrossRef]
37. Macpherson, L.J.; Hwang, S.W.; Miyamoto, T.; Dubin, A.E.; Patapoutian, A.; Story, G.M. More than cool: Promiscuous relationships of menthol and other sensory compounds. *Mol. Cell Neurosci.* **2006**, *32*, 335–343. [CrossRef]
38. Stange, E.F.; Schroeder, B.O. Microbiota and mucosal defense in IBD: An update. *Expert Rev. Gastroenterol. Hepatol.* **2019**, *13*, 963–976. [CrossRef]
39. Kaji, I.; Yasuoka, Y.; Karaki, S.; Kuwahara, A. Activation of TRPA1 by luminal stimuli induces EP4-mediated anion secretion in human and rat colon. *Am. J. Physiol. Gastrointest. Liver Physiol.* **2012**, *302*, G690–G701. [CrossRef]
40. Liebe, F.; Liebe, H.; Kaessmeyer, S.; Sponder, G.; Stumpff, F. The TRPV3 channel of the bovine rumen: Localization and functional characterization of a protein relevant for ruminal ammonia transport. *Pflugers Arch.* **2020**, *472*, 693–710. [CrossRef] [PubMed]
41. Schrapers, K.T.; Sponder, G.; Liebe, F.; Liebe, H.; Stumpff, F. The bovine TRPV3 as a pathway for the uptake of Na+, Ca2+, and NH4+. *PLoS ONE* **2018**, *13*, e0193519. [CrossRef] [PubMed]
42. Peier, A.M.; Reeve, A.J.; Andersson, D.A.; Moqrich, A.; Earley, T.J.; Hergarden, A.C.; Story, G.M.; Colley, S.; Hogenesch, J.B.; McIntyre, P.; et al. A Heat—Sensitive TRP channel expressed in keratinocytes. *Science* **2002**, *296*, 2046–2049. [CrossRef] [PubMed]
43. Xu, H.; Ramsey, I.S.; Kotecha, S.A.; Moran, M.M.; Chong, J.A.; Lawson, D.; Ge, P.; Lilly, J.; Silos-Santiago, I.; Xie, Y.; et al. TRPV3 is a calcium-permeable temperature-sensitive cation channel. *Nature* **2002**, *418*, 181–186. [CrossRef] [PubMed]
44. Smith, G.D.; Gunthorpe, M.J.; Kelsell, R.E.; Hayes, P.D.; Reilly, P.; Facer, P.; Wright, J.E.; Jerman, J.C.; Walhin, J.P.; Ooi, L.; et al. TRPV3 is a temperature-sensitive vanilloid receptor-like protein. *Nature* **2002**, *418*, 186–190. [CrossRef] [PubMed]
45. Boudry, G.; Perrier, C. Thyme and cinnamon extracts induce anion secretion in piglet small intestine via cholinergic pathways. *J. Physiol. Pharmacol.* **2008**, *59*, 543–552.
46. Van Liefferinge, E.; Van Noten, N.; Degroote, J.; Vrolix, G.; Van Poucke, M.; Peelman, L.; Van Ginneken, C.; Roura, E.; Michiels, J. Expression of Transient Receptor Potential Ankyrin 1 and Transient Receptor Potential Vanilloid 1 in the Gut of the Peri-Weaning Pig Is Strongly Dependent on Age and Intestinal Site. *Animals* **2020**, *10*, 2417. [CrossRef]

47. Gonzalez-Mariscal, L.; Contreras, R.G.; Bolivar, J.J.; Ponce, A.; Chavez De Ramirez, B.; Cereijido, M. Role of calcium in tight junction formation between epithelial cells. *Am. J. Physiol.* **1990**, *259*, C978–C986. [CrossRef]
48. Meoli, L.; Gunzel, D. Channel functions of claudins in the organization of biological systems. *Biochim. Biophys. Acta Biomembr.* **2020**, *1862*, 183344. [CrossRef]
49. Barrett, K.E.; Keely, S.J. Chloride secretion by the intestinal epithelium: Molecular basis and regulatory aspects. *Annu. Rev. Physiol.* **2000**, *62*, 535–572. [CrossRef]
50. Ueda, T.; Yamada, T.; Ugawa, S.; Ishida, Y.; Shimada, S. TRPV3, A thermosensitive channel is expressed in mouse distal colon epithelium. *Biochem. Biophys. Res. Commun.* **2009**, *383*, 130–134. [CrossRef] [PubMed]
51. Bischof, M.; Olthoff, S.; Glas, C.; Thorn-Seshold, O.; Schaefer, M.; Hill, K. TRPV3 endogenously expressed in murine colonic epithelial cells is inhibited by the novel TRPV3 blocker 26E01. *Cell Calcium* **2020**, *92*, 102310. [CrossRef] [PubMed]
52. Barry, P.H.; Lynch, J.W. Liquid junction potentials and small cell effects in patch-clamp analysis. *J. Membr. Biol.* **1991**, *121*, 101–117. [CrossRef] [PubMed]
53. May, O.; Yu, H.; Riederer, B.; Manns, M.P.; Seidler, U.; Bachmann, O. Short-term regulation of murine colonic NBCe1-B (electrogenic Na+/HCO3(-) cotransporter) membrane expression and activity by protein kinase C. *PLoS ONE* **2014**, *9*, e92275. [CrossRef]
54. Bachmann, O.; Juric, M.; Seidler, U.; Manns, M.P.; Yu, H. Basolateral ion transporters involved in colonic epithelial electrolyte absorption, anion secretion and cellular homeostasis. *Acta Physiol.* **2011**, *201*, 33–46. [CrossRef]
55. Ballout, J.; Diener, M. The role of HCO3(-) in propionate-induced anion secretion across rat caecal epithelium. *Pflugers Arch.* **2021**. [CrossRef] [PubMed]
56. Tang, L.; Fatehi, M.; Linsdell, P. Mechanism of direct bicarbonate transport by the CFTR anion channel. *J. Cyst. Fibros.* **2009**, *8*, 115–121. [CrossRef]
57. Seidler, U.; Blumenstein, I.; Kretz, A.; Viellard-Baron, D.; Rossmann, H.; Colledge, W.H.; Evans, M.; Ratcliff, R.; Gregor, M. A functional CFTR protein is required for mouse intestinal cAMP-, cGMP- and Ca(2+)-dependent HCO3- secretion. *J. Physiol.* **1997**, *505*(Pt. 2), 411–423. [CrossRef]
58. Johnstone, T.B.; Agarwal, S.R.; Harvey, R.D.; Ostrom, R.S. cAMP Signaling Compartmentation: Adenylyl Cyclases as Anchors of Dynamic Signaling Complexes. *Mol. Pharmacol.* **2018**, *93*, 270–276. [CrossRef]
59. Nakanishi, T.; Tamai, I. Roles of Organic Anion Transporting Polypeptide 2A1 (OATP2A1/SLCO2A1) in Regulating the Pathophysiological Actions of Prostaglandins. *AAPS J.* **2017**, *20*, 13. [CrossRef]
60. Nakanishi, T.; Nakamura, Y.; Umeno, J. Recent advances in studies of SLCO2A1 as a key regulator of the delivery of prostaglandins to their sites of action. *Pharmacol. Ther.* **2021**, *223*, 107803. [CrossRef] [PubMed]
61. Chan, B.S.; Satriano, J.A.; Pucci, M.; Schuster, V.L. Mechanism of prostaglandin E2 transport across the plasma membrane of HeLa cells and Xenopus oocytes expressing the prostaglandin transporter "PGT". *J. Biol. Chem.* **1998**, *273*, 6689–6697. [CrossRef] [PubMed]
62. Konya, V.; Marsche, G.; Schuligoi, R.; Heinemann, A. E-type prostanoid receptor 4 (EP4) in disease and therapy. *Pharmacol. Ther.* **2013**, *138*, 485–502. [CrossRef]
63. Takafuji, V.; Cosme, R.; Lublin, D.; Lynch, K.; Roche, J.K. Prostanoid receptors in intestinal epithelium: Selective expression, function, and change with inflammation. *Prostaglandins Leukot. Essent. Fatty Acids* **2000**, *63*, 223–235. [CrossRef] [PubMed]
64. Lejeune, M.; Moreau, F.; Chadee, K. Loss of EP2 receptor subtype in colonic cells compromise epithelial barrier integrity by altering claudin-4. *PLoS ONE* **2014**, *9*, e113270. [CrossRef]
65. Matsumoto, Y.; Nakanishi, Y.; Yoshioka, T.; Yamaga, Y.; Masuda, T.; Fukunaga, Y.; Sono, M.; Yoshikawa, T.; Nagao, M.; Araki, O.; et al. Epithelial EP4 plays an essential role in maintaining homeostasis in colon. *Sci. Rep.* **2019**, *9*, 15244. [CrossRef]
66. Blikslager, A.T.; Pell, S.M.; Young, K.M. PGE2 triggers recovery of transmucosal resistance via EP receptor cross talk in porcine ischemia-injured ileum. *Am. J. Physiol. Gastrointest. Liver Physiol.* **2001**, *281*, G375–G381. [CrossRef]
67. Bjarnason, I.; Scarpignato, C.; Holmgren, E.; Olszewski, M.; Rainsford, K.D.; Lanas, A. Mechanisms of Damage to the Gastrointestinal Tract from Nonsteroidal Anti-Inflammatory Drugs. *Gastroenterology* **2018**, *154*, 500–514. [CrossRef]
68. Ilhan, Z.E.; Marcus, A.K.; Kang, D.W.; Rittmann, B.E.; Krajmalnik-Brown, R. pH-Mediated Microbial and Metabolic Interactions in Fecal Enrichment Cultures. *mSphere* **2017**, *2*. [CrossRef] [PubMed]
69. Louis, P.; Scott, K.P.; Duncan, S.H.; Flint, H.J. Understanding the effects of diet on bacterial metabolism in the large intestine. *J. Appl. Microbiol.* **2007**, *102*, 1197–1208. [CrossRef] [PubMed]
70. Garcia, M.A.; Yang, N.; Quinton, P.M. Normal mouse intestinal mucus release requires cystic fibrosis transmembrane regulator-dependent bicarbonate secretion. *J. Clin. Investig.* **2009**, *119*, 2613–2622. [CrossRef]
71. Nilius, B.; Appendino, G. Tasty and healthy TR(i)Ps. The human quest for culinary pungency. *EMBO Rep.* **2011**, *12*, 1094–1101. [CrossRef] [PubMed]
72. Braun, H.-S.; Sponder, G.; Pieper, R.; Aschenbach, J.R.; Deiner, C. GABA selectively increases mucin-1 expression in isolated pig jejunum. *Genes Nutr.* **2015**, *10*, 47. [CrossRef] [PubMed]
73. Rosendahl, J.; Braun, H.S.; Schrapers, K.T.; Martens, H.; Stumpff, F. Evidence for the functional involvement of members of the TRP channel family in the uptake of Na(+) and NH4 (+) by the ruminal epithelium. *Pflugers. Arch.* **2016**, *468*, 1333–1352. [CrossRef]
74. Abdoun, K.; Stumpff, F.; Wolf, K.; Martens, H. Modulation of electroneutral Na transport in sheep rumen epithelium by luminal ammonia. *Am. J. Physiol. Gastrointest. Liver Physiol.* **2005**, *289*, G508–G520. [CrossRef] [PubMed]

Supplementary Materials

The TRPA1 Agonist Cinnamaldehyde Induces Secretion of HCO_3^- by the Porcine Colon (Supplement)

David Manneck [1], Gisela Manz [1], Hannah-Sophie Braun [2], Julia Rosendahl [2] and Friederike Stumpff [1,*]

[1] Institute of Veterinary Physiology, Department of Veterinary Medicine, Freie Universität Berlin, Oertzenweg 19b, 14163 Berlin, Germany; david.manneck@fu-berlin.de (D.M.); gisela.manz@fu-berlin.de (G.M.)
[2] PerformaNat GmbH, Hohentwielsteig 6, 14163 Berlin, Germany; hannah-sophie.braun@fu-berlin.de (H.-S.B.); rosendahl@performanat.de (J.R.)
* Correspondence: stumpff@zedat.fu-berlin.de; Tel.: +49-30-838-62595

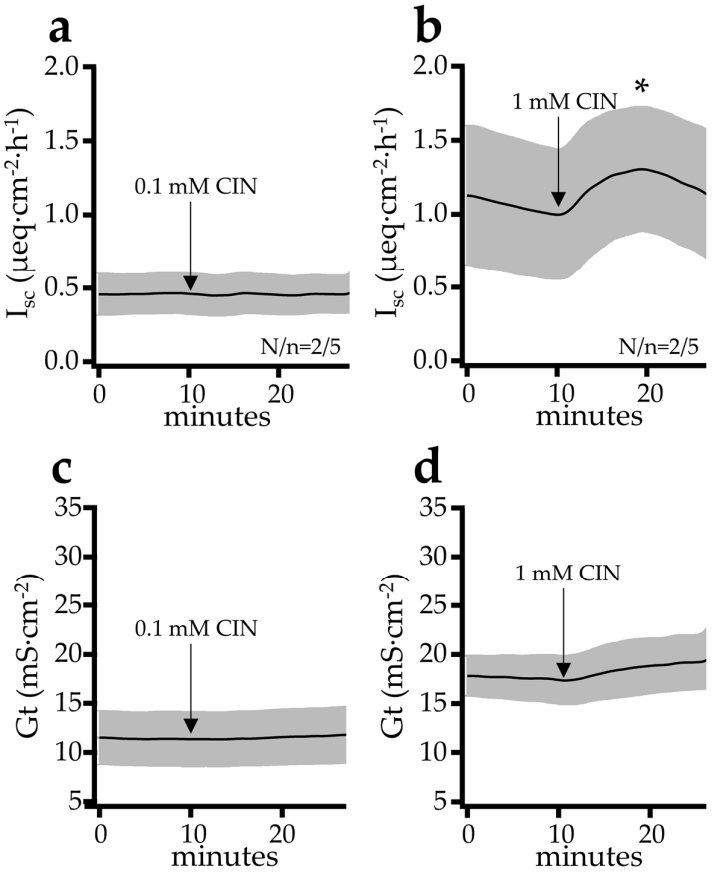

Figure 1. Effect of the TRPA1 agonist cinnamaldehyde at a concentration of 100 µmol·l^{-1} (**a,c**) and 1 mmol·l^{-1} (**b,d**) on I_{sc} and G_t in the Ussing chamber using jejunal tissue of pigs. After the addition of 1 mmol·l^{-1} cinnamaldehyde, a significant increase on the I_{sc} and a trend for G_t could be observed, which was absent when a concentration of 100 µmol·l^{-1} was added. Significant differences are marked as * ($P < 0.05$). N/n = number of animals/number of tissues, identical for G_t and I_{sc}.

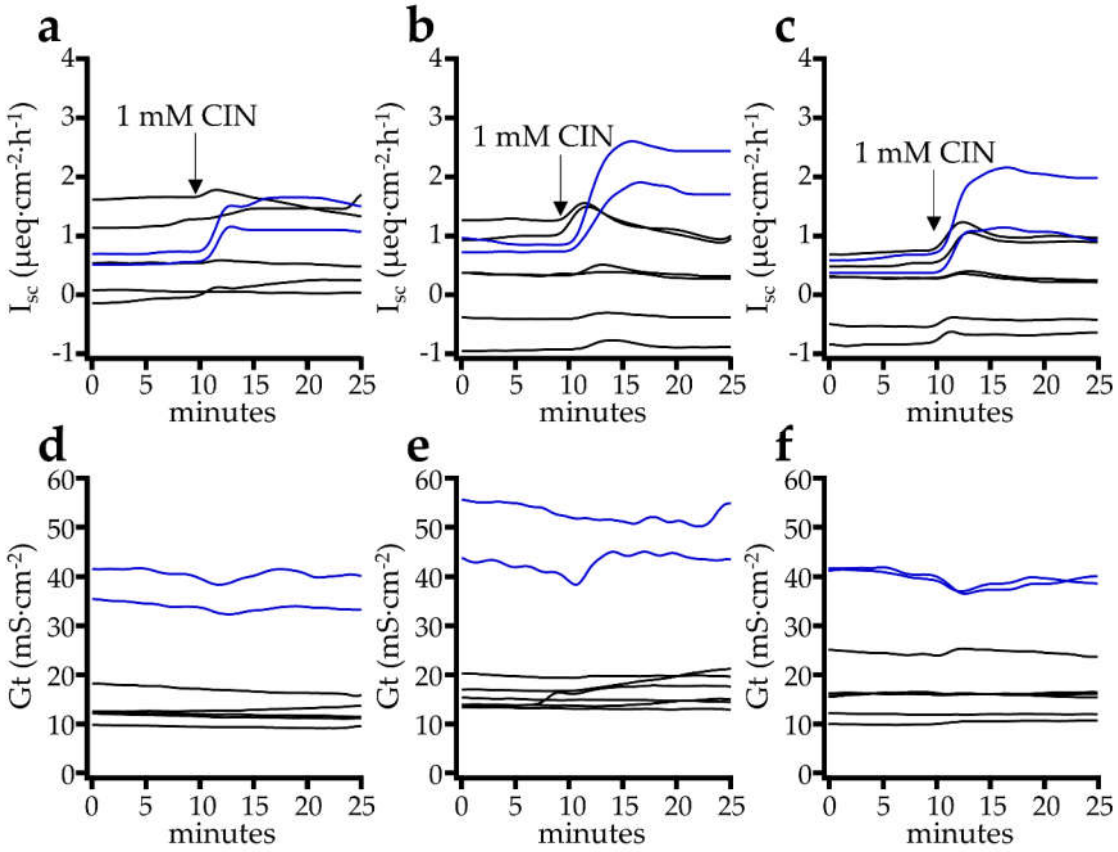

Figure S2. Effect of the TRPA1 agonist cinnamaldehyde (CIN) at a concentration of 1 mmol·l^{-1} after mucosal (**a, d**), serosal (**b, e**), or bilateral addition (**c, f**) on I_{sc} and G_t in the Ussing chamber using jejunal tissue of pigs. After addition, an increase in I_{sc} was observed after mucosal ($P = 0.054$), serosal ($P = 0.008$) and after bilateral addition ($P = 0.011$). However, G_t barely changed after addition in all 3 groups and was not significantly altered. Some tissues were obtained from older pigs from a commercial slaughterhouse (blue lines), while the black lines reflect responses of younger pigs slaughtered within a controlled study as in the rest of the manuscript.

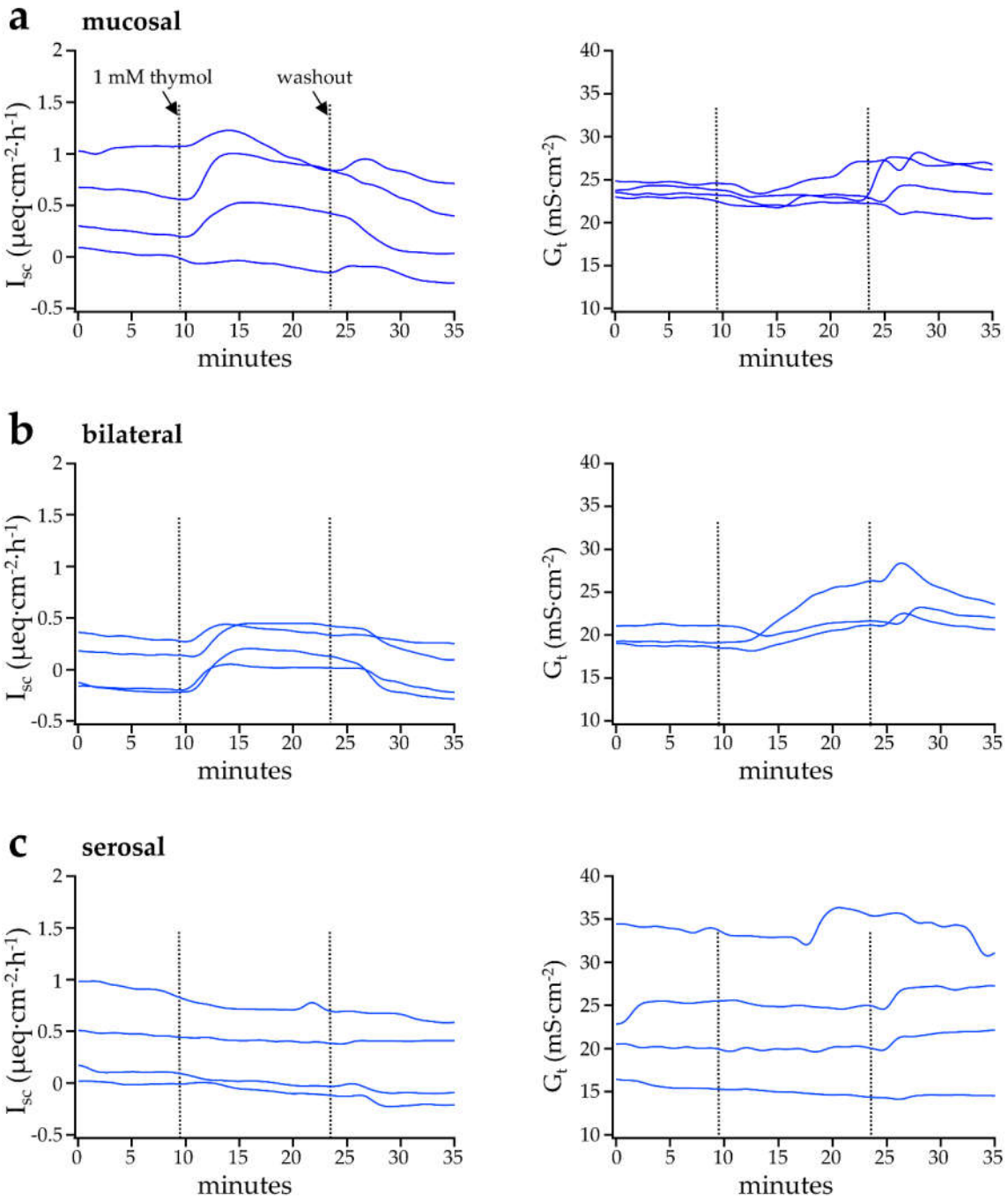

Figure S3. Effect of thymol at a concentration of 1 mmol·l^{-1} after mucosal (**a**), bilateral (**b**), or serosal addition (**c**) on I_{sc} and G_t in the Ussing chamber using colonic tissue of pigs. After mucosal and bilateral addition, a significant increase in I_{sc} and G_t was observed in most tissues, although the effects were absent with serosal addition.

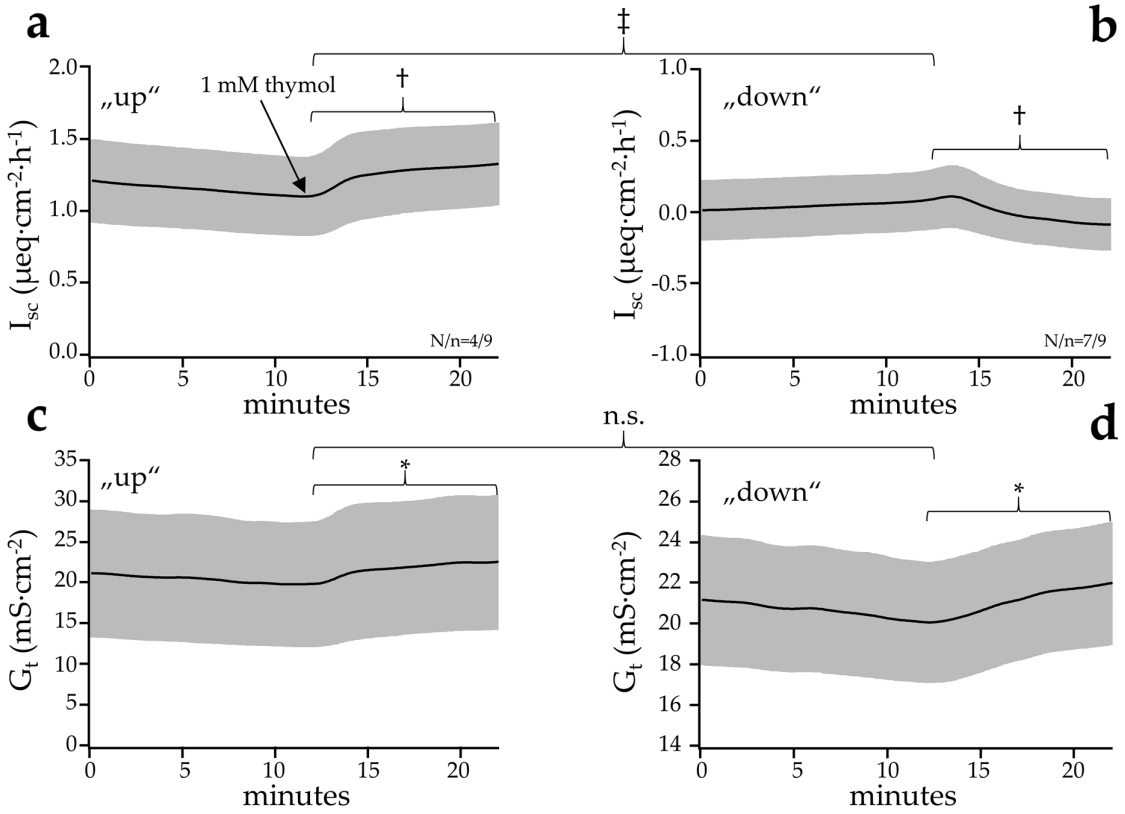

Figure S4. Effect of a bilateral application of thymol on the I_{sc} and G_t of the jejunum of pigs. Data are given as means ± SEM. In some tissues an increase („up“) in I_{sc} could be observed after thymol addition (**a**), whereas in other tissues a decrease or no effect („down“) was observed (**b**). An increase in G_t was observed in all tissues after thymol addition, ruling out barrier effects as a cause for increases in I_{sc} (**c, d**). The significance bars within graphs compare values taken immediately prior to addition of the agonist and after an incubation time of 10 minutes. The significance bars between graphs indicate that in the jejunum, the I_{sc} values were higher in the "up" group from the start. Significant differences are marked as *, †, or ‡ ($P < 0.05$, $P < 0.01$ or $P < 0.001$). N/n = number of animals/number of tissues, identical for G_t and I_{sc}

Table 1. Solutions used in the Ussing chamber experiments. Mucosal and serosal solutions differed only by the addition of 16 mmol·l^{-1} glucose (serosal) and mannitol (mucosal), respectively, unless otherwise indicated. Solutions were adjusted to 300 mosmol·kg^{-1} with mannitol and were titrated to a pH of 7.4 (Tris, HCl).

Item (mmol·l^{-1})	**Standard**	**Na^+ free[1]**	**Cl^- low**	**HCO_3^- free**	**Ca^{2+} free**	**EGTA[2]**
NaCl	120	0	0	120	120	120
$NaHCO_3$	25	0	25		25	25
NaH_2PO_4	0.32	0	0.32	0.32	0.32	0.32
$MgSO_4$	1	1	1	1	1	1.15
KCl	6.3	5.98	6.3	6.3	2	6.3
$CaCl_2$	2	2	2	2	0	0
EGTA	0	0	0	0	0	1
NMDGCl	0	120.32	0	0	0	4
Choline-HCO_3	0	25	0	0	0	0
KH_2PO_4	0	0.32	0	0	0	0
NaGlu	0	0	120	25	0	0
HEPES	0	0	0	10	0	0

[1] Na+ free solution was used as mucosal free only or bilateral free solution. [2] The Ca^{2+} free solution with EGTA was used only on the mucosal side, the serosal side contained the standard solution.

6. General Discussion

6.1. Electrogenic Transport of NH_4^+ in Porcine Intestinal Tissues

The first part of this thesis focused on the effects of luminal ammonium administration in the different gastrointestinal compartments of pigs in the Ussing chamber model. The aim was to answer the question whether ammonium is absorbed by electrogenic processes and whether the involvement of TRP channels might play a role. Data were published in Paper 1 (**Chapter 4**) (Manneck et al. 2021a).

In a first step, ingesta samples from different segments of the porcine gastrointestinal tract were investigated. Ammonia concentrations in the mmol range were measurable in all compartments, with a steady increase from the duodenum with ~1.8 $mmol \cdot l^{-1}$ to the colon with ~16.5 $mmol \cdot l^{-1}$ (**Paper 1**, Table 2). These values give some orientation, but it should be noted that the ammonia concentrations in the intestinal segments can deviate greatly from these values, depending on the composition of the feed. Thus, diets with increased protein and low crude fiber show significantly higher ammonia concentrations compared to diets with reduced protein or increased crude fiber (Pieper et al. 2014, 2012; Stumpff et al. 2013).

In the subsequent experiments with the Ussing chamber technique, it was found that following the luminal application of an solution containing ammonium, there was a significant increase in the short circuit current (I_{sc}) and conductance (G_t) in the different segments (**Paper 1**, Figure 5 & 6, Table 4) that was reversible upon washout. This suggests that there is uptake of NH_4^+ ions across the epithelium, since electroneutral uptake in the form of NH_3 would cause no change in I_{sc}. However, an ammonia-induced stimulation of the secretion of Cl^- or HCO_3^- could have similar effects. Accordingly, experiments with the withdrawal of these anions were performed which showed comparable results. Notably, in studies with rat colon, Cermak et al. (2002, 2000) also observed an increase in I_{sc} after luminal administration of 30 $mmol \cdot l^{-1}$ ammonium, but this maneuver had no effect on the serosal to mucosal or net flux of radioactively labeled $^{36}Cl^-$. The same authors showed that at pH 7.4, luminal ammonium had an inhibitory effect on Na^+ absorption. Cermak et al. (2002, 2000) ruling out the possibility that ammonia stimulated Na^+ transport. A similar inhibition of Na^+ transport by luminal ammonia was observed in the rumen at pH 7.4, although at the more physiological pH of 6.4, Na^+ transport was stimulated (Abdoun et al. 2005), with both results most likely reflecting effects of intracellular pH on sodium-proton exchange (NHE). These results suggest that at least some transport of ammonia occurs in the form of NH_4^+, which can take place either through paracellular or transcellular pathways.

Since a gradient for NH_4^+ was present in these experiments, increased paracellular transport due to the (reversible) opening of tight junction proteins cannot be excluded. In Caco-2 cells, reduced transepithelial resistance and increased dextran fluxes were observed by the administration of ammonium at various concentrations (Yokoo et al. 2021). However, changes in the paracellular barrier are typically observed in studies only after several hours (Yokoo et al. 2021). In the studies performed in this thesis, the effects were observed immediately after administration of ammonium and quickly returned to the original levels after washout.

In a further approach, divalent cations, which are known to block most TRP channels, were removed in the presence of ammonia, resulting in a further increase in I_{sc} that was again reversible. An increase of the I_{sc} could also be observed when divalent cations were removed with an identical NaCl solution on both sides of the tissue. Since the potential across the tissue was clamped to 0 mV, this divalent-sensitive I_{sc} cannot be explained by paracellular involvement, since there was no electrochemical gradient present to serve as a driving force (**Paper 1**, Figure 5 & 6, Table 3). These experiments prove that the tissue expresses a divalent sensitive, transcellular conductance to Na^+. It appears likely that the divalent sensitive uptake of NH_4^+ occurred through the same transcellular pathway. However, it should be stressed that in particular under Ussing chamber conditions, a paracellular leak pathway or one mediated by tight junctions may well have contributed to the NH_4^+ induced current.

Several mechanisms could play a role in the transcellular transport of NH_4^+ across gastrointestinal tissues. Given their ubiquitous distribution, K^+ channels are an option that should not be ruled out (Rubino et al. 2019; Hall et al. 1992). However, the fact that the pathway was found to be divalent sensitive and permeable not only to NH_4^+, but also to Na^+ argues against K^+ selective channels and for the involvement of nonselective cation channels. As discussed in the introduction, transport of NH_4^+ via non-selective cation channels has emerged over the years from more detailed investigations of both Xenopus oocytes and of the ruminal epithelium by a variety of authors (Liebe et al. 2022, 2020; Rabbani et al. 2018; Schrapers et al. 2018; Rosendahl et al. 2016; Lu et al. 2014; Abdoun et al. 2005; Bödeker and Kemkowski 1996; Burckhardt and Frömter 1992).

It appears likely that in particular at less acidic pH, additional transport in the form of NH_3 takes place, for example, via rhesus proteins (Caner et al. 2015; Nakhoul et al. 2010, 2005), via aquaporins or via urea transporters (Weiner and Verlander 2017; Geyer et al. 2013a; Gunther and Wright 1983). Furthermore, an uptake of NH_4^+ via NHE as proposed for rat colon should not be ruled out (Cermak et al. 2002, 2000), although it cannot explain the increase in I_{sc}. An involvement of NKCC appears unlikely, since this transporter is basolaterally expressed in the intestine. An additional increase in the conductance of the paracellular pathway is a possibility that cannot and should not be ruled out.

6.2. Expression of TRP Channels in the Porcine Gastrointestinal Tract

Due to their low selectivity for various cations and as described above, TRP channels are prime candidate proteins that might mediate the transport of NH_4^+. Surprisingly little is known about the expression of the various TRP channels by tissues of the gastrointestinal tract. This is likely due to the low expression level of some channels in many tissues. In this context, note that carriers such as NHE typically do not transport more than 10^2 to 10^4 ions per second and molecule. Conversely, ion channels typically conduct around 10^7 to 10^8 ions per second and molecule (Fakler 2019), so that expression levels are typically only a small fraction of those observed for carriers. In addition, some TRP channels, such as TRPV5 and TRPV6 show very strong similarities (Peng et al. 1999), making primer and antibody design difficult. Primer design is further complicated by additional splice variants of the channels or variations in the predicted sequences. One aim of the current thesis was to fill some of these gaps and to compare the expression of mRNA for several different TRP channels in different parts of the porcine gastrointestinal tract.

Arguably, fairly much is known about the function and expression of TRPV6 in the gastrointestinal tract. This channel was classically known as ECaC2 or “epithelial calcium channel” since it plays an important role in the absorption of calcium (van Goor et al. 2017; Christakos et al. 2016; Schröder and Breves 2006). The current investigation confirms that the highest expression is found in the mucosa of the duodenum (Schröder and Breves 2006; Nijenhuis et al. 2003; Hinterding 2002), with lower expression in the mucosa of the cardia of the stomach, jejunum, caecum and colon (**Paper 1**, Figure 1). A TRPV5 primer was successfully constructed that showed a reliable band with weak expression in the duodenum, jejunum, and ileum by conventional PCR in gel electrophoresis, but no primer could be designed for qPCR studies that showed reliable separation from TRPV6, which is a problem that other authors have already described (Hinterding 2002). However, TRPV5 is thought to play a minor role in the gut (Christakos et al. 2016).

Much less is known about TRPM6 and TRPM7 channels, which are highly selective for magnesium and therefore play significant roles in the absorption and homeostasis of this ion (Schlingmann et al. 2007; Voets et al. 2004b). In the current study of the porcine gut, mRNA for both channels was detected in all tissues of the mucosa and muscularis of the gastrointestinal tract (**Paper 1**, Figure 1). TRPM6 showed higher mRNA expression in the epithelium of the jejunum, caecum and colon, whereas TRPM7 seemed to be ubiquitous, which is in line with the proposed function of this channel as a general “housekeeper” of cellular Mg^{2+} homeostasis (Dimke et al. 2011). Although no data were found on the expression distribution of TRPM6 and TRPM7 in porcine intestinal segments, the results are consistent with the literature in other species (Holzer 2011; Rondón et al. 2008).

In contrast, TRPM8, which also belongs to the melastatin group, is less selective and conducts Na^+ and Ca^{2+} (Janssens et al. 2016). In addition, TRPM8 can be activated by several phytogenic agents, such as menthol and thymol (Almaraz et al. 2014; Ortar et al. 2012; Bautista et al. 2007). The expression of TRPM8, though, could not be detected in the gastrointestinal tissues of porcine mucosa and muscularis. This is consistent with mouse and human studies, where mRNA was also not detected in the intestinal segments (Mihara et al. 2010; Penuelas et al. 2007; Fonfria et al. 2006). However, some authors also describe an expression of TRPM8 in the mucosa of the stomach and small intestine of mice (Zhang et al. 2004) or in the muscularis and mucosa of the distal colon in humans (Amato et al. 2020).

Likewise, TRPV1 could not be detected in the mucosa and muscularis of the intestinal segments of the pigs in this study. However, studies of the human and mouse intestine have demonstrated TRPV1 expression in the distal colon and rectum, although expression levels were either very low or not detectible in the remaining areas of the gastrointestinal tract, being almost exclusively restricted to nerve fibers (Rizopoulos et al. 2018; Matsumoto et al. 2009; Funakoshi et al. 2006). The low expression level might explain why TRPV1 could not be detected in the experiments performed in this thesis. Furthermore, samples were taken from the mid-colon, and not from the distal colon, where expression appears to be significantly lower (Matsumoto et al. 2009).

The expression of TRPV2 in the gastrointestinal tract has also been insufficiently examined. Studies of mice have shown that mRNA of TRPV2 is expressed in the muscularis of the stomach and small intestine, but not in the mucosa (Zhang et al. 2004). In contrast, TRPV2 expression has been described in the mucosa of the colon in humans (Toledo Mauriño et al. 2020) and in the small intestine of laying hens (Gloux et al. 2019). Moreover, TRPV2 expression has been detected mainly in neurons of the gastrointestinal tract of mice and rats, but not in epithelial cells (Kashiba et al. 2004; Zhang et al. 2004). In our study of the porcine gut, TRPV2 mRNA expression was mainly seen in the mucosa of the small intestine, especially in the jejunum and ileum (**Paper 1**, Figure 1). In the mucosa of the stomach and colon, as well as in the muscularis of the gastrointestinal tract, expression levels of TRPV2 were weak.

The expression of TRPV3 by transporting cells of the colon has long been described, but the function of this protein remains mysterious (Nilius et al. 2014; Holzer 2011). Due to its importance for NH_4^+ transport by the ruminal epithelium, detection of TRPV3 was performed both on the level of mRNA and on the protein level in this study, which led to some interesting observations. At the mRNA level, TRPV3 expression was detected exclusively in the mucosa of caecum and colon (**Paper 1**, Figure 1). However, further studies on the protein level showed that the epitope to which the TRPV3 antibody bound was expressed by all intestinal segments (**Paper 1**, Figure 3). A similar result was observed in immunohistological studies, where

expression of TRPV3 could be detected in all intestinal segments, albeit mainly localized to the apical membrane of the transporting epithelia, in addition to the gastric pits of the stomach (**Paper 1**, Figure 4). Furthermore, only the colon showed an additional weak band at the expected level of ~90 kDa, with a shorter band detected at ~60 kDa in all other tissues, including the colon (**Paper 1**, Figure 3).

Inconsistencies between mRNA and protein expression are not unusual and have been described in the literature many times (Greco et al. 2018; Cheng et al. 2016), so that various possibilities for this are likely. Xu et al. (2006) showed that mRNA expression is mainly found basally in the epithelial layers of the tongue, and the amount of TRPV3 protein seems to increase with progressive differentiation and epithelial migration. Since intestinal cells also migrate from the crypt base and differentiate further during this process, a similar mechanism is also conceivable here. Thus, high TRPV3 mRNA expression would be expected in the new intestinal cells in the crypt region, but high TRPV3 protein expression in the villus tip, as was found in this study. Indeed, rat colon showed that mRNA expression of TRPV3 was higher in crypt cells than in residual tissue (Kaji et al. 2012). As villi are very prominent in the small intestine, mRNA expression may not be detectable in mucosa samples due to insufficient levels of TRPV3 mRNA.

However, another very likely reason for the mismatches between mRNA and protein expression of TRPV3 are different splice variants, which would also explain the differences observed in the Immunoblots. Various splice variants have been described for TRP channels, frequently leading to functional changes (Ramsey et al. 2006; Vázquez and Valverde 2006). In the case of TRPV3, several variants have been found (Yang and Zhu 2014; Smith et al. 2002; Xu et al. 2002). Thus, in addition to the full ~90 kDa protein, a shorter ~60 kDa variant has been described in the mouse and bovine species (**Paper 1**, Supporting Tables A2 and A3), the full sequences of which are available (XM_015458625.2, NM_001099024.1, NM_145099.3, XM_006533348.3) (Church et al. 2009; Zimin et al. 2009). In addition, there is evidence for both of these variants in human and bovine keratinocytes (Liebe et al. 2021, 2020; Szöllősi et al. 2018). Since the TRPV3 channel is remarkably well preserved between different species (see Alignment in **Paper 1**, Supporting Table A3), and given the size of the bands in the immunoblots, it appears quite likely that the porcine species also expresses both of these TRPV3 variants.

The initial goal was therefore to find a primer that would be suitable for different splice variants described. However, creating a suitable TRPV3 primer for both splice variants proved challenging and thus no suitable primer could be found, despite several attempts, as they always produced more than one prominent melting curve in PCR. In retrospect, this is not surprising since the short splice variant is a truncated part of the long splice variant and any

primer that will amplify the short variant should also amplify the long variant, thus producing at least two melting curves.

Seen from this perspective, the discrepancy between the PCR and the Immunohistochemical results are explicable. Both variants of TRPV3 contain the epitope of the murine antibody that was used, and it thus bound to both the short ~60 kDa and the long ~90 kDa variant. Conversely, the primer for amplification of mRNA only bound to the long, ~90 kDa variant. It would thus appear that only the colon and the caecum expressed the full-length TRPV3 variant, while the shorter variant was expressed by all tissues of the porcine intestinal tract. Notably, the short variant does not include the pore region of the channel (see alignment in the supplement of Liebe et al. 2022). The truncated ~60 kDa splice variants of TRPV3 are thus unlikely to serve as channels and their function remains mysterious. But it is intriguing to note that fully functional TRPV3 channels are expressed by those gastrointestinal organs with the highest rate of ammonia absorption, namely, the colon, the caecum and (in ruminants) the rumen.

Ueda et al. (2009) examined the expression of some TRP channels in murine intestinal sections and detected expression at the mRNA level in the distal colon but not in the stomach, duodenum, or proximal colon. Inspection of the primer used in that study reveals that it was also only suitable for the longer ~90 kDa variant. At the protein level, the distal colon also showed two prominent bands at different heights, but verification of the antibody used by Ueda is not possible due to lack of information on the binding epitope. Studies on TRPV3 mRNA expression in humans showed that very weak expression could also be detected in the stomach and small intestine, also using a primer that detected the full length of the gene (Xu et al. 2002). The authors showed in further Northern blot analyses that a splice variant probably exists in the stomach. De Petrocellis et al. (2012) demonstrated expression of TRPV3 mRNA in the jejunum and ileum of mice.

TRPV4 expression was also examined at the mRNA and protein levels. This showed that at the mRNA level, expression was found in the mucosa and muscularis in all gastrointestinal sections, with the highest expression in the stomach (**Paper 1**, Figure 1). At the protein level, this picture could be confirmed and thus a clear band at the expected ~90 kDa level could be seen in the examined mucosa samples of the different segments (**Paper 1**, Figure 2). Apart from the stomach, however, another band at the level of ~80 kDa could be detected. This could be due to a splice variant as described in other studies (Toft-Bertelsen and MacAulay 2021; Pritschow et al. 2011; Hartmannsgruber et al. 2007). Immunohistological studies of TRPV4 showed a similar picture to TRPV3, where staining was mainly found in the apical membrane of superficial epithelial cells in the intestinal segments and in the gastric pits of the stomach (**Paper 1**, Figure 4). In the literature, TRPV4 expression has been reported in

the stomach (Mihara et al. 2016), small intestine (De Petrocellis et al. 2012) as well as in the colon (Toledo Mauriño et al. 2020; D'Aldebert et al. 2011). TRPV4 is known as an osmosensor and this may be its primary function in the gastrointestinal tract, explaining its ubiquitous distribution.

TRPA1 was detected at the mRNA level primarily in the mucosa of the caecum and colon, but also to a lesser extent in the stomach, duodenum, and jejunum. (**Paper 2**, Figure 1). In the muscularis of the gastrointestinal tract and in the mucosa of the ileum, the expression of TRPA1 was below the detection limit. It was not possible to find a suitable TRPA1 antibody for the pig because all antibodies used showed multiple or no bands in the Western blots performed, indicating nonspecific binding. The additional mouse samples in these experiments, which served as controls, made it clear that they were suitable for use in mice, as proposed by the distributer.

Van Liefferinge et al. (2020) used a TRPA1 antibody that showed strong colocalization with chromogranin A positive cells in the pyloric region of the stomach of pigs in immunohistochemical studies, suggesting predominant expression in gastrin-releasing cells. In the small intestine, staining was associated with colocalization with GLP-1 positive cells in the same study. However, the authors did not mention how the antibody used was validated. Nevertheless, a consistent picture emerges in the literature, where TRPA1 expression in the gastrointestinal tract is described mainly in enteroendocrine cells (Bellono et al. 2017; Cho et al. 2014; Nozawa et al. 2009) and in peripheral nerve fibers (Yang et al. 2008; Zhang et al. 2004).

6.3. Possible Involvement of TRP Channels in the Transport of NH_4^+

Molecular biological evidence in tissues alone is not sufficient to assess predictions about the function or relevance of the genes in question. Therefore, further studies using agonists declared to be specific were performed to determine whether there was functional relevance in the colon of TRPV3 and TRPV4, since expression for these two channels was detectable at the mRNA and protein levels in gastrointestinal tissues. Unfortunately, to date there is neither a highly specific agonist nor an antagonist for TRPV3, but 2-APB is considered a reliable and high potent agonist for TRPV3 (Hu et al. 2009). However, 2-APB also has agonistic effects on TRPV1, TRPV2, and TRPA1 (Gao et al. 2016; Hinman et al. 2006). In addition, it shows antagonistic effects on TRPC3, TRPC4, TRPC5, TRPC6, TRPC7, TRPM7, TRPM8 and TRPP1 (Talavera et al. 2020; Chokshi et al. 2012; Harteneck and Gollasch 2011; Hu et al. 2004) with no effects described for TRPV6 (Hu et al. 2004). In the experiments performed, 2-APB showed marked functional effects in the colonic mucosa with increased G_t

and decrease I_{sc} under conditions with NaCl Ringer on both sides of the tissue (**Paper 1**, Figure 7).

On the basis of these effects, functional involvement of those TRP channels on which 2-APB acts antagonistically appears unlikely, because this should have resulted in a decrease in both I_{sc} and G_t, as observed in the rat caecum (Pouokam and Diener 2019). The involvement of TRPV1 should also be regarded as unlikely, as no mRNA expression was detected in the colon and TRPV1 has been detected almost exclusively in nerve fibers in the literature. For TRPV2, no expression in the superficial epithelium has been described so far either, which also suggests an involvement as unlikely (Zhang et al. 2004). This leaves TRPV3 or TRPA1. Activation of TRPA1 by the specific agonists cinnamaldehyde or allyl isothiocyanates always caused a reliable increase in I_{sc} in studies conducted with the colon of pigs, mice, rats, and humans (**Paper 2;** Fothergill et al., 2016; Kaji et al., 2012). Conversely, TRPV3 also has a high permeability to K^+ - which may be the reason why the G_t rose whereas the I_{sc} decreased.

The selectivity for cations is substantially different in TRPA1 and TRPV3. For permeation through an ion channel, the ions must interact with the binding site of the channel of the pore structure (Talavera and Nilius 2011; Owsianik et al. 2006). According to Eisenman's theory the biophysical properties of a pore and of the ions in question determine the extent to which these cations are conducted, leading to a total of 11 different permeability sequences (Table 1; Eisenman 1962). This model, which has been remarkably useful for modulation of channel permeation over many decades, assumes that permeation is determined by the competition between the energy released when an ion binds to the pore and the energy required for its dehydration. If the TRP channels in question are now observed, it becomes apparent that TRPA1 follows an Eisenman sequence XI (Talavera et al. 2020), whereas TRPV3 follows an Eisenman sequence IV (Liebe et al. 2020; Owsianik et al. 2006). Accordingly, activation of TRPA1 in the colon is expected to primarily increase absorption of Na^+ with increasing I_{sc}, whereas activation of TRPV3 is expected to increase both absorption of Na^+ and secretion of K^+, with the ultimate impact on I_{sc} depending on the exact electrochemical gradients. If the tissue in question has a very negative membrane potential, an initial increase in I_{sc} can be expected, reflecting influx of Na^+, as observed in studies of the rumen (Liebe et al. 2022; Rosendahl et al. 2016). As the membrane potential becomes more depolarized due to the influx of Na^+ or is less negative from the start, K^+ secretion will predominate, and the I_{sc} will decrease, as observed in the performed studies. In this context, the increase in G_t could be due to an increase in the opening of ion channels, an increase in the paracellular conductance or a combination of both.

Table 1 Eisenman sequences with associated selectivity of cations (Eisenman 1962)

Sequence	Selectivity
I	$Cs^+ > Rb^+ > K^+ > Na^+ > Li^+$
IIa	$Cs^+ > K^+ > Rb^+ > Na^+ > Li^+$
II	$Rb^+ > Cs^+ > K^+ > Na^+ > Li^+$
IIIa	$K^+ > Cs^+ > Rb^+ > Na^+ > Li^+$
III	$Rb^+ > K^+ > Cs^+ > Na^+ > Li^+$
IV	$K^+ > Rb^+ > Cs^+ > Na^+ > Li^+$
V	$K^+ > Rb^+ > Na^+ > Cs^+ > Li^+$
VI	$K^+ > Na^+ > Rb^+ > Cs^+ > Li^+$
VII	$Na^+ > K^+ > Rb^+ > Cs^+ > Li^+$
VIII	$Na^+ > K^+ > Rb^+ > Li^+ > Cs^+$
IX	$Na^+ > K^+ > Li^+ > Rb^+ > Cs^+$
X	$Na^+ > Li^+ > K^+ > Rb^+ > Cs^+$
XI	$Li^+ > Na^+ > K^+ > Rb^+ > Cs^+$

Since TRPV4 also follows an Eisenman sequence IV (Owsianik et al. 2006; Voets et al. 2002) and there is similar expression in the colon compared to TRPV3, activation of TRPV4 should lead to identical results. Indeed, using the highly specific TRPV4 agonist GSK1016790A (Thorneloe et al. 2017, 2008), a decrease in I_{sc} with a concomitant increase in G_t (**Paper 1**, Figure 7) was observed. However, it should be noted that the concentration of the agonist was relatively high compared to what is effective in patch clamping (Liebe et al. 2022). In conjunction with the molecular biological data, functional expression of TRPV3 may play important roles in the uptake of NH_4^+ from the colon, with contributions of TRPV4 playing a role throughout the intestine, in particular when the channel is activated by osmotic challenges.

Studies in neurons have shown that ammonia causes activation of TRPC1, TRPV1, and TRPA1 channels (Balakrishnan and Mironov 2020; Dhaka et al. 2009). The activation of TRPA1 is thought to function via the modification of intracellular cysteine residues (Dhaka et al. 2009), a mechanism also described for cinnamaldehyde and allyl isothiocyanate (Macpherson et al. 2007; Hinman et al. 2006). Furthermore, studies using the patch-clamp technique showed that HEK-293 cells overexpressing the bovine or human TRPV3 exhibit a conductance for NH_4^+ that is nearly twice that for Na^+ (Liebe et al. 2021, 2020; Schrapers et al. 2018). But other TRP channels also show conductivity for NH_4^+, as shown for TRPV4 and TRPV6 (Liebe et al. 2022; Voets et al. 2004a).

Transcellular transport of NH_4^+ should result in minimal changes of cytosolic pH (Figure 2) although an acidification is expected if NH_4^+ is subsequently deprotonated. This can be the case if efflux occurs partially as NH_3 or if NH_3 is sequestered in organelles and converted to nitrogenous compounds (Musa-Aziz et al. 2009b). Transport of NH_3, in contrast, should lead to an increase in intracellular pH, as more protons are bound.

It should be stressed that in a majority of cell types exposed to solutions containing NH_4^+, the influx of NH_3 initially predominates, leading to a rapid alkalinization (Worrell et al. 2004; Helbig et al. 1988). Subsequently, a slower acidification can be observed (Boron 2004; Thomas 1984). After washout of NH_4^+, the cell returns to a cytosolic pH that is more acidic than at the beginning of the experiment. The classical explanation for the acidification of cells by what is known as the "NH_4Cl-prepuls technique" is that initially, influx of NH_3 predominates until there is an equilibration of NH_3, preventing further influx of NH_3 (Boron 2004). However, there is simultaneously an influx of NH_4^+, which dissociates into NH_3 and H^+ until equilibrium prevails across the membrane for this ion as well. After removal of external NH_4Cl, outflow occurs predominantly in the form of NH_3, which leads to acidification of the cell, while efflux of NH_4^+ is prevented by the negative membrane potential (Marcaggi and Coles 2001; Boron and De Weer 1976).

However, not all cells respond in this manner. Experiments on native Xenopus oocytes have shown that an immediate acidification of intracellular pH occurs after the addition of ammonium chloride, suggesting that from the start, influx of NH_4^+ predominates (Liebe et al. 2020; Musa-Aziz et al. 2009b; Burckhardt and Frömter 1992). Unlike the immediate pH recovery observed in most cell types, washout after an NH_4Cl prepuls in Xenopus Oocytes is very slow, suggesting a very limited permeability of the membrane to NH_3. A similar picture was also seen in astrocytes (Nagaraja and Brookes 1998) or the epithelium of the rumen (Rosendahl et al. 2016; Lu et al. 2014). Furthermore, in the ruminal epithelium, application of NH_4Cl at pH 6.4 stimulated uptake of Na^+ via NHE, further arguing for an uptake of ammonia in the protonated form as NH_4^+ (Abdoun et al. 2005).

Our attempts to observe the effects of NH_4Cl on native porcine epithelium using double-barrelled ion-selective microelectrodes failed despite extensive attempts, which may have been due to the fragility of the single-layered epithelial cells. In the rumen, multiple layers of cells are covered by the thick layers of the stratum corneum, which greatly facilitates such experiments (Rosendahl et al. 2016; Lu et al. 2014).

6.4. Effect of Phytogenic Agents and Modes of Action in the Intestine

The second part of this thesis focused on the electrophysiological effects of phytogenic TRP modulators in the jejunum and especially the colon of pigs. Data were published in Paper

2 (**Chapter 5**) (Manneck et al. 2021b). The use of these phytogenic substances could be particularly interesting from a pharmacological point of view to improve health. However, little is known so far about the exact mode of action of these agonists. Further complicating matters is the fact that many of the phytogenic agents appear to have other, non-TRP-mediated mechanisms of action.

To investigate the effect of the potent TRPA1 agonist cinnamaldehyde on colonic epithelium, the underlying mechanisms were investigated in Ussing chambers with the help of different blockers and solutions. Addition of 100 µmol·l^{-1} cinnamaldehyde under NaCl Ringer conditions showed no effects in the colon or jejunum (**Paper 2**, Figure 2 and Supplementary Materials Figure S1). However, at a concentration of 1 mmol·l^{-1} cinnamaldehyde, there was an increase in I_{sc} and G_t, which was reversible after washout. As discussed above, the increase in I_{sc} under conditions with no electrochemical gradient present must represent transcellular transport energized by a primary active transport process, such as the Na^+-K^+-ATPase.

Similar observations were made in studies using rat colon (Kaji et al. 2012), mouse duodenum and colon (Fothergill et al. 2016) or porcine jejunum (Boudry and Perrier 2008). However, here a smaller concentration of 100 µmol·l^{-1} cinnamaldehyde showed significant effects. One reason for this could be the mucus layer of the colon or also a different genetic background of the animals. However, it should be noted that other research groups at the laboratory also only saw effects at higher concentrations in the jejunum of pigs with the same genetic background, even when using other phytogenic agents. Interestingly, when using colon tissue from adult pigs from the slaughterhouse, a much greater increase in I_{sc} was observed after the addition of 1 mmol·l^{-1} cinnamaldehyde. This could be due to a different genetic background, but also to the age difference or the fact that these animals were fasted before slaughter in contrast to the younger animals. However, in the course of the study it became clear that the use of slaughter animals should be considered inappropriate for several reasons: 1) The baselines of I_{sc} and G_t showed greater variation between animals. 2) Tissue removal is delayed due to the slaughter process, which may result in reduced tissue viability. 3) Clearly stronger animal-dependent differences in the effects could be observed, although the causes (e.g. impaired vitality) for this were always unclear. A striking observation was that theophylline (which stimulates Cl^- secretion via a cAMP dependent pathway from crypt cells) continued to show effects, while agents with effects on apically expressed channels often showed no effect. This suggests that cells of the surface epithelium may have been degraded by various processes following slaughter, although crypt cells remained intact. Reasons for this may include insufficient supply with oxygen through the thick mucus layer followed by microbial invasion.

It can be assumed that apical receptors for cinnamaldehyde are necessary for the observed electrophysiological effects in the colon, since they were observed only after the addition of 1 mmol·l^{-1} cinnamaldehyde on the mucosal side or after bilateral addition, but not after serosal addition (**Paper 2**, Figure 3). As a receptor, TRPA1 is the main candidate, since it shows apical epithelial expression in the colon and small intestine, especially in enteroendocrine cells (Bellono et al. 2017; Kaji et al. 2012) and was detected by us in the mucosa of the porcine colon via qPCR. For this reason, further studies were conducted using different blockers or solutions to better understand the mechanism of action. It was found that the manipulation of cation concentration and their channels mainly showed an effect on G_t, whereas the manipulation of anion concentration and their channels mainly had an effect on I_{sc} (**Paper 2**, Figure 4, Table 1 & 2). Thus, removal of divalent calcium ions significantly increased the cinnamaldehyde-induced increase in G_t, whereas removal of monovalent Na^+ ions resulted in a reduction of the G_t increase. This seems logical, since it has already been demonstrated that divalent cations can have a blocking effect on TRP channels, so that their elimination can lead to increased transport of monovalent cations (Schrapers et al. 2018; Owsianik et al. 2006). The reduction of the G_t increase after Na^+ elimination can be explained by the fact that a reduced transport of cations through the TRP channels occurs, with paracellular transport a further option. Channel-mediated effects are supported by the effect of quinidine, a nonspecific blocker of cation channels, which also reduced the cinnamaldehyde-induced G_t increase. However, it should also be noted at this point that for the solutions in which Na^+ was eliminated, $NMDG^+$ was substituted as a compensating substance. $NMDG^+$ is a very large cation, but studies showed that despite its size, it can also be transported to some extent through cation channels (Schrapers et al. 2018; Xu et al. 2002). Here, it probably has a similar blocking effect as divalent cations, which may have led to an additional blocking effect on the G_t increase. Differences in the cinnamaldehyde-induced I_{sc} increase compared to control could not be observed under these interventions, most likely because efflux of K^+ occurs in addition to influx of Na^+, so that a block of both conductances by quinidine does not lead to a change in the net transport of ions.

The I_{sc} increase after cinnamaldehyde addition in the colon is mainly due to the secretion of anions, especially HCO_3^-, via a prostaglandin-mediated cascade. This can be concluded from the fact that the cyclooxygenase inhibitor indomethacin led to a significant reduction of the cinnamaldehyde-induced I_{sc} increase, which was also seen after the elimination of HCO_3^- from the solution. This conclusion is further supported by effects of the non-specific anion channel blocker NPPB, which also decreased the cinnamaldehyde-induced I_{sc} rise. Cl^- ions appear to play a minor role in this response, as the basolateral NKCC1 blocker bumetanide or removal of Cl^- ions from the solution did not show significant I_{sc} effects.

A similar prostaglandin-dependent activation of anion secretion has been observed after activation of TRPA1 by luminal application of the synthetic TRPA1 agonist allyl isothiocyanate (AITC) in the colon of humans, rats, and mice (Fothergill et al. 2016; Kaji et al. 2012). The exact reasons for this remain to be clarified, but some speculation is possible. Prostanoids such as PGE2 are anions that are synthesized from membrane phospholipids via cyclooxygenase-mediated pathways and secreted. Signalling ends when the anionic prostaglandin is taken up into the cytosol via an electrogenic anion exchanger, OATP2A1 (SLCOA1), after which the prostaglandin is degraded by cytosolic enzymes (Nakanishi et al. 2021; Nakanishi and Tamai 2017). It is possible to speculate that opening of TRPA1 by agonists such as AITC or cinnamaldehyde leads to a depolarization of the cell after influx of Na^+ and Ca^{2+}. This depolarization would interfere with the reuptake of negatively charged PGE2 via OATP2A1, leading to increased binding of PGE2 to its receptor EP4 with subsequent formation of cAMP and secretion via CFTR.

But other hypotheses are possible. Thus, following activation of TRPA1 in enterochromaffin cells, a release of serotonin has been reported (Bellono et al. 2017; Nozawa et al. 2009). Serotonin, in turn, leads to the secretion of HCO_3^- after binding to its receptors and is well studied in the duodenum (Hansen and Witte 2008). Serotonin also leads to HCO_3^- secretion in the colon, as shown by studies in the rat (Kaji et al. 2015). On the other hand, it is not clear how prostaglandin signalling comes into this model of cinnamaldehyde effects. Furthermore, studies with mouse duodenum and colon showed that blocking of the serotonin receptors 5-HT_3 and 5-HT_4 did not result in any change in the induced current after the addition of AITC, so further research is needed on this aspect (Fothergill et al. 2016).

Intracellular organelles, such as the endoplasmic reticulum, endosomes, etc., could also play a role, since TRP channels are frequently expressed by subcellular membranes, but research on their precise role is lacking (Gees et al. 2010). Notably, activation of the EP4 receptor may also lead to increased formation of mucins (Akaba et al. 2018; Belley and Chadee 1999). This assumption is also confirmed by in vivo results in rats, where cinnamaldehyde supplementation led to increased expression of the mucin gene Muc2 (Qi et al. 2021).

When the TRPV3 agonist thymol was used, a more variable response pattern was observed, and the effects were mostly animal-specific. Although the addition of thymol also always led to an increase in G_t, the I_{sc} responses were highly variable (**Paper 2**, Figure 5, Supplementary Materials Figure S4). In some cases, there was an increase in I_{sc}, but in many tissues, a direct decrease in I_{sc} was observed. A similar picture was also seen in a few experiments with other TRP agonists, such as carvacrol or linalool. In contrast to the relatively specific phenylpropanoid TRPA1 agonist cinnamaldehyde, thymol, carvacrol and linalool are monoterpenes and activate TRPV3, but also TRPA1 (Nilius et al. 2012; Vogt-Eisele et al.

2007). As discussed above, TRPA1 has a higher selectivity for Na^+ and Ca^{2+} over K^+ than TRPV3. Activation of TRPV3 should thus lead to increased efflux of intracellular K^+ with a corresponding decrease in I_{sc}, as was seen after the addition of the TRPV3 agonist 2-APB (**Paper 1**, Figure 7). Conversely, an increase in I_{sc} could follow TRPA1 activation, as was observed after application of cinnamaldehyde. Interestingly, even in tissues that showed an increase in I_{sc}, thymol led to lower increases in I_{sc} than cinnamaldehyde, despite a similar increase in G_t. This may indicate a combined effect of thymol on both Na^+ absorption and K^+ secretion (**Paper 2**, Figure 6e).

Interestingly, the TRPA1 blocker HC-030031 blocked the thymol-induced I_{sc} in the rat colon (Kaji et al. 2011). Furthermore, a neuronal component may also be involved, as experiments in porcine small intestine showed that thymol-induced current could be inhibited by tetrodotoxin (Blocker of voltage-gated sodium channels of nerve cells) and hexamethonium (nicotinic receptor antagonist) (Boudry and Perrier 2008). However, this could not be confirmed with experiments in rat colon (Kaji et al. 2011). Accordingly, these TRP agonists appear to have additional mechanisms of action that remain to be explored in more detail. This is also true for effects of cinnamaldehyde on the jejunum. In contrast to the colon, where apical application was necessary, in the jejunum a basolateral application also led to effects (**Paper 2**, Figure 3, Supplementary Materials Figure S2). This suggests a more complex mechanism of action, possibly involving submucosal neurons.

6.5. Practical Application of Phytogenic Agents in Livestock Feeding and their Effects on Performance, Health and the Environment

In livestock feeding, the described TRP modulators are increasingly being used with positive effects on animal performance and health. Thus, many studies show a positive effect of phytogenic components on daily growth performance or feed conversion rate (Franz et al. 2010; Costa et al. 2013; Windisch et al. 2008). It is possible to speculate that this effect may be related to enhanced uptake of cations from the diet, such as Ca^{2+}, but possibly also Mg^{2+} or other trace minerals.

In addition, some studies have also shown that the substances used have effects on fecal ammonia production. Unfortunately, most of these studies worked with natural compounds such as dried spices, herbs or essential oils, so that the exact concentration of the individual active ingredients is often unknown and further additional effects may occur due to other active ingredients. Feeding *mentha piperita* (menthol) to caecal fistulated pigs was shown to result in a reduction in the emissions of ammonia from the caecal content (Ushida et al. 2002). When a mixture of fenugreek, clove (eugenol) and cinnamon (cinnamaldehyde) was used on weaned piglets, a numerical reduction in ammonia emissions were observed (Kim et

al. 2015; Cho et al. 2005). Similar effects were also observed in chickens, where feeding essential oil from oregano (thymol, carvacrol), anise (anethol) and citrus peel powder (citral) reduced ileal ammonium concentration (Hong et al. 2012). However, provided that more ammonia was absorbed from the ileum following the application of these TRP channel agonists, this would have led to a higher rate of renal excretion, with the negative effects mentioned in the introduction. It is thus clear that far more work needs to be done.

It is commonly believed that the positive effects of phytogenic agents on animal growth and reduced emission of ammonia are due to a change in the microbiota with concomitant reduction of pathogens, toxins and their metabolites, such as ammonia or biogenic amines (Windisch et al. 2008). Frequently, a “destabilization” of the bacterial membrane is mentioned as a causative effect. Given the ubiquitous expression of TRP channels, an opening of these channels by the herbal agonists with subsequent influx of Ca^{2+} and bacterial apoptosis appears to be more likely. However this may be, it should be noted that relatively high concentrations are required for antimicrobial activity (Franz et al. 2010; Calsamiglia et al. 2007) that are not tolerated in animal feed. In addition, many of the active components are rapidly absorbed into the body or even degraded to inactive forms. Thus, studies with the use of carvarcrol, thymol, eugenol or trans-cinnamaldehyde in pigs showed that up to 100 % are already absorbed in the stomach and proximal intestine (Van Noten et al. 2020; Michiels et al. 2008). Microencapsulation of these substances may delay absorption (Omonijo et al. 2018), but it remains questionable how much of the active ingredients are still available in sufficient concentration in the segments of the large intestine. Indeed, Piva et al. (2007) showed that microencapsulation of vanillin resulted in detectable concentrations in the stomach, as well as in the proximal and distal jejunum, but not in the ileum or colon. Nevertheless, some studies have demonstrated that feeding phytogenic agents results in a change in the intestinal flora of pigs (Vanrolleghem et al. 2019; Maenner et al. 2011; Castillo et al. 2006; Manzanilla et al. 2004). It remains to be clarified whether the alteration of the microbiota, especially in distal intestinal segments, is due to the antimicrobial effect of the phytogenic agents or whether other mechanisms are causative, such as altered availability of nutrients including proteins, or a higher rate of secretion of pro- or antibacterial substrates, buffers or enzymes from more proximal intestinal segments in response to TRP channel activation.

In comparison, targeted activation of TRP channels in the intestinal tract, including the colon, could be achieved with much lower concentrations of the phytogenic agents, since they are already effective in the lower µmol range (Talavera et al. 2020; Premkumar 2014). In this context, activation of bicarbonate secretion (e.g. via cinnamaldehyde) should be useful for buffering colonic pH and thus, stabilizing the microbial flora. Furthermore, activation of TRP channels could increase the influx of NH_4^+ into the epithelial intestinal cell. Metabolization and

synthesis of amino acids such as glutamine and arginine may already partially occur here (Eklou-Lawson et al. 2009; James et al. 1998a, b). Moreover, activity of glutamine synthetase is higher in colonocytes than in enterocytes of small intestine (Andriamihaja et al. 2010). Thus, feeding of phytogenic agents with menthol as the main substance in sheep showed an increase in amino acids such as glutamine, glutamate, asparagine and aspartate in blood serum (Patra et al. 2019). Glutamine serves multiple functions in the body. Thus, it serves as a major source of energy for enterocytes. Furthermore, glutamine serves as a transport shuttle for ammonia to the kidney, where deamination follows with secretion of NH_3 and subsequent binding of protons. On the other hand, glutamine is considered a semi-essential amino acid that serves as a precursor of other non-essential amino acids. Glutamine can be rate-limiting for performance, in particular during infection, pregnancy, growth or milk production (Xiao et al. 2016; d'Paula et al. 2014; Meijer et al. 1993). Accordingly, the positive effect on growth and feed conversion rate by the use of phytogenic agents could be partly due to increased metabolization of ammonia to amino acids and proteins by initial activation of TRP channels. This potential effect of TRP channel agonists should be further investigated in future studies.

7. Summary

Functional and molecular biological studies of the absorption of ammonia across porcine intestinal epithelia

The high ammonia emissions associated with pig fattening have serious consequences for the health of the animals, the people who care for them, and the global climate. For example, about 50 % of fattening pigs undergo severe pneumonia with identifiable scarring of the lung tissue in the course of their lives (Hillen et al. 2014; Maes et al. 2001; Grest et al. 1997). The source of this ammonia is degradation of protein within the gut, which is absorbed, detoxified by the liver and renally excreted. Most steps of this process have been investigated in detail. However, the mechanism by which ammonia is absorbed from the intestine continues to be unclear. Previous studies suggest that certain members of the TRP channel family contribute to uptake of ammonia in the form of NH_4^+ from the rumen. The aims of the present thesis were to investigate evidence for a channel-mediated uptake of NH_4^+ from the various parts of the porcine intestine, to study the expression of certain relevant members of the TRP family by the gut and to explore the effects of selected phytogenic agonists with a potential effect on these channels. A better understanding of the absorption mechanisms from the gastrointestinal tract of the pig is a prerequisite for the development of rational strategies in breeding and feeding with the aim of reducing ammonia excretion in fattening farms.

Within the context of the two studies presented in this thesis, the expression levels of nine different TRP channels were studied and compared at mRNA level in the stomach (cardia and fundus), duodenum, jejunum, ileum, caecum and colon, always distinguishing between tissues of epithelial or muscular origin. While TRPV2, TRPV3, TRPV4, TRPV6, TRPM6, TRPM7, and TRPA1 could be detected in various segments of the porcine gastrointestinal tract, no evidence could be found for the expression of TRPV1 and TRPM8. Two channels with potential relevance for NH_4^+ transport, TRPV3 and TRPV4, were investigated further at protein level by immunoblot and immunohistochemistry, showing a predominant staining of the apical membrane of the epithelium in all segments. While TRPV4 was expressed throughout the gastrointestinal tract, mRNA data suggest that expression of the full-length TRPV3 protein is limited to those segments with the highest absorption of ammonia, namely caecum and colon. Via the Ussing chamber technique, functional evidence of TRPV3 and TRPV4 was obtained using the selective agonists 2-APB and GSK106790A. In line with a functional expression of these channels, electrogenic transport of NH_4^+ could be observed and was found to be further enhanced by the removal of divalent cations. In conjunction, the results suggest that the transport of NH_4^+ across the caecum and colon of the pigs may involve TRPV3, with possible further contributions of TRPV4.

In the second study, the electrophysiological effects of the TRPA1 agonist cinnamaldehyde and the TRPV3 and TRPA1 agonist thymol were investigated in the colon of pigs. For this purpose, the Ussing chamber technique and the use of different blockers and solutions were used to investigate the mechanism of action in more detail. It was shown that the effect of cinnamaldehyde in the colon is most likely due to HCO_3^- mediated secretion by a prostaglandin-mediated signalling cascade following activation of TRPA1. In contrast, the electrophysiological effects after thymol addition were diverse, suggesting different mechanisms of action, which need to be investigated in more detail in further studies.

The results presented provide an overview of the expression pattern of nine different TRP channels in seven different parts of the porcine gastrointestinal tract. Furthermore, evidence is presented for the electrogenic transport of ammonia in the form of NH_4^+. Functional data suggest a direct involvement of TRPV3 and TRPV4 in colonic transport, while TRPA1 modulates transport via a prostaglandin-dependent signalling cascade. By targeted modulation of these channels, e.g. by phytogenic agents, it seems possible to influence the transport and metabolism of cations, including the physiologically relevant NH_4^+ ion. Compounds with a selective inhibitory effects on the absorption of NH_4^+ from the hindgut are thus conceivable, but have yet to be developed. However, the use of currently available phytogenic agents, such as cinnamaldehyde, may result in other positive effects, such as the stimulation of bicarbonate secretion with buffering of protons in the lumen.

8. Zusammenfassung

Funktionelle und molekularbiologische Untersuchungen zur Resorption von Ammoniak über intestinale Epithelien des Schweins

Die mit der Schweinemast verbundenen hohen Ammoniakemissionen haben schwerwiegende Folgen für die Gesundheit der Tiere, der Menschen, die sie versorgen, und das Weltklima. So erleiden etwa 50 % der Mastschweine im Laufe ihres Lebens eine schwere Lungenentzündung mit nachweisbarer Vernarbung des Lungengewebes (Hillen et al. 2014; Maes et al. 2001; Grest et al. 1997). Die Quelle des Ammoniaks ist der Abbau von Eiweiß im Darm, welches absorbiert, von der Leber entgiftet und über die Nieren ausgeschieden wird. Die meisten Schritte dieses Prozesses sind im Detail untersucht worden. Der Mechanismus, über den Ammoniak aus dem Darm absorbiert wird, ist jedoch nach wie vor unklar. Frühere Studien legen nahe, dass bestimmte Mitglieder der TRP-Kanalfamilie zur Aufnahme von Ammoniak in Form von NH_4^+ aus dem Pansen beitragen. Ziel der vorliegenden Arbeit war es, Hinweise für eine kanalvermittelte Aufnahme von NH_4^+ aus den verschiedenen Teilen des Schweinedarms zu überprüfen, die Expression bestimmter relevanter Mitglieder der TRP-Familie im Darm zu ermitteln und die Auswirkungen bestimmter phytogener Agonisten mit potenzieller Wirkung auf diese Kanäle zu untersuchen. Ein besseres Verständnis der Absorptionsmechanismen aus dem Magen-Darm-Trakt des Schweins ist eine Voraussetzung für die Entwicklung rationaler Strategien in der Zucht und Fütterung mit dem Ziel, die Ammoniakausscheidung in Mastbetrieben zu reduzieren.

Im Rahmen der beiden in dieser Arbeit vorgestellten Studien wurden die Expressionsniveaus von neun verschiedenen TRP-Kanälen auf mRNA-Ebene in Magen (Kardia und Fundus), Duodenum, Jejunum, Ileum, Zäkum und Kolon untersucht und verglichen, wobei zwischen den Geweben auf epithelialem oder muskulärem Ursprung unterschieden wurde. Während TRPV2, TRPV3, TRPV4, TRPV6, TRPM6, TRPM7 und TRPA1 in verschiedenen Segmenten des Magen-Darm-Trakts von Schweinen nachgewiesen werden konnten, gab es keine Hinweise auf die Expression von TRPV1 und TRPM8. Zwei Kanäle mit potenzieller Relevanz für den NH_4^+-Transport, TRPV3 und TRPV4, wurden auf Proteinebene mittels Immunoblot und Immunhistochemie weiter untersucht und zeigten eine überwiegende Färbung der apikalen Membran des Epithels in allen Segmenten. Während TRPV4 im gesamten Gastrointestinaltrakt exprimiert wurde, deuten die mRNA-Daten darauf hin, dass die Expression des TRPV3-Proteins in voller Länge auf die Segmente mit der höchsten Ammoniakaufnahme, nämlich Zäkum und Kolon, beschränkt ist. Mit Hilfe der Ussing-Kammertechnik wurde ein funktioneller Nachweis von TRPV3 und TRPV4 unter Verwendung der selektiven Agonisten 2-APB und GSK106790A erbracht. Im Einklang mit einer

funktionellen Expression dieser Kanäle konnte ein elektrogener Transport von NH_4^+ beobachtet werden, der durch die Entfernung von zweiwertigen Kationen noch verstärkt wurde. Die Ergebnisse deuten darauf hin, dass am Transport von NH_4^+ durch das Zäkum und dem Kolon von Schweinen TRPV3 beteiligt sein könnte, wobei TRPV4 möglicherweise weitere Beiträge leistet.

In der zweiten Studie wurden die elektrophysiologischen Wirkungen des TRPA1-Agonisten Zimtaldehyd und des TRPV3- und TRPA1-Agonisten Thymol im Kolon von Schweinen untersucht. Zu diesem Zweck wurde die Ussing-Kammertechnik und die Verwendung verschiedener Blocker und Lösungen eingesetzt, um den Wirkungsmechanismus genauer zu untersuchen. Es zeigte sich, dass die Wirkung von Zimtaldehyd im Dickdarm höchstwahrscheinlich auf eine HCO_3^- vermittelte Sekretion durch eine Prostaglandin-vermittelte Signalkaskade nach Aktivierung von TRPA1 zurückzuführen ist. Im Gegensatz dazu waren die elektrophysiologischen Effekte nach Thymol-Zugabe vielfältig, was auf unterschiedliche Wirkmechanismen hindeutet, die in weiteren Studien noch genauer untersucht werden müssen.

Die vorgestellten Ergebnisse geben einen Überblick über das Expressionsmuster von neun verschiedenen TRP-Kanälen in sieben verschiedenen Teilen des Magen-Darm-Trakts von Schweinen. Darüber hinaus gibt es Hinweise auf den elektrogenen Transport von Ammoniak in Form von NH_4^+. Funktionelle Daten deuten auf eine direkte Beteiligung von TRPV3 und TRPV4 am Transport im Kolon hin, während TRPA1 den Transport über eine Prostaglandin-abhängige Signalkaskade moduliert. Durch gezielte Modulation dieser Kanäle, z. B. durch phytogene Wirkstoffe, scheint es möglich, den Transport und den Stoffwechsel von Kationen, einschließlich des physiologisch relevanten NH_4^+-Ions, zu beeinflussen. Wirkstoffe mit einer selektiven Hemmwirkung auf die Absorption von NH_4^+ aus dem Dickdarm sind daher denkbar, müssen aber noch entwickelt werden. Die Verwendung derzeit verfügbarer Phytogene, wie z. B. Zimtaldehyd, kann jedoch zu anderen positiven Effekten führen, wie z. B. zur Stimulation der Bikarbonatsekretion mit Pufferung von Protonen im Lumen.

9. References

Abdoun K, Stumpff F, Wolf K, Martens H (2005): Modulation of electroneutral Na transport in sheep rumen epithelium by luminal ammonia. Am J Physiol Gastrointest Liver Physiol, 289:G508–G520. https://doi.org/10.1152/ajpgi.00436.2004

Akaba T, Komiya K, Suzaki I, Kozaki Y, Tamaoki J, Rubin BK (2018): Activating prostaglandin E2 receptor subtype EP4 increases secreted mucin from airway goblet cells. Pulm Pharmacol Ther, 48:117–123. https://doi.org/10.1016/j.pupt.2017.11.001

Al-Awqati Q (1999): One hundred years of membrane permeability: does Overton still rule? Nat Cell Biol, 1:E201–E202. https://doi.org/10.1038/70230

Almaraz L, Manenschijn J-A, de la Peña E, Viana F (2014): TRPM8. In: Nilius B, Flockerzi V (eds) Mammalian Transient Receptor Potential (TRP) Cation Channels: Volume I. 1st edition, Springer, Berlin, Heidelberg, pp 547–579. ISBN 978-3-642-54215-2

Amato A, Terzo S, Lentini L, Marchesa P, Mulè F (2020): TRPM8 Channel Activation Reduces the Spontaneous Contractions in Human Distal Colon. Int J Mol Sci, 21:5403. https://doi.org/10.3390/ijms21155403

Amlal H, Soleimani M (1997): K^+/NH_4^+ antiporter: a unique ammonium carrying transporter in the kidney inner medulla. Biochim Biophys Acta Biomembr, 1323:319–333. https://doi.org/10.1016/S0005-2736(96)00200-3

Anderson WG, Nawata CM, Wood CM, Piercey-Normonore MD, Weihrauch D (2012): Body fluid osmolytes and urea and ammonia flux in the colon of two chondrichthyan fishes, the ratfish, *Hydrolagus colliei*, and spiny dogfish, *Squalus acanthias*. Comp Biochem Physiol A Mol Integr Physiol, 161:27–35. https://doi.org/10.1016/j.cbpa.2011.08.017

Andriamihaja M, Davila A-M, Eklou-Lawson M, Petit N, Delpal S, Allek F, Blais A, Delteil C, Tomé D, Blachier François (2010): Colon luminal content and epithelial cell morphology are markedly modified in rats fed with a high-protein diet. Am J Physiol Gastrointest Liver Physiol, 299:G1030–G1037. https://doi.org/10.1152/ajpgi.00149.2010

Aronson PS, Suhm MA, Nee J (1983): Interaction of external H^+ with the Na^+-H^+ exchanger in renal microvillus membrane vesicles. J Biol Chem, 258:6767–6771. https://doi.org/10.1016/S0021-9258(18)32287-7

Assentoft M, Kaptan S, Schneider H-P, Deitmer JW, de Groot BL (2016): Aquaporin 4 as a NH_3 Channel*. J Biol Chem, 291:19184–19195. https://doi.org/10.1074/jbc.M116.740217

Attmane-Elakeb A, Boulanger H, Vernimmen C, Bichara M (1997): Apical Location and Inhibition by Arginine Vasopressin of K^+/H^+ Antiport of the Medullary Thick Ascending Limb of Rat Kidney. J Biol Chem, 272:25668–25677. https://doi.org/10.1074/jbc.272.41.25668

Bach M, Häußermann U, Klement L, Knoll L, Breuer L, Weber T, Fuchs S, Heldstab J, Reutimann J, Schäppi B (2020): Reaktive Stickstoffflüsse in Deutschland 2010 - 2014 (DESTINO Bericht 2). Umweltbundesamt, Dessau-Roßlau. ISSN 1862-4804

Baday S, Orabi EA, Wang S, Lamoureux G, Bernèche S (2015): Mechanism of NH_4^+ Recruitment and NH_3 Transport in Rh Proteins. Structure, 23:1550–1557. https://doi.org/10.1016/j.str.2015.06.010

Balakrishnan S, Mironov SL (2020): Instant activation of TRP channels by NH_4^+ promotes neuronal bursting and glutamate spikes in CA1 neurons. Curr Res Physiol, 3:20–29. https://doi.org/10.1016/j.crphys.2020.05.002

Balemans D, Boeckxstaens GE, Talavera K, Wouters MM (2017): Transient receptor potential ion channel function in sensory transduction and cellular signaling cascades underlying visceral hypersensitivity. Am J Physiol Gastrointest Liver Physiol, 312:G635–G648. https://doi.org/10.1152/ajpgi.00401.2016

Baluška F, Mancuso S, Volkmann D (eds) (2006): Communication in plants: neuronal aspects of plant life. 1st edition, Springer, Berlin, New York. ISBN 978-3-540-28516-8

Bautista DM, Siemens J, Glazer JM, Tsuruda PR, Basbaum AI, Stucky CL, Jordt S-E, Julius D (2007): The menthol receptor TRPM8 is the principal detector of environmental cold. Nature, 448:204–208. https://doi.org/10.1038/nature05910

Béline F (2002): Nitrogen transformations during biological aerobic treatment of pig slurry: effect of intermittent aeration on nitrous oxide emissions. Bioresour Technol, 83:225–228. https://doi.org/10.1016/S0960-8524(01)00219-X

Bell JM, Feild AL (1911): THE DISTRIBUTION OF AMMONIA BETWEEN WATER AND CHLOROFORM. J Am Chem Soc, 33:940–943. https://doi.org/10.1021/ja02219a013

Belley A, Chadee K (1999): Prostaglandin E2 stimulates rat and human colonic mucin exocytosis via the EP4 receptor. Gastroenterology, 117:1352–1362. https://doi.org/10.1016/S0016-5085(99)70285-4

Bellono NW, Bayrer JR, Leitch DB, Castro K, Zhang C, O'Donnel TA, Brierley SM, Ingraham HA, Julius D (2017): Enterochromaffin Cells Are Gut Chemosensors that Couple to Sensory Neural Pathways. Cell, 170:185-198.e16. https://doi.org/10.1016/j.cell.2017.05.034

Bergen WG, Wu G (2009): Intestinal Nitrogen Recycling and Utilization in Health and Disease. J Nutr, 139:821–825. https://doi.org/10.3945/jn.109.104497

Bianchi BR, Zhang X-F, Reilly RM, Kym PR, Yao BB, Chen J (2012): Species Comparison and Pharmacological Characterization of Human, Monkey, Rat, and Mouse TRPA1 Channels. J Pharmacol Exp Ther, 341:360–368. https://doi.org/10.1124/jpet.111.189902

Bindelle J, Leterme P, Buldgen A (2008): Nutritional and environmental consequences of dietary fibre in pig nutrition: a review. Biotechnol Agron Soc Environ, 12:69-80

Bischof M, Olthoff S, Glas C, Thorn-Seshold O, Schaefer M, Hill K (2020): TRPV3 endogenously expressed in murine colonic epithelial cells is inhibited by the novel TRPV3 blocker 26E01. Cell Calcium, 92:102310. https://doi.org/10.1016/j.ceca.2020.102310

Bödeker D, Kemkowski J (1996): Participation of NH_4^+ in total ammonia absorption across the rumen epithelium of sheep (*Ovis aries*). Comp Biochem Physiol A Mol Integr Physiol, 114:305–310. https://doi.org/10.1016/0300-9629(96)00012-6

Bookstein C, DePaoli AM, Xie Y, Niu P, Musch MW, Rao MC, Chang EB (1994): Na^+/H^+ exchangers, NHE-1 and NHE-3, of rat intestine. Expression and localization. J Clin Invest, 93:106–113. https://doi.org/10.1172/JCI116933

Boron WF (2010): Sharpey-Schafer Lecture: Gas channels. Exp Physiol, 95:1107–1130. https://doi.org/10.1113/expphysiol.2010.055244

Boron WF (2004): Regulation of intracellular pH. Adv Physiol Educ, 28:160–179. https://doi.org/10.1152/advan.00045.2004

Boron WF, Waisbren SJ, Modlin IM, Geibel JP (1994): Unique permeability barrier of the apical surface of parietal and chief cells in isolated perfused gastric glands. J Exp Biol, 196:347–360. https://doi.org/10.1242/jeb.196.1.347

Boron WF, De Weer P (1976): Intracellular pH transients in squid giant axons caused by CO_2, NH_3, and metabolic inhibitors. J Gen Physiol, 67:91–112. https://doi.org/10.1085/jgp.67.1.91

Boudry G, Perrier C (2008): Thyme and cinnamon extracts induce anion secretion in piglet small intestine via cholinergic pathways. J Physiol Pharmacol, 59:543–552

Bourgeois S, Bounoure L, Christensen EI, Ramakrishnan SK, Houillier P, Devuyst O, Wagner CA (2013): Haploinsufficiency of the Ammonia Transporter Rhcg Predisposes to Chronic Acidosis. J Biol Chem, 288:5518–5529. https://doi.org/10.1074/jbc.M112.441782

Braun H-S, Schrapers KT, Mahlkow-Nerge K, Stumpff F, Rosendahl J (2019): Dietary supplementation of essential oils in dairy cows: evidence for stimulatory effects on nutrient absorption. Animal, 13:518–523. https://doi.org/10.1017/S1751731118001696

Bromberg PA, Robin ED, Forkner CE (1960): THE EXISTENCE OF AMMONIA IN BLOOD *IN VIVO* WITH OBSERVATIONS ON THE SIGNIFICANCE OF THE NH_4^+–NH_3 SYSTEM. J Clin Invest, 39:332–341. https://doi.org/10.1172/JCI104044

Burckhardt BC, Frömter E (1992): Pathways of NH_3/NH_4^+ permeation across Xenopus laevis oocyte cell membrane. Pflugers Arch - Eur J Physiol, 420:83–86. https://doi.org/10.1007/BF00378645

Cai S, Wu L, Yuan S, Liu G, Wang Y, Fang L, Xu D (2021): Carvacrol alleviates liver fibrosis by inhibiting TRPM7 and modulating the MAPK signaling pathway. Eur J Pharmacol, 898:173982. https://doi.org/10.1016/j.ejphar.2021.173982

Calsamiglia S, Busquet M, Cardozo PW, Castillejos L, Ferret A (2007): Invited Review: Essential Oils as Modifiers of Rumen Microbial Fermentation. J Dairy Sci, 90:2580–2595. https://doi.org/10.3168/jds.2006-644

Caner T, Abdulnour-Nakhoul S, Brown K, Islam MT, Hamm LL, Nakhoul NL (2015): Mechanisms of ammonia and ammonium transport by rhesus-associated glycoproteins. Am J Physiol Cell Physiol, 309:C747–C758. https://doi.org/10.1152/ajpcell.00085.2015

Canh TT, Aarnink AJA, Schutte JB, Sutton A, Langhout DJ, Verstegen MWA (1998): Dietary protein affects nitrogen excretion and ammonia emission from slurry of growing–finishing pigs. Livest Prod Sci, 56:181–191. https://doi.org/10.1016/S0301-6226(98)00156-0

Castillo M, Martín-Orúe SM, Roca M, Manzanilla EG, Badiola I, Perez JF, Gasa J (2006): The response of gastrointestinal microbiota to avilamycin, butyrate, and plant extracts in early-weaned pigs. J Anim Sci, 84:2725–2734. https://doi.org/10.2527/jas.2004-556

Catterall WA, Chandy KG, Clapham DE, Gutman GA, Hofmann F, Harmar AJ, Abernethy DR, Spedding M (2003): International Union of Pharmacology: Approaches to the Nomenclature of Voltage-Gated Ion Channels. Pharmacol Rev, 55:573–574. https://doi.org/10.1124/pr.55.4.5

Cavins JF, Friedman M (1967): New amino acids derived from reactions of epsilon-amino groups in proteins with alpha, beta-unsaturated compounds. Biochemistry, 6:3766–3770. https://doi.org/10.1021/bi00864a021

Cenac N, Altier C, Chapman K, Liedtke W, Zamponi G, Vergnolle N (2008): Transient Receptor Potential Vanilloid-4 Has a Major Role in Visceral Hypersensitivity Symptoms. Gastroenterology, 135:937-946.e2. https://doi.org/10.1053/j.gastro.2008.05.024

Cermak R, Minck K, Lawnitzak C, Scharrer E (2002): Ammonia Inhibits Sodium and Chloride Absorption in Rat Distal Colon. Exp Physiol, 87:311–319. https://doi.org/10.1113/eph8702331

Cermak R, Lawnitzak C, Scharrer E (2000): Influence of ammonia on sodium absorption in rat proximal colon. Pflugers Arch - Eur J Physiol, 440:619–626. https://doi.org/10.1007/s004240000309

Chen W, Xu B, Xiao A, Liu L, Fang X, Liu R, Turlova E, Barszczyk A, Zhong X, Sung CLF, Britto LR, Feng Z-P, Sun H-S (2015): TRPM7 inhibitor carvacrol protects brain from neonatal hypoxic-ischemic injury. Mol Brain, 8:11. https://doi.org/10.1186/s13041-015-0102-5

Cheng L, de la Monte S, Ma J, Hong J, Tong M, Cao W, Behar K, Bancani P, Harnett KM (2009): HCl-activated neural and epithelial vanilloid receptors (TRPV1) in cat esophageal mucosa. Am J Physiol Gastrointest Liver Physiol, 297:G135–G143. https://doi.org/10.1152/ajpgi.90386.2008

Cheng Z, Teo G, Krueger S, Rock TM, Koh HWL, Choi H (2016): Differential dynamics of the mammalian mRNA and protein expression response to misfolding stress. Mol Syst Biol, 12:855. https://doi.org/10.15252/msb.20156423

Cho H-J, Callaghan B, Bron R, Bravo DM, Furness JB (2014): Identification of enteroendocrine cells that express TRPA1 channels in the mouse intestine. Cell Tissue Res, 356:77–82. https://doi.org/10.1007/s00441-013-1780-x

Cho JH, Chen YJ, Min BJ, Kim HJ, Kwon OS, Shon KS, Kim IH, Kim SJ, Asamer A (2005): Effects of Essential Oils Supplementation on Growth Performance, IgG Concentration and Fecal Noxious Gas Concentration of Weaned Pigs. Asian Australas J Anim Sci, 19:80–85. https://doi.org/10.5713/ajas.2006.80

Choe H, Sackin H, Palmer LG (2000): Permeation properties of inward-rectifier potassium channels and their molecular determinants. J Gen Physiol, 115:391–404. https://doi.org/10.1085/jgp.115.4.391

Chokshi R, Fruasaha P, Kozak JA (2012): 2-Aminoethyl diphenyl borinate (2-APB) inhibits TRPM7 channels through an intracellular acidification mechanism. Channels, 6:362–369. https://doi.org/10.4161/chan.21628

Christakos S, Dhawan P, Verstuyf A, Verlinden L, Carmeliet G (2016): Vitamin D: Metabolism, Molecular Mechanism of Action, and Pleiotropic Effects. Physiol Rev, 96:365–408. https://doi.org/10.1152/physrev.00014.2015

Chu Y, Cohen BE, Chuang H (2020): A single TRPV1 amino acid controls species sensitivity to capsaicin. Sci Rep, 10:8038. https://doi.org/10.1038/s41598-020-64584-2

Church DM, Goodstadt L, Hillier LW, Zody MC, Goldstein S, She X, Bult CJ, Agarwala R, Cherry JL, DiCuccio M, Hlavina W, Kapustin Y, Meric P, Maglott D, Birtle Z, Marques AC, Graves T, Zhou S, Teague B, Potamousis K, Churas C, Place M, Herschleb J, Runnheim R, Forrest D, Amos-Landgraf J, Schwartz DC, Cheng Z, Lindblad-Toh K, Eichler EE, Ponting CP (2009): Lineage-Specific Biology Revealed by a Finished Genome Assembly of the Mouse. PLoS Biol, 7:e1000112. https://doi.org/10.1371/journal.pbio.1000112

Clapham DE (2003): TRP channels as cellular sensors. Nature, 426:517-524 https://doi.org/426:517-524. 10.1038/nature02196

Cosens DJ, Manning A (1969): Abnormal Electroretinogram from a Drosophila Mutant. Nature, 224:285–287. https://doi.org/10.1038/224285a0

Cosme D, Estevinho MM, Rieder F, Magro F (2021): Potassium channels in intestinal epithelial cells and their pharmacological modulation: a systematic review. Am J Physiol Cell Physiol, 320:C520–C546. https://doi.org/10.1152/ajpcell.00393.2020

Costa LB, Luciano FB, Miyada VS, Gois FD (2013): Review article: Herbal extracts and organic acids as natural feed additives in pig diets. S Afr J Anim Sci, 43:181–193. https://doi.org/10.4314/sajas.v43i2.9

Cougnon M, Bouyer P, Jaisser F, Edelmann A, Planelles G (1999): Ammonium transport by the colonic H^+-K^+-ATPase expressed in *Xenopus* oocytes. Am J Physiol Cell Physiol, 277:C280–C287. https://doi.org/10.1152/ajpcell.1999.277.2.C280

Csekő K, Beckers B, Keszthelyi D, Helyes Z (2019): Role of TRPV1 and TRPA1 Ion Channels in Inflammatory Bowel Diseases: Potential Therapeutic Targets? Pharmaceuticals, 12:48. https://doi.org/10.3390/ph12020048

d'Paula JT, Martinez RLV, de Almeida Craveiro Alves TL, Katurchi S, Mélo M, Kutschenko M, Nogueira ET, da Costa Cordeiro Manso HEC, Filho HCM (2014): Blood and Milk Glutamine + Glutamate and Milk Composition in Lactating Holstein Cows in Semi-Arid of Brazil. Open J Vet Med, 04:322–328. https://doi.org/10.4236/ojvm.2014.412039

D'Aldebert E, Cenac N, Rousset P, Martin L, Rolland C, Chapman K, Selves J, Alric L, Vinel J-P, Vergnolle N (2011): Transient Receptor Potential Vanilloid 4 Activated Inflammatory Signals by Intestinal Epithelial Cells and Colitis in Mice. Gastroenterology, 140:275-285.e3. https://doi.org/10.1053/j.gastro.2010.09.045

Darragh AJ, Cranwell PD, Moughan PJ (1994): Absorption of lysine and methionine from the proximal colon of the piglet. Br J Nutr, 71:739–752. https://doi.org/10.1079/BJN19940181

de la Hoz RE, Schlueter DP, Rom WN (1996): Chronic lung disease secondary to ammonia inhalation injury: a report on three cases. Am J Ind Med, 29:209–214. https://doi.org/10.1002/(SICI)1097-0274(199602)29:2<209::AID-AJIM12>3.0.CO;2-7

De Petrocellis L, Orlando P, Moriello AS, Aviellp G, Stoff C, Izzo AA, Di Marzo V (2012): Cannabinoid actions at TRPV channels: effects on TRPV3 and TRPV4 and their potential relevance to gastrointestinal inflammation: Plant cannabinoids and TRPV channels. Acta Physiol (Oxf), 204:255–266. https://doi.org/10.1111/j.1748-1716.2011.02338.x

Deglaire A, Bos C, Tomé D, Moughan PJ (2009): Ileal digestibility of dietary protein in the growing pig and adult human. Br J Nutr, 102:1752–1759. https://doi.org/10.1017/S0007114509991267

den Dekker E, Hoenderop JGJ, Nilius B, Bindels RJM (2003): The epithelial calcium channels, TRPV5 & TRPV6: from identification towards regulation. Cell Calcium, 33:497–507. https://doi.org/10.1016/S0143-4160(03)00065-4

Desai BN, Clapham DE (2005): TRP channels and mice deficient in TRP channels. Pflugers Arch - Eur J Physiol, 451:11–18. https://doi.org/10.1007/s00424-005-1429-z

Dhaka A, Uzzell V, Dubin AE, Mathur J, Petrus M, Bandell M, Patapoutian A (2009): TRPV1 Is Activated by Both Acidic and Basic pH. J Neurosci, 29:153–158. https://doi.org/10.1523/JNEUROSCI.4901-08.2009

Diener M (2021): How to manage N waste in the intestine? Acta Physiol (Oxf), 233:e13711. https://doi.org/10.1111/apha.13711

Dietrich A, Chubanov V, Kalwa H, Rost BR, Gudermann T (2006): Cation channels of the transient receptor potential superfamily: Their role in physiological and pathophysiological processes of smooth muscle cells. Pharmacol Ther, 112:744–760. https://doi.org/10.1016/j.pharmthera.2006.05.013

Dimke H, Hoenderop JGJ, Bindels RJM (2011): Molecular basis of epithelial Ca^{2+} and Mg^{2+} transport: insights from the TRP channel family. J Physiol, 589:1535–1542. https://doi.org/10.1113/jphysiol.2010.199869

Doihara H, Nozawa K, Kojima R, Kawabata-Shoda E, Yokoyama T, Ito H (2009): QGP-1 cells release 5-HT via TRPA1 activation; a model of human enterochromaffin cells. Mol Cell Biochem, 331:239–245. https://doi.org/10.1007/s11010-009-0165-7

Donham KJ (1991): Association of environmental air contaminants with disease and productivity in swine. Am J Vet Res, 52:1723–1730

Eisenman G, Latorre R, Miller C (1986): Multi-ion conduction and selectivity in the high-conductance Ca^{++}-activated K^{+} channel from skeletal muscle. Biophys J, 50:1025–1034. https://doi.org/10.1016/S0006-3495(86)83546-9

Eisenman G (1962): Cation Selective Glass Electrodes and their Mode of Operation. Biophys J, 2:259–323. https://doi.org/10.1016/S0006-3495(62)86959-8

Eklou-Lawson M, Bernard F, Neveux N, Chaumontet C, Bos C, Davila-Gay A-M, Tomé D, Cynober L, Blachier F (2009): Colonic luminal ammonia and portal blood l-glutamine and l-arginine concentrations: a possible link between colon mucosa and liver ureagenesis. Amino Acids, 37:751–760. https://doi.org/10.1007/s00726-008-0218-3

von Engelhardt W, Breves G (2010): Physiologie der Haustiere. 3rd edition, Enke, Stuttgart. ISBN 978-3-8304-1039-3

Etschmann B, Heipertz KS, von der Schulenburg A, Schweigel M (2006): A vH^+-ATPase is present in cultured sheep ruminal epithelial cells. Am J Physiol Gastrointest Liver Physiol, 291:G1171–G1179. https://doi.org/10.1152/ajpgi.00099.2006

Fakler B (2019): Grundlagen der zellulären Erregbarkeit. In: Brandes R, Lang F, Schmidt RF (eds) Physiologie des Menschen: mit Pathophysiologie. Springer, 32nd edition, Berlin, Heidelberg, pp 38–54. ISBN 978-3-662-56468-4

Faussone-Pellegrini M-S, Taddei A, Bizzoco E, Bizzoco E, Lazzeri M, Vannucchi MG Bechi P (2005): Distribution of the vanilloid (capsaicin) receptor type 1 in the human stomach. Histochem Cell Biol, 124:61–68. https://doi.org/10.1007/s00418-005-0025-9

Fiati Kenston SS, Song X, Li Z, Zhao J (2019): Mechanistic insight, diagnosis, and treatment of ammonia-induced hepatic encephalopathy: Ammonia-induced hepatic encephalopathy. J Gastroenterol Hepatol, 34:31–39. https://doi.org/10.1111/jgh.14408

Fonfria E, Murdock PR, Cusdin FS, Benham CD, Kelsell RE, McNulty S (2006): Tissue Distribution Profiles of the Human TRPM Cation Channel Family. J Recept Signal Transduct Res, 26:159–178. https://doi.org/10.1080/10799890600637506

Fothergill L, Callaghan B, Rivera L, Lieu TM, P DP, Cho H-J, Bravo DM, Furness JB (2016): Effects of Food Components That Activate TRPA1 Receptors on Mucosal Ion Transport in the Mouse Intestine. Nutrients, 8:623. https://doi.org/10.3390/nu8100623

Franz C, Baser K, Windisch W (2010): Essential oils and aromatic plants in animal feeding - a European perspective. A review. Flavour Fragr J, 25:327–340. https://doi.org/10.1002/ffj.1967

Funakoshi K, Nakano M, Atobe Y, Goris RC, Kadota T, Yazama F (2006): Differential development of TRPV1-expressing sensory nerves in peripheral organs. Cell Tissue Res, 323:27–41. https://doi.org/10.1007/s00441-005-0013-3

Ganz P, Ijato T, Porras-Murrilo R, Stührwohldt N, Ludewig U (2020): A twin histidine motif is the core structure for high-affinity substrate selection in plant ammonium transporters. J Biol Chem, 295:3362–3370. https://doi.org/10.1074/jbc.RA119.010891

Gao L, Yang P, Qin P, Lu Y, Li X, Tian Q, Li Y, Xie C, Tian J, Thang C, Tian C, Zhu MX, Yao J (2016): Selective potentiation of 2-APB-induced activation of TRPV1–3 channels by acid. Sci Rep, 6:20791. https://doi.org/10.1038/srep20791

Garg LC, Narang N (1988): Ouabain-insensitive K-adenosine triphosphatase in distal nephron segments of the rabbit. J Clin Invest, 81:1204–1208. https://doi.org/10.1172/JCI113436

Gazzarrini S, Lejay L, Gojon A, Ninnemann O, Frommer WB, von Wirén N (1999): Three functional transporters for constitutive, diurnally regulated, and starvation-induced uptake of ammonium into Arabidopsis roots. Plant Cell, 11:937–948. https://doi.org/10.1105/tpc.11.5.937

Gees M, Colsoul B, Nilius B (2010): The Role of Transient Receptor Potential Cation Channels in Ca^{2+} Signaling. Cold Spring Harb Perspect Biol, 2:a003962. https://doi.org/10.1101/cshperspect.a003962

Geiger S, Patra AK, Schrapers KT, Braun HS, Aschenbach JR (2021): Menthol stimulates calcium absorption in the rumen but not in the jejunum of sheep. J Dairy Sci, 104:3067–3081. https://doi.org/10.3168/jds.2020-19372

Gerber PJ, Hristov AN, Henderson B, Makkar H, Oh J, Lee C, Meinen R, Montes F, Firkins J, Rotz A, Dell C, Adesogan AT, Yang WZ, Tricarico JM, Kebreab E, Waghorn G, Dijkstra J, Oosting S (2013): Technical options for the mitigation of direct methane and nitrous oxide emissions from livestock: a review. Animal, 7:220–234. https://doi.org/10.1017/S1751731113000876

Geupel M, Richter S, Schlesinger L (2021): Stickstoff – Element mit Wirkung. Umweltbundesamt, Dessau-Roßlau. ISSN 2363-829X

Geyer RR, Musa-Aziz R, Enkavi G, Mahinthichaichan P, Tajkhorshid E, Boron WF (2013a): Movement of NH_3 through the human urea transporter B: a new gas channel. Am J Physiol Renal Physiol, 304:F1447–F1457. https://doi.org/10.1152/ajprenal.00609.2012

Geyer RR, Parker MD, Toye AM, Boron WF, Musa-Aziz R (2013b): Relative CO_2/NH_3 Permeabilities of Human RhAG, RhBG and RhCG. J Membr Biol, 246:915–926. https://doi.org/10.1007/s00232-013-9593-0

Gloux A, Le Roy N, Brionne A, Bonin E, Juanchich A, Benzoni G, Piketty M-L, Prié D, Nys Y, Gautron J, Narcy A, Duclos MJ (2019): Candidate genes of the transcellular and paracellular calcium absorption pathways in the small intestine of laying hens. Poult Sci, 98:6005–6018. https://doi.org/10.3382/ps/pez407

Greco G, Hagen F, Meißner S, Shen Z, Lu Z, Amasheh S, Aschenbach JR (2018): Effect of individual SCFA on the epithelial barrier of sheep rumen under physiological and acidotic luminal pH conditions. J Anim Sci, 96:126–142. https://doi.org/10.1093/jas/skx017

Grest P, Keller H, Sydler T, Pospischil A (1997): The prevalence of lung lesions in pigs at slaughter in Switzerland. Schweiz Arch Tierheilkd, 139:500–506

Gunther RD, Wright EM (1983): Na^+, Li^+ and Cl^- transport by brush border membranes from rabbit jejunum. J Membr Biol, 74:85–94. https://doi.org/10.1007/BF01870497

Haas M, Forbush B (1998): The Na-K-Cl Cotransporters. J Bioenerg Biomembr, 30:161–172. https://doi.org/10.1023/A:1020521308985

Hakvoort TBM, He Y, Kulik W, Vernuelen JLM, Duijst S, Ruijter JM, Runge JH, Deutz NEP, Koehler SE, Lamers WH (2017): Pivotal role of glutamine synthetase in ammonia detoxification. Hepatology, 65:281–293. https://doi.org/10.1002/hep.28852

Hall MC, Koch MO, McDougal WS (1992): Mechanism of Ammonium Transport by Intestinal Segments Following Urinary Diversion: Evidence For Ionized Nh_4^+ Transport Via K^+-Pathways. J Urol, 148:453–457. https://doi.org/10.1016/S0022-5347(17)36627-2

Handlogten ME, Hong S-P, Zhang L, Vander AW, Steinbaum ML Campgell-Thompson M, Weiner ID (2005): Expression of the ammonia transporter proteins Rh B glycoprotein and Rh C glycoprotein in the intestinal tract. Am J Physiol Gastrointest Liver Physiol, 288:G1036–G1047. https://doi.org/10.1152/ajpgi.00418.2004

Hansen MB, Witte A-B (2008): The role of serotonin in intestinal luminal sensing and secretion. Acta Physiol (Oxf), 193:311–323. https://doi.org/10.1111/j.1748-1716.2008.01870.x

Hardwick LL, Jones MR, Brautbar N, Lee DB (1991): Magnesium absorption: mechanisms and the influence of vitamin D, calcium and phosphate. J Nutr, 121:13–23. https://doi.org/10.1093/jn/121.1.13

Harrington AM, Hughes PA, Martin CM, Yang J, Joel I, Isaacs, NJ, Blackshaw AL, Brierley SM (2011): A novel role for TRPM8 in visceral afferent function. PAIN, 152:1459–1468. https://doi.org/10.1016/j.pain.2011.01.027

Harteneck C, Gollasch M (2011): Pharmacological Modulation of Diacylglycerol-Sensitive TRPC3/6/7 Channels. Curr Pharm Biotechnol, 12:35–41. https://doi.org/10.2174/138920111793937943

Hartmannsgruber V, Heyken W-T, Kacik M, Kaistha A, Grgic I, Harteneck C, Liedtke W, Hoyer J, Köhler R (2007): Arterial Response to Shear Stress Critically Depends on Endothelial TRPV4 Expression. PLoS One, 2:e827. https://doi.org/10.1371/journal.pone.0000827

Heginbotham L, MacKinnon R (1993): Conduction properties of the cloned Shaker K^+ channel. Biophys J, 65:2089–2096. https://doi.org/10.1016/S0006-3495(93)81244-X

Heitzmann D, Warth R (2008): Physiology and Pathophysiology of Potassium Channels in Gastrointestinal Epithelia. Physiol Rev, 88:1119–1182. https://doi.org/10.1152/physrev.00020.2007

Helbig H, Korbmacher C, Stumpff F, Coca-Prados M, Wiederholt M (1988): Na^+/H^+ exchange regulates intracellular pH in a cell clone derived from bovine pigmented ciliary epithelium. J Cell Physiol, 137:384–389. https://doi.org/10.1002/jcp.1041370225

Hillen S, von Berg S, Köhler K, Reinacher M, Willems H, Reiner G (2014): Occurrence and severity of lung lesions in slaughter pigs vaccinated against Mycoplasma hyopneumoniae with different strategies. Prev Vet Med, 113:580–588. https://doi.org/10.1016/j.prevetmed.2013.12.012

Hinman A, Chuang H -h., Bautista DM, Julius D (2006): TRP channel activation by reversible covalent modification. Proc Natl Acad Sci, 103:19564–19568. https://doi.org/10.1073/pnas.0609598103

Hinterding T (2002): Expression der Ca^{2+}-Kanäle ECaC1 und ECaC2 im Dünndarm von Saug- und Absetzferkeln. Published online https://elib.tiho-hannover.de/receive/etd_mods_00002714

Hoenderop JGJ (2003): Homo- and heterotetrameric architecture of the epithelial Ca^{2+} channels TRPV5 and TRPV6. EMBO J, 22:776–785. https://doi.org/10.1093/emboj/cdg080

Holtug K, Laverty G, Árnason SS, Skadhauge E (2009): NH^{4+} secretion in the avian colon. An actively regulated barrier to ammonium permeation of the colon mucosa. Comp Biochem Physiol A Mol Integr Physiol, 153:258–265. https://doi.org/10.1016/j.cbpa.2009.02.023

Holzer P (2011): TRP Channels in the Digestive System. Curr Pharm Biotechnol, 12:24–34. https://doi.org/10.2174/138920111793937862

Hong J-C, Steiner T, Aufy A, Lien T-F (2012): Effects of supplemental essential oil on growth performance, lipid metabolites and immunity, intestinal characteristics, microbiota and carcass traits in broilers. Livest Sci, 144:253–262. https://doi.org/10.1016/j.livsci.2011.12.008

Hosoya T, Matsumoto K, Tashima K, Nakamura H, Fujino T, Murayama SH (2014): TRPM8 has a key role in experimental colitis-induced visceral hyperalgesia in mice. Neurogastroenterol Motil, 26:1112–1121. https://doi.org/10.1111/nmo.12368

Hu H, Grandl J, Bandell M, Petrus M, Patapoutian A (2009): Two amino acid residues determine 2-APB sensitivity of the ion channels TRPV3 and TRPV4. Proc Natl Acad Sci, 106:1626–1631. https://doi.org/10.1073/pnas.0812209106

Hu H-Z, Gu Q, Wang C, Colton CK, Tang J, Kinoshita-Kawada M, Lee L-Y, Wood JD, Zhu MX (2004): 2-aminoethoxydiphenyl borate is a common activator of TRPV1, TRPV2, and TRPV3. J Biol Chem, 279:35741–35748. https://doi.org/10.1074/jbc.M404164200

Inoue H, Kozlowski SD, Klein JD, Bailey JL, Sands JM, Bagnasco SM (2005): Regulated expression of renal and intestinal UT-B urea transporter in response to varying urea load. Am J Physiol Renal Physiol, 289:F451–F458. https://doi.org/10.1152/ajprenal.00376.2004

Issa CM, Hambly BD, Wang Y, Maleki S, Wand W, Fei J, Bao S (2014): TRPV2 in the Development of Experimental Colitis. Scand J Immunol, 80:307–312. https://doi.org/10.1111/sji.12206

James LA, Lunn PG, Elia M (1998a): Glutamine metabolism in the gastrointestinal tract of the rat assessed by the relative activities of glutaminase (EC 3.5.1.2) and glutamine synthetase (EC 6.3.1.2). Br J Nutr, 79:365–372. https://doi.org/10.1079/BJN19980061

James LA, Lunn PG, Middleton S, Elia M (1998b): Distribution of Glutaminase and Glutamine Synthetase Activities in the Human Gastrointestinal Tract. Clin Sci (Lond), 94:313–319. https://doi.org/10.1042/cs0940313

Janas S, Seghers F, Schakman O, Alsady M, Deen P, Vriens J, Tissir F, Nilius B, Loffing J, Gailly P, Devuyst O (2016): TRPV4 is associated with central rather than nephrogenic osmoregulation. Pflugers Arch - Eur J Physiol, 468:1595–1607. https://doi.org/10.1007/s00424-016-1850-5

Jang Y, Lee Y, Kim SM, Yang YD, Jung J, Oh U (2012): Quantitative analysis of TRP channel genes in mouse organs. Arch Pharm Res, 35:1823–1830. https://doi.org/10.1007/s12272-012-1016-8

Janssens A, Gees M, Toth BI, Ghosh D, Mulier M, Vennekens R, Vriens J, Talavera K, Voets T (2016): Definition of two agonist types at the mammalian cold-activated channel TRPM8. eLife, 5:e17240. https://doi.org/10.7554/eLife.17240

Jardín I, López JJ, Diez R, Sánchez-Collado J, Cantonero C, Albarrán L, Woodard GE, Redondo PC, Salido GM, Smani T, Rosado JA (2017): TRPs in Pain Sensation. Front Physiol, 8:392. https://doi.org/10.3389/fphys.2017.00392

Javelle A, Lupo D, Li X-D, Merrick M, Chami M, Ripoche P, Winkler FK (2007): Structural and mechanistic aspects of Amt/Rh proteins. J Struct Biol, 158:472–481. https://doi.org/10.1016/j.jsb.2007.01.004

Kaji I, Akiba Y, Said H, Narimatsu K, Kaunitz JD (2015): Luminal 5-HT stimulates colonic bicarbonate secretion in rats: Luminal 5-HT-evoked colonic HCO_3^- secretion. Br J Pharmacol, 172:4655–4670. https://doi.org/10.1111/bph.13216

Kaji I, Yasuoka Y, Karaki S, Kuwahara A (2012): Activation of TRPA1 by luminal stimuli induces EP_4 -mediated anion secretion in human and rat colon. Am J Physiol Gastrointest Liver Physiol, 302:G690–G701. https://doi.org/10.1152/ajpgi.00289.2011

Kaji I, Karaki S, Kuwahara A (2011): Effects of luminal thymol on epithelial transport in human and rat colon. Am J Physiol Gastrointest Liver Physiol, 300:G1132–G1143. https://doi.org/10.1152/ajpgi.00503.2010

Karashima Y, Damann N, Prenen J, Talavera K, Segal A, Voets T, Nilius B (2007): Bimodal Action of Menthol on the Transient Receptor Potential Channel TRPA1. J Neurosci, 27:9874–9884. https://doi.org/10.1523/JNEUROSCI.2221-07.2007

Karim Z, Szutkowska M, Vernimmen C, Bichara M (2005): Renal Handling of NH_3/NH_4^+: Recent Concepts. Nephron Physiol, 101:p77–p81. https://doi.org/10.1159/000087575

Kashiba H, Uchida Y, Takeda D, Nishigori A, Ueda Y, Kuribayashi K, Ohshima M (2004): TRPV2-immunoreactive intrinsic neurons in the rat intestine. Neurosci Lett, 366:193–196. https://doi.org/10.1016/j.neulet.2004.05.069

Kavolelis B (2006): Impact of Animal Housing Systems on Ammonia Emission Rates. Pol J Environ Stud, 15:739–745

Kedei N, Szabo T, Lile JD, Treanor JJ, Olah Z, Iadarola MJ, Blumberg PM (2001): Analysis of the Native Quaternary Structure of Vanilloid Receptor 1. J Biol Chem, 276:28613–28619. https://doi.org/10.1074/jbc.M103272200

Kholif AE, Hassan AA, Matloup OH, El Ashry GM (2020): Top-dressing of chelated phytogenic feed additives in the diet of lactating Friesian cows to enhance feed utilization and lactational performance. Ann Anim Sci, 21:657-673. https://doi.org/10.2478/aoas-2020-0086

Kiela PR, Ghishan FK (2016): Physiology of Intestinal Absorption and Secretion. Best Pract Res Clin Gastroenterol, 30:145–159. https://doi.org/10.1016/j.bpg.2016.02.007

Kim IH, Lee SI, Devi SM (2015): Effect of phytogenics on growth performance, fecal score, blood profiles, fecal noxious gas emission, digestibility, and intestinal morphology of weanling pigs challenged with Escherichia coli K88. Pol J Vet Sci, 18:557-564

Kinne R, Kinne-Saffran E, Schütz H, Schölermann B (1986): Ammonium transport in medullary thick ascending limb of rabbit kidney: Involvement of the Na^+, K^+, Cl^--cotransporter. J Membr Biol, 94:279–284. https://doi.org/10.1007/BF01869723

Kinsella JL, Aronson PS (1981): Interaction of NH_4^+ and Li^+ with the renal microvillus membrane Na^+-H^+ exchanger. Am J Physiol Cell Physiol, 241:C220–C226. https://doi.org/10.1152/ajpcell.1981.241.5.C220

Kirkhorn SR, Garry VF (2000): Agricultural Lung Diseases. Environ Health Perspect, 108:705-712. https://doi.org/10.1289/ehp.00108s4705

Kitchen P, Day RE, Salman MM, Conner MT, Bill RM, Conner AC (2015): Beyond water homeostasis: Diverse functional roles of mammalian aquaporins. Biochim Biophys Acta Gen Subj, 1850:2410–2421. https://doi.org/10.1016/j.bbagen.2015.08.023

Knepper MA, Packer R, Good DW (1989): Ammonium transport in the kidney. Physiol Rev, 69:179–249. https://doi.org/10.1152/physrev.1989.69.1.179

Kollmann P, Elfers K, Maurer S, Klingenspor M, Schemann M, Mazzuoli-Weber G (2020): Submucosal enteric neurons of the cavine distal colon are sensitive to hypoosmolar stimuli. J Physiol, 598:5317–5332. https://doi.org/10.1113/JP280309

Krawielitzki K, Zebrowska T, Schadereit R, Kowalczyk J, Hennig U, Wünsche J, Hermmann U (1990): Determining of Nitrogen Absorption and Nitrogen Secretion in Different Sections of the Pig's Intestine by Digesta Exchange between ^{15}N Labelled and Unlabelled Animals. Arch Tierernaehr, 40:25–37. https://doi.org/10.1080/17450399009428378

Kunert-Keil C, Bisping F, Krüger J, Brinkmeier H (2006): Tissue-specific expression of TRP channel genes in the mouse and its variation in three different mouse strains. BMC Genomics, 7:159. https://doi.org/10.1186/1471-2164-7-159

Kurtz I, Balaban RS (1986): Ammonium as a substrate for Na^+-K^+-ATPase in rabbit proximal tubules. Am J Physiol Renal Physiol, 250:F497–F502. https://doi.org/10.1152/ajprenal.1986.250.3.F497

Leonhard-Marek S, Stumpff F, Brinkmann I, Breves G, Martens H (2005): Basolateral Mg^{2+}/Na^+ exchange regulates apical nonselective cation channel in sheep rumen epithelium via cytosolic Mg^{2+}. Am J Physiol Gastrointest Liver Physiol, 288:G630-45. https://doi.org/10.1152/ajpgi.00275.2004

Liebe F, Liebe H, Sponder G, Mergler S, Stumpff F (2022): Effects of $butyrate^-$ on ruminal Ca^{2+} transport: evidence for the involvement of apically expressed TRPV3 and TRPV4 channels. Pflugers Arch - Eur J Physiol, 474:315-342. https://doi.org/10.1007/s00424-021-02647-7

Liebe F, Liebe H, Kaessmeyer S, Sponder G, Stumpff F (2020): The TRPV3 channel of the bovine rumen: localization and functional characterization of a protein relevant for ruminal ammonia transport. Pflugers Arch - Eur J Physiol, 472:693–710. https://doi.org/10.1007/s00424-020-02393-2

Liebe H, Liebe F, Sponder G, Hedtrich S, Stumpff F (2021): Beyond Ca^{2+} signalling: the role of TRPV3 in the transport of NH_4^+. Pflugers Arch - Eur J Physiol, 473:1859-1884. https://doi.org/10.1007/s00424-021-02616-0

Liebich H-G (2010): Funktionelle Histologie der Haussäugetiere und Vögel: Lehrbuch und Farbatlas für Studium und Praxis. 5th edition, Schattauer Verlag, Stuttgart. ISBN 978-3-7945-2692-5

Lieder B, Hoi J, Burian N, Hans J, Holik A-K, Marquez LRB, Ley JP, Hatt H, Somoza V (2020): Structure-Dependent Effects of Cinnamaldehyde Derivatives on TRPA1-Induced Serotonin Release in Human Intestinal Cell Models. J Agric Food Chem, 68:3924–3932. https://doi.org/10.1021/acs.jafc.9b08163

Litman T, Søgaard R, Zeuthen T (2009): Ammonia and Urea Permeability of Mammalian Aquaporins. In: Beitz E (ed) Aquaporins. 1st edition, Springer, Berlin, Heidelberg, pp 327–358. ISBN: 978-3-540-79885-9

Liu Z, Peng J, Mo R, Hui C, Huang C-H (2001): Rh Type B Glycoprotein Is a New Member of the Rh Superfamily and a Putative Ammonia Transporter in Mammals. J Biol Chem, 276:1424–1433. https://doi.org/10.1074/jbc.M007528200

Liu Z, Chen Y, Mo R, Hui C, Cheng J-F, Mohandas N, Huang C-H (2000): Characterization of Human RhCG and Mouse Rhcg as Novel Nonerythroid Rh Glycoprotein Homologues Predominantly Expressed in Kidney and Testis*. J Biol Chem, 275:25641–25651. https://doi.org/10.1074/jbc.M003353200

Liu Z, Huang CH (1999): The mouse Rhl1 and Rhag genes: sequence, organization, expression, and chromosomal mapping. Biochem Genet, 37:119–138. https://doi.org/10.1023/a:1018726303397

Lu Z, Stumpff F, Deiner C, Rosendahl J, Braun H, Abdoun K, Aschenbach JR, Martens H (2014): Modulation of sheep ruminal urea transport by ammonia and pH. Am J Physiol Regul Integr Comp Physiol, 307:R558–R570. https://doi.org/10.1152/ajpregu.00107.2014

Lucas P, Ukhanov K, Leinders-Zufall T, Zufall F (2003): A Diacylglycerol-Gated Cation Channel in Vomeronasal Neuron Dendrites Is Impaired in TRPC2 Mutant Mice: Mechanism of Pheromone Transduction. Neuron, 40:551–561. https://doi.org/10.1016/S0896-6273(03)00675-5

Lucien N, Bruneval P, Lasbennes F, Belair M-F, Mandet C, Cartron J-P, Bailly P, Trinh-Trang-Tan M-M (2005): UT-B1 urea transporter is expressed along the urinary and gastrointestinal tracts of the mouse. Am J Physiol Regul Integr Comp Physiol, 288:R1046–R1056. https://doi.org/10.1152/ajpregu.00286.2004

Lynch MB, O'Shea CJ, Sweeney T, Callan JJ, O'Doherty JV (2008): Effect of crude protein concentration and sugar-beet pulp on nutrient digestibility, nitrogen excretion, intestinal fermentation and manure ammonia and odour emissions from finisher pigs. Animal, 2:425–434. https://doi.org/10.1017/S1751731107001267

Macpherson LJ, Dubin AE, Evans MJ, Marr F, Schultz PG, Cravatt BF, Patapoutian A (2007): Noxious compounds activate TRPA1 ion channels through covalent modification of cysteines. Nature, 445:541–545. https://doi.org/10.1038/nature05544

Maenner K, Vahjen W, Simon O (2011): Studies on the effects of essential-oil-based feed additives on performance, ileal nutrient digestibility, and selected bacterial groups in the gastrointestinal tract of piglets. J Anim Sci, 89:2106–2112. https://doi.org/10.2527/jas.2010-2950

Maes DG, Deluyker H, Verdonck M, de Kruif A, Ducatelle R, Castryck F, Miry C, Vriejns B (2001): Non-infectious factors associated with macroscopic and microscopic lung lesions in slaughter pigs from farrow-to-finish herds. Vet Rec, 148:41–46. https://doi.org/10.1136/vr.148.2.41

Manneck D, Braun H-S, Schrapers KT, Stumpff F (2021a): TRPV3 and TRPV4 as candidate proteins for intestinal ammonium absorption. Acta Physiol (Oxf), 233:e13694. https://doi.org/10.1111/apha.13694

Manneck D, Manz G, Braun H-S, Rosendahl J, Stumpff F (2021b): The TRPA1 Agonist Cinnamaldehyde Induces the Secretion of HCO_3^- by the Porcine Colon. Int J Mol Sci, 22:5198. https://doi.org/10.3390/ijms22105198

Manzanilla EG, Perez JF, Martin M, Kamel C, Baucells F, Gasa J (2004): Effect of plant extracts and formic acid on the intestinal equilibrium of early-weaned pigs. J Anim Sci, 82:3210–3218. https://doi.org/10.2527/2004.82113210x

Marcaggi P, Coles JA (2001): Ammonium in nervous tissue: transport across cell membranes, fluxes from neurons to glial cells, and role in signalling. Prog Neurobiol, 64:157–183. https://doi.org/10.1016/S0301-0082(00)00043-5

Mardini H, Record C (2013): Pathogenesis of hepatic encephalopathy: lessons from nitrogen challenges in man. Metab Brain Dis, 28:201–207. https://doi.org/10.1007/s11011-012-9362-2

Marini AM, Soussi-Boudekou S, Vissers S, Andre B (1997): A family of ammonium transporters in Saccharomyces cerevisiae. Mol Cell Biol, 17:4282–4293. https://doi.org/10.1128/MCB.17.8.4282

Martens H, Leonhard-Marek S, Röntgen M, Stumpff F (2018): Magnesium homeostasis in cattle: absorption and excretion. Nutr Res Rev, 31:114–130. https://doi.org/10.1017/S0954422417000257

Massa F, Sibaev A, Marsicano G, Blaudzun H, Storr M, Lutz B (2006): Vanilloid receptor (TRPV1)-deficient mice show increased susceptibility to dinitrobenzene sulfonic acid induced colitis. J Mol Med (Berl), 84:142–146. https://doi.org/10.1007/s00109-005-0016-2

Matsumoto K, Kurosawa E, Terui H, Hosoya T, Tashima K, Murayama T, Priestley JV, Harie S (2009): Localization of TRPV1 and contractile effect of capsaicin in mouse large intestine: high abundance and sensitivity in rectum and distal colon. Am J Physiol Gastrointest Liver Physiol, 297:G348–G360. https://doi.org/10.1152/ajpgi.90578.2008

Meijer GAL, van der Meulen J, van Vuuren AM (1993): Glutamine is a potentially limiting amino acid for milk production in dairy cows: A hypothesis. Metabolism, 42:358–364. https://doi.org/10.1016/0026-0495(93)90087-5

Michiels A, Piepers S, Ulens T, Vam Ransbeeck N, Del Pozo Sacristán R, Sierens A, Haesebrouck F, Demeyer P, Maes D (2015): Impact of particulate matter and ammonia on average daily weight gain, mortality and lung lesions in pigs. Prev Vet Med, 121:99–107. https://doi.org/10.1016/j.prevetmed.2015.06.011

Michiels J, Missotten J, Dierick N, Fremaut D, Maene P, De Smet S (2008): *In vitro* degradation and *in vivo* passage kinetics of carvacrol, thymol, eugenol and *trans*-cinnamaldehyde along the gastrointestinal tract of piglets: *In vitro* degradation and *in vivo* passage kinetics of essential oils in piglets. J Sci Food Agric, 88:2371–2381. https://doi.org/10.1002/jsfa.3358

Mihara H, Suzuki N, Boudaka AA, Muhammad JS, Tominaga M, Tabuchi Y, Sugiyama T (2016): Transient receptor potential vanilloid 4-dependent calcium influx and ATP release in mouse and rat gastric epithelia. World J Gastroenterol, 22:5512-5519. https://doi.org/10.3748/wjg.v22.i24.5512

Mihara H, Suzuki N, Yamawaki H, Tominaga M, Sugiyama T (2013): TRPV2 ion channels expressed in inhibitory motor neurons of gastric myenteric plexus contribute to gastric adaptive relaxation and gastric emptying in mice. Am J Physiol Gastrointest Liver Physiol, 304:G235–G240. https://doi.org/10.1152/ajpgi.00256.2012

Mihara H, Boudaka A, Shibasaki K, Yamanaka A, Sugiyama T, Tominaga M (2010): Involvement of TRPV2 Activation in Intestinal Movement through Nitric Oxide Production in Mice. J Neurosci, 30:16536–16544. https://doi.org/10.1523/JNEUROSCI.4426-10.2010

Minke B, Wu C-F, Pak WL (1975): Induction of photoreceptor voltage noise in the dark in Drosophila mutant. Nature, 258:84–87. https://doi.org/10.1038/258084a0

Montell C (2011): The history of TRP channels, a commentary and reflection. Pflugers Arch - Eur J Physiol, 461:499–506. https://doi.org/10.1007/s00424-010-0920-3

Montell C, Birnbaumer L, Flockerzi V, Bindels RK, Bruford EA, Caterina MJ, Clapham DE, Harteneck C, Heller S, Julius D, Kojima I, Mori Y, Penner R, Prawitt D, Scharenberg AM, Schultz G, Shimizu N, Zhu MX (2002): A Unified Nomenclature for the Superfamily of TRP Cation Channels. Mol Cell, 9:229–231. https://doi.org/10.1016/S1097-2765(02)00448-3

Montell C, Rubin GM (1989): Molecular characterization of the Drosophila trp locus: a putative integral membrane protein required for phototransduction. Neuron, 2:1313–1323. https://doi.org/10.1016/0896-6273(89)90069-x

Muller C, Morales P, Reggio PH (2019): Cannabinoid Ligands Targeting TRP Channels. Front Mol Neurosci, 11:487. https://doi.org/10.3389/fnmol.2018.00487

Musa-Aziz R, Chen L-M, Pelletier MF, Boron WF (2009a): Relative CO_2/NH_3 selectivities of AQP1, AQP4, AQP5, AmtB, and RhAG. Proc Natl Acad Sci, 106:5406–5411. https://doi.org/10.1073/pnas.0813231106

Musa-Aziz R, Jiang L, Chen L-M, Behar KL, Boron WF (2009b): Concentration-Dependent Effects on Intracellular and Surface pH of Exposing Xenopus oocytes to Solutions Containing NH_3/NH_4^+. J Membr Biol, 228:15–31. https://doi.org/10.1007/s00232-009-9155-7

Nagaraja TN, Brookes N (1998): Intracellular acidification induced by passive and active transport of ammonium ions in astrocytes. Am J Physiol Cell Physiol, 274:C883–C891. https://doi.org/10.1152/ajpcell.1998.274.4.C883

Nagatomo K, Kubo Y (2008): Caffeine activates mouse TRPA1 channels but suppresses human TRPA1 channels. Proc Natl Acad Sci, 105:17373–17378. https://doi.org/10.1073/pnas.0809769105

Nakamura S, Amlal H, Galla JH, Soleimani M (1999): NH_4^+ secretion in inner medullary collecting duct in potassium deprivation: Role of colonic H^+-K^+-ATPase. Kidney Int, 56:2160–2167. https://doi.org/10.1046/j.1523-1755.1999.00780.x

Nakanishi T, Nakamura Y, Umeno J (2021): Recent advances in studies of SLCO2A1 as a key regulator of the delivery of prostaglandins to their sites of action. Pharmacol Ther, 223:107803. https://doi.org/10.1016/j.pharmthera.2021.107803

Nakanishi T, Tamai I (2017): Roles of Organic Anion Transporting Polypeptide 2A1 (OATP2A1/SLCO2A1) in Regulating the Pathophysiological Actions of Prostaglandins. AAPS J, 20:13. https://doi.org/10.1208/s12248-017-0163-8

Nakhoul NL, Abdulnour-Nakhoul SM, Boulpaep EL, Rabon E, Schmidt E, Hamm LL (2010): Substrate specificity of Rhbg: ammonium and methyl ammonium transport. Am J Physiol Cell Physiol, 299:C695–C705. https://doi.org/10.1152/ajpcell.00019.2010

Nakhoul NL, DeJong H, Abdulnour-Nakhoul SM, Boulpaep EL, Hering-Smith K, Hamm LL (2005): Characteristics of renal Rhbg as an NH_4^+ transporter. Am J Physiol Renal Physiol, 288:F170–F181. https://doi.org/10.1152/ajprenal.00419.2003

Neuhäuser B, Dynowski M, Ludewig U (2014): Switching substrate specificity of AMT/MEP/Rh proteins. Channels, 8:496–502. https://doi.org/10.4161/19336950.2014.967618

Nickel R, Schummer A, Seiferle E (2004): Lehrbuch der Anatomie der Haustiere, Band II: Eingeweide. 9th edition, Enke, Stuttgart. ISBN 978-3-8304-4152-6

Nijenhuis T, Hoenderop JGJ, van der Kemp AWCM, Bindels RJM (2003): Localization and Regulation of the Epithelial Ca^{2+} Channel TRPV6 in the Kidney. Clin J Am Soc Nephrol, 14:2731–2740. https://doi.org/10.1097/01.ASN.0000094081.78893.E8

Nilius B, Bíró T, Owsianik G (2014): TRPV3: time to decipher a poorly understood family member!. J Physiol, 592:295–304. https://doi.org/10.1113/jphysiol.2013.255968

Nilius B, Bíró T (2013): TRPV3: a 'more than skinny' channel. Exp Dermatol, 22:447–452. https://doi.org/10.1111/exd.12163

Nilius B, Appendino G, Owsianik G (2012): The transient receptor potential channel TRPA1: from gene to pathophysiology. Pflugers Arch - Eur J Physiol, 464:425–458. https://doi.org/10.1007/s00424-012-1158-z

Nilius B, Owsianik G (2011): The transient receptor potential family of ion channels. Genome Biol, 12:218. https://doi.org/10.1186/gb-2011-12-3-218

Nilius B, Prenen J, Owsianik G (2011): Irritating channels: the case of TRPA1: Puzzling properties of TRPA1. J Physiol, 589:1543–1549. https://doi.org/10.1113/jphysiol.2010.200717

Nozawa K, Kawabata-Shoda E, Doihara H, Kojima R, Okada H, Mochizuki S, Sano Y, Inamura K, Matsushime H, Koizumi T, Yokoyama T, Ito H (2009): TRPA1 regulates gastrointestinal motility through serotonin release from enterochromaffin cells. Proc Natl Acad Sci, 106:3408–3413. https://doi.org/10.1073/pnas.0805323106

Omonijo FA, Kim S, Guo T, Wang Q, Gong J, Lahaye L, Bodin J-C, Nyachoti M, Liu S, Yang C (2018): Development of Novel Microparticles for Effective Delivery of Thymol and Lauric Acid to Pig Intestinal Tract. J Agric Food Chem, 66:9608–9615. https://doi.org/10.1021/acs.jafc.8b02808

Ortar G, Morera L, Schiano Moriello A, Morera E, Nalli M, Di Marzo V, De Petrocellis L (2012): Modulation of thermo-transient receptor potential (thermo-TRP) channels by thymol-based compounds. Bioorg Med Chem Lett, 22:3535–3539. https://doi.org/10.1016/j.bmcl.2012.03.055

O'Shea CJ, Lynch B, Lynch MB, Callan JJ, O'Doherty JV (2009): Ammonia emissions and dry matter of separated pig manure fractions as affected by crude protein concentration and sugar beet pulp inclusion of finishing pig diets. Agric Ecosyst Environ, 131:154–160. https://doi.org/10.1016/j.agee.2009.01.019

Owsianik G, Talavera K, Voets T, Nilius B (2006): PERMEATION AND SELECTIVITY OF TRP CHANNELS. Annu Rev Physiol, 68:685–717. https://doi.org/10.1146/annurev.physiol.68.040204.101406

Patra AK, Geiger S, Schrapers KT, Braun H-S, Gehlen H, Starke A, Pieper R, Cieslak A, Szumacher-Strabel M, Aschenbach JR (2019): Effects of dietary menthol-rich bioactive lipid compounds on zootechnical traits, blood variables and gastrointestinal function in growing sheep. J Animal Sci Biotechnol, 10:86. https://doi.org/10.1186/s40104-019-0398-6

Peiris M, Weerts ZZRM, Aktar R, Masclee AAM, Blackshaw A, Keszthelyi D (2021): A putative anti-inflammatory role for TRPM8 in irritable bowel syndrome—An exploratory study. Neurogastroenterol Motil, https://doi.org/10.1111/nmo.14170

Peng J-B, Chen X-Z, Berger UV, Vassilev PM, Tsukaguchi H, Brown EM, Hediger MA (1999): Molecular Cloning and Characterization of a Channel-like Transporter Mediating Intestinal Calcium Absorption. J Biol Chem, 274:22739–22746. https://doi.org/10.1074/jbc.274.32.22739

Penuelas A, Tashima K, Tsuchiya S, Matsumoto K, Nakamura T, Horie S, Yano S (2007): Contractile effect of TRPA1 receptor agonists in the isolated mouse intestine. Eur J Pharmacol, 576:143–150. https://doi.org/10.1016/j.ejphar.2007.08.015

Philippe F-X, Cabaraux J-F, Nicks B (2011): Ammonia emissions from pig houses: Influencing factors and mitigation techniques. Agric Ecosyst Environ, 141:245–260. https://doi.org/10.1016/j.agee.2011.03.012

Pieper R, Boudry C, Bindelle J, Vahjen W, Zentek J (2014): Interaction between dietary protein content and the source of carbohydrates along the gastrointestinal tract of weaned piglets. Arch Anim Nutr, 68:263–280. https://doi.org/10.1080/1745039X.2014.932962

Pieper R, Kröger S, Richter JF, Wang J, Martin L, Bindelle J, Htoo JK, von Smolinski D, Vahjen W, Zentek J, Van Kessel AG (2012): Fermentable Fiber Ameliorates Fermentable Protein-Induced Changes in Microbial Ecology, but Not the Mucosal Response, in the Colon of Piglets. J Nutr, 142:661–667. https://doi.org/10.3945/jn.111.156190

Pingle SC, Matta JA, Ahern GP (2007): Capsaicin Receptor: TRPV1 A Promiscuous TRP Channel. In: Flockerzi V, Nilius B (eds) Transient Receptor Potential (TRP) Channels. 1st edition, Springer, Berlin, Heidelberg, pp 155–171. ISBN 978-3-540-34891-7

Piva A, Pizzamiglio V, Morlacchini M, Tedeschi M, Piva G (2007): Lipid microencapsulation allows slow release of organic acids and natural identical flavors along the swine intestine. J Anim Sci, 85:486–493. https://doi.org/10.2527/jas.2006-323

Pottosin I, Dobrovinskaya O (2014): Non-selective cation channels in plasma and vacuolar membranes and their contribution to K^+ transport. J Plant Physiol, 171:732–742. https://doi.org/10.1016/j.jplph.2013.11.013

Pouokam E, Diener M (2019): Segmental differences in ion transport in rat caecum. Pflugers Arch - Eur J Physiol, 471:1007–1023. https://doi.org/10.1007/s00424-019-02276-1

Premkumar LS (2014): Transient Receptor Potential Channels as Targets for Phytochemicals. ACS Chem Neurosci, 5:1117–1130. https://doi.org/10.1021/cn500094a

Pritschow BW, Lange T, Kasch J, Kunert-Weil C, Liedtke W, Brinkmeier H (2011): Functional TRPV4 channels are expressed in mouse skeletal muscle and can modulate resting Ca^{2+} influx and muscle fatigue. Pflugers Arch - Eur J Physiol, 461:115–122. https://doi.org/10.1007/s00424-010-0883-4

Qi L, Mao H, Lu X, Shi T, Wang J (2021): Cinnamaldehyde Promotes the Intestinal Barrier Functions and Reshapes Gut Microbiome in Early Weaned Rats. Front Nutr, 8:748503. https://doi.org/10.3389/fnut.2021.748503

Qin N, Neeper MP, Liu Y, Hutchinson TL, Lubin ML, Flores CM (2008): TRPV2 is activated by cannabidiol and mediates CGRP release in cultured rat dorsal root ganglion neurons. J Neurosci, 28:6231–6238. https://doi.org/10.1523/JNEUROSCI.0504-08.2008

Rabbani I, Braun H-S, Akhtar T, Liebe F, Rosendahl J, Grunau M, Tietjen U, Masood S, Kaessmeyer S, Günzel D, Rehmann H, Stumpff F (2018): A comparative study of ammonia transport across ruminal epithelia from *Bos indicus* crossbreds versus *Bos taurus*. Anim Sci J, 89:1692–1700. https://doi.org/10.1111/asj.13107

Ramachandran R, Hyun E, Zhao L, Lapointe TK, Chapman K, Hirota CL, Ghosh S, McKemy DD, Vergnolle N, Beck PL, Altier C, Hollenberg MD (2013): TRPM8 activation attenuates inflammatory responses in mouse models of colitis. Proc Natl Acad Sci, 110:7476–7481. https://doi.org/10.1073/pnas.1217431110

Ramirez M, Fernandez R, Malnic G (1999): Permeation of NH_3/NH_4^+ and cell pH in colonic crypts of the rat. Pflugers Arch - Eur J Physiol, 438:508–515. https://doi.org/10.1007/s004249900077

Ramsey IS, Delling M, Clapham DE (2006): AN INTRODUCTION TO TRP CHANNELS. Annu Rev Physiol, 68:619–647. https://doi.org/10.1146/annurev.physiol.68.040204.100431

Rizopoulos T, Papadaki-Petrou H, Assimakopoulou M (2018): Expression Profiling of the Transient Receptor Potential Vanilloid (TRPV) Channels 1, 2, 3 and 4 in Mucosal Epithelium of Human Ulcerative Colitis. Cells, 7:61. https://doi.org/10.3390/cells7060061

Roberts DM, Tyerman SD (2002): Voltage-Dependent Cation Channels Permeable to NH_4^+, K^+, and Ca^{2+} in the Symbiosome Membrane of the Model Legume *Lotus japonicus*. Plant Physiol, 128:370–378. https://doi.org/10.1104/pp.010568

Romero-Gómez M, Jover M, Galán JJ, Ruiz A (2009): Gut ammonia production and its modulation. Metab Brain Dis, 24:147–157. https://doi.org/10.1007/s11011-008-9124-3

Rondón LJ, Groenestege WMT, Rayssiguier Y, Mazur A (2008): Relationship between low magnesium status and TRPM6 expression in the kidney and large intestine. Am J Physiol Regul Integr Comp Physiol, 294:R2001–R2007. https://doi.org/10.1152/ajpregu.00153.2007

Roper SD (2014): TRPs in Taste and Chemesthesis. In: Nilius B, Flockerzi V (eds) Mammalian Transient Receptor Potential (TRP) Cation Channels: Volume II. 1st edition, Springer, Berlin, Heidelberg, pp 827–871. ISBN 978-3-319-05160-4

Rosendahl J, Braun HS, Schrapers KT, Martens H, Stumpff F (2016): Evidence for the functional involvement of members of the TRP channel family in the uptake of Na^+ and NH_4^+ by the ruminal epithelium. Pflugers Arch - Eur J Physiol, 468:1333–1352. https://doi.org/10.1007/s00424-016-1835-4

Rubino JG, Wilson JM, Wood CM (2019): An in vitro analysis of intestinal ammonia transport in fasted and fed freshwater rainbow trout: roles of NKCC, K^+ channels, and Na^+, K^+ ATPase. J Comp Physiol B, 189:549–566. https://doi.org/10.1007/s00360-019-01231-x

Rushton L (2007): Occupational causes of chronic obstructive pulmonary disease. Rev Environ Health, 22:195–212. https://doi.org/10.1515/reveh.2007.22.3.195

Salomon F-V, Geyer H, Gille U (2008): Anatomie für die Tiermedizin. 2nd edition, Enke, Stuttgart. ISBN 978-3-8304-1075-1

Schlingmann KP, Waldegger S, Konrad M, Chubanov V, Gudermann T (2007): TRPM6 and TRPM7—Gatekeepers of human magnesium metabolism. Biochim Biophys Acta Mol Basis Dis, 1772:813–821. https://doi.org/10.1016/j.bbadis.2007.03.009

Schrapers KT, Sponder G, Liebe F, Liebe H, Stumpff F (2018): The bovine TRPV3 as a pathway for the uptake of Na^+, Ca^{2+}, and NH_4^+. PLoS One, 13:e0193519. https://doi.org/10.1371/journal.pone.0193519

Schröder B, Breves G (2006): Mechanisms and regulation of calcium absorption from the gastrointestinal tract in pigs and ruminants: comparative aspects with special emphasis on hypocalcemia in dairy cows. Anim Health Res Rev, 7:31–41. https://doi.org/10.1017/S1466252307001144

Schröder B, Vössing S, Breves G (1999): In vitro studies on active calcium absorption from ovine rumen. J Comp Physiol B Biochem Syst Environ Physiol, 169:487–494. https://doi.org/10.1007/s003600050246

Schröder B, Rittmann I, Pfeffer E, Breves G (1997): In vitro studies on calcium absorption from the gastrointestinal tract in small ruminants. J Comp Physiol B Biochem Syst Environ Physiol, 167:43–51. https://doi.org/10.1007/s003600050046

Shibasaki K (2016): TRPV4 ion channel as important cell sensors. J Anesth, 30:1014–1019. https://doi.org/10.1007/s00540-016-2225-y

Smith GD, Gunthorpe MJ, Kelsell RE, Hayes PD, Reilly P, Facer P, Wright JE, Jerman JC, Walhin J-P, Ooi L, Egerton J, Charles KJ, Smart D, Randall AD, Anand P, David JB (2002): TRPV3 is a temperature-sensitive vanilloid receptor-like protein. Nature, 418:186–190. https://doi.org/10.1038/nature00894

Soupene E, He L, Yan D, Kustu S (1998): Ammonia acquisition in enteric bacteria: physiological role of the ammonium/methylammonium transport B (AmtB) protein. Proc Natl Acad Sci U S A, 95:7030–7034. https://doi.org/10.1073/pnas.95.12.7030

Spanaki C, Plaitakis A (2012): The Role of Glutamate Dehydrogenase in Mammalian Ammonia Metabolism. Neurotox Res, 21:117–127. https://doi.org/10.1007/s12640-011-9285-4

Spoelstra SF (1979): Volatile fatty acids in anaerobically stored piggery wastes. Neth J Agri Sci, 27:60–66. https://doi.org/10.18174/njas.v27i1.17071

Stombaugh DP, Teague HS, Roller WL (1969): Effects of Atmospheric Ammonia on the Pig. J Anim Sci, 28:844–847. https://doi.org/10.2527/jas1969.286844x

Stotz SC, Vriens J, Martyn D, Clardy J, Clapham DE (2008): Citral Sensing by TRANSient Receptor Potential Channels in Dorsal Root Ganglion Neurons. PLoS One, 3:e2082. https://doi.org/10.1371/journal.pone.0002082

Stumpff F, Lodemann U, Van Kessel AG, Pieper R, Klingspor S, Wolf K, Martens H, Zentek J, Aschenbach JR (2013): Effects of dietary fibre and protein on urea transport across the cecal mucosa of piglets. J Comp Physiol B, 183:1053–1063. https://doi.org/10.1007/s00360-013-0771-2

Szöllősi AG, Vasas N, Angyal Á, Kistamás K, Nánási, PP, Mihály J, Béke G, Herczeg-Lisztes E, Szegedi A, Kawada N, Yanagida T, Mori T, Kemény L, Bírßo T (2018): Activation of TRPV3 Regulates Inflammatory Actions of Human Epidermal Keratinocytes. J Invest Dermatol, 138:365–374. https://doi.org/10.1016/j.jid.2017.07.852

Takaishi M, Uchida K, Suzuki Y, Matsui H, Shimada T, Fujita F, Tominaga M (2016): Reciprocal effects of capsaicin and menthol on thermosensation through regulated activities of TRPV1 and TRPM8. J Physiol Sci, 66:143–155. https://doi.org/10.1007/s12576-015-0427-y

Talavera K, Startek JB, Alvarez-Collazo J, Boonen Bm Alpizar YA, Sanchez A, Naert R, Nilius B (2020): Mammalian Transient Receptor Potential TRPA1 Channels: From Structure to Disease. Physiol Rev, 100:725–803. https://doi.org/10.1152/physrev.00005.2019

Talavera K, Nilius B (2011): Electrophysiological Methods for the Study of TRP Channels. In: Zhu MX (ed) TRP Channels. 1st edition, CRC Press/Taylor & Francis, Boca Raton (FL), pp. G508-G520. ISBN 978-1-138-11616-0

Thomas GH, Mullins JG, Merrick M (2000): Membrane topology of the Mep/Amt family of ammonium transporters. Mol Microbiol, 37:331–344. https://doi.org/10.1046/j.1365-2958.2000.01994.x

Thomas RC (1984): Experimental displacement of intracellular pH and the mechanism of its subsequent recovery. J Physiol, 354:3P-22P. https://doi.org/10.1113/jphysiol.1984.sp015397

Thorneloe KS, Cheung M, Holt DA, Willette RN (2017): PROPERTIES OF THE TRPV4 ACTIVATOR GSK1016790A AND the TRPV4 ANTAGONIST GSK2193874. Physiol Rev, 97:1231–1232. https://doi.org/10.1152/physrev.00019.2017

Thorneloe KS, Sulpizio AC, Lin Z, Figueroa DJ, Clouse AK, McCafferty GP, Chendrimada TP, Lashinger ESR, Gordon E, Evans L, Misajet BA, DeMarini DJ, Nation JH, Casillas LN, Marquis RW, Votta BJ, Sheardown SA, Xu X, Brooks DP, Laping NJ, Westfall TD (2008): *N* -((1 *S*)-1-{[4-((2 *S*)-2-{[(2,4-Dichlorophenyl)sulfonyl]amino}-3-hydroxypropanoyl)-1-piperazinyl]carbonyl}-3-methylbutyl)-1-benzothiophene-2-carboxamide (GSK1016790A), a Novel and Potent Transient Receptor Potential Vanilloid 4 Channel Agonist Induces Urinary Bladder Contraction and Hyperactivity: Part I. J Pharmacol Exp Ther, 326:432–442. https://doi.org/10.1124/jpet.108.139295

Toft-Bertelsen TL, MacAulay N (2021): TRPing to the Point of Clarity: Understanding the Function of the Complex TRPV4 Ion Channel. Cells, 10:165. https://doi.org/10.3390/cells10010165

Toledo Mauriño JJ, Fonseca-Camarillo G, Furuzawa-Carballeda J, Barreto-Zuñiga R, Martínez Benítez B, Granados J, Yamamoto-Furusho JK (2020): TRPV Subfamily (TRPV2, TRPV3, TRPV4, TRPV5, and TRPV6) Gene and Protein Expression in Patients with Ulcerative Colitis. J Immunol Res, 2020:1–11. https://doi.org/10.1155/2020/2906845

Ueda T, Yamada T, Ugawa S, Ishida Y, Shimida S (2009): TRPV3, a thermosensitive channel is expressed in mouse distal colon epithelium. Biochem Biophys Res Commun, 383:130–134. https://doi.org/10.1016/j.bbrc.2009.03.143

Umweltbundesamt (2021): Ammoniak, Geruch und Staub. Accessed 07.02.2022 at 12:38 from https://www.umweltbundesamt.de/themen/boden-landwirtschaft/umweltbelastungen-der-landwirtschaft/ammoniak-geruch-staub#emissionen-der-landwirtschaft

Ushida K, Maekawa M, Arakawa T (2002): Influence of Dietary Supplementation of Herb Extracts on Volatile Sulfur Production in Pig Large Intestine. J Nutr Sci Vitaminol, (Tokyo) 48:18–23. https://doi.org/10.3177/jnsv.48.18

Uzura R, Takahashi K, Saito S, Tominaga M, Ohta T (2020): Reduction of extracellular sodium evokes nociceptive behaviors in the chicken via activation of TRPV1. Brain Res, 1747:147052. https://doi.org/10.1016/j.brainres.2020.147052

van der Wielen N, Moughan PJ, Mensink M (2017): Amino Acid Absorption in the Large Intestine of Humans and Porcine Models. J Nutr, 147:1493–1498. https://doi.org/10.3945/jn.117.248187

van Goor MKC, Hoenderop JGJ, van der Wijst J (2017): TRP channels in calcium homeostasis: from hormonal control to structure-function relationship of TRPV5 and TRPV6. Biochim Biophys Acta Mol Cell Res, 1864:883–893. https://doi.org/10.1016/j.bbamcr.2016.11.027

Van Liefferinge E, Van Noten N, Degroote J, Vrolix G, Van Poucke M, Peelman L, Van Ginneken C, Roura E, Michiels J (2020): Expression of Transient Receptor Potential Ankyrin 1 and Transient Receptor Potential Vanilloid 1 in the Gut of the Peri-Weaning Pig Is Strongly Dependent on Age and Intestinal Site. Animals, 10:2417. https://doi.org/10.3390/ani10122417

Van Noten N, Van Liefferinge E, Degroote J, De Smet S, Desmet T, Michiels J (2020): Fate of Thymol and Its Monoglucosides in the Gastrointestinal Tract of Piglets. ACS Omega, 5:5241–5248. https://doi.org/10.1021/acsomega.9b04309

Vanrolleghem W, Tanghe S, Verstringe S, Bruggemann G, Papadopoulos D, Trevisi P, Zentek J, Sarrazin S, Dewulf J (2019): Potential dietary feed additives with antibacterial effects and their impact on performance of weaned piglets: A meta-analysis. Vet J, 249:24–32. https://doi.org/10.1016/j.tvjl.2019.04.017

Vázquez E, Valverde MA (2006): A review of TRP channels splicing. Semin Cell Dev Biol, 17:607–617. https://doi.org/10.1016/j.semcdb.2006.11.004

Vennekens R, Vriens J, Nilius B (2008): Herbal Compounds and Toxins Modulating TRP Channels. Curr Neuropharmacol, 6:79–96. https://doi.org/10.2174/157015908783769644

Vincent F, Duncton MAJ (2011): TRPV4 Agonists and Antagonists. Curr Top Med Chem, 11:2216–2226. https://doi.org/10.2174/156802611796904861

Voets T, Prenen J, Vriens J, Watanabe H, Janssens A, Wissenbach U, Bödding M, Droogmans G, Nilius B (2002): Molecular Determinants of Permeation through the Cation Channel TRPV4. J Biol Chem, 277:33704–33710. https://doi.org/10.1074/jbc.M204828200

Voets T, Janssens A, Droogmans G, Nilius B (2004a): Outer Pore Architecture of a Ca^{2+}-selective TRP Channel. J Biol Chem, 279:15223–15230. https://doi.org/10.1074/jbc.M312076200

Voets T, Nilius B, Hoefs S, van der Kemp AWCM, Droogmans G, Bindels RJM, Hoenderop JGJ (2004b): TRPM6 Forms the Mg^{2+} Influx Channel Involved in Intestinal and Renal Mg^{2+} Absorption. J Biol Chem, 279:19–25. https://doi.org/10.1074/jbc.M311201200

Vogt-Eisele AK, Weber K, Sherkheli MA, Vielhaber G, Panten J, Gisselmann G, Hatt H (2007): Monoterpenoid agonists of TRPV3: Monoterpenoid agonists of TRPV3. Br J Pharmacol, 151:530–540. https://doi.org/10.1038/sj.bjp.0707245

Von Essen S, Romberger D (2003): The respiratory inflammatory response to the swine confinement building environment: the adaptation to respiratory exposures in the chronically exposed worker. J Agric Saf Health, 9:185–196. https://doi.org/10.13031/2013.13684

Waisbren SJ, Geibel JP, Modlin IM, Boron WF (1994): Unusual permeability properties of gastric gland cells. Nature, 368:332–335. https://doi.org/10.1038/368332a0

Walker RL, Hume JR, Horowitz B (2001): Differential expression and alternative splicing of TRP channel genes in smooth muscles. Am J Physiol Cell Physiol, 280:C1184–C1192. https://doi.org/10.1152/ajpcell.2001.280.5.C1184

Walker V (2009): Ammonia toxicity and its prevention in inherited defects of the urea cycle. Diabetes Obes Metab, 11:823–835. https://doi.org/10.1111/j.1463-1326.2009.01054.x

Wall SM (1996): NH_4^+ augments net acid secretion by a ouabain-sensitive mechanism in isolated perfused inner medullary collecting ducts. Am J Physiol Renal Physiol, 270:F432–F439. https://doi.org/10.1152/ajprenal.1996.270.3.F432

Wathes DC, Clempson AM, Pollott GE (2013): Associations between lipid metabolism and fertility in the dairy cow. Reprod Fertil Dev, 25:48-61. https://doi.org/10.1071/RD12272

Weiner ID, Verlander JW (2017): Ammonia Transporters and Their Role in Acid-Base Balance. Physiol Rev, 97:465–494. https://doi.org/10.1152/physrev.00011.2016

Weiner ID, Verlander JW (2016): Recent advances in understanding renal ammonia metabolism and transport. Curr Opin Nephrol Hypertens, 25:436–443. https://doi.org/10.1097/MNH.0000000000000255

Weiner ID, Hamm LL (2007): Molecular Mechanisms of Renal Ammonia Transport. Annu Rev Physiol, 69:317–340. https://doi.org/10.1146/annurev.physiol.69.040705.142215

Wilkens MR, Richter J, Fraser DR, Liesegang A, Breves G, Schröder B (2012): In contrast to sheep, goats adapt to dietary calcium restriction by increasing intestinal absorption of calcium. Comp Biochem Physiol A Mol Integr Physiol, 163:396–406. https://doi.org/10.1016/j.cbpa.2012.06.011

Wilkens MR, Kunert-Keil C, Brinkmeier H, Schröder B (2009): Expression of calcium channel TRPV6 in ovine epithelial tissue. Vet J, 182:294–300. https://doi.org/10.1016/j.tvjl.2008.06.020

Windisch W, Schedle K, Plitzner C, Kroismayr A (2008): Use of phytogenic products as feed additives for swine and poultry1. J Anim Sci, 86:E140–E148. https://doi.org/10.2527/jas.2007-0459

Worrell RT, Oghene J, Matthews JB (2004): Ammonium effects on colonic Cl^- secretion: anomalous mole fraction behavior. Am J Physiol Gastrointest Liver Physiol, 286:G14–G22. https://doi.org/10.1152/ajpgi.00196.2003

Wrong O (1978): Nitrogen metabolism in the gut. Am J Clin Nutr, 31:1587–1593. https://doi.org/10.1093/ajcn/31.9.1587

Xiao B, Dubin AE, Bursulaya B, Viswanath V, Jegla TJ, Patapoutian A (2008): Identification of Transmembrane Domain 5 as a Critical Molecular Determinant of Menthol Sensitivity in Mammalian TRPA1 Channels. J Neurosci, 28:9640–9651. https://doi.org/10.1523/JNEUROSCI.2772-08.2008

Xiao D, Zeng L, Yao K, Kong X, Wu G, Yin Y (2016): The glutamine-alpha-ketoglutarate (AKG) metabolism and its nutritional implications. Amino Acids, 48:2067–2080. https://doi.org/10.1007/s00726-016-2254-8

Xu H, Delling M, Jun JC, Clapham DE (2006): Oregano, thyme and clove-derived flavors and skin sensitizers activate specific TRP channels. Nat Neurosci, 9:628–635. https://doi.org/10.1038/nn1692

Xu H, Ramsey IS, Kotecha SA, Moran MM, Chong JA, Lawson D, Ge P, Liily J, Silos-Santiago I, Xie Y, DiStefano PS, Curtis R, Clapham DE (2002): TRPV3 is a calcium-permeable temperature-sensitive cation channel. Nature, 418:181–186. https://doi.org/10.1038/nature00882

Xu L, Han Y, Chen X, Aierken A, Wen H, Zheng W, Wang H, Lu X, Zhao Z, Ma C, Liang P, Yang W, Yang S, Yang F (2020): Molecular mechanisms underlying menthol binding and activation of TRPM8 ion channel. Nat Commun, 11:3790. https://doi.org/10.1038/s41467-020-17582-x

Yang B, Zhao D, Solenov E, Verkman AS (2006): Evidence from knockout mice against physiologically significant aquaporin 8-facilitated ammonia transport. Am J Physiol Cell Physiol, 291:C417–C423. https://doi.org/10.1152/ajpcell.00057.2006

Yang J, Li Y, Zuo X, Zhen Y, Yu Y, Gao L (2008): Transient receptor potential ankyrin-1 participates in visceral hyperalgesia following experimental colitis. Neurosci Lett, 440:237–241. https://doi.org/10.1016/j.neulet.2008.05.093

Yang P, Zhu MX (2014): TRPV3. In: Nilius B, Flockerzi V (eds) Mammalian Transient Receptor Potential (TRP) Cation Channels: Volume I. 1st edition, Springer, Berlin, Heidelberg, pp 273–291. ISBN 978-3-642-54215-2

Yokoo K, Yamamoto Y, Suzuki T (2021): Ammonia impairs tight junction barriers by inducing mitochondrial dysfunction in Caco-2 cells. FASEB J, 35:e21854. https://doi.org/10.1096/fj.202100758R

Zervas S, Zijlstra RT (2002): Effects of dietary protein and fermentable fiber on nitrogen excretion patterns and plasma urea in grower pigs. J Anim Sci, 80:3247. https://doi.org/10.2527/2002.80123247x

Zhang L, Jones S, Brody K, Costa M, Brookes SJH (2004): Thermosensitive transient receptor potential channels in vagal afferent neurons of the mouse. Am J Physiol Gastrointest Liver Physiol, 286:G983–G991. https://doi.org/10.1152/ajpgi.00441.2003

Zhu C, Chen Z, Jiang Z (2016): Expression, Distribution and Role of Aquaporin Water Channels in Human and Animal Stomach and Intestines. Int J Mol Sci, 17:1399. https://doi.org/10.3390/ijms17091399

Zidi-Yahiaoui N, Mouro-Chanteloup I, D'Ambrosio A-M, Lopez C, Gane P, Le Van Kim C, Cartron J-P, Colin Y, Ripoche P (2005): Human Rhesus B and Rhesus C glycoproteins: properties of facilitated ammonium transport in recombinant kidney cells. Biochem J, 391:33–40. https://doi.org/10.1042/BJ20050657

Zimin AV, Delcher AL, Florea L, Kelley DR, Schatz MC, Puiu D, Hanrahan F, Pertea G, Van Tassell CP, Sonstegard TS, Marçais G, Roberts M, Subramanian P, Yorke JA, Salzberg SL (2009): A whole-genome assembly of the domestic cow, Bos taurus. Genome Biol, 10:R42. https://doi.org/10.1186/gb-2009-10-4-r42

Zirkle KW, Nolan BT, Jones RR, Weyer PJ, Ward MH, Wheeler DC (2016): Assessing the relationship between groundwater nitrate and animal feeding operations in Iowa (USA). Sci Total Environ, 566–567:1062–1068. https://doi.org/10.1016/j.scitotenv.2016.05.130

List of Publications

Publications (peer reviewed)

2021

Manneck, D., Braun, H.-S., Schrapers, K.T., Stumpff, F., (2021): TRPV3 and TRPV4 as candidate proteins for intestinal ammonium absorption. Acta Physiol (Oxf), 233:e13694. https://doi.org/10.1111/apha.13694

Manneck, D., Manz, G., Braun, H.-S., Rosendahl, J., Stumpff, F., (2021): The TRPA1 Agonist Cinnamaldehyde Induces the Secretion of HCO_3^- by the Porcine Colon. Int J Mol Sci, 22:5198. https://doi.org/10.3390/ijms22105198

Stumpff, F., **Manneck, D.**, Martens, H., (2021): News in caecal signalling: the role of propionate in microbial-epithelial crosstalk. Pflugers Arch – Eur J Physiol, 473:853-854 https://doi.org/10.1007/s00424-021-02579-2

2019

Stumpff, F., **Manneck, D.**, Martens, H., (2019): Unravelling the secrets of the caecum. Pflugers Arch – Eur J Physiol, 471:925-926 https://doi.org/10.1007/s00424-019-02292-1

Abstracts in Proceedings & Participation in Conferences

2021

Manneck, D.; Schrapers, K.T.; Stumpff, F. (2021):
Effect of thymol on electrophysiological parameters in the porcine jejunum and colon ex vivo.
75. Jahrestagung der Gesellschaft für Ernährungsphysiologie (GfE)
Berlin – 16.03.-18.03.2021
In: Frankfurt am Main (Germany): DLG-Verlag GmbH. Proceedings of the Society of Nutrition Physiology: Berichte der Gesellschaft für Ernährungsphysiologie; volume 30 (2021), S. 103

2019

Manneck, D.; Schrapers, K. S.; Braun, H.-S.; Stumpff, F. (2019):
Evidence for functional involvement of TRPA1 and TRPV3 in ion transport across the colon of pigs
98. DPG (Deutsche Physiologische Gesellschaft)
Ulm – 30.09.-02.10.2019
In: Acta Physiologica; 229(S719), S. 130-131.

2018

Manneck, D.; Schrapers, K.; Stumpff, F. (2018):
Evidence for the stimulation of multiple conductances by cinnamaldehyde in the porcine colon.
Tagung der DVG-Fachgruppe Physiologie und Biochemie der Deutschen Veterinärmedizinischen Gesellschaft
Wien – 21.02.-23.02.2018.
In: 23. Tagung der Fachgruppe Physiologie und Biochemie der Deutschen Veterinärmedizinischen Gesellschaft: PROGRAMM & ABSTRACTS – Veterinärmedizinische Universität Wien (Hrsg.), Wien, S. 64

Manneck D.; Schrapers K.T.; Stumpff F. (2018):
Effects of cinnamaldehyde on electrophysiological parameters of the porcine colon in vitro
72. Jahrestagung der Gesellschaft für Ernährungsphysiologie (GfE)
Göttingen – 13.03.-15.03.2018.
In: Frankfurt am Main (Germany): DLG-Verlag GmbH. Proceedings of the Society of Nutrition Physiology: Berichte der Gesellschaft für Ernährungsphysiologie; volume 27 (2018), S. 57

2017

Manneck, D.; Schrapers, K. T.; Braun, H. S.; Rosendahl, J.; Stumpff, F. (2017):
A Study on NH_4^+-induced currents across the gastrointestinal epithelium of pigs.
71. Jahrestagung der Gesellschaft für Ernährungsphysiologie (GfE)
Göttingen – 14.03.-16.03.2017
In: Frankfurt am Main (Germany): DLG-Verlag GmbH. Proceedings of the Society of Nutrition Physiology: Berichte der Gesellschaft für Ernährungsphysiologie; volume 26 (2017), S. 36
Veterinärmedizinische Universität Wien (Hrsg.), Wien, S. 64

Manneck D.; Schrapers K.T.; Braun, H. S.; Rosendahl, J.; Stumpff, F. (2017):
Effects of luminal NH_4^+ on epithelial transport in porcine gastrointestinal epithelia.
Deutsche Physiologische Gesellschaft
Greifswald – 16.03.-18.03.2017.
In: Acta Physiologica Scandinavica; 219(S711), S. A01–A05

Acknowledgements

Die Anfertigung dieser Dissertation wäre ohne die Hilfe einiger besonderer Menschen nicht möglich gewesen, bei denen ich mich an dieser Stelle herzlich bedanken möchte.

Zunächst möchte ich mich bei **Prof. Dr. Friederike Stumpff** für die Betreuung meiner Promotion bedanken. Du standest mir zu jeder Zeit als Ratgeberin zur Seite und hattest dabei stets ein Ohr für die kleinen und auch größeren Probleme. Du hast mir gezeigt, dass es sich lohnt manchmal out of the box zu denken, gleichzeitig aber auch die kleinen Details nicht außer Acht gelassen werden sollten.

Ein herzliches Dankeschön geht außerdem an die Mitarbeitenden im Institut für Veterinär-Physiologie. Ein besonderer Dank geht dabei an **Katharina Söllig**, die mich bei vielen Fragen tatkräftig unterstützt hat und dank ihrer optimistischen und herzlichen Art dafür sorgte, dass man auch nach dem fünften Anlauf nicht aufgab. Bei **Gisela Manz** möchte ich mich vor allem bei der tatkräftigen Unterstützung im Patch-Labor bedanken, ohne die Einiges nicht möglich gewesen wäre. Ebenso möchte ich mich bei **Martin Grunau** bedanken, der in der Ussing-Kammer stets geholfen hat, wenn etwas nicht funktioniert hat, wie es eigentlich sollte und gleichzeitig immer viel Geduld bewies. Bei **Susanne Trappe** möchte ich mich für die tolle Unterstützung in der Zellkultur und der Mikroskopie herzlich bedanken. Ein großes Dankeschön geht außerdem an **Prof. Dr. Jörg Aschenbach**, der mir die Möglichkeit gab, am Institut zu promovieren, sowie mit wertvollen Hinweisen und Ratschlägen unterstützte.

Ein weiteres großes Dankeschön richte ich an **Dr. Hannah-Sophie Braun, Dr. Julia Rosendahl** und **Dr. Katharina Schrapers**, die mich vor allem in der Anfangszeit tatkräftig unterstützt haben und stets ein offenes Ohr hatten.

Zuletzt gilt mein ganz besonderer Dank meinen **Eltern** und **Kevin Niehage**, die mich stets in allen Hoch- und Tieflagen des Lebens unterstützen. Ohne euch wäre diese Arbeit nicht möglich gewesen, weshalb ich meinen Dank für euren grenzenlosen Rückhalt nicht in Worte fassen kann.

Funding Sources

Ich bedanke mich bei der Akademie für Tiergesundheit, die meine Promotion mit einem Stipendium unterstützt hat.

Conflict of Interest

Die Arbeiten wurden finanziell unterstützt durch die PerformaNat GmbH. Es besteht kein Interessenkonflikt durch die finanzielle Unterstützung der Arbeiten.

Statement of Authorship

Hiermit bestätige ich, dass ich die vorliegende Arbeit selbstständig angefertigt habe. Ich versichere, dass ich ausschließlich die angegebenen Quellen und Hilfen in Anspruch genommen habe.

Potsdam, den 21.10.2022 David Manneck

Druck: Mensch und Buch Verlag Berlin